INFORMATION TO USERS

This manuscript has been reproduced from the microfilm master. UMI films the text directly from the original or copy submitted. Thus, some thesis and dissertation copies are in typewriter face, while others may be from any type of computer printer.

The quality of this reproduction is dependent upon the quality of the copy submitted. Broken or indistinct print, colored or poor quality illustrations and photographs, print bleedthrough, substandard margins, and improper alignment can adversely affect reproduction.

In the unlikely event that the author did not send UMI a complete manuscript and there are missing pages, these will be noted. Also, if unauthorized copyright material had to be removed, a note will indicate the deletion.

Oversize materials (e.g., maps, drawings, charts) are reproduced by sectioning the original, beginning at the upper left-hand corner and continuing from left to right in equal sections with small overlaps.

Photographs included in the original manuscript have been reproduced xerographically in this copy. Higher quality 6" x 9" black and white photographic prints are available for any photographs or illustrations appearing in this copy for an additional charge. Contact UMI directly to order.

Bell & Howell Information and Learning
300 North Zeeb Road, Ann Arbor, MI 48106-1346 USA

UMI®
800-521-0600

METALLOCENE-CATALYZED SEMI-BATCH AND CONTINUOUS POLYMERIZATION OF ETHYLENE

By

PAUL A. CHARPENTIER, M.Sc.

A Thesis

Submitted to the School of Graduate Studies

in Partial Fulfillment of the Requirements

for the Degree

Doctor of Philosophy

McMaster University

DOCTOR OF PHILOSOPHY (1997) McMaster University

(Chemical Engineering) Hamilton, Ontario

TITLE: Metallocene-Catalyzed Semi-Batch and Continuous Polymerization of Ethylene

AUTHOR: Paul A. Charpentier, H.BSc. (York University, Canada)
M.Sc. (University of Waterloo, Canada)

SUPERVISOR: Professor Archie E. Hamielec

NUMBER OF PAGES: xxii, 210

ABSTRACT

An integrated methodology has been utilized to analyze the factors that affect the activity of metallocene catalysts and the microstructure of the polymers produced under various reaction conditions for both semi-batch and continuous solution polymerization of ethylene. The highly active metallocene catalyst system Cp_2ZrCl_2/MAO was focused on in order to determine the fundamental kinetic rate constants, and a thorough characterization of the polymer microstructure was carried out using high temperature size exclusion chromatography (SEC), carbon-13 nuclear magnetic resonance spectroscopy (^{13}C NMR), differential scanning calorimetry (DSC) and shear thinning behavior as determined by I_{10}/I_2.

In the semi-batch polymerization of ethylene in toluene utilizing Cp_2ZrCl_2/MAO, the shape of the polymerization rate-time curves were found to depend on monomer diffusion rates with low ethylene concentrations and poor sparging/mixing impellers giving steady-states while high ethylene concentrations and superior impellers led to decay-type curves. Increasing temperature increased the catalyst activity with an activation energy for propagation (E_p) of 28.5 kJ/mol while strongly decreasing PE MWs. Several types of commercial and developmental aluminoxanes were studied which indicated that the structure and type of aluminoxane co-catalyst did not influence the MWD of PE although significantly influenced the catalyst activity. Mixing additional TMA with MAO

was found not to alter the MWD. For all conditions studied at temperatures between 20-90 °C in semi-batch, the PE produced was found to approximate Flory's most probable distribution for a single site-type catalyst. The rate constants for propagation, β-scission and chain transfer to ethylene at 70 °C were found to be $k_p = 2.7\times10^4$ $(M\cdot s)^{-1}$, $k_{tr,\beta} = 0.27$ s^{-1} and $k_{tr,M} \cong 3.8$ $(M\cdot s)^{-1}$. Long chain branches per 1000 carbons (λ_N) up to 1.2 were found and the ratio of melt flow indexes indicating shear thinning, I_{10}/I_2, were found up to 15.

A high pressure, high temperature CSTR was utilized for the solution polymerization of ethylene at 1500 psig in toluene using the metallocene catalyst system Cp_2ZrCl_2/MAO/TMA. Increasing Cp_2ZrCl_2 concentration led to a decrease in PE MWs while the catalyst activity increased. With increasing temperature between 140-200 °C, the MWs of PE decreased and polydispersities increased while the catalyst activity decreased with an apparent activation energy of -93 kJ/mol. The deactivation of the catalyst is first-order with rate constant $k_d=2.1\times10^{-3}$ s^{-1} while $k_p = 5\times10^3$ $(M\cdot s)^{-1}$ and $k_{tr,\beta}=3$ s^{-1} at 140 °C. λ_N's up to 0.6 were found and I_{10}/I_2 were found up to 6.

ACKNOWLEDGEMENTS

I wish to express my gratitude to several people that helped me during the course of my Ph.D. program at McMaster University.

First, I am particularly indebted to my thesis supervisor, Professor Archie E. Hamielec for his guidance and encouragement throughout this work. Working with Professor Hamielec for the past four years was certainly a privilege and an extremely enriching experience. I am also grateful to my thesis co-supervisor, Professor Michael Brook and to Professor Shiping Zhu, both of whom have contributed invaluably to this thesis.

I owe thanks to Dr. Joao Soares for his advice and encouragement throughout this work. I owe thanks to Dr. Jesus M. Vela-Estrada for his discussions with me during his short stay at McMaster during my thesis work.

I would like to express my gratitude to some of the present and former staff members of the McMaster Institute for Polymer Production Technology for their kind help during the past four years: Mr. Doug Keller, Mr. Greg Emery, and especially to Dr. Kris Kostanski for help with DSC, running GPC samples besides advice on numerous other topics. Thanks also to Dr. Brian Sayer for help with ^{13}C and ^{27}Al NMR and thanks to Peter Hajak and Daryoosh Beigzadeh for help with the research CSTR setup and to Dajing Yan for performing several MFIs.

TABLE OF CONTENTS

LIST OF FIGURES

CHAPTER 2 Page

CHAPTER 3

CHAPTER 4

CHAPTER 5

APPENDIX A

LIST OF TABLES

NOMENCLATURE

CCD	Chemical Composition Distribution
CSTR	Continuous Stirred Tank Reactor
atm	Atmosphere (s)
Cp	Cyclopentadienyl
E_a	Activation Energy (kJ/mol)
HDPE	High Density Polyethylene
LCB	Long Chain Branching
LLDPE	Linear Low Density Polyethylene
M	Monomer
MAO	Methylaluminoxane
MWD	Molecular Weight Distribution
PDI	Polydispersity Index
PE	Polyethylene
PS	Polystyrene
k_p	Propagation Rate Constant (L/mol·s)
GPC	Gel Permeation Chromatography
R_p	Rate of Polymerization (mol/s)
RTD	Residence Time Distribution

SCB	Short Chain Branching
T	Temperature (°C)
τ	Termination/Propagation Ratio
Z-N	Ziegler-Natta Catalyst

PREFACE TO THESIS

This thesis has been divided into five separate chapters and an appendix. The first chapter is an introductory chapter and provides: a) an introduction to metallocene polymerization and the different synthetic methods for producing high density polyethylene (HDPE) and linear low density polyethylene (LLDPE) and what advantages metallocene catalysts provide over the traditional routes for producing these polymers; and b) the objectives of this thesis. The main objectives of this thesis were to determine the factors that effect the activity of metallocene catalysts and the microstructure of the polyethylene (PE) polymer produced and particularly to determine the effect of the aluminoxane co-catalyst on the activity of the metallocene catalyst and the microstructure of the PE produced.

Chapters 2-5 consist of four papers that have been submitted to various academic journals. These papers contain all of the significant research and analysis that was performed in this thesis. Chapter 2 investigates the polymerization of ethylene utilizing the metallocene catalyst, Cp_2ZrCl_2. This metallocene catalyst is one of the simplest of the metallocene catalysts, easy to obtain through commercial sources, and gives one of the highest activities for the polymerization of ethylene of any of the metallocene catalysts. Additionally, most of the research up to this time in metallocene polymerization has been performed by chemists. The chemist's main interest has been in synthesizing different metallocene catalysts,

determining their structure and the type of polymer that they produce, normally at a single experimental condition. Also the ability to make novel tactic polymers as well as to produce highly isotactic polypropylene (iPP) has been a focus of their research. However, the effect of the polymerization conditions such as reactor temperature and monomer concentration have largely been ignored. Thus, a systematic investigation was undertaken to examine the main experimental variables including ethylene concentration, impeller geometry, polymerization temperature, and catalyst concentration. Additionally, polymerization time, hydrogen concentration, octene-1 concentration and transition metal type were investigated. The main experimental measurements were polymerization activity ((kg PE/(g Zr·hr·[ethylene])) and the produced PE MWD through the use of high temperature GPC. The polymerizations were determined to be mass-transfer limited relatively early during experimentation and this mass-transfer limitation was attempted to be minimized by choosing appropriate experimental conditions i.e. agitator with a relatively large d/D and a low catalyst concentration. The determined rate constants in semi-batch are thus apparent rate constants.

Chapter 3 is devoted to the effects of the aluminoxane co-catalyst on the polymerization of ethylene utilizing the metallocene catalyst Cp_2ZrCl_2. These experiments were performed in semi-batch during the time period of the experiments from Chapter 2. However, as this body of experimental work was

found to be distinct and unique from the material of Chapter 2, it was published separately. Various aluminoxane co-catalysts were either purchased or donated by Akzo-Nobel or Albemarle Corporation. Additionally, trimethylaluminum (TMA) was investigated as to its effect in the polymerization of ethylene, along with the presence of an aluminoxane.

Originally in my experimental work, I was going to investigate copolymerization and supporting the metallocene catalysts on inorganic supports and to compare these to homogeneous (nonsupported) polymerization. However, my research objectives at this time were changed to design, build and operate a continuous solution polymerization reactor for studying polyolefins utilizing metallocene catalysts. Chapter 4 describes this reactor and polymerization experiments utilizing the metallocene catalyst Cp_2ZrCl_2/MMAO and TMA to polymerize ethylene. A systematic investigation was performed studying the variables; polymerization temperature, reactor residence time, ethylene concentration in the feed, and catalyst concentration. The Al/Zr ratio was not investigated in these experiments and the total Al/Zr ratio was held constant at 1000 with 600 coming from TMA and 400 from MAO. As previous experiments had demonstrated that the feed pumps were quite sensitive to aluminoxane and could be damaged by this co-catalyst, it was decided to make the concentration of aluminoxane as low as possible for these experiments while maintaining a

reproducible polymerization. As the catalyst and co-catalyst were diluted into separate feed tanks which were pumped separately, protection of the catalyst was found necessary. TMA was added to the catalyst feed tank in order to protect the catalyst from deactivation by impurities in the solvent. It was found that the polymerization could be made reproducible by this technique.

Chapter 5 of this thesis deals with experimental evidence indicating the presence of long chain branching (LCBing) in PE produced from semi-batch and continuous solution polymerization of ethylene utilizing the simple metallocene catalyst Cp_2ZrCl_2. LCBing is a relatively unexplored area of metallocene polymerization and it is mainly believed that an open faced catalyst such as the Dow Chemical Company's constrained geometry catalyst is required in solution polymerization to produce significant long chain branching which will effect shear thinning. One of the main experimental difficulties encountered in this study is the difficulty in accurately determining the frequency of long chain branching utilizing ^{13}C NMR. Much more experimental evidence is required to accurately determine the frequency of branching and how to maximize this branching.

The appendix of this thesis is given to explore the results from Chapter 4 where the PE PDIs were found to increase with increasing polymerization temperature. The appendix explores the deconvolution of the experimental GPC curves to determine the number of Flory's most probably distributions and thus the

number of site types. It appears from these results that the number of site types may be increasing with temperature in this high temperature range from 140-200 °C.

CHAPTER 1 - INTRODUCTION

1.1 *General Considerations*

Low density polyethylene (LDPE), high density polyethylene (HDPE), and linear low density polyethylene (LLDPE) are three of the major tonnage commodity polymers which will reach a capacity of approximately 17 million tons of LDPE, 17 million tons of HDPE and 15 million tons of LLDPE in world plastic sales for 1997 (Kuhlke, 1994). Presently, polyethylene polymers are commercially produced using: a) free-radical initiators, b) Phillips type catalysts, c) Ziegler-Natta catalysts, and d) metallocene catalysts, with the importance of free radical polyethylene polymers decreasing.

Low density polyethylene (LDPE) has been commercially produced since the 1930s by free-radical mechanisms in high temperature, high pressure processes (e.g., autoclave at 150-200 MPa, 180-290 °C or tubular reactors at 250-350 MPa, 140-180 °C) (Whiteley et al., 1992). As the chain end radical is the active site, the active site structure cannot be varied and the structure of the LDPE produced cannot be varied by the type of initiator. Due to the free radical polymerization mechanism, the LDPE polymer produced is both highly long chain branched (LCBed) and short chain branched (SCBed) which leads to the low density. (Hamielec & Tobita, 1992). The LCBing provides this polymer with good shear

thinning, making it easy to process. Due to its poor mechanical and physical properties, LDPE is used primarily in the manufacture of films. According to the Stanford Research Institute (SRI), the production of LDPE has not grown over the last 5 years (Sinclair, 1994). Due to the expense of LDPE plants, their lack of flexibility, and the fact that in the future metallocene produced resins with LCBing can take the place of LDPE with improved performance, it is likely that the production of LDPE will be phased out.

The Phillips Petroleum Company pioneered the development of silica-supported chromium oxide catalysts (CrO_3/SiO_2) which are presently the most widely used catalysts for HDPE production (James, 1987). These catalysts produce HDPE with a broad MWD which provide good shear thinning (Karol, 1995). Ziegler-Natta catalysts (e.g. $TiCl_4$/TMA) have evolved through several generations since their discovery in 1953 but basically are composed of two components: i) a transition metal salt from Groups IV-VIII (catalyst component), and ii) a metal alkyl from groups I-III (co-catalyst component) (Boor, 1979). As only broad structural changes can be made to these catalysts, traditionally, a polyolefin manufacturer designs a HDPE/LLDPE polymer for a particular application by selecting the polymerization process and the comonomer and by adjusting the process conditions to control the polymers melt flow index (MFI) (the MFI I_2 is correlated roughly with the M_w molecular weight) and the density of the polymer for a desired end-use application.

Both the Phillips and Ziegler-Natta catalysts have several different site-types. Each of the individual site-types instantaneously produce polymer with i) Flory's most probable distribution with polydispersity index M_w/M_n =2 and M_z/M_w = 1.5 (Flory, 1953), and ii) a copolymer (if comonomer present) described by Stockmayer's bivariate distribution (Stockmayer, 1945). These multiple site-type catalysts give rise to polymers with broad MWDs and copolymers with broad chemical composition distributions (CCD refers to the distribution of composition among the polymer chains), each of which can only be partially controlled. For these copolymers, the low molecular weight fractions possess higher than average comonomer content (i.e., high SCBing content). This low molecular weight, high comonomer percent fraction is the waxy, hexane extractable fraction of the polymer. The high MW fraction produced with the traditional Phillips or Z-N catalyst consists mainly of PE homopolymer molecules containing little SCBing. This high MW fraction is highly crystalline and is responsible for higher haze and higher peak melting point (MP) of Z-N resins. Polyethylenes made using classical Z-N catalysts and Phillips chromium oxide catalysts are linear with no measurable levels of LCBing.

Metallocene catalysts are turning out to be truly a revolution to the production of both specialty and commodity polyolefins. The main advantages of metallocene catalysts are that they can provide extremely high productivities (Kaminsky, 1983; Chien, 1988) and, as they are complex organometallic species, their structure can be modified to an almost limitless number of possibilities by

variation of: a) ligand type, b) bridge joining ligands, c) substituents on ligand and bridge to modify the steric and electronic surroundings of the transition metal and, d) the transition metal (Hamielec & Soares, 1996). The well defined and controllable metallocene structure allows formation of unique and specific active site-types (normally one per catalyst) compared to a multi-sited Phillips or Z-N catalyst where there is very little control of the individual site-types. Each site-type gives a unique activity, chain transfer to propagation rate, reactivity ratio and stereoselectivity so that by variation of the catalyst site structure, each of these can be tailored to give a polymer with a desired blend of properties. These catalysts can be customized to fit a specific process and will allow a single reactor to produce many diverse grades and types of polymer.

For certain processes, particularly slurry and gas phase polymerization, supporting the metallocene catalysts on high surface area inorganic particles is necessary. Gas phase polymerization has revolutionized the production of HDPE/LLDPE/PP/EPR since the 1970s as well as being considered the process of choice for many future types of polymers that metallocene polymerization will allow (Karol, 1995). Supporting the metallocene can reduce the amount of expensive MAO required for polymerization and provides a means for stabilizing the unusual oxidation states and/or coordination numbers of the metal. Another advantage of supporting metallocenes is that different metallocenes can be supported on the same support to produce polymers with optimum properties for specific applications. Unfortunately, the supported metallocene catalyst also gives

a significantly lower activity than the same non-supported catalyst due to the immobility of the catalyst on the support material.

In addition to homopolymerization of ethylene and other α-olefins, metallocenes can be employed for copolymerization of α-olefins using conditions essentially identical to those used for homopolymerization. Certain metallocenes with open structures such as monocyclopentadienyl metallocenes allow high incorporation of higher α-olefin comonomers to readily control the density of a polymer not achievable with a traditional heterogeneous Phillips or Z-N catalyst. (Lai et al., 1993). These catalysts can also polymerize and copolymerize many unusual monomers and combinations of monomers that are not possible with traditional Z-N catalysts. This allows polymer products to be produced with uniform composition and specific desired properties.

Metallocene catalysts produce LLDPE copolymers with a much narrower CCD than that produced by a conventional Phillips or Z-N catalyst. Because of the narrow CCD, the metallocene produced copolymers have very little low molecular weight polymer with high amounts of SCBing. This provides low hexane extractables content which is good for food and drug applications. Similarly, very little highly crystallizable high molecular weight polymer with low amounts of short chain branching is produced. This is important for film and other applications requiring low haze and good clarity (Speed et al., 1991). Metallocene LLDPE copolymers are ideal for shrink film applications because of the narrower

melting point (MP) range and lower peak MP due to the narrow MWD and CCD than those from traditional copolymers (VandderSanden et al., 1993). The lower peak MP is due to the lower amount of highly crystalline high MW fraction present in heterogeneous copolymers which melts at a higher temperature. Metallocene LLDPE copolymers also can be used in sealing applications where low seal initiation temperatures are important (Walton, et al., 1994). These resins give a lower seal initiation temperature with simultaneous higher toughness and strength than resins produced by multi-site catalysts.

Metallocene catalysts also give the ability to control the shear-thinning behavior of the polymer by the formation of long chain branches (LCBs). The frequency of long chain branches is believed to be controlled by the variation of the metallocene structure and the manipulation of reactor conditions (Lai et al., 1993; Soares and Hamielec, 1996). Metallocene polymers are reported to have higher zero shear viscosity (due to the narrow MWD), higher melt elasticity and higher shear sensitivity (from the presence of long chain branches) than a standard Z-N catalyzed LLDPE at the same MI and density (Swogger, 1992).

1.2 *Objectives of the Thesis*

The objective of this research was to study the factors that affect the activity of metallocene catalysts and the microstructure of the polyethylene polymer produced. This was carried out both in semi-batch and in continuous solution polymerization. An integrated methodology was utilized for

polymerization analysis consisting of the determination of fundamental kinetic rate constants, and a thorough characterization of the polymer microstructure using high temperature size exclusion chromatography (SEC), carbon-13 nuclear magnetic resonance spectroscopy (^{13}C NMR), differential scanning calorimetry (DSC) and shear thinning as determined by I_{10}/I_2.

The simple metallocene catalyst, Cp_2ZrCl_2, is one of the most active metallocenes known for the polymerization of ethylene but its polymerization behavior has not been well established. Various models have been proposed in the literature which have assumed the presence of more than one site-type for Cp_2ZrCl_2 due to the measured PE MWDs being greater than 3 and the presence of bimodal distributions. The metallocene system Cp_2ZrCl_2/MAO was analyzed in order to determine: a) if Cp_2ZrCl_2 is a single site-type catalyst; b) the effects of polymerization conditions on the rate of polymerization and polymer molecular weight distribution (MWD); and, c) to measure kinetic rate constants for kinetic model development.

The effect of the structure and degree of oligomerization of the aluminoxane co-catalyst on the activity of the metallocene catalyst Cp_2ZrCl_2 and its effect on the MWD of produced PE has not been well established. The effect of additional TMA on the activity and MWD of produced PE has also not been established. The role of the aluminoxane co-catalyst in the active catalytic site-type is still very much in question and a thorough polymerization and polymer

characterization study was undertaken to elucidate its role with the metallocene catalyst Cp_2ZrCl_2.

A semi-batch reactor was utilized to study the kinetics of ethylene homopolymerization using the unsupported metallocene catalyst system Cp_2ZrCl_2/MAO. This reactor type was also used to investigate the aluminoxane and aluminum alkyl co-catalysts in the homopolymerization of ethylene. The microstructure of the polymer produced during this stage was further analyzed with SEC, ^{13}C NMR, DSC, and I_{10}/I_2 measurements.

In industry, the manufacture of polyolefins is performed exclusively with continuous reactors while most academic researchers who study metallocene catalysts are chemists and use batch or semi-batch autoclaves because they are not familiar with continuous reactors. Certain aspects of the polymer microstructure are also believed best controlled with a continuous stirred tank reactor (CSTR), such as the formation of higher levels of long-chain branches. These factors led to the design, sizing and assembling of a high temperature high pressure research CSTR for the air-sensitive polymerization of olefins using metallocene catalysts. This CSTR was used to study the kinetics of ethylene solution polymerization using the unsupported metallocene catalyst Cp_2ZrCl_2/MAO. The microstructure of the polymer produced during this stage was further analyzed with SEC, ^{13}C NMR, DSC, and I_{10}/I_2 measurements.

The importance of having a detailed understanding of the polymerization phenomena using metallocene catalysts cannot be overstated. These catalysts are a

part in all future plans for producing commodity and specialty polyolefins mainly due to: a) extremely high activities, so less catalyst and co-catalyst are necessary for production; and, b) they will allow vast improvements in product quality as they allow one to control the polymer microstructure in an unprecedented manner. An understanding of how the metallocene catalyst activity and the polymer microstructure can be affected by the type of metallocene catalyst, the type of aluminoxane cocatalyst, and the process conditions is highly desirable.

CHAPTER 2 - SEMI-BATCH POLYMERIZATION OF ETHYLENE UTILIZING METALLOCENE DICHLORIDE/ METHYL ALUMINOXANE - DIFFUSION LIMITATIONS

P.A. Charpentier, A.E. Hamielec*, S. Zhu

Department of Chemical Engineering

McMaster University, Hamilton, Ontario, Canada L8S 4L7

M. A. Brook

Department of Chemistry

McMaster University, Hamilton, Ontario, Canada L8S 4M1

Manuscript submitted to *AIChE J*, August 4, 1997

Keywords: metallocene catalyst, methylaluminoxane, polyethylene, semi-batch polymerization, diffusion, kinetic analysis

Author to whom correspondence should be addressed.

Email: hamielec@mcmaster.ca

Phone: (905) 525-9140 ext 24950

Fax: (905) 528-5114.

2.1 Abstract

This paper presents a systematic investigation on ethylene polymerization utilizing the metallocene catalyst Cp_2ZrCl_2/MAO. Experimental variables include: ethylene concentration, catalyst concentration, temperature, polymerization time, hydrogen concentration, octene-1 concentration, transition metal type, and impeller type. Measurements included catalyst activity, polyethylene (PE) molecular weights (MWs) and distributions (PDIs), and PE melting temperature. The shape of the polymerization rate-time curves was found to depend on monomer diffusion rates. Low ethylene concentrations and poor sparging/mixing impellers gave steady-states in the rate curves while high ethylene concentrations and superior impellers led to decay-type curves. The polymerization of ethylene with Cp_2ZrCl_2/MAO was found to give polymer with Flory's most probable distribution for a single site-type catalyst for all conditions studied. Increasing temperature increased the catalyst activity with an activation energy for propagation of ΔE_p of 28.5 kJ/mol and strongly decreased PE MWs. The rate constants for propagation, β-scission and chain transfer to ethylene at 70 °C were found to be $k_p = 2.7\times10^4$ $(M^{-0.8}\cdot s^{-1})$, $k_{tr,\beta} = 0.27$ s^{-1} and $k_{tr,M} \cong 3.8$ $(M\cdot s)^{-1}$.

2.2 Introduction

Metallocene catalysis is having a revolutionary effect on the commercialization of both specialty and commodity polyolefins. The main advantages of metallocene catalysts is that they are extremely active (Kaminsky, 1983; Chien, 1988) and their structure can be modified to give an almost limitless number of active site types by variation of: a) ligand type, b) bridge joining ligands, c) substituents on ligand and bridge to modify steric and electronic surroundings of transition metal and d) transition metal type (Hamielec and Soares, 1996). This well defined and controllable catalyst structure allows formation of unique and specific active site-types (normally one site type per catalyst) compared to a traditional Ziegler-Natta (Z-N) catalyst (e.g. $TiCl_4$/TMA) which is a multi site-type catalyst with very little control of the site-types. Each site type gives narrow molecular weight distributions (MWDs) (Chien, 1988; Kaminsky, 1987) with polydispersity indexes (PDIs) approaching 2 as defined by Flory's most probable MWD (Flory, 1953) and extremely narrow chemical composition distributions (CCDs) in the formation of copolymers, as defined by Stockmayer's bivariate distribution (Stockmayer, 1945). Each site-type gives a unique activity, chain transfer to propagation rate, reactivity ratio and stereoselectivity so that by variation of catalyst site structure, each of these can be tailored to give a polymer with a desired blend of properties. These catalysts also give the ability to control the polymer structure and the rheology of the formed polymer chains by variation

of catalyst structure and manipulation of reactor conditions to form long chain branches (LCBs) (Lai et al., 1993; Soares and Hamielec, 1996).

There are several potential advantages to the study of homogeneous non-supported metallocene polymerization such as a) ideal polymerization behavior producing polymer with Flory's most probable distribution for a single site-type catalyst, which if you support the catalyst, may create additional site-types or modify the original site-type; b) non-encapsulation of catalyst particles with polymer creating intra-particle mass and heat transfer gradients which complicate kinetic interpretation such as that found with traditional heterogeneous Z-N polymerization; c) easier to separate the catalyst and co-catalyst residues from the polymer at the end of the polymerization; d) formation of unique polymer morphology and formation of LCBs; and e) significantly higher activities than supported polymerization.

Various attempts have been made to model the kinetics of ethylene polymerization utilizing the simple metallocene catalyst system, Cp_2ZrCl_2/MAO, such as that given by Chien and Wang (1990), Vela Estrada and Hamielec (1994). These models have assumed the presence of more than one site-type due to the measured PE MWDs being greater than 3 and the presence of bimodal distributions. In the present investigation we have carried out a systematic experimental investigation of the Cp_2ZrCl_2/MAO system in the semi-batch polymerization of ethylene in order to determine a) if Cp_2ZrCl_2 is a single site-type catalyst; b) the effects of polymerization conditions on the rate of polymerization

and polymer molecular weight distribution (MWD) and c) to measure kinetic rate constants for kinetic model development. This most simple metallocene catalyst remains one of the most active metallocenes known for the polymerization of ethylene (Kaminsky, 1983) but a great deal of its ethylene polymerization behavior has not yet been well characterized.

2.3 Experimental

2.3.1 *Materials*

Fisher Optima toluene was used as diluent for all reactions and purified by distillation over sodium benzyl ketyl. The diluent was stored in a stainless steel cylinder and continually sparged with ultra high purity (UHP) argon until used. No contact with the atmosphere was allowed at any time. Research grade ethylene was purchased from Matheson Gas and purified by passing over beds of Alphagaz catalyst and then molecular sieves to remove O_2 and H_2O respectively. UHP hydrogen (99.999 %) was purchased from Matheson Gas and purified by passing over Alphagaz beds to remove O_2 and molecular sieves to remove H_2O. Octene-1 was purchased from Aldrich Chemical and distilled over sodium, then stored over 5 Å molecular sieves and sparged with UHP nitrogen until use. MAO studied was purchased from Akzo-Nobel or donated by Albemarle Corporation. All MAO was used as received. TMA 2.0M in toluene, zirconocene dichloride, hafnocene dichloride, and titanocene dichloride were purchased from Aldrich Chemical and

used as received. All manipulations of catalyst and co-catalyst were performed in a Vacuum Atmospheres glovebox which reduces the impurities O_2 and H_2O to a few ppm. UHP nitrogen (99.999%) and UHP argon (99.999%) were purchased from Matheson Gas and further purified by passing through columns containing catalyst to remove O_2, and molecular sieves to remove H_2O.

2.3.2 *Reactor Setup and Control*

The semi-batch reactor utilized for all polymerization experiments is an Autoclave Engineers 1 L stainless steel kettle with necessary reactant inlets and with a magnetic stirring drive equipped with 2" Dispersimax impeller (see Figure 2.1). All wetted parts were either 316 stainless-steel or Teflon.

The control of temperature was performed with a Thermo Electric Tempstar III Controller with an integrated circuit control board utilizing a PID algorithm in a time proportional heating of an Autoclave Engineers furnace and the time proportional actuation of a solenoid valve for allowing cooling fluid through the cooling coil of the reactor. A Lauda RMS-20 Refrigerating Circulator was used for providing cooling fluid at a constant temperature. This type of control was found sufficient to maintain the reaction temperature at set-point $\pm$ 0.2 °C. The reactor temperature was monitored continuously by a J-type thermocouple placed in a thermocouple well of the reactor. Ethylene flow to the reactor was measured by a Sierra Instruments Model 830 thermal mass flowmeter.

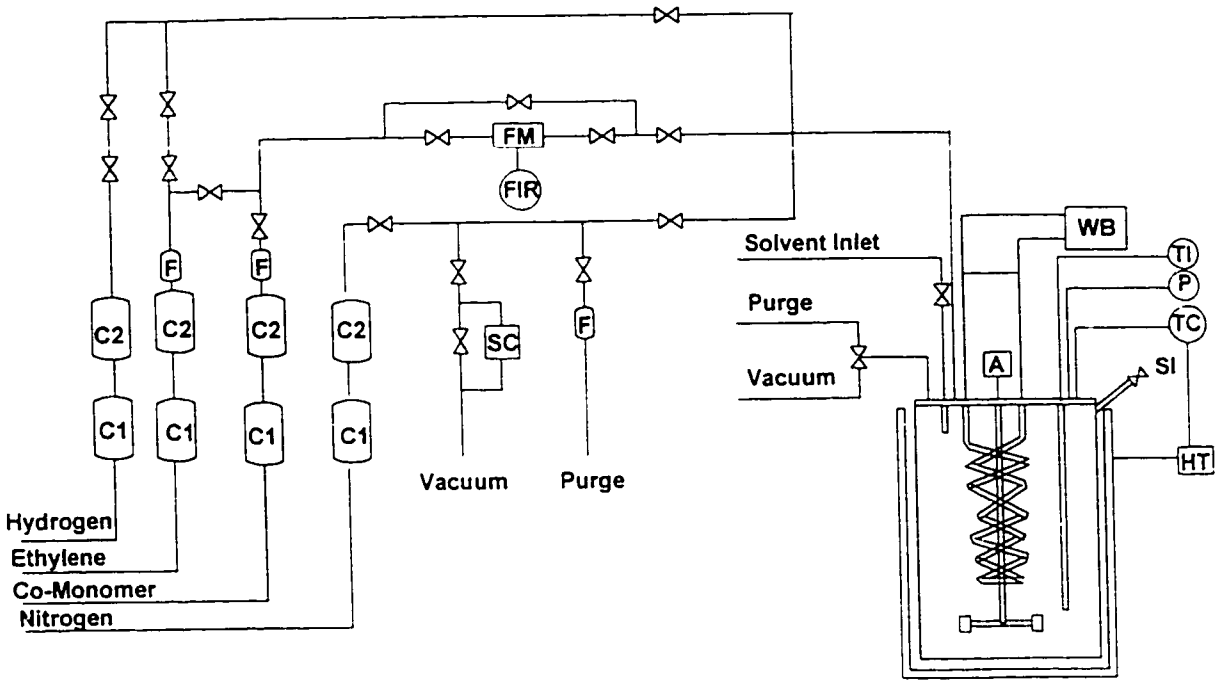

C1 = Oxygen Trap
C2 = Water Trap
F = Filter
FM = Flowmeter
FIR = Flow Indicator
WB = Water Bath
TI = Temperature Indicator
A = Agitator
P = Pressure Gauge
HT = Temperature Controller
TC = Thermocouple

Figure 2.1 - Overview of the semi-batch reactor system used in this study.

2.3.3 *Polymerization Procedure*

All experiments were performed at 1200 rpm, in toluene. A stainless steel cylinder attached to a load cell was utilized to transfer a weighed amount of diluent to the nitrogen purged reactor with additional subsequent purging of the reactor with nitrogen, then ethylene. The co-catalyst was injected by syringe into the reactor next, then the reactor was pressurized with ethylene. For the copolymerization runs, a measured amount of octene-1 was also injected into the reactor prior to the ethylene pressurization. The polymerization was initiated by injection of the metallocene catalyst into the pressurized reactor 5 minutes after injection of co-catalyst. The reaction was terminated by depressurizing and injection of methanol into the reactor. The formed PE was washed with acidic methanol to remove MAO residue, then methanol, filtered and dried under vacuum.

2.3.4 *High Temperature GPC*

All GPC measurements were performed with a Waters-Millipore SEC instrument model 150-C high temperature GPC with a differential refractive index detector at 140 °C using TCB as solvent. The following operation conditions were adopted: 1) column and sample compartment temperature, 140 °C; 2) flow rate of mobile phase, 1.0 mL/min; 3) sample injection volume, 200 μL; 4) no

sample spinning; 5) no sample filtering; 6) sample concentration, 0.1 wt % in 1,2,4-trichlorobenzene (TCB).

Calibration of the high temperature GPC was performed at 140 °C directly with a calibration curve obtained using narrow MWD PE standards purchased from the National Bureau of Standards. Additionally, both narrow MWD polystyrene (PS) standards from Tosoh Corporation and broad MWD PE standards from American Polymer Standards and Polymer Laboratories Ltd. were used to check the calibration curve. The Mark-Houwink constants for the universal calibration curve were $K_{PS} = 1.21 \times 10^{-4}$ and $a_{PS} = 0.707$ and were $K_{PE} = 3.92 \times 10^{-4}$ and $a_{PE} = 0.725$.

2.3.5 *Differential Scanning Calorimetry (DSC)*

All polymer melting points and heats of fusion were measured with a DuPont model 910 DSC which was calibrated with an Indium standard. Weighed polymer samples (2-3 mg) were transferred to DSC pans, heated up to 180 °C at a heating rate of 10 °C/min, cooled to 50 °C, then repeated.

2.4 Results

2.4.1 *Effect of Ethylene Concentration on Polymerization*

Figure 2.2(A) illustrates how the polymerization rate-time curves are affected by ethylene concentration in the reactor. It is clear that increasing the ethylene concentration (by increasing ethylene pressure in the reactor headspace) leads from a steady-state type rate curve at low ethylene concentrations to a decay-type rate curve at high ethylene concentrations. We have defined activity here as A = kg PE/(g Zr·[ethylene]·hr) utilizing the saturated concentration of ethylene in the diluent rather than the absolute pressure of ethylene in the reactor headspace in order to account for monomer solubility differences due to diluent type and reaction temperature. The saturated concentration of ethylene in the diluent toluene was estimated by the published data (Gerrard, 1980) and was confirmed by the measured values for various partial pressures of ethylene in the reactor headspace. Figure 2.2(B) shows how the average catalyst activity is affected by the ethylene concentration. An increase in ethylene concentration was found to lead to an increase in catalyst activity over the range of 0.03 - 0.26 mol/L (5-50 psia). Using this definition of activity, an increase in ethylene concentration, with other variables held constant, should not affect catalyst activity. A discrepancy from this indicates that the polymerization rate may be mass transfer limited.

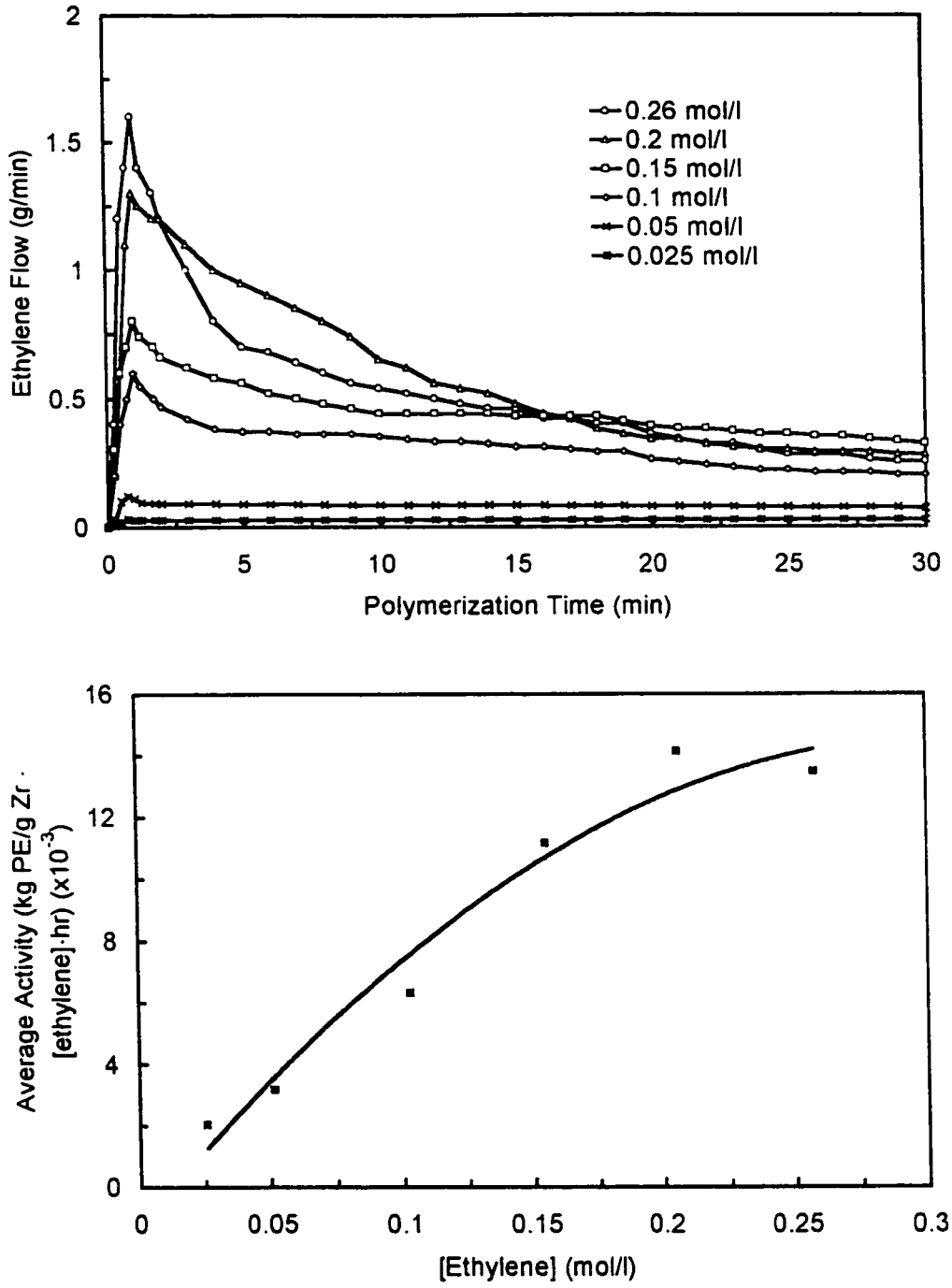

Figure 2.2 Effect of the ethylene concentration in toluene on (A) polymerization rate-time curves, (B) catalyst activity (kg PE/(g Zr·[ethylene]·hr)). The polymerization conditions were: T = 70 °C, $[Cp_2ZrCl_2]$ = 0.7 μM, Al/Zr = 1600.

Figure 2.3(A) illustrates the relationship between ethylene concentration and the PE MWs produced (M_n, M_w and M_z). The PE MWs increase significantly with increasing monomer concentration over the range 0.03-0.1 mol/L (5-20 psia), then level off and become independent of concentration up to the maximum concentration studied, 0.26 mol/L (50 psia). Figure 2.3(B) illustrates the relationship between ethylene concentration and PE PDIs which are observed to decrease essentially linearly with increasing ethylene concentration over the range studied, approaching the values of Flory's most probable distribution of M_w/M_n = 2.0 and M_z/M_w = 1.5 for a single site-type catalyst.

In addition to the diffusion limitation of monomer with this highly active catalyst, it is clear from the experimental observations that chain transfer to ethylene is a significant termination mechanism and cannot be ignored in kinetic analysis, particularly at high ethylene concentrations. If the chain transfer to monomer were not significant, any change in the ethylene concentration would result in different PE MWs. However, the PE MWs remain unchanged with increasing ethylene concentration in the range of 0.1-0.26 mol/L (refer to Figure 2.3(A)).

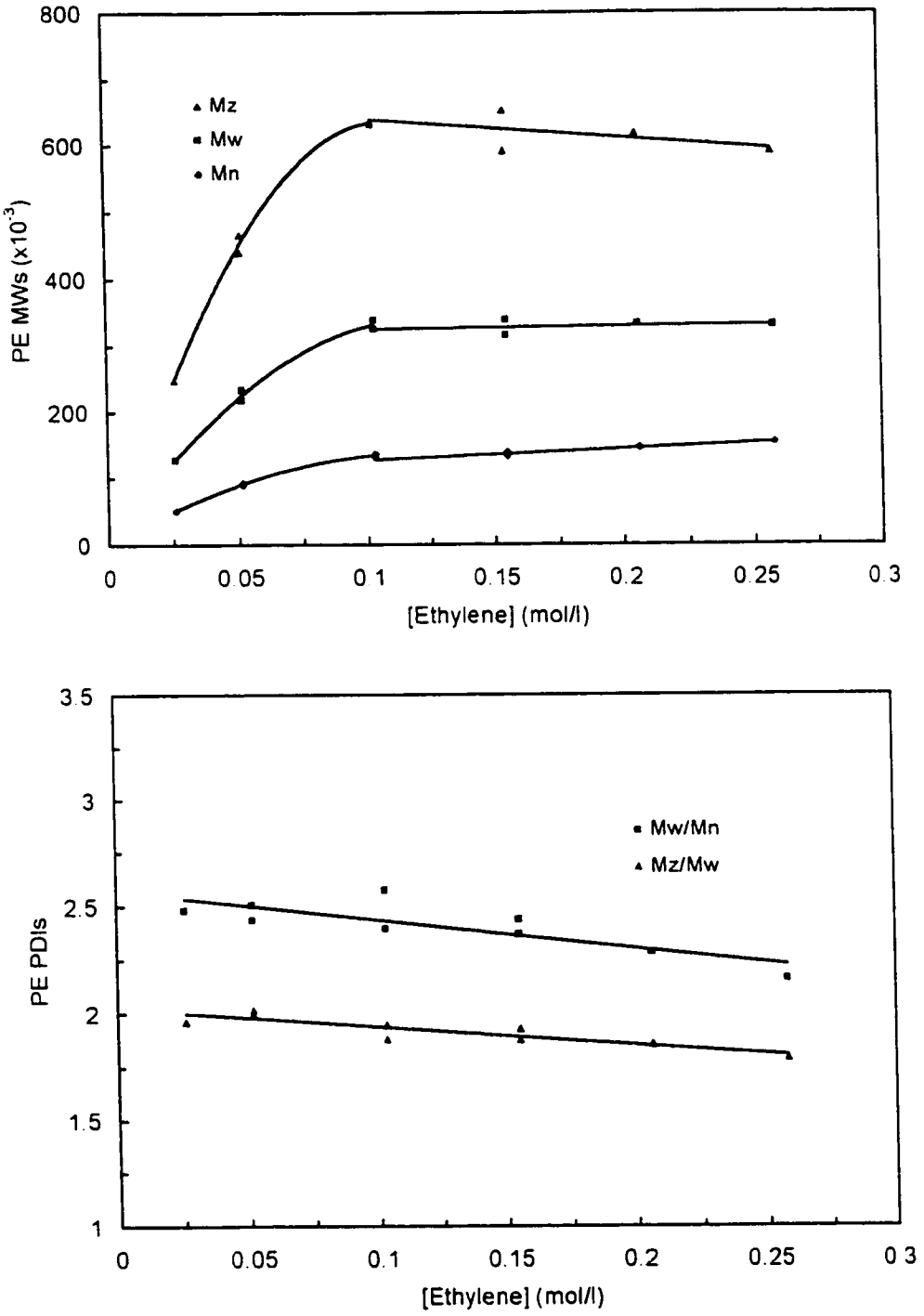

Figure 2.3 Effect of the ethylene concentration in toluene on (A) PE MWs and (B) PE PDIs. The polymerization conditions were: T = 70 °C, [Cp_2ZrCl_2] = 0.7 μM, Al/Zr = 1600.

2.4.2 *Effect of Impeller Type on Ethylene Polymerization*

Four different impellers were studied as to their effect on the polymerization of ethylene. These are: a) 1.25" turbine (d/D = 0.42); b) 1.75" turbine (d/D = 0.58); c) Autoclave Engineers 1.25" dispersimax (d/D = 0.42) and d) Autoclave Engineers 2" dispersimax. (d/D = 0.67). The two turbine impellers studied gave little to no ethylene sparging in the reactor so mass transfer of monomer was limited to diffusion through the diluent from the reactor headspace. The dispersimax impellers were able to give dispersimax action or ethylene sparging to the reactor by transfer of gas from a hole in the agitator shaft located in the reactor headspace through the impeller as illustrated schematically in Figure 2.4. The 2" dispersimax impeller utilized an RPM of 1200 whereas the other agitators utilized an agitator RPM of 1500.

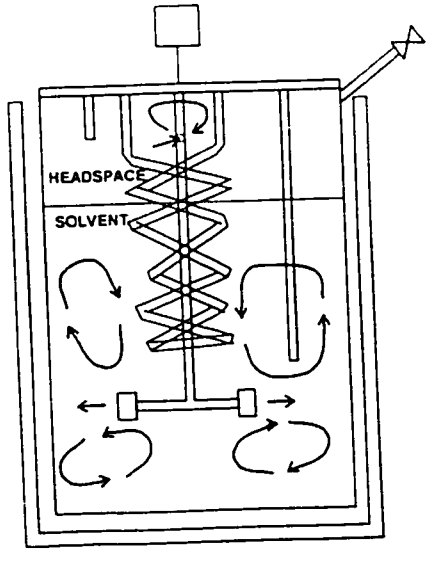

Figure 2.4 Schematic of the interior of the reactor with sparging provided by an Autoclave Engineers Dispersimax impeller.

Figure 2.5(A) gives the rate-time curves for these four different agitators in the polymerization of ethylene. It is apparent that the impeller and ethylene sparging were very important for uptake of ethylene by the catalyst which indicates that the polymerizations were mass-transfer limited. Figure 2.5(B) gives both the maximum and average activities of the Cp_2ZrCl_2/MAO catalyst system for the different impellers studied. The maximum activity is calculated using the maximum from the rate-time curves while the average activity is calculated from the total weight of polymer collected for a given polymerization time (both in units of kgPE/(gZr·[ethylene]·hr). The ethylene sparging in the reactor provided by the dispersimax impeller configuration yielded higher uptake of monomer by the catalyst than that by the turbine impellers. For both turbine and dispersimax impellers the larger diameters gave higher R_p curves. The larger diameter of the impeller (higher d/D value) gives better mixing in the viscous polymerization medium and hence better mass transfer of monomer to the catalytically active site types. It is clear that the 2" dispersimax impeller gave the least monomer diffusion limited system of the various impellers studied.

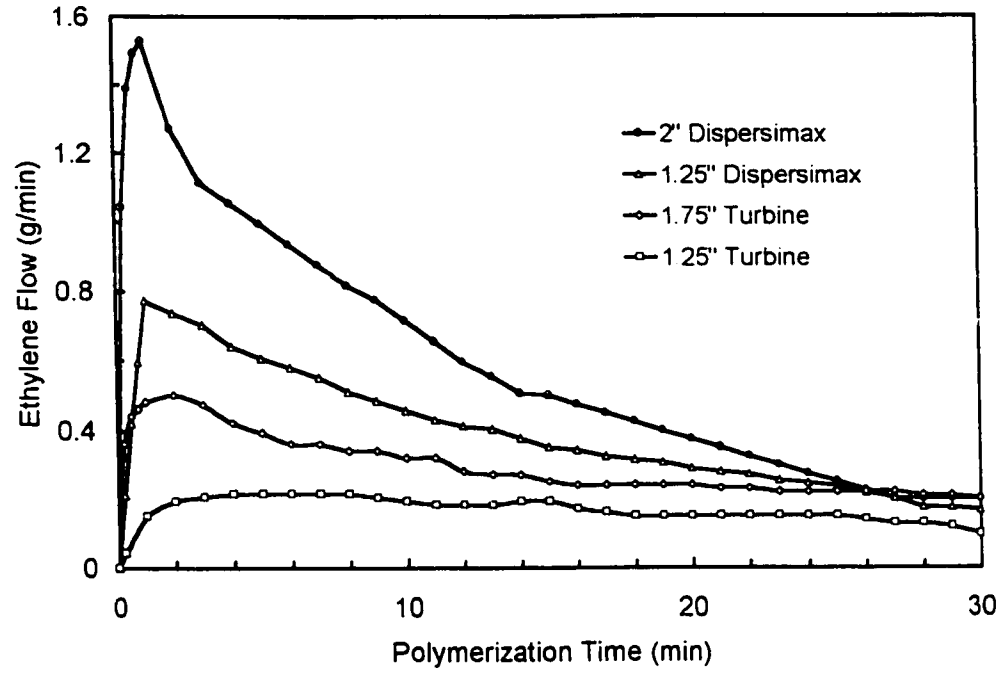

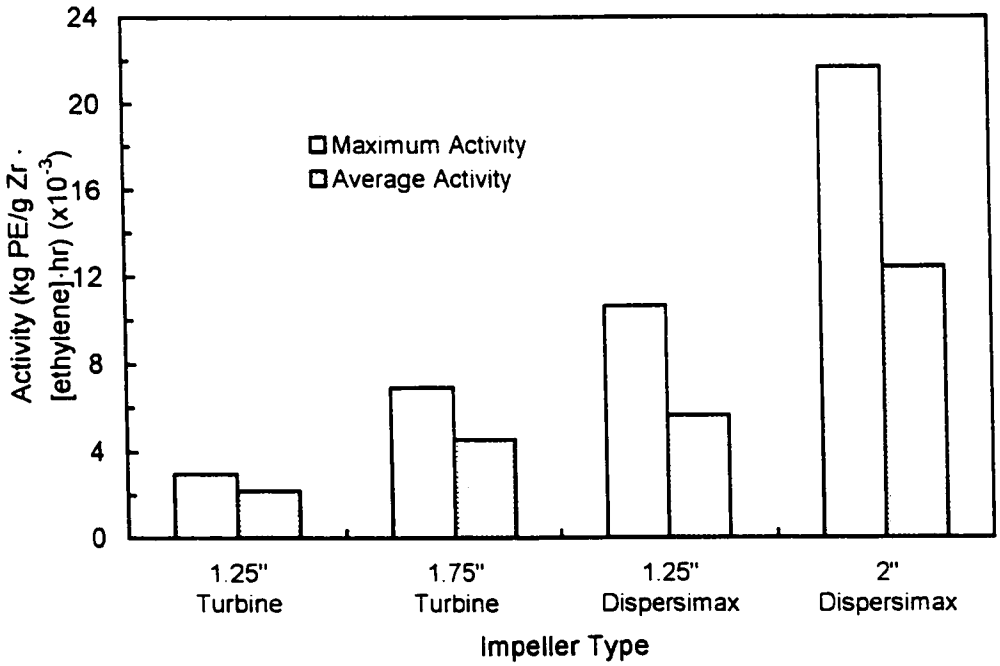

Figure 2.5 Effect of the impeller type on (A) polymerization rate-time curves, (B) catalyst activity (kg PE/(g Zr·[ethylene]·hr)). The polymerization conditions were: T = 70 °C, $[Cp_2ZrCl_2]$ = 0.7 μM, Al/Zr = 1600, [ethylene] = 0.1 mol/L.

Figure 2.6(A) gives the PE MWs for the four different agitators studied. There is a slight increase in the MWs for the dispersimax impellers which provide superior sparging of monomer in the reactor and decrease any mass transfer limitation. Figure 2.6(B) illustrates that the PDIs are not significantly affected by the agitator and approximate those predicted from Flory's most probable distribution. The 1.25" Dispersimax does give a slightly higher M_w/M_n than the other agitators which may be caused by the higher polymerization rate R_p due to the ethylene sparging but lack of mixing of the larger d/D value which causes greater monomer and temperature gradients in the reactor.

2.4.3 *Effect of Zirconocene Dichloride Concentration on Ethylene Polymerization*

Figure 2.7 illustrates the relationship between catalyst concentration and average activity. It is clear that the catalyst activity decreases rather significantly with increasing catalyst concentration. This decrease of activity is attributed to the active site-types being starved for monomer with this high activity catalyst. Figure 2.8(A) shows how the PE MWs decrease significantly with increasing catalyst concentration which is also indicative that the catalyst site types are starved for monomer. Figure 2.8(B) shows that PE PDIs generally increase slightly with increasing catalyst concentration.

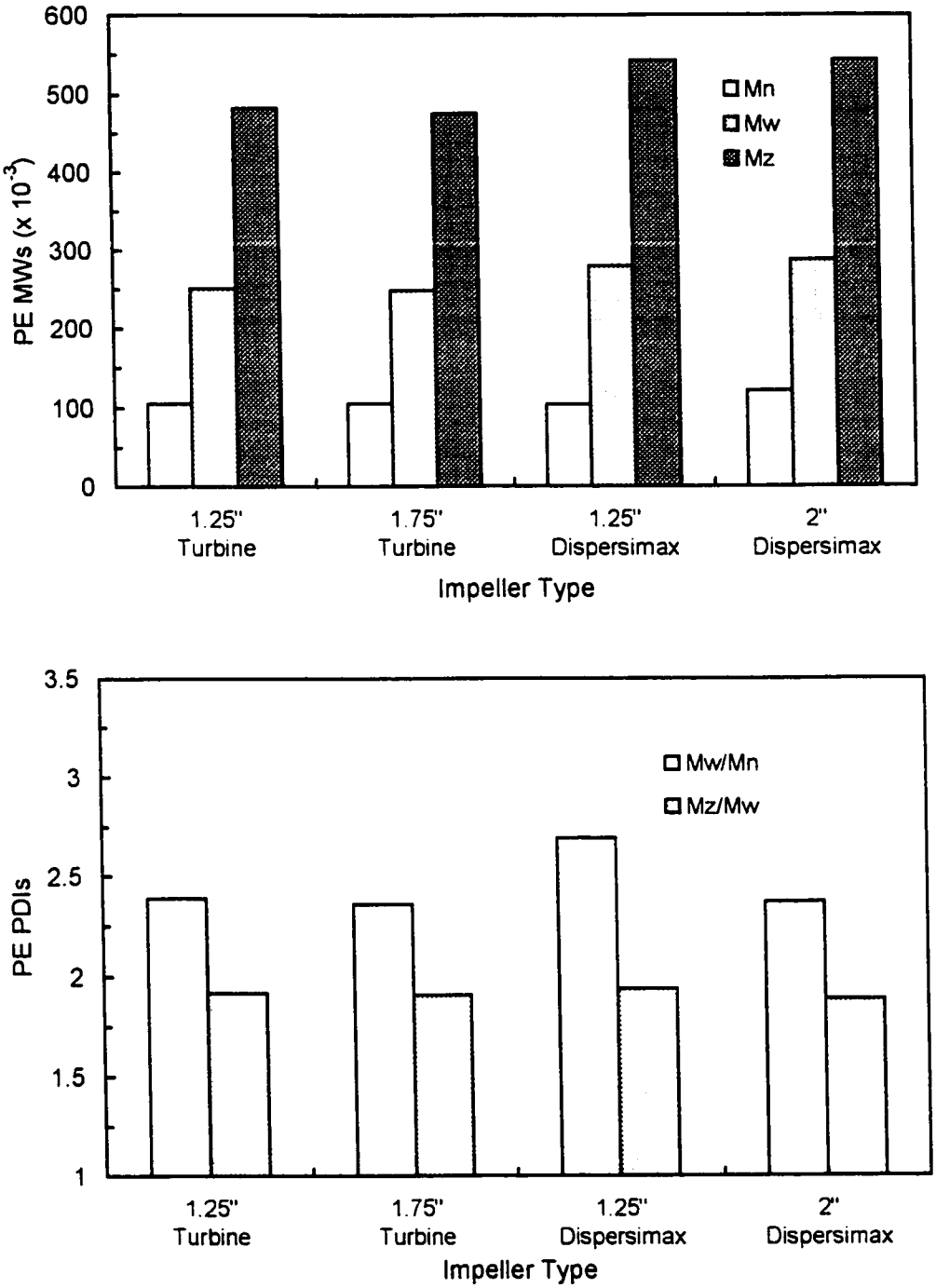

Figure 2.6 Effect of the impeller type on (A) PE MWs and (B) PE PDIs. The polymerization conditions were: T = 70 °C, [Cp_2ZrCl_2] = 0.7 μM, Al/Zr = 1600, [ethylene] = 0.1 mol/L.

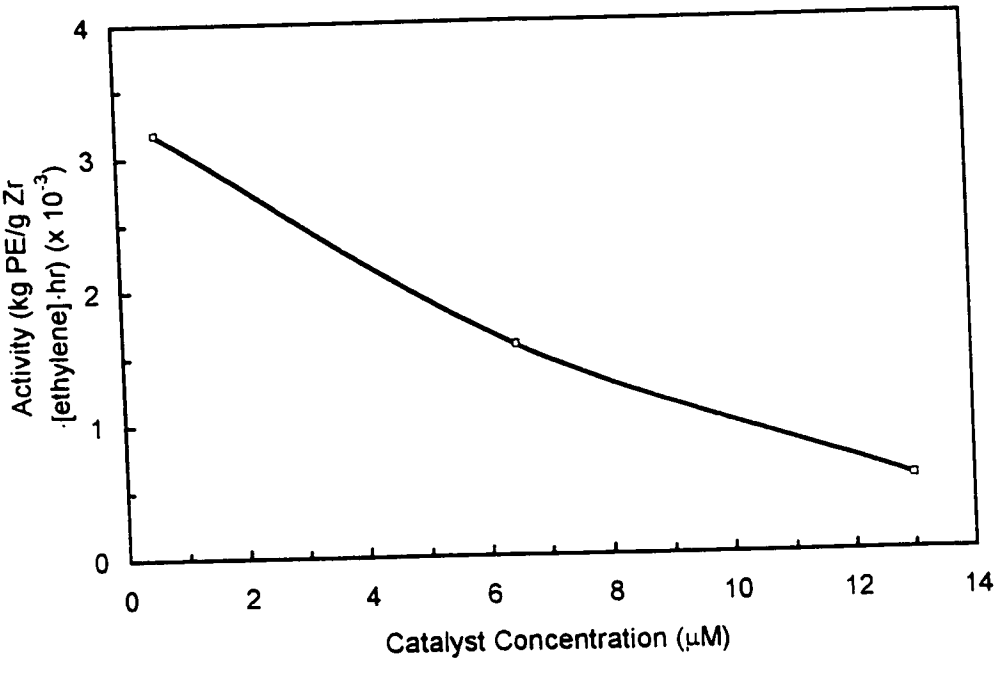

Figure 2.7 Effect of the Cp_2ZrCl_2 catalyst concentration on catalyst activity (kg PE/(g Zr·[ethylene]·hr)). The polymerization conditions were: T = 70 °C, Al/Zr = 1600, [ethylene] = 0.05 mol/L.

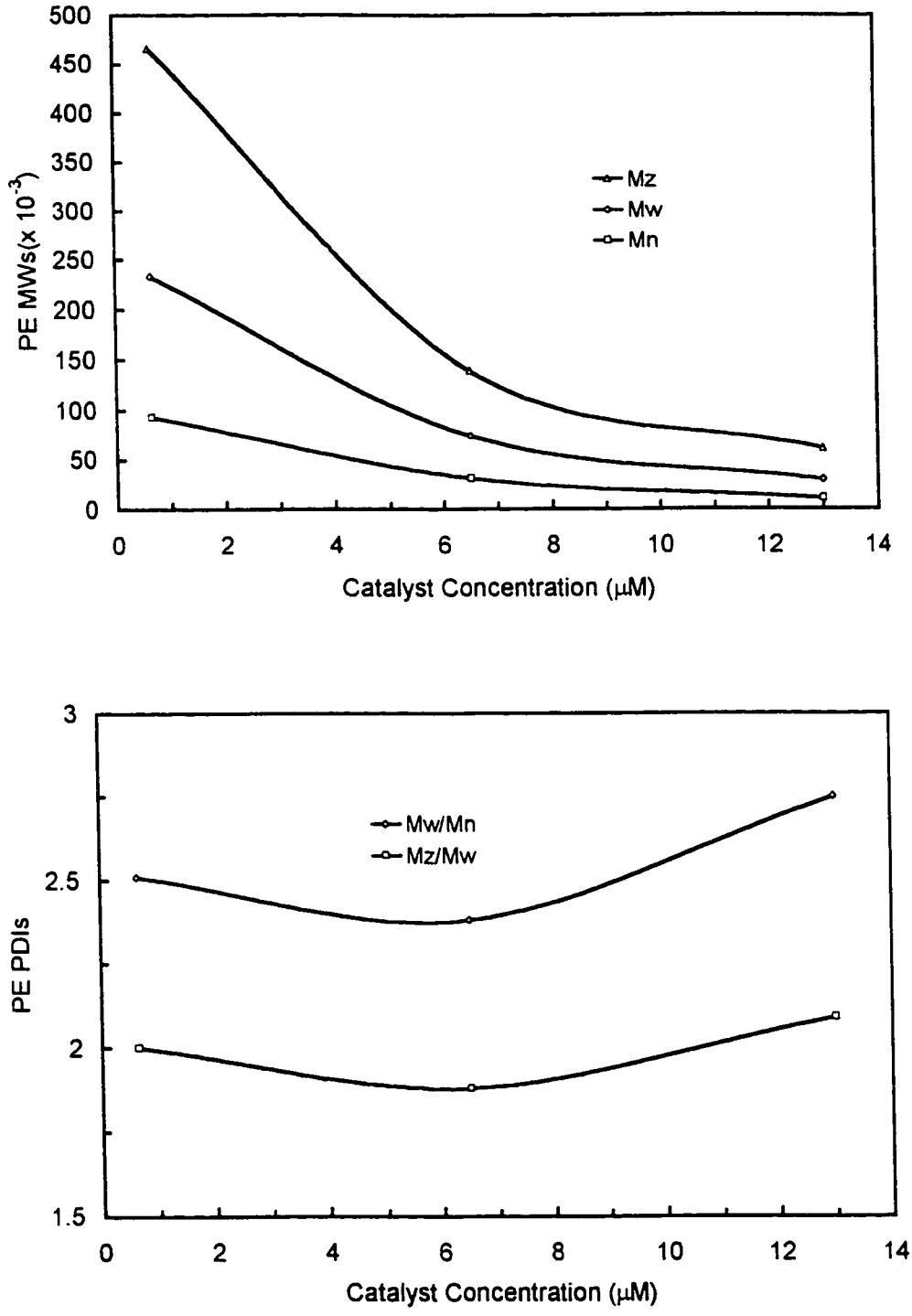

Figure 2.8 Effect of the Cp_2ZrCl_2 catalyst concentration on (A) PE MWs and (B) PE PDIs. The polymerization conditions were: T = 70 °C, Al/Zr = 1600, [ethylene] = 0.05 mol/L.

2.4.4 *Effect of Temperature on Ethylene Polymerization*

The effect of temperature on ethylene polymerization utilizing Cp_2ZrCl_2/MAO in toluene has been investigated under two different experimental conditions i.e. high and low monomer diffusion limitation conditions. For the high monomer diffusion limitation condition (low monomer concentration, high Cp_2ZrCl_2 concentration and 1.25" dispersimax), Figure 2.9(A) gives the rate-time curves for various polymerization temperatures. The rate was highest at 70 °C where a steady-state value was reached. The rate-time curves were similar for 50 and 90 while for 20 °C the rate was much lower. Figure 2.9(B) gives the activity versus temperature curve for polymerization temperatures between 10-90 °C where we see that the average activity increases almost linearly with increasing polymerization temperature. As the temperature increases, the ethylene concentration in toluene decreases (under a constant ethylene pressure in the reactor headspace) which is accounted for in this definition of activity. Figure 2.9(B) also gives an alternative activity versus temperature curve where we replace ethylene concentration with ethylene pressure and we see that a maximum in the curve appears at 70 °C which is what we would expect based on the rate-time curves. Figure 2.10(A) illustrates how increasing polymerization temperatures decrease PE MWs significantly while Figure 2.10(B) shows how increasing polymerization temperatures generally decreases PE PDIs. Notice for this high diffusion limited condition that the variability in the PE PDIs is quite significant.

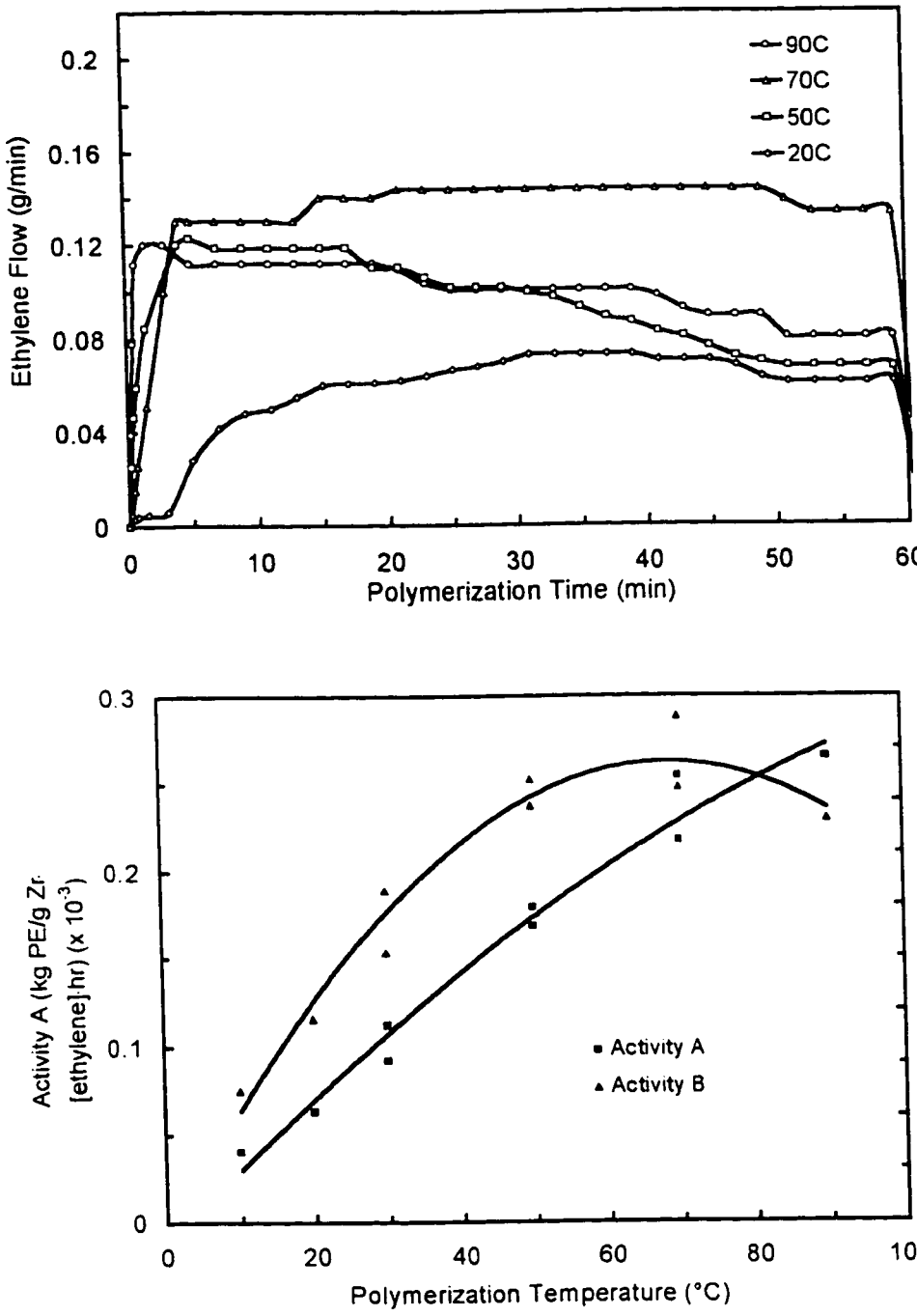

Figure 2.9 Effect of the polymerization temperature on (A) polymerization rate-time curves, (B) catalyst activity (A = kg PE/(g Zr·[ethylene]·hr)) and (B = kg PE/g Zr·atm ethylene·hr)). The polymerization conditions were: $[Cp_2ZrCl_2]$ = 13 μM, Al/Zr = 1600, [ethylene] = 0.05 mol/L, impeller type = 1.25" Dispersmax.

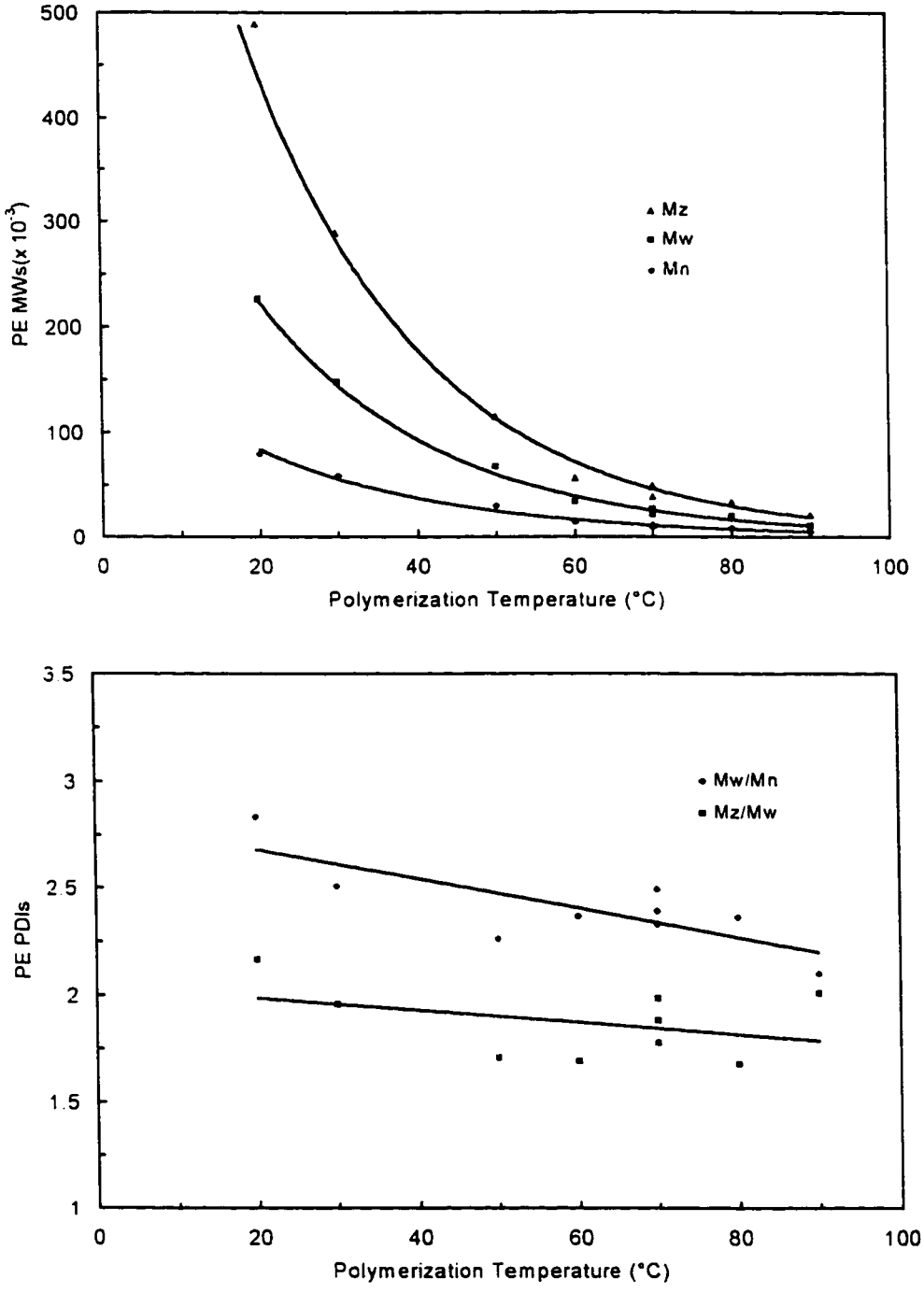

Figure 2.10 Effect of the polymerization temperature on (A) PE MWs and (B) PE PDIs. The polymerization conditions were: [Cp_2ZrCl_2] = 13 μM, Al/Zr = 1600, [ethylene] = 0.05 mol/L, impeller type = 1.25" Dispersmax.

For ethylene polymerization under minimal monomer diffusion limitation conditions (high monomer concentration, low Cp_2ZrCl_2 concentration and 2" dispersimax), three temperatures from 50-90 °C were investigated. Figure 2.11(A) gives the polymerization rate-time curves for these three polymerization temperatures. All three temperatures gave an immediate maximum (less than 1 minute) with a sharp decay in the rate-time curves which was sharpest for 70 °C which had the highest initial rate of polymerization. Figure 2.11(B) gives the activity versus temperature curves. Again we see a maximum for activity around 70 °C. Figure 2.12(A) illustrates how increasing polymerization temperatures decrease PE MWs essentially linearly over the temperature range 50-90 °C. Figure 2.12(B) shows that increasing polymerization temperature linearly decreases the PE PDIs towards the limit of Flory's most probable distribution with M_w/M_n = 2.0 and M_z/M_w = 1.5. The decrease in the PE PDIs with increasing temperature is believed to be due to a lower apparent viscosity of the reaction mixture from the higher polymerization temperature which provides a more uniform polymerization medium with lower mass and heat transfer gradients.

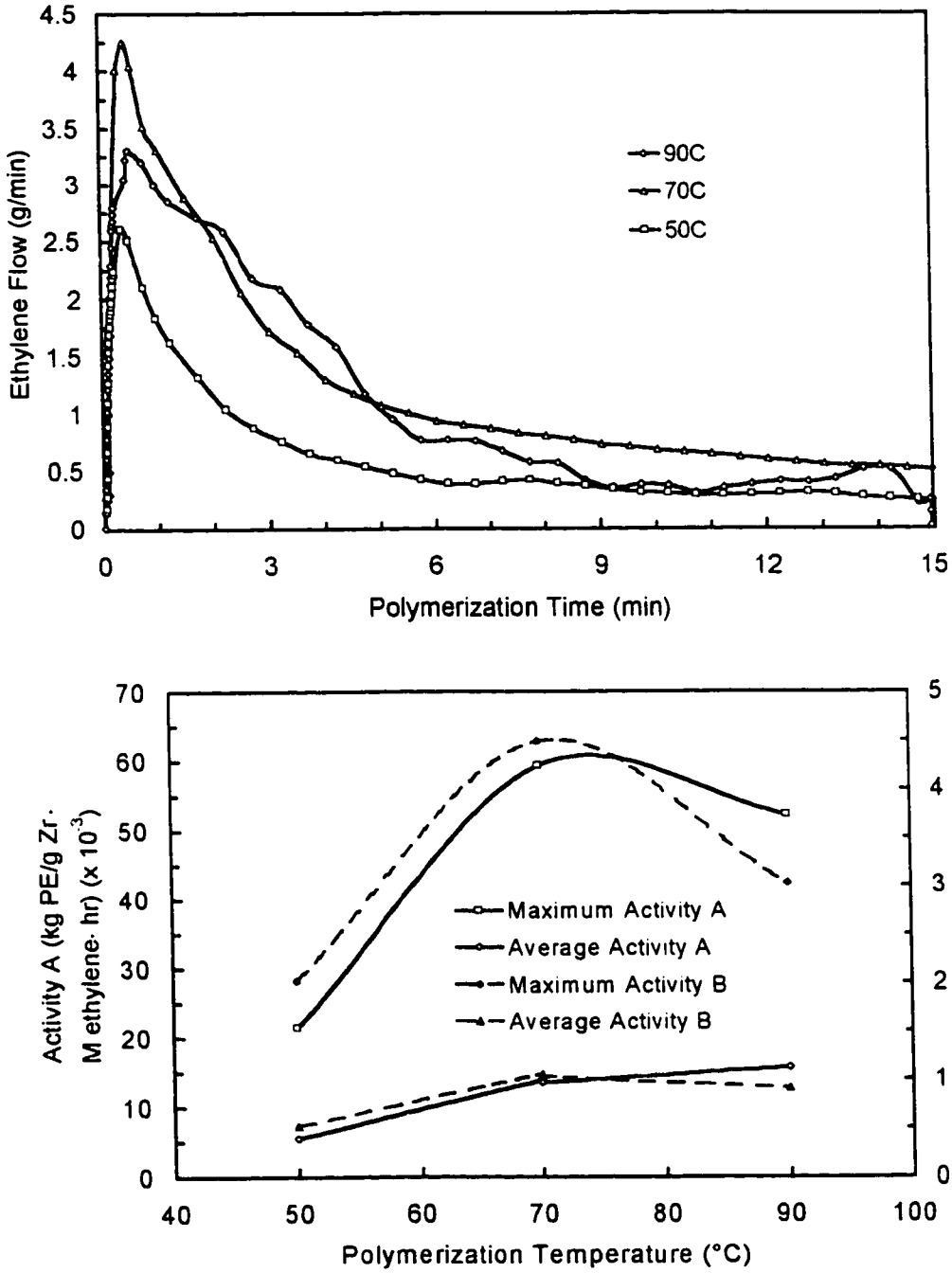

Figure 2.11 Effect of the polymerization temperature on (A) polymerization rate-time curves, (B) catalyst activity (A = kg PE/(g Zr·[ethylene]·hr)) and (B = kg PE/g Zr·atm ethylene·hr)). The polymerization conditions were: $[Cp_2ZrCl_2]$ = 0.65 μM, Al/Zr = 1600, [ethylene] = 0.18 mol/L, impeller type = 2" Dispersmax.

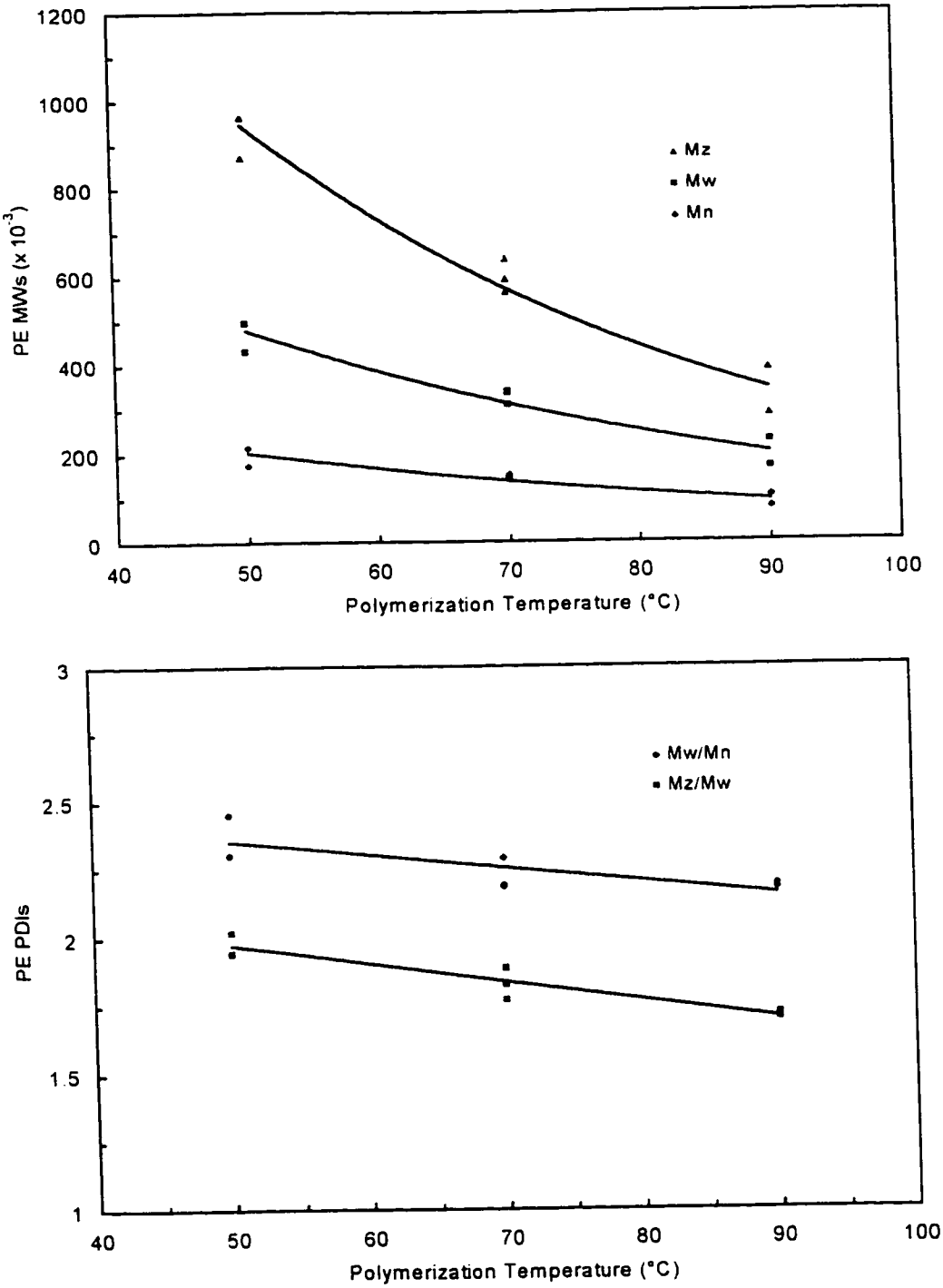

Figure 2.12 Effect of the polymerization temperature on (A) PE MWs and (B) PE PDIs. The polymerization conditions were: [Cp_2ZrCl_2] = 0.65 μM, Al/Zr = 1600, [ethylene] = 0.18 mol/L, impeller type = 2" Dispersmax.

Changing the polymerization temperature affects several conditions in the reactor, notably changing the monomer concentration. We have shown above that the polymerization of ethylene with Cp_2ZrCl_2/MAO in toluene is sensitive to monomer concentration, particularly in the low concentration range. The change in PE MWs with temperature will be most affected under the first set of conditions with a lower monomer concentration and a higher catalyst concentration which we have shown to be significantly diffusion limited. Another significant problem with studying the effects in the homogeneous semi-batch polymerization of ethylene is the change in apparent viscosity of the polymerization medium with temperature. The lower polymerization temperatures cause extremely high apparent viscosity. This can lead to problems with local monomer and temperature gradients in the reactor. Even with the above reservations, it is clear that metallocene polymerization of ethylene with Cp_2ZrCl_2/MAO is sensitive to the polymerization temperature and that τ (termination/propagation ratio) increases with increasing temperature.

2.4.5 Effect of Length of Polymerization Time on Ethylene Polymerization

For the polymerization of ethylene with Cp_2ZrCl_2/MAO in toluene at 70 °C, the effects of the length of the polymerization time on the PE MWs and PDIs, before quenching by addition of methanol and removal of monomer by venting, are given in Figures 2.13(A) and (B). It is clear that the length of the polymerization time is not significantly affecting the PE MWs and PDIs under these conditions

and that chain transfer to polymer is not a significant termination mechanism or the PE MWs would be decreasing as the polymer/active site ratio in the reactor increases with time.

2.4.6 Effect of Hydrogen on Ethylene Polymerization

In Figure 2.14(A) we see the rate-time curves for the polymerization of ethylene with increasing concentrations of hydrogen in the polymerization medium while Figure 2.14(B) gives the activity versus the concentration of hydrogen. The concentration of hydrogen in the diluent was estimated from published data for various partial pressures of hydrogen in the reactor headspace (Gerrard, 1980). It is clear from these results that hydrogen does decrease the polymerization rate of the Cp_2ZrCl_2/MAO catalyst significantly. This is consistent with the idea that the chain transfer reaction by hydrogen occurs as shown in Equation (1) and that the metallocene hydride product is less reactive to insertion of monomer (as shown in Equation (2)) than the active metallocene alkyl form of the metallocene catalyst (Jordan, 1988).

$$\text{cat-P} + H_2 \rightarrow \text{cat-H} + \text{PH} \qquad (1)$$

$$\text{cat-H} + \text{M} \rightarrow \text{cat-P} \qquad (2)$$

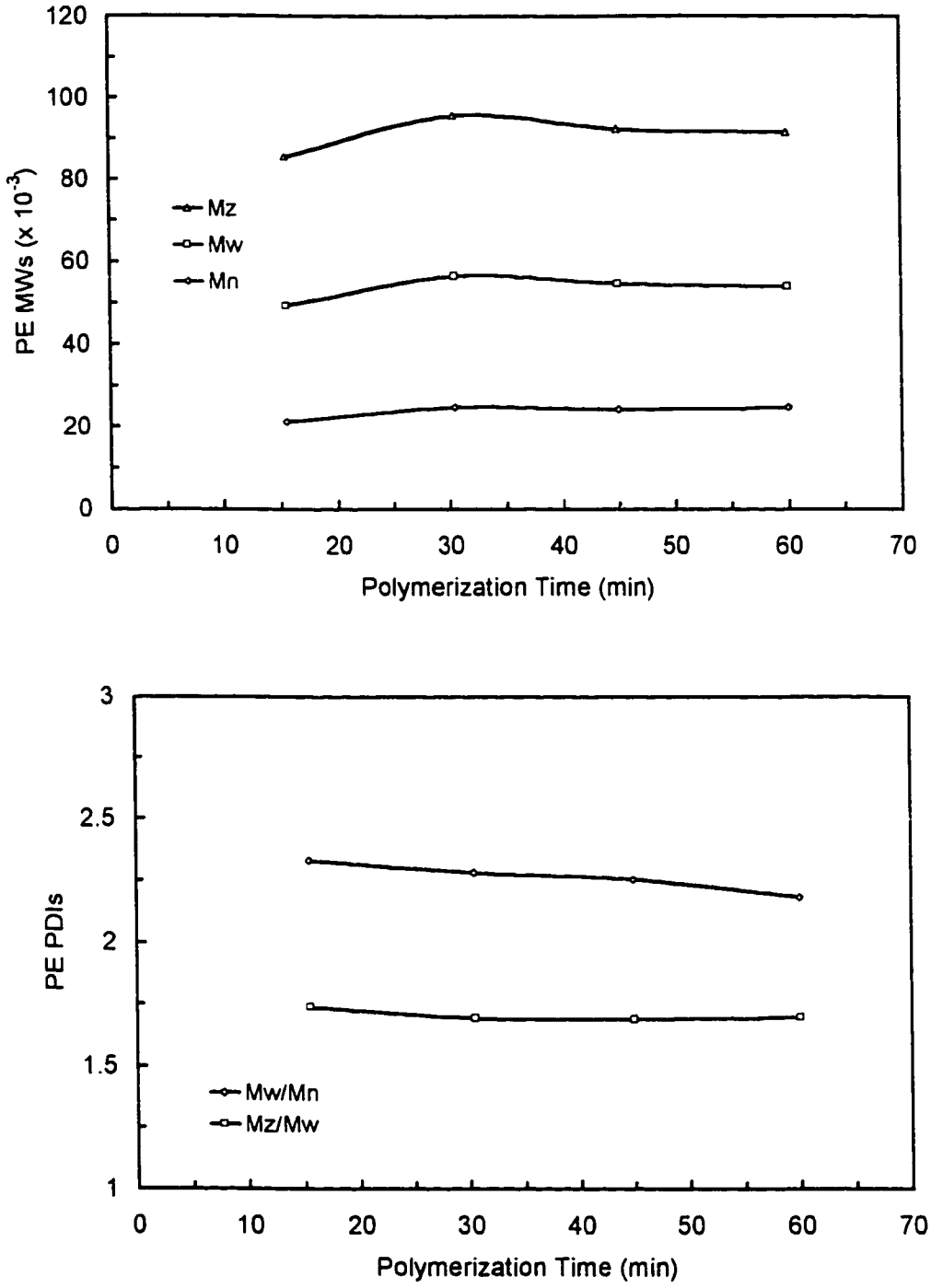

Figure 2.13 Effect of the length of polymerization on (A) PE MWs (B) PE PDIs. The polymerization conditions were: T = 70 °C, [Cp_2ZrCl_2] = 13 μM, Al/Zr = 1600, [ethylene] = 0.05 mol/L.

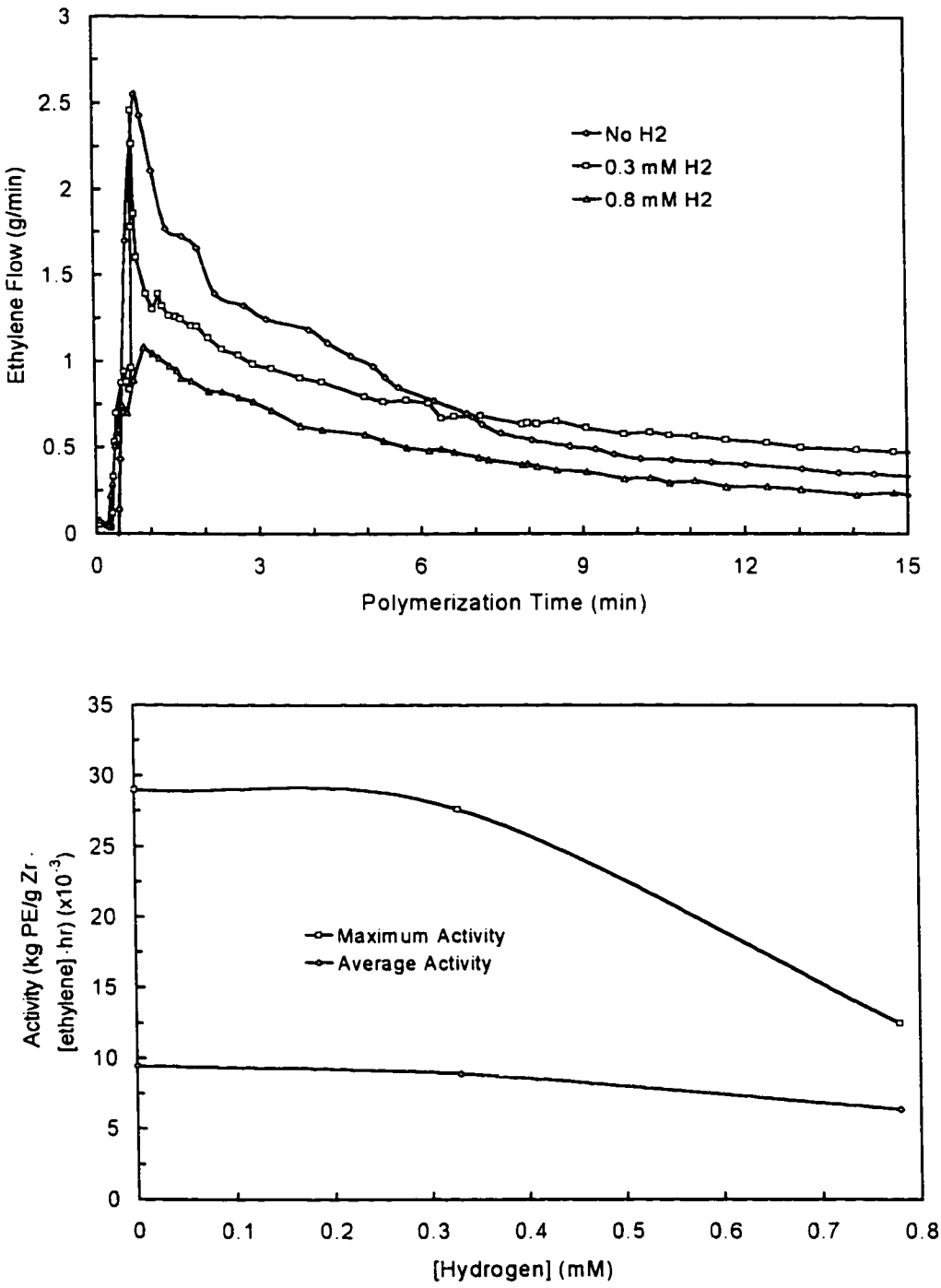

Figure 2.14 Effect of the hydrogen concentration on (A) polymerization rate-time curves, (B) catalyst activity (kg PE/(g Zr·[ethylene]·hr)). The polymerization conditions were: T = 70 °C, $[Cp_2ZrCl_2]$ = 0.65 μM, Al/Zr = 1600, [ethylene] = 0.18 mol/L.

Although the metallocene hydride product is less reactive to insertion of monomer than the active alkyl form of zirconocene, less extreme levels of hydrogen should not lower the catalyst activity significantly for the polymerization of ethylene. In practice, much lower levels of hydrogen would be used for controlling the MWs of ethylene polymers produced by metallocene catalysts (< 0.1 %) (Lai et al, 1993).

We see in Figure 2.15(A) that hydrogen at these overly high levels led to a drastic lowering of PE MWs. Figure 2.15(B) gives the PE PDIs produced with increasing amounts of hydrogen. Note the lowering of M_w/M_n very close to the limiting value of 2.0 for Flory's most probable distribution. This slight lowering of M_w/M_n may be due to the low PE MWs which give a much lower apparent viscosity to the reaction mixture so temperature gradients and monomer gradients within the reactor are more uniform. From these results it is clear that the polymerization of ethylene with Cp_2ZrCl_2 using hydrogen as a chain transfer agent obeys Flory's most probable distribution and does not increase the PE MWD or increase the number of active site types.

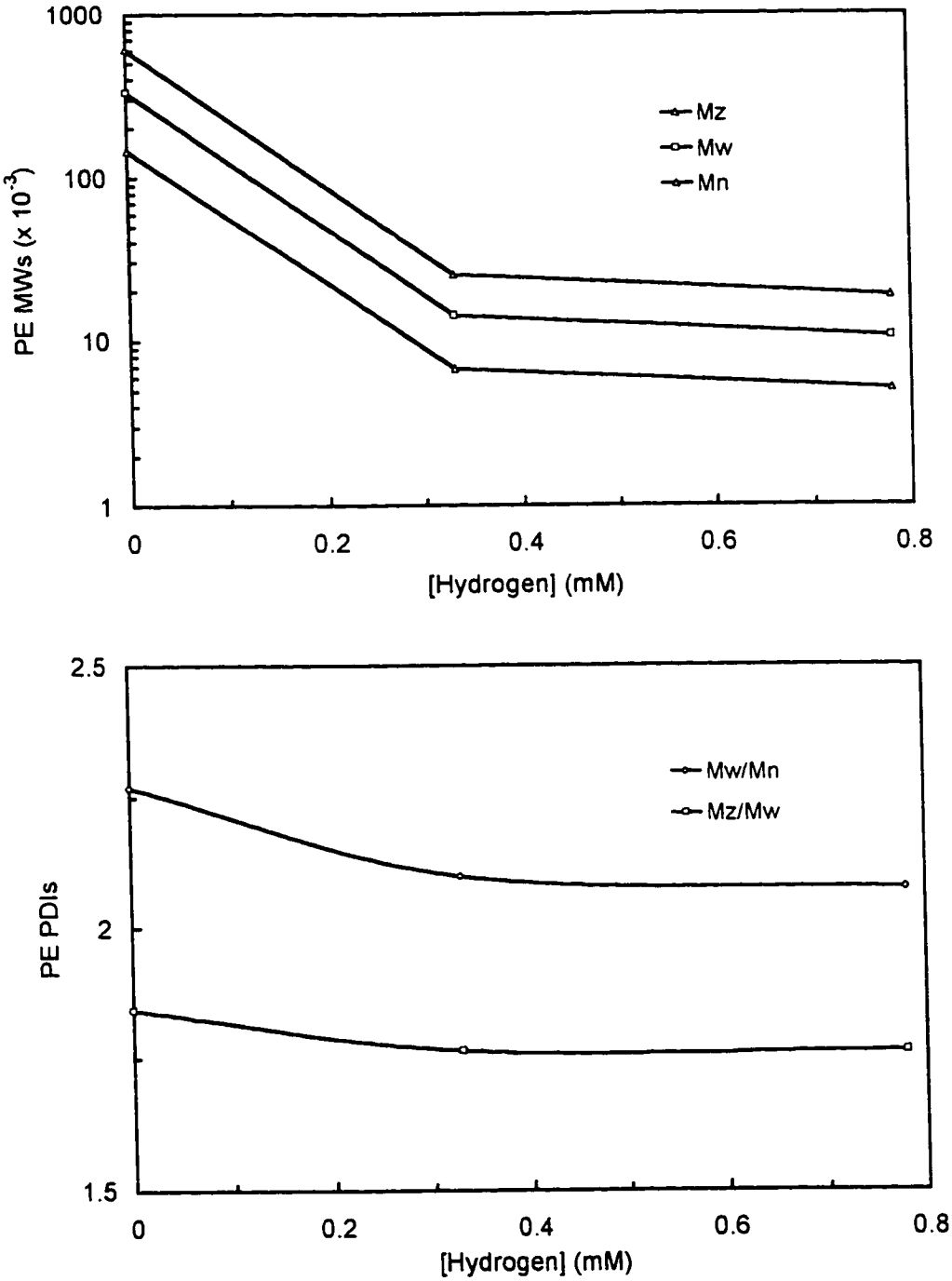

Figure 2.15 Effect of the hydrogen concentration on (A) PE MWs and (B) PE PDIs. The polymerization conditions were: T = 70 °C, $[Cp_2ZrCl_2]$ = 0.65 μM, Al/Zr = 1600, [ethylene] = 0.18 mol/L.

2.4.7 *Effect of Octene-1 Comonomer on Ethylene Polymerization*

Figure 2.16 shows the rate-time curves for different copolymerizations containing octene-1 comonomer in the reaction mixture. The added octene gives a slightly higher initial rate of polymerization which is maintained throughout the copolymerization compared to homopolymerization of ethylene which shows a rapid decay in the rate-time curve. The lower concentration of comonomer was found to give a higher initial and sustained rate. This rate enhancement and closer behavior to steady-state effect is believed to be due to the effect of the comonomer which when incorporated into a polyethylene chain to give a short chain branch (SCB), prevents precipitation of the LLDPE chains. Precipitation of the PE chains may reduce the concentration of active sites in solution in the homopolymerization of ethylene.

Figure 2.17 gives the DSC traces of the ethylene-octene copolymers which give a single sharp peak illustrating that the chemical composition distribution (CCD) of the copolymer is quite uniform corresponding to that predicted by Stockmayer's bivariate distribution. The single sharp peak is also indicative of a single catalytic site-type for this metallocene catalyst.

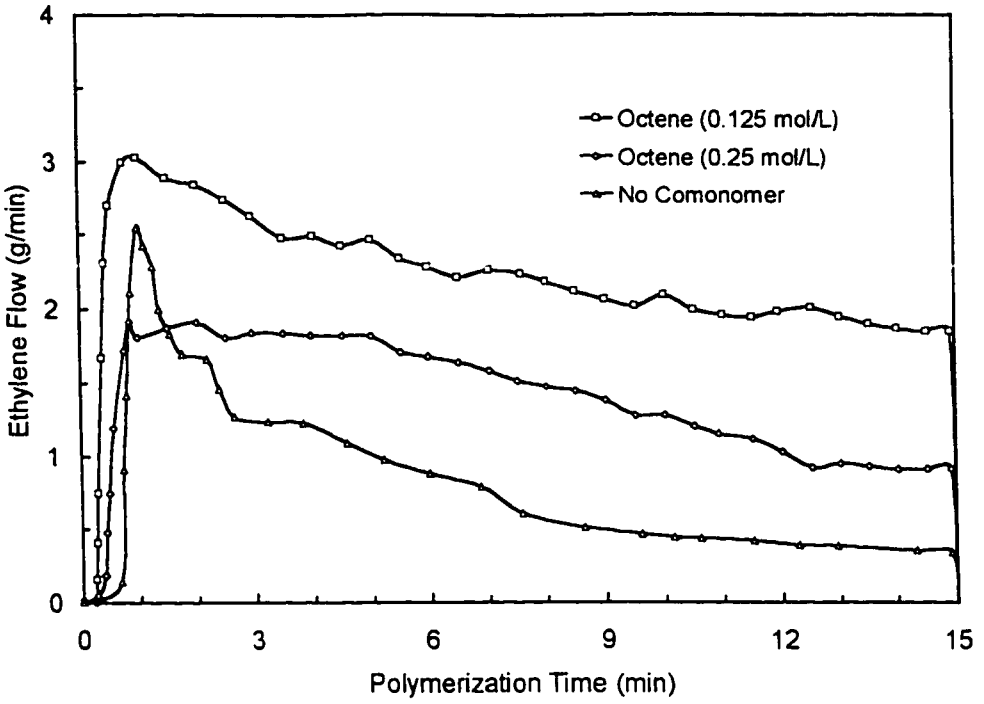

Figure 2.16 Effect of octene-1 on the polymerization rate-time curves. The polymerization conditions were: T = 70 °C, $[Cp_2ZrCl_2]$ = 0.7 μM, Al/Zr = 1600, [ethylene] =0.18 mol/L.

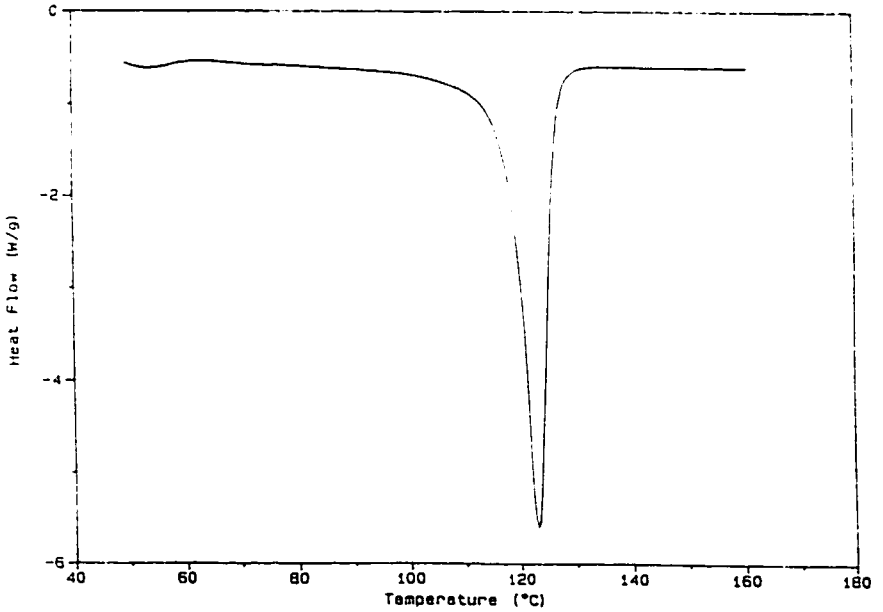

Figure 2.17 DSC Curve of ethylene-octene copolymer. The polymerization conditions were the same as Figure 2.16.

2.4.8 *Effect of Transition Metal of Metallocene Dichloride on Ethylene Polymerization*

In Figure 2.18 we see the rate-time curves for the polymerization of ethylene at 70 °C with the three metallocene dichloride catalysts: Cp_2TiCl_2, Cp_2ZrCl_2, and Cp_2HfCl_2. For the activity of the catalyst; $Cp_2ZrCl_2 >> Cp_2HfCl_2 > Cp_2TiCl_2$ with only the zirconium analog giving significant activity at 70 °C. Figures 2.19(A) and (B) give the PE MWs and PDIs for the three different metallocene dichloride catalysts. Going down Group IVB of the Periodic Table from Ti to Zr to Hf led to significant increases in PE MWs and a slight increase in the PDIs of the formed PE although all of these catalysts appear to approximate Flory's most probable distribution for a single site-type catalyst. The effect on PE MWs indicates that the transition metal has a significant effect on the termination/propagation ratio τ and the higher the atomic number of the transition metal of Group IVB, the lower the value for τ.

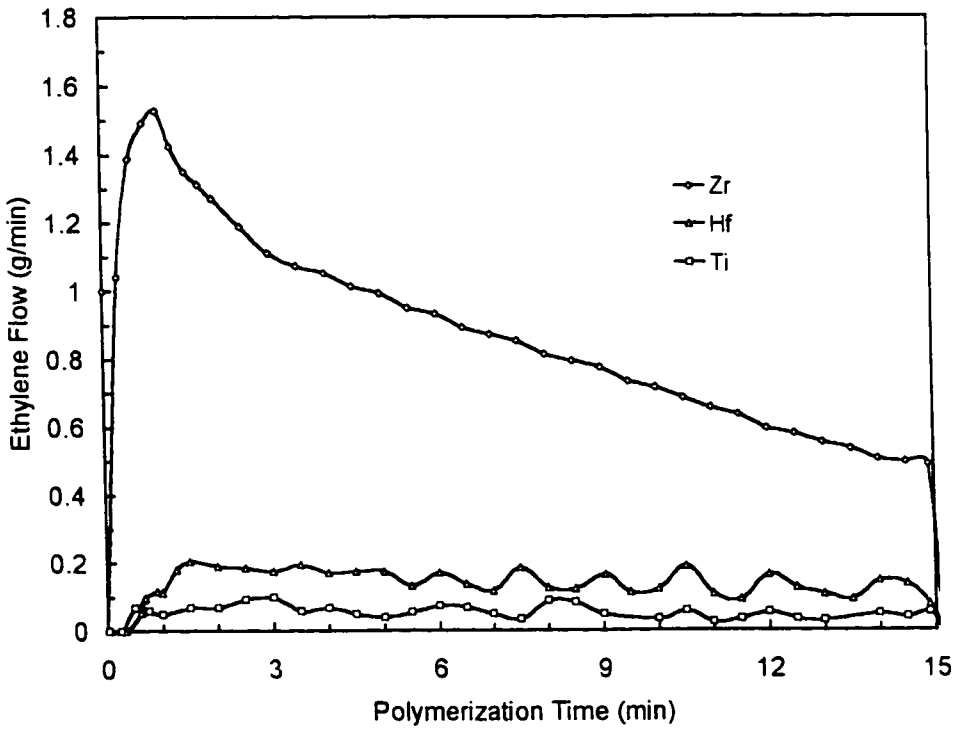

Figure 2.18 Effect of the type of metallocene dichloride transition metal on polymerization rate-time curves. The polymerization conditions were: T = 70 °C, [Cp_2ZrCl_2] = 0.65 μM, Al/Zr = 1600, [ethylene] = 0.18 mol/L.

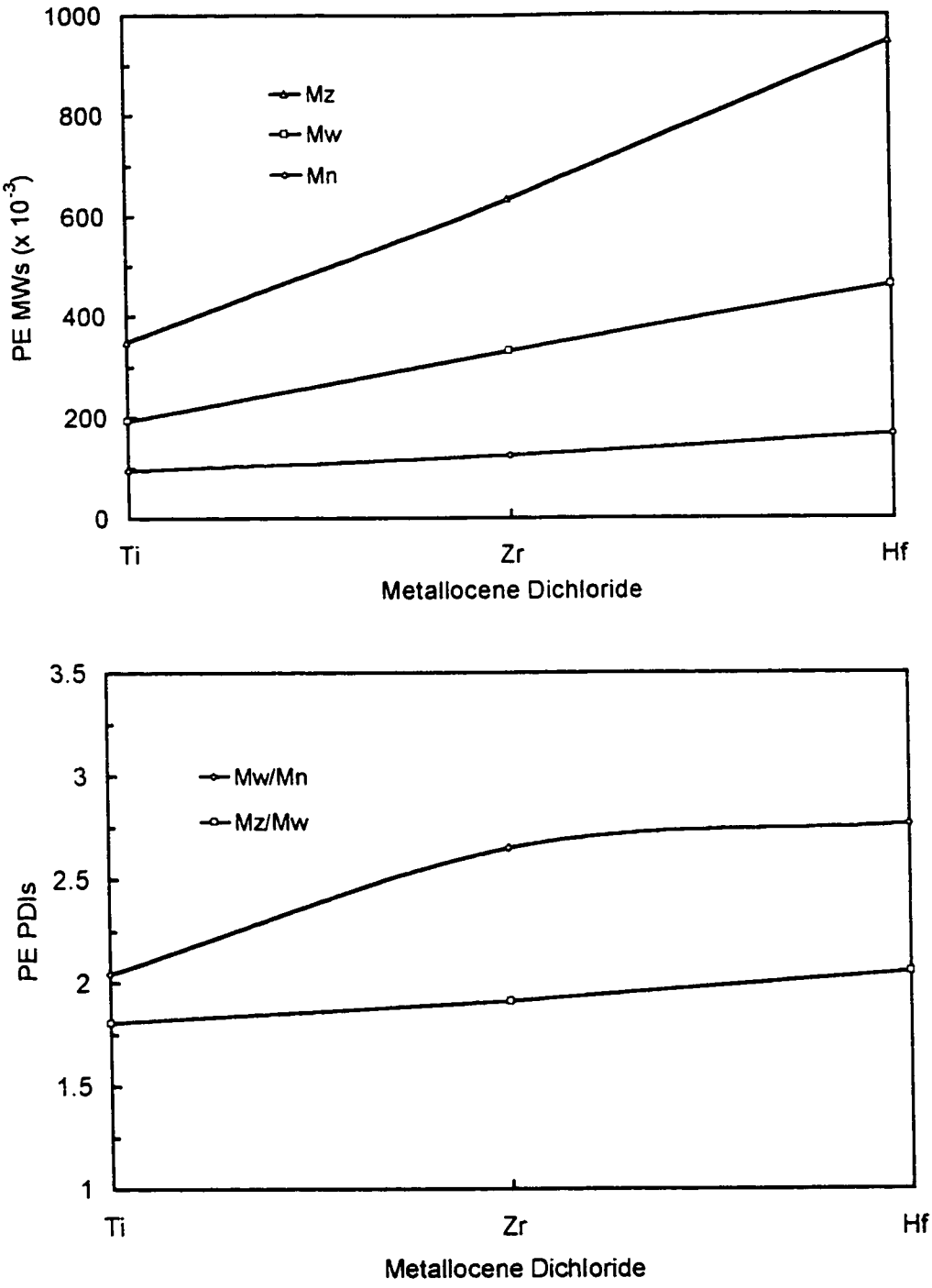

Figure 2.19 Effect of the type of metallocene dichloride transition metal on (A) PE MWs and (B) PE PDIs. The polymerization conditions were: T = 70 °C, $[Cp_2ZrCl_2]$ = 0.65 μM, Al/Zr = 1600, [ethylene] = 0.18 mol/L.

2.5 Discussion

For the Cp_2ZrCl_2/MAO catalyst system, less than 1 μmol/L of catalyst was found necessary to catalyze the polymerization of ethylene in semi-batch. This low concentration of catalyst (< 0.1 ppm compared to solvent) means that impurities in the ppm range in the solvent and monomer will lead to catalyst deactivation and hence impurities must be reduced to the ppb range to prevent significant catalyst deactivation. These impurities can never be totally removed from the solvent and monomer and it is likely that metallocene active sites are consumed to a significant extent by deactivation. The active site generated when a metallocene catalyst is activated by the co-catalyst MAO is widely believed to have a large degree of cationic behavior (Jordan, 1988). Like a carbocation in cationic polymerization, the propagating metallocene active site is very reactive and hence vulnerable to impurities in the reaction medium. For an unsupported metallocene catalyst in which the catalyst is mobile in the solution phase, the catalyst is particularly sensitive to any impurities which are also mobile in the solution phase. A supported catalyst is relatively immobile when suspended in solution and hence is much less sensitive to impurities in the solution phase. Unfortunately, the supported metallocene catalyst also gives significantly lower activity than the same non-supported catalyst due to the immobility of the catalyst on the support material.

MAO is widely believed to aid in mopping up impurities in the diluent such as H_2O and O_2 and we have found that a higher Al/Zr ratio will lead to a more reproducible polymerization (Charpentier et al. 1997). It was found necessary to lower impurity levels in the diluent down to levels where the impurity/active-site levels were sufficiently low to provide a reproducible polymerization. For these extremely high activity non-supported metallocene catalysts, polymerization problems occur as the higher the activity of the catalyst, the lower the required concentration of catalyst necessary for a highly efficient polymerization. As the catalyst concentration is decreased, the impurity/active-site ratio inevitably increases with a resultant decrease in polymerization reproducibility and activity. Thus as the catalyst becomes more active, in order to take advantage of that activity and to improve reproducibility, impurity levels in the polymerization system must be decreased by higher purity ingredients and/or increased scavenger levels.

Except for a true living polymerization, the rates of all polymerization systems change with time. Details of the change with time for a traditional heterogeneous Ziegler-Natta system normally depend on the type of catalyst and co-catalyst, type of monomer, monomer pressure and temperature. We have found that the polymerization of ethylene with Cp_2ZrCl_2/MAO, when initiated by catalyst injected into a pressurized reactor under minimal diffusion limitation conditions (good mixing and high ethylene concentration), exhibits an almost instantaneous maximum in R_p (less than 1 minute) with a resultant quasi-

exponential decay in activity. No real steady-state in the ethylene polymerization was commonly observed. On the other hand, with poor mixing and/or low monomer concentration, rate-time curves were produced with an apparent steady-state. However, the catalyst activities and PE molecular weights were significantly lowered indicating that the catalysts were starved for monomer. It has been found by an ab-initio molecular dynamics study in the metallocene catalyzed polymerization of ethylene that the insertion time of ethylene into the bridged zirconocene complex $(SiH_2Cp_2)ZrCH_3^+$ is only about 170 femto-seconds (Iarlori, 1995). They found that there is no significant barrier of activation for the ethylene insertion step. This very fast insertion time gives additional evidence for a polymerization that can be diffusion limited at low ethylene concentrations.

The rapid decay observed in the rate-time curves may be caused by polymer precipitation with removal of active sites from solution. The presence of the octene-1 comonomer is believed to form SCBs in the PE chains which help prevent precipitation of the chains from solution and give rise to the observed steady-state in the rate-time curves. In the homogeneous polymerization of ethylene at low temperatures (<90 °C) utilizing a metallocene/MAO catalyst system, the precipitation kinetics are complicated and believed responsible for much of the polymerization behavior. We often assume that all the polymerization occurs in the solvent phase rather than a two phase type polymerization where some polymerization is occurring additionally in a polymer rich phase. We have found evidence for significant amounts of long chain branch formation (LCBing) in

the semi-batch polymerization of ethylene under the above reported conditions which may indicate some polymerization is occurring in a polymer-rich phase (Chapentier, 1977).

Several methods may be employed to prevent PE precipitation in low temperature slurry polymerization utilizing metallocene catalysts. Extremely high Al/Zr ratios due to a high excess of MAO will presumably lead to a more constant polymerization rate-time curve due to the MAO oligomers helping to prevent precipitation of the PE chains. Of course, this method is extremely expensive and separating the MAO from the PE is not an easy nor cheap task and unrealistic for a commercial operation. Also, MAO-free cationic catalysts are now being developed and commercialized which require no MAO and provide both high activity and give high MWs, although MAO may still be employed at low concentrations to act as an impurity scavenger (Lai, et. al, 1993, Charpentier, et al., 1997). Employing a comonomer will also help prevent precipitation of PE chains which will lead to a more steady polymerization rate-time curve as we have seen above.

The higher the MW of the PE chains, the higher the apparent viscosity in the reaction medium. This high viscosity results in low heat transfer coefficients in a stirred reactor which greatly aggravates the problem of heat removal and can cause significant reactor fouling. Producing low MW PE in slurry will give less problems with viscosity than higher MW PE and a technology employing a homogeneous metallocene catalyst in slurry producing low MW PE chains is more

reasonable than one producing higher MW PE. Higher polymerization temperatures help to reduce the apparent viscosity by giving polymers with lower MW and reducing the viscosity of the reaction mixture. At the temperatures in slurry that we have reported in this work, high apparent viscosity's and significant reactor fouling were observed. However, at higher temperatures in solution polymerization (> 140°C) with a research CSTR, no viscosity problems were encountered with this catalyst system (Charpentier, et. al., 1997).

In unsupported metallocene polymerization of ethylene in slurry or solution, there are no heterogeneous particles for the polymer to form from such as that found with traditional Z-N polymerization. This lack of powder properties of the PE chains in slurry greatly increases the viscosity of the reacting medium. Supporting the metallocene catalyst on a spherical macrosupport particle consisting of spherical primary crystallite particles may greatly improve the apparent viscosity of the polymerization. The spherical primary crystallite particles will act as a template for polymerization of PE which will grow radially outwards in a fashion similar to that encountered in a traditional Z-N polymerization (often called *replication*). Another way to reduce apparent viscosity would be to use a prepolymerization with either a spherical Z-N catalyst or a spherical supported metallocene catalyst to: a) slow down the initial R_p; b) provide good "replication"; and c) provide good bulk density. Then, in a second step, use homogenous metallocene polymerization to take advantage of the extremely high activities and narrow MWD and other favorable physical properties.

We will now attempt a basic kinetic analysis of Cp_2ZrCl_2/MAO with the realization that diffusion limitation of monomer and high apparent viscosity significantly influence this high activity polymerization system. Unfortunately, there is no simple method for measuring the number of active sites for metallocene polymerization. Chien et al (1987) has determined for the Cp_2ZrCl_2/MAO system that the number of active sites is close to 100 % of the catalyst concentration. Thus, for kinetic analysis purposes we will approximate the active site concentration to be the catalyst concentration. The two termination mechanisms that we will analyze are: 1) β-hydride elimination and 2) chain transfer to monomer. Chain transfer to hydrogen is also a very important method for controlling the PE MWs as metallocene catalysts are extremely sensitive to hydrogen. Another likely method for chain termination, not investigated here, is with the use of comonomers which appear to generate hydrogen when incorporated into the PE chain by certain metallocene catalysts (Brinen and Muhle, 1997). As metallocenes are extremely sensitive to hydrogen, this mechanism significantly lowers LLDPE MWs.

The polymerization rate R_p is given by:

$$R_p = k_p [C^*] [M]^{\alpha} \qquad (3)$$

where R_p = rate of propagation (M/s^{-1})

k_p = propagation rate constant $(M \cdot s)^{-1}$

C^* = active site concentration (M)

M = reactor ethylene concentration (M)

α = the reaction order w.r.t. monomer.

Rearranging Equation (3) yields

$$\ln(R_p/[C^*]) = \alpha \ln([M]) + \ln(k_p) \qquad (4)$$

where $R_p/[C^*]$ is calculated by the mole of ethylene consumed divided by the mole of zirconium and the polymerization time. The plot of ln $(R_p/[C^*])$ versus ln [ethylene] is given in Figure 2.20. The slope of the graph gives the reaction order w.r.t. monomer of 1.8 instead of 1.0 which may be indicative of a polymerization that is diffusion limited w.r.t. monomer. From the y intercept we can calculate a k_p value for these conditions of 2.7×10^{4} $(M^{-0.8}\cdot s^{-1})$.

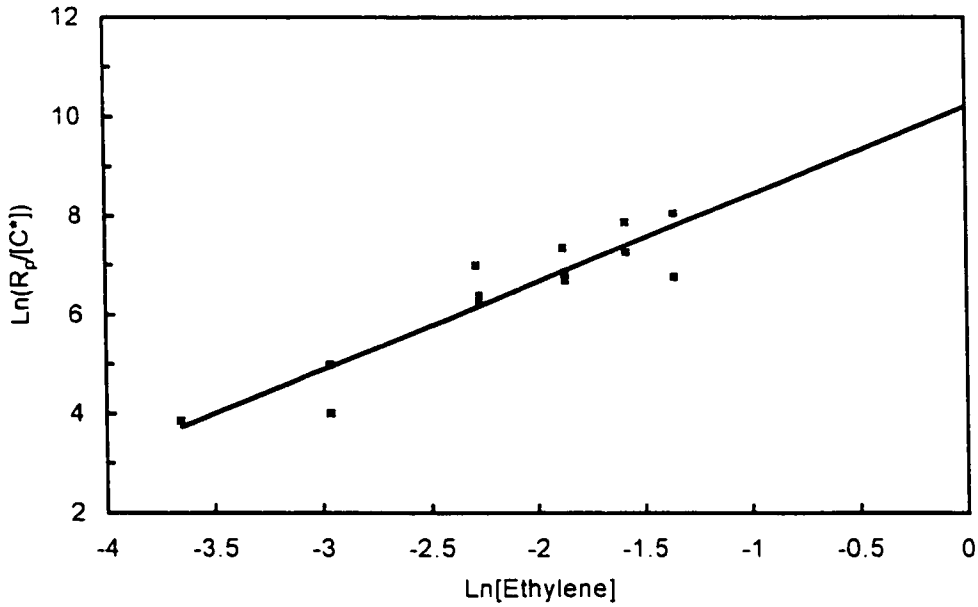

Figure 2.20 Plot of $\log(R_p/[C^*])$ versus log[Ethylene] to estimate reaction order. The points are experimental data and the line is a linear least-square regression fit to the points. The polymerization conditions were: T = 70 °C, $[Cp_2ZrCl_2]$ = 0.7 μM, Al/Zr = 1600.

The temperature dependence of the propagation rate constant is given by the Arrhenius equation.

$$k_p = A_p \exp(-\Delta E_p/RT) \quad (5)$$

and by rearranging Equation (3) yields

$$\ln (R_p/([C^*][M]^{\alpha})) = -\Delta E_p/RT + \ln(A_p) \quad (6)$$

The activation energy of propagation, ΔE_p, can be estimated from the slope of the curve of $\ln (R_p/[M]^{\alpha})$ versus 1/T, as shown in Figure 2.21. Both sets of experiments studying temperature, with one set of experimental conditions in the temperature range of 10-90 °C under diffusion limited conditions and the other set of experimental conditions in the temperature range 50-90 °C under less diffusion limited conditions, give identical values for ΔE_p of 28.5 kJ/mol or 6.8 kcal/mol. It is interesting to compare this result to the solution polymerization of ethylene in toluene at 140-200 °C using Cp_2ZrCl_2/MAO, where we found highly negative activation energies due to increasing catalyst deactivation with temperature (Charpentier et al., 1997).

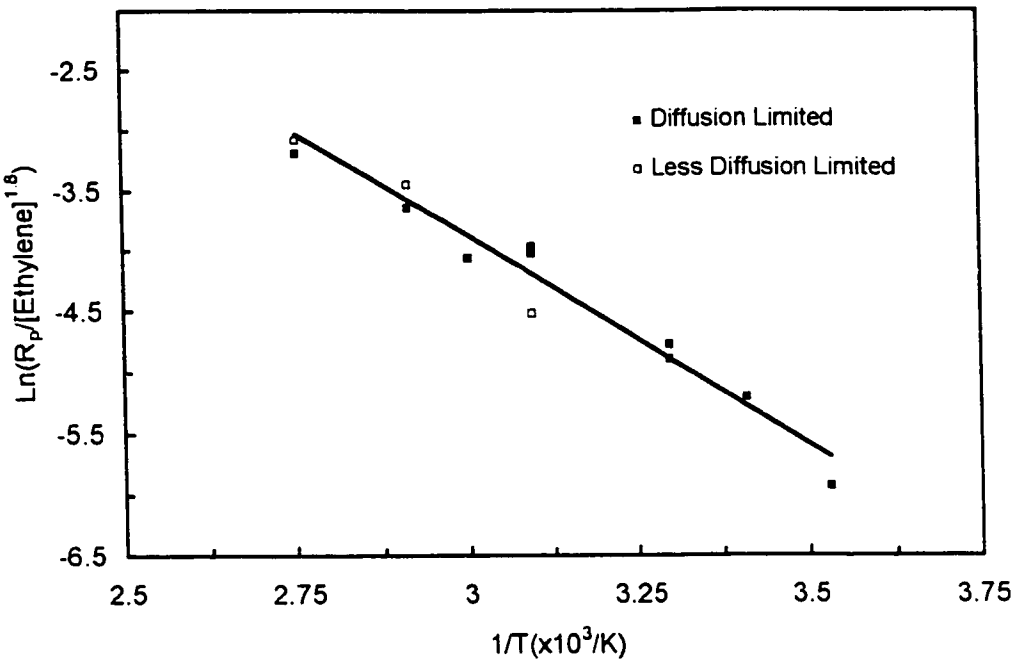

Figure 2.21 Plot of ln(Rp/([C*][ethylene])) versus 1/T to get activation energy. The points are experimental data and the line is a linear least-square regression fit to the points. The polymerization conditions were: (A) $[Cp_2ZrCl_2]$ = 13 μM, Al/Zr = 1600; (B) $[Cp_2ZrCl_2]$ = 0.7 μM, Al/Zr = 1600.

The spontaneous process of the β-hydride elimination, $k_{tr,\beta}$ is widely recognized as the primary mechanism for termination of polymer chains when using metallocene/MAO catalysts (Chien, 1985). The value of $k_{tr,\beta}$ can be obtained from the variation of number average molecular weight with monomer concentration according to the following equation (H_2 absent):

$$m/M_n = k_{tr,M}/k_p + k_{tr,\beta}/(k_p[M]) + k_{tr,Al}/(k_p[M]) \qquad (7)$$

where m is the molecular weight of the monomeric unit (28 for PE). Since $k_{tr,\beta} \approx 25\ k_{tr,Al}$ (Chien and Wang, 1990) we can ignore $k_{tr,Al}$ and thus,

$$m/M_n = k_{tr,M}/k_p + k_{tr,\beta}/(k_p[M]) \quad (8)$$

From the slope and intercept of m/M_n versus $[ethylene]^{-1}$ in Figure 2.22, we obtain $k_{tr,\beta}/k_p = 9.9 \times 10^{-6}$ mol/L and $k_{tr,M}/k_p = 1.4 \times 10^{-4}$. Since $k_p = 2.7 \cdot 10^4$ $(M^{-0.8} \cdot s^{-1})$, $k_{tr,\beta} = 0.27$ s^{-1} and $k_{tr,M} \cong 3.8$ $(M \cdot s)^{-1}$ for the conditions $[Cp_2ZrCl_2] = 0.67$ μM, Al/Zr = 1,600, T = 70 °C.

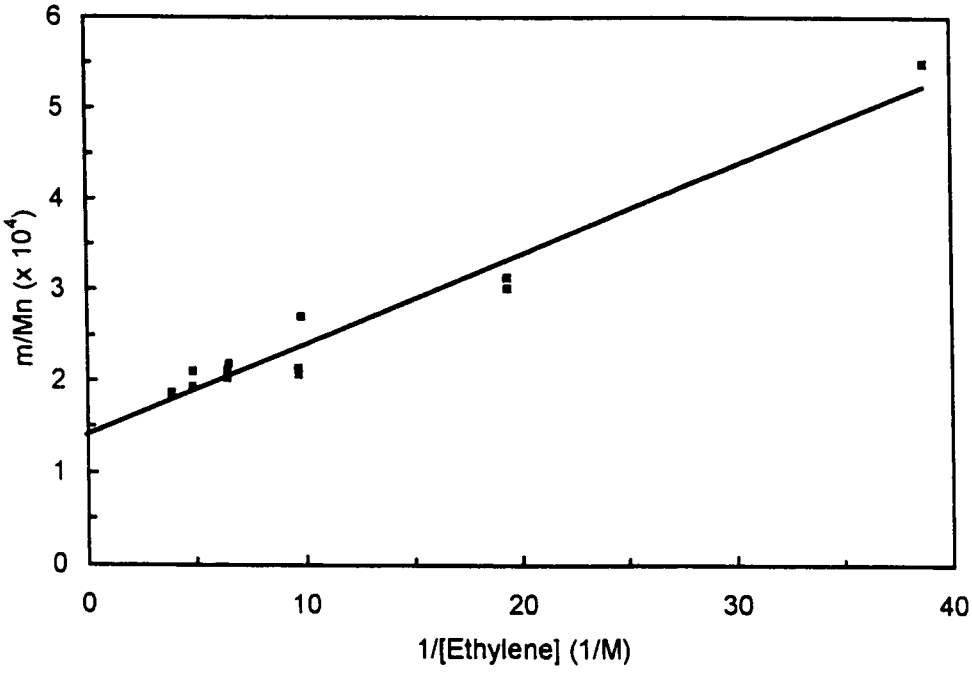

Figure 2.22 Plot of m/Mn versus 1/[Ethylene] to estimate kinetic parameters. The points are experimental data and the line is a linear least-square regression fit to the points. The polymerization conditions were: T = 70 °C, $[Cp_2ZrCl_2] = 0.7$ μM, Al/Zr = 1600.

2.6 Conclusions

In the polymerization of ethylene utilizing the metallocene catalyst system Cp_2ZrCl_2/MAO in toluene, the shape of the polymerization rate-time curves was found to depend on ethylene concentration with low ethylene concentrations giving steady-states and higher ethylene concentrations leading to decay-type curves. Various impellers were studied which also gave steady-state or decay-type curves depending on their ability to sparge the reactor with ethylene. PE MWs increased to a plateau with increasing ethylene concentration while PE PDIs decreased. Superior sparging and mixing impellers also slightly increased PE MWs and decreased PDIs. This behavior is attributed to the extremely high activity of the Cp_2ZrCl_2/MAO system which causes significant diffusion limitation of ethylene at low ethylene concentration or lack of significant sparging and mixing ability of the impeller. Addition of comonomer was found to prevent decay-type curves and give a steady-state. This behavior was attributed to the precipitation of PE chains removing active sites from solution which is reduced by use of a comonomer. The length of polymerization time was found to have no effect on PE MWs or PDIs indicating no chain transfer to polymer. High temperature GPC measurements of the PE approximated Flory's most probable distribution from a single site-type catalyst for all temperatures studied. Activity increased with increasing temperature from 10-90 °C. Increasing temperature strongly decreased PE MWs and lowered PDIs towards those predicted by Flory's distribution. Increasing

Cp_2ZrCl_2 concentration significantly decreased PE MWs and led to a slight increase in PDIs. Hydrogen decreased the activity of Cp_2ZrCl_2/MAO and strongly decreased PE MWs while PDIs were not significantly affected. Increasing the transition metal from Ti to Zr to Hf was found to increase PE MWs steadily although only the Zr analog had significant activity. PE PDIs were not strongly affected by the transition metal type. Deviations from Flory's most probable distribution are believed to be due to the high viscosity of polymerization encountered whose effects cause temperature, monomer, and active site gradients within the polymerization reactor.

2.7 Acknowledgments

We greatly appreciate the financial support from the Natural Sciences and Engineering Research Council of Canada (NSERC) for this work. We also thank Albemarle Corporation for donation of MAO co-catalyst and to Dr. Kris Kostanski for analysis of PE samples by GPC.

2.8 Notation

ΔH_f	heat of fusion
° C	degrees Celsius
δ	chemical shift in ppm relative to TMS (NMR)
CCD	chemical composition distribution

atm	atmosphere (s)
Cp	cyclopentadienyl
E_a	activation energy (kJ/mol)
HDPE	high density polyethylene
LLDPE	linear low density polyethylene
MAO	methylaluminoxane
M	monomer
PDI	polydispersity Index
PE	polyethylene
PS	polystyrene
k_p	propagation rate constant (L/mol·s)
GPC	gel permeation chromatography
R_p	rate of polymerization (mol/s)
SCB	short chain branching
T	temperature (°C)
TCB	1,2,4 trichlorobenzene
τ	termination/propagation ratio

2.9 Literature Cited

Brinen, J.L.; Muhle, M.E. *Polymer Reaction Engineering III*, **1997**.

Charpentier, P.; Hamielec, A.E.; Zhu, S., Brook, M. "Effect of Aluminoxane on Semi-Batch Polymerization of Ethylene Using Zirconocene Dichloride"; Submitted for publication to *Polymer*, 1997

Charpentier, P.; Zhu, S.; Hamielec A.E., Brook, M "Continuous Solution Polymerization of Ethylene using the Metallocene Catalyst System, Zirconocene Dichloride/MMAO/TMA"; Submitted for publication to *Ind. Eng. Chem. Res.*, 1997

Chien, J.C.W., Wang, B.P. *J. Polym. Sci., Polym. Chem. Ed.* **1988**, 26, 3089.

Chien, J.C.W. ,Wang, B.P. *J. Polym. Sci., Polym. Chem. Ed.* **1990**, 28, 15.

Flory, P.J. in "Principles of Polymer Chemistry", Cornell University Press, Ithaca, New York, 1953, p.161.

Gerrard, W. in "Gas Solubilities-Widespread Applications", Pergamon Press, New York, 1980.

Gerrard, W. in "Solubility of Gases and Liquids-A Graphic Approach", Plenum Press, New York, 1976.

Hamielec, A.E., Soares, J.P. *Progr. Polym. Sci.*. **1996**, 21, 651

Iarlori, S.; Buda, F. *Macromol. Symp.* **1995**, 89, 369.

Jordan, R.F.; *J. Chem. Educ.* **1988**, 65,4.

Kaminsky, W. in "Transition Metal Catalyzed Polymerization" (Ed. R.P. Quirk), vol.4, MMI Press, London, 1983, p.225

Kaminsky, W., Miri, M., Sinn, H., Woldt, R. *Makromol. Chem., Rapid Commun.* **1983**, 4, 417

Kaminsky, W., Kolper, K., Niedoba, S. *Makromol. Chem., Makromol. Symp.* **1986**, 3, 377.

Kaminsky, W., Bark, A., Speihl, R., Moller-Lindenhof, N., Niedoba, S. in "Transition Metals and Organometallics: Catalysts for Olefin Polymerization" (Eds W. Kaminsky and H. Sinn), Springer-Verlag, Berlin, 1988, p.291

Kaminsky, W. in "Catalytic Polymerization of Olefins" (Eds. T. Keii and K. Soga), Kodansha, Tokyo, 1986, p.293

Lahti, M.; Koivumaki, J.; Seppala, J.V. *Angew. Makromol. Chemie*, **1996**, 236, 139.

Lai, S. Y.; Wilson, J.R.; Knight, G.W.; Stevens, J.C.; Chum, P.W.S. (to Dow Chemical Co.). Elastic substantially linear olefin polymers, U.S. Patent 5,272,236, **1993**.

Lai, S.Y.; Wilson, J.R.; Knight, G.W.; Stevens, J.C. (to Dow Chemical Co.). Elastic substantially linear olefin polymers, U.S. Patent Application WO 93/08221, **1993**.

Soares, J.P.; Hamielec, A. E. *Macromol. Theory Simul.* **1996**, 5, 547.

Vela Estrada, J.M.; Hamielec, A.E. *Polymer*, **1994**, 35, 808.

CHAPTER 3 - EFFECT OF ALUMINOXANE ON SEMI-BATCH POLYMERIZATION OF ETHYLENE USING ZIRCONOCENE DICHLORIDE

P.A. Charpentier, A.E. Hamielec*, S. Zhu

Department of Chemical Engineering

McMaster University, Hamilton, Ontario, Canada L8S 4L7

M. A. Brook

Department of Chemistry

McMaster University, Hamilton, Ontario, Canada L8S 4M1

Manuscript submitted to *Polymer*, July 30, 1997

Keywords: metallocene catalyst, aluminoxane, polyethylene, semi-batch polymerization

Author to whom correspondence should be addressed.

Email: hamielec@mcmaster.ca

Phone: (905) 525-9140 ext 24950

Fax: (905) 528-5114.

3.1 Abstract

Several types of commercial and developmental aluminoxanes were studied in the semi-batch polymerization of ethylene using bis(cyclopentadienyl) zirconium dichloride (Cp_2ZrCl_2). High temperature gel permeation chromatography (GPC) measurements of polyethylene (PE) formed using various types of aluminoxanes approximated Flory's most probable distribution from a single site-type with PE M_w/M_n's approaching 2.0 for polymerization temperatures ranging from 50-90 °C. The structure and type of aluminoxane co-catalyst were found not to influence the molecular weight distribution (MWD) of PE although to influence the activity of Cp_2ZrCl_2 catalyst. In general, modified methylaluminoxanes (MMAOs) and methylaluminoxanes (MAOs) were found to have similar activities whereas isobutylaluminoxane (IBAO) gave a very low activity for the polymerization of ethylene. Increasing isobutyl content in the aluminoxane co-catalyst led to a continual decrease in catalyst activity. Increasing aluminum/zirconium (Al/Zr) molar ratio, by increasing the MAO concentration, led to increasing catalyst activity up to a maximum activity at an Al/Zr molar ratio of 2400. Like the structure and type of the aluminoxane co-catalyst, the Al/Zr molar ratio was found not to influence the PE MWD. Mixing in additional trimethylaluminum (TMA) with MAO was found not to alter the MWD but gave lower activity at similar Al/Zr molar ratios than that from MAO itself.

3.2 Introduction

Metallocene polymerization is a revolution in the polymer industry for producing both specialty and commodity polyolefins. The main advantages of metallocene catalysts is that they are extremely active (Kaminsky, 1983; Chien, 1988) and their structure can be modified to an almost limitless number of possibilities by variation of: a) ligand type, b) bridge joining ligands, c) substituents on ligand and bridge to modify steric and electronic and surroundings of transition metal and d) transition metal type (Hamielec and Soares, 1996). This well defined and controllable catalyst structure allows formation of unique and specific active site-types (normally one per catalyst) compared to a traditional Ziegler-Natta (Z-N) catalyst (e.g. $TiCl_4$/TMA) which is a multi site-type catalyst with very little control of the site-types. Each site type gives narrow molecular weight distributions (MWDs) (Chien, 1988; Kaminsky, 1987) with polydispersity indexes (PDIs) approaching 2 as defined by Flory's most probable MWD (Flory, 1953) and extremely narrow chemical composition distributions (CCDs) in the formation of copolymers, as defined by Stockmayer's bivariate distribution (Stockmayer, 1945). Each site-type gives a unique activity, chain transfer to propagation rate, reactivity ratio and stereoselectivity so that by variation of catalyst site structure, each of these can be tailored to give a polymer with a desired blend of properties. These catalysts also provide the potential to control the polymer structure and the rheology of the formed polymer chains by variation of catalyst structure and

manipulation of reactor conditions to form long chain branches (LCBs) (Lai et al., 1993; Soares and Hamielec, 1996).

Until 1973, it was assumed that homogeneous Group IV-B metallocene catalysts were inactive in olefin polymerization. However, it was surprisingly found that when water was added to bis(cyclopentadienyl) titaniumdimethyl/trimethylaluminum (TMA), $(C_5H_5)_2Ti(CH_3)_2$ /$Al(CH_3)_3$, system, the activity increased to such a degree that ethylene could be polymerized (Long & Breslow, 1975; Andresen, 1976). The reaction of water with TMA has been found to eliminate methane and to form an aluminum-oxygen-aluminum structure (Figure 3.1) which has been called methylaluminoxane or MAO (Boleslawsky, 1976; Sinn, 1980).

MAO can be prepared in several different methods by the careful controlled partial hydrolysis of an alkylaluminum. The reaction of water with alkylaluminum is extremely rapid and highly exothermic and careful synthetic routes are necessary for its controlled and safe formation. In the laboratory, often the hydrated salt method is utilized for formation of aluminoxane which consists of reacting a hydrated salt such as hydrated aluminum, copper, or iron sulfate with TMA or other trialkylaluminums (Kaminsky and Hahnsen,1985; Welborn Jr. and Tornqvist,1987) (Figure 3.1).

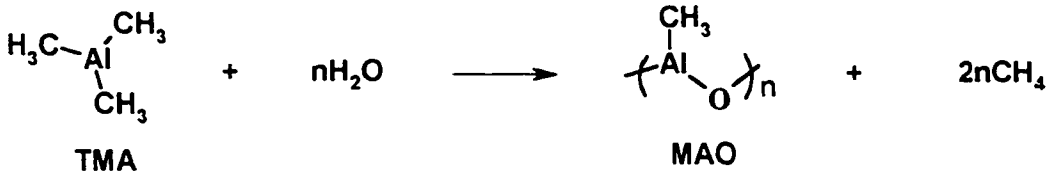

Figure 3.1 Formation of methylaluminoxane (MAO): a) basic formation of MAO by reaction of trimethylaluminum (TMA) with water; b) hydrated salt method of formation of MAO by reaction of TMA with hydrated aluminum sulfate.

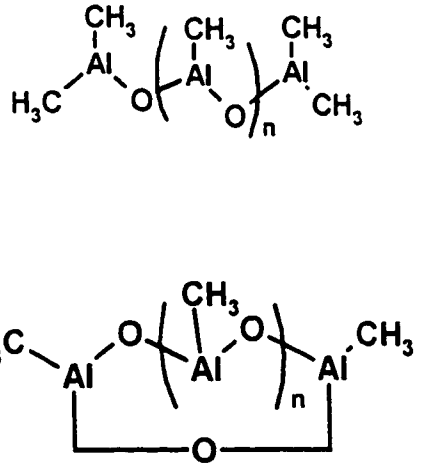

Figure 3.2 Forms of MAO: a) linear; b) cyclic.

Several other methods for synthesizing aluminoxanes have been reported which generally involve either a wet solvent (Manyik et.al., 1967) and/or gas to control the aluminoxane formation (Brintzinger, 1982; Kaminsky, 1983; Giannetti, 1985). However, there are several disadvantages with these methods including long reaction times with hydrated salts, low yields (50% or lower), potential of explosion and formation of solid by-products, small amounts of the transition metal when using hydrated iron or copper sulfate (Razuvaev, 1975; Giannetti, 1985), use of low temperatures (-10 °C and below) in order to obtain optimum yields, poor reproducibility, use of expensive raw materials or unusual reactors (Schoenthal and Slaugh, 1988) and conditions (Schoenthal and Slaugh, 1988) etc. (Kaminsky, 1987). Due to these disadvantages, these methods are not favored industrially and various other methods are employed (Crapo, 1990), such as directly contacting trialkylaluminum with water vapor or atomized water vapor under carefully controlled conditions (Deavenport, 1991).

All of the above synthetic techniques to produce aluminoxanes inevitably produce aluminoxanes with different structures, different degrees of oligomerization, and different amounts of unreacted TMA. Both cyclic and linear oligomers have been proposed to be produced in the formation of aluminoxanes with a degree of oligomerization between 10-20 (Sinn, 1988) (Figure 3.2). More recently, 3-D cage structures with four-coordinate aluminum centers have been demonstrated for aluminoxanes produced from $Al(tBu)_3$ (Barron, 1994) with similar structures demonstrated for methylaluminoxanes (Sinn, 1995). These cage

structures are theorized to be involved in the interaction between aluminoxane and transition metal in an active catalyst site with the aluminoxane involved in more than just catalyst activation (Barron, 1995).

It has also been demonstrated that in the partial hydrolysis of TMA to MAO some unreacted TMA always remains in the MAO solution (Howie, 1993, Hagendorf, 1995) even when the solution is dried under vacuum (Tritto, 1993). By ^{13}C NMR spectroscopy, Tritto et al. found that TMA is most likely bound to MAO, bridging two or more MAO chains together and that the amount of TMA influences the active cationic metallocene concentration (Tritto, 1995). A cage structure has been reported which contains unreacted TMA inside a 3-D MAO cage (Sinn, 1995). However, presently the exact structure of the MAO oligomer is unknown as studies to analyze this system suffer from the dynamic behavior of MAO, which by multiple equilibria such as disproportionation, changes its size and structure with both temperature and solvent (Belov, 1995; Tritto, 1996). The term "black box" is used to describe the inherent difficulties in trying to elucidate the structure of MAO (Barron, 1995).

Hydrolysis of aluminoxane to give a gas/Al ratio gives an indication of the structure of aluminoxane. Conventional MAO, when hydrolyzed, gives methane as the sole gaseous product from methyl aluminum species. A form of MAO known as modified methylaluminoxane (MMAO) can be formed by the reaction of TMA with a tetraalkyldialuminoxane containing ethyl or higher alkyl groups with the optional presence of water (Crapo, 1991) (Figure 3.3). Unlike conventional

MAO, MMAO contains alkyl substituents derived from tetraalkyldialuminoxane and/or polyalkylaluminoxane and gives C2+ products such as isobutane, n-butane etc. upon hydrolysis. The mole % methane and mole % higher alkane depend on the relative quantity of TMA to polyalkyldialuminoxane introduced. IBAO is a type of MAO that consists entirely of isobutyl groups with no methyl groups present and can be formed from diisobutylaluminoxane (Figure 3.3).

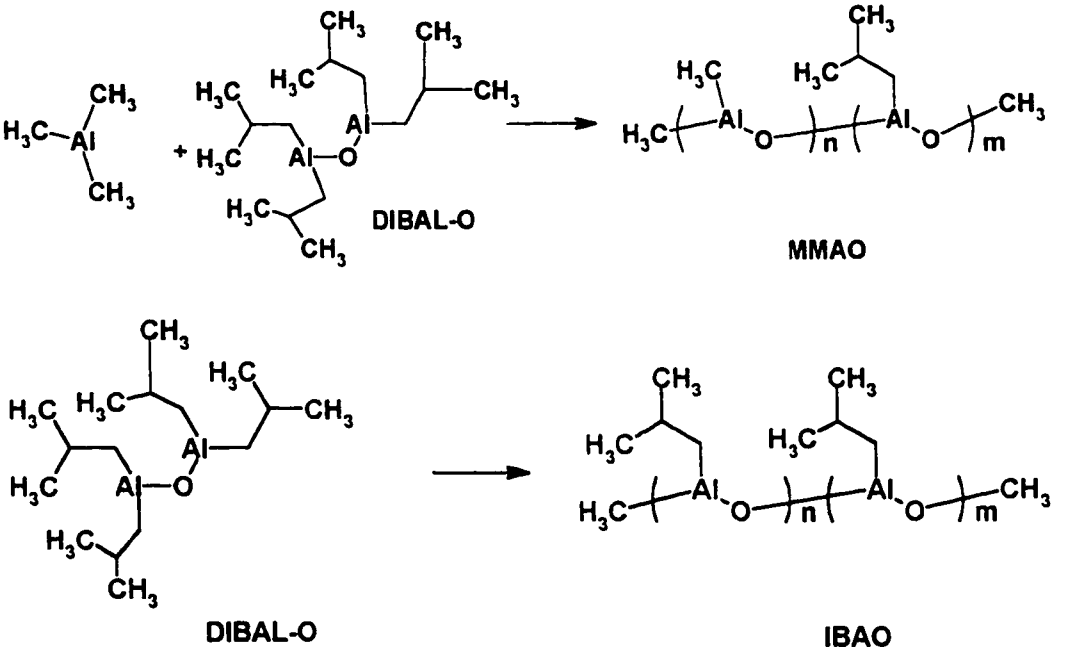

Figure 3.3 Formation of a) MMAO by reacting TMA with tetraisobutyldialumin oxane (DIBAL-O) b) IBAO by reacting DIBAL-O.

Advantages of MMAO over conventional MAO are due to the isobutyl groups of MMAO which lead to high solubility in both aliphatic and aromatic solvents whereas conventional MAOs exhibit only limited solubility in aliphatic solvents. Aliphatic or saturated hydrocarbon solvents are preferred for industrial solution and slurry ethylene polymerization and are also believed superior for the

formation of long chain branches (Soares & Hamielec, 1996). MMAO has the additional advantage of having a longer shelf life than conventional MAO which tends to gel over time and hence lose its cocatalytic ability (Tritto, 1996).

The interactions of oligomeric MAO with unreacted TMA and metallocene catalyst are complicated and unknown. The MAO co-catalyst is believed to alkylate the metallocene catalyst and functions as a Lewis acid promoting the formation of an active cationic form of metallocene catalyst (Jordan, 1986). It has been found by ^{1}H and ^{13}C NMR studies with $Cp_2Ti(CH_3)(X)$ complexes where X is CH_3 or Cl, that 1) MAO was a better alkylating agent than TMA and 2) MAO had a greater capacity for producing and stabilizing cation-like complexes than TMA (Tritto, 1993). This study, and several others for similar systems, found that the following equilibrium takes place:

$$Cp_2TiMe^{+}[\text{-}Al(Me)O\text{-}]^{-}_{n} \leftrightarrow Cp_2TiMe^{+}S[\text{-}Al(Me)O\text{-}]^{-}_{n} \qquad (1)$$

where S is a solvent molecule and that the active catalytic species ($Cp_2TiMe^{+}S[\text{-}Al(Me)O\text{-}]^{-}_{n}$) is a cation-like species. The equilibrium is believed to be shifted to the right for higher Al/Group IV metal molar ratios, thus increasing the concentration of the active cationic catalyst and hence increasing the activity of the catalyst. Of course, a maximum activity will be produced at a certain co-catalyst/catalyst ratio depending on various conditions such as catalyst type and concentration, co-catalyst type and concentration, solvent type (especially polarity), impurity/active site concentration, temperature, and monomer concentration in the diluent.

The structure of aluminoxane has been reported to have a marked influence on the activity of a metallocene/aluminoxane catalytic system with methylaluminoxane (MAO) being reported to give higher activity than other aluminoxanes such as ethylaluminoxane (EAO) or isobutylaluminoxane (IBAO) (Kaminsky, 1988). Increasing the degree of oligomerization of aluminoxane is also reported to increase the catalytic activity (Kaminsky, 1980). The effect of the structure and degree of oligomerization of aluminoxane co-catalyst on the MWD of produced PE has not been well established. It has been suggested for the polymerization of ethylene using Cp_2ZrCl_2/MAO that the PE MW decreases when the concentration of aluminoxane increases (Michiels, 1995). For the same system, when using an additional alkylaluminum, the PE MWs were found to increase with increasing concentration of TMA or TEA through a maximum at a TMA/MAO or TEA/MAO ratio of about 0.5 with decreasing PE MWs at higher ratios. Increasing the TIBA/MAO ratio gave a decrease in PE MW (Michiels, 1995; Resconi, 1991). TIBA was suggested to give PE MWs that were higher than those obtained with TMA or TEA due to the bulkier isobutyl group in aluminum alkyl which reduced the occurrence of chain transfer to aluminum (Michiels, 1995).

The role of aluminoxane co-catalyst in the active catalytic site-type is still very much in question and a thorough polymerization and polymer characterization study was undertaken to elucidate its role with the metallocene catalyst Cp_2ZrCl_2. This paper deals with the investigation of the effects of various commercial and

developmental aluminoxanes on the catalyst activity and resulting polymer MWD in the ethylene polymerization. The addition of extra TMA to MAO was also studied to determine its role in the catalyst activation and site-type formation.

3.3 Experimental

3.3.1 *Materials*

Fisher Optima toluene was used as diluent for all reactions and purified by distillation over sodium benzyl ketyl. Research grade ethylene was purchased from Matheson Gas and purified by passing over beds of CuO catalyst and then molecular sieves. The MAOs studied were purchased either from Akzo-Nobel or donated by Albemarle Corporation. All MAOs were used as received without further purification. TMA 2.0 M in toluene and zirconocene dichloride were purchased from Aldrich Chemical and used as received. All manipulations of catalyst and co-catalyst were performed in a Vacuum Atmospheres glovebox which reduces the impurities O_2 and H_20 to less than 1 ppm.

3.3.2 *Reactor Setup and Method of Polymerization*

The polymerization reactor utilized for all experiments is an Autoclave Engineers 1 L autoclave with 2" dispersimax impeller. All wetted parts were either 316 stainless-steel or teflon. All experiments were performed at 1200 rpm, in toluene. A weighed amount of diluent was transferred to the nitrogen purged

reactor with additional purging of the reactor with nitrogen, then ethylene. Co-catalyst was injected by syringe into the reactor next, then the reactor was pressurized with ethylene. The polymerization was initiated by injection of catalyst into the reactor within 5 minutes of injection of co-catalyst. The reactor temperature was monitored continuously by a J type thermocouple placed in a thermocouple well of the reactor. Temperature was maintained ± 0.2 °C. Ethylene flow to the reactor was measured by a Sierra Instruments Model 830 thermal mass flowmeter. The reaction was terminated by depressurizing and injection of methanol into the reactor. The formed PE was washed with acidic methanol to remove MAO residue, then methanol, filtered and dried under vacuum.

3.3.3 *High Temperature GPC*

All GPC measurements were performed with a Waters-Millipore SEC instrument model 150-C high temperature GPC with a differential refractive index detector at 140 °C using 1,2,4-trichlorobenzene (TCB) as solvent. The following operation conditions were adopted: 1) column and sample compartment temperature, 140 °C; 2) flow rate of mobile phase, 1.0 mL min^{-1}; 3) sample injection volume, 200 μL; 4) no sample spinning: 5) no sample filtering; 6) sample concentration, 0.1 wt % in TCB.

Calibration of the high temperature GPC was performed at 140 °C directly with a calibration curve obtained using narrow MWD PE standards purchased from the National Bureau of Standards. Additionally, both narrow MWD polystyrene (PS) standards from Tosoh Corporation and broad MWD PE standards from American Polymer Standards and Polymer Laboratories Ltd. were used to check the calibration curve. The Mark-Houwink constants for the calibration curve were for $K_{PS} = 1.21 \times 10^{-4}$ and $a_{PS} = 0.707$ and for $K_{PE} = 3.92 \times 10^{-4}$ and $a_{PE} = 0.725$.

3.4 Results

3.4.1 *Effect of Aluminoxane Structure on Catalyst Activity*

Ten different commercially supplied MAOs were studied at a polymerization temperature of 70 °C and an Al/Zr molar ratio of 1600. Table 3.1 lists the MAOs studied with their composition while Table 3.2 summarizes the polymerization activity and gives the resultant PE MWs and PDIs.

Table 3.1. Types and Composition of Aluminoxanes Studied

MAO	Structure	Composition	Stabilizers
Akzo PMAO-S1*	$-(Al(CH_3)O)-$	> 99 % Methane	Yes
Akzo PMAO-S2*	$-(Al(CH_3)O)-$	> 99 % Methane	Yes
Akzo PMAO-372	$-(Al(CH_3)O)-$	> 99 % Methane	No
Akzo MMAO-3A	$(Al(CH_3)O)_m$-(Al(i-Bu)O)$_n$	29 mol % Isobutane	-
Akzo MMAO-4	$(Al(CH_3)O)_m$-(Al(i-Bu)O)$_n$	12 mol % Isobutane	-
Akzo IBAO 0.65*	(Al(i-Bu)O)	$H_2O/Al = 0.65$	-
Akzo IBAO 0.80*	(Al(i-Bu)O)	$H_2O/Al = 0.80$	-
Akzo DIBAL-O	$(i\text{-}Bu)_2AlOAl(i\text{-}Bu)_2$	-	-
A-MAO 25010*	$-(Al(CH_3)O)-$	N/A	-
A-DMAO*	$-(Al(CH_3)O)-$	N/A	-
A-27000*	$-(Al(CH_3)O)-$	N/A	-
A-MAO	$-(Al(CH_3)O)-$	N/A	-

*Developmental MAOs

Table 3.2. Polymerization Results of 10 Aluminoxanes

MAO Type	Max. Activity ($x10^{-3}$) **	Avg. Activity ($x10^{-3}$) **	M_n ($x\ 10^{-3}$)	M_w ($x\ 10^{-3}$)	M_z ($x\ 10^{-3}$)	M_w/M_n	M_z/M_w
Akzo PMAO	58.7	11.9	143	347	650	2.42	1.88
Akzo PMAO-S2	42.3	10.4	147	345	639	2.34	1.88
Akzo MMAO-3A	48.6	13.6	147	337	637	2.29	1.89
Akzo MMAO-4	53.5	13	155	351	649	2.26	1.85
Akzo IBAO 0.65	4	3.6	137	335	643	2.45	1.92
Akzo IBAO 0.80	2.3	1.6	144	341	650	2.37	1.90
Akzo DIBAL-O	0	0	-	-	-	-	-
A-29000	25	8.4	141	327	604	2.31	1.85
A-27000	29	9.9	156	340	621	2.17	1.83
A-25010	27.8	7.2	140	332	630	2.36	1.90
A-MAO	29	9	147	354	665	2.41	1.88

* Polymerization Conditions: Temperature = 70 °C; $[Zr]_0$ = 0.65 μM; Al/Zr = 1600; [ethylene] = 0.18 mol/L; solvent = toluene

** Activity = kgPE/(g Zr·[ethylene]·hr)

Figure 3.4 gives the rate-time traces for different Akzo aluminoxanes containing different amounts of isobutyl content. From this figure we see that the highly active MAOs (0-30 % iBu content) gave an almost immediate maximum (less than 1 minute) in the rate of polymerization after initiation by injection of catalyst into the pressurized reactor. The almost instantaneous maximum in polymerization is followed by a rapid decay in the rate. We have discussed this behavior more thoroughly in another publication (Charpentier et al., 1997). The two IBAOs studied gave much lower and more constant rate-time curves with slower initiation and an apparent steady-state.

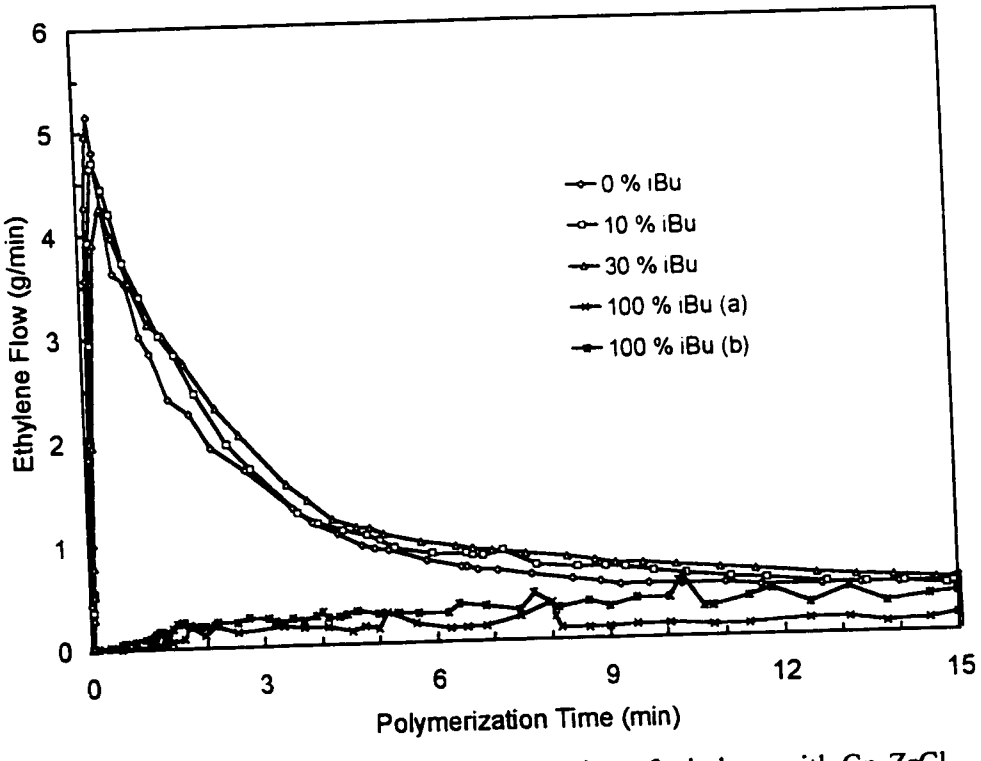

Figure 3.4 Rate-time curves for the polymerization of ethylene with Cp_2ZrCl_2 utilizing different aluminoxanes. The polymerization conditions were: T = 70 °C, [ethylene] = 0.18 mol/L, [Zr] = 0.65 μM, Al/Zr = 1600, diluent = toluene.

Figure 3.5 plots the catalyst activity versus % iBu content in the aluminoxane co-catalyst with the upper curve (maximum activity) being determined from the maximum in the rate-time curves and the lower curve (average activity) being determined from the overall rate-time curves. We have defined activity here as A = kg PE/(g Zr·[ethylene]·hr) using the concentration of ethylene in the diluent. The top trace illustrates the relationship of decreasing maximum activity with increasing iBu content in aluminoxane. Plain MAO (0 % iBu) gives the highest maximum activity while MMAO with 12 mol % i-butyl content gives a slightly higher maximum activity than MMAO with 29 mol % i-butyl content. The two 100 % i-butyl aluminoxanes (IBAOs) give significantly lower maximum activities than MMAOs or plain MAO IBAO with the H_2O/Al ratio of 0.65 gives slightly higher activity than IBAO with H_2O/Al ratio of 0.80. The bottom trace shows the relationship of average activity over 15 minutes of polymerization time versus % iBu content in aluminoxane. Here we see that the activity increases very slightly with increasing % iBu content from 0-30 % iBu. The two IBAOs again give much lower activities. Thus, the activities in the polymerization of ethylene utilizing Cp_2ZrCl_2/aluminoxane are very similar using either MAOs or MMAOs as co-catalysts but much lower for IBAO co-catalysts. Table 2 also gives the activities for various developmental Albemarle MAOs containing various unknown additives which provide similar activities to those from Akzo.

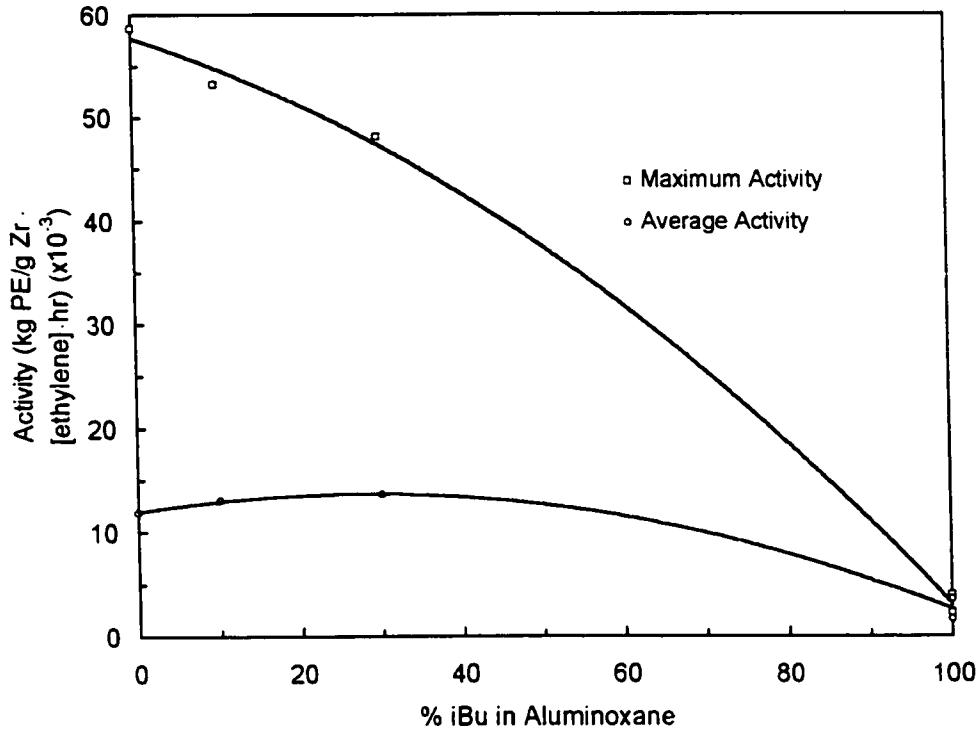

Figure 3.5 Plot of catalyst activity versus % isobutyl content in aluminoxane for the polymerization of ethylene with Cp_2ZrCl_2. The points are experimental data. The polymerization conditions were: T = 70 °C, [ethylene] = 0.18 mol/L, [Zr] = 0.65 μM, Al/Zr = 1600, diluent = toluene.

3.4.2 *Effect of Aluminoxane on PE MWD*

Figure 3.6 provides the plots of PE MWs and PDIs versus the % iBu content in the aluminoxane co-catalyst. It is clear from these plots that the % iBu content in aluminoxane co-catalyst has no discernible effect on the PE MWs and PDIs. Additionally, Figure 3.7 provides the plots of PE MWs and PDIs for each of the 10 different aluminoxanes studied at this particular set of polymerization conditions which were found to minimize diffusion limitations (Charpentier et al., 1997); i.e. temperature = 70 °C, [ethylene] = 0.18 mol/L, Al/Zr molar ratio = 1600

and [Cp_2ZrCl_2] =0.7 μM.. The lines are least-square regression lines through the data points which show that each of the aluminoxane co-catalysts produce identical PE samples, independent of the type of aluminoxane.

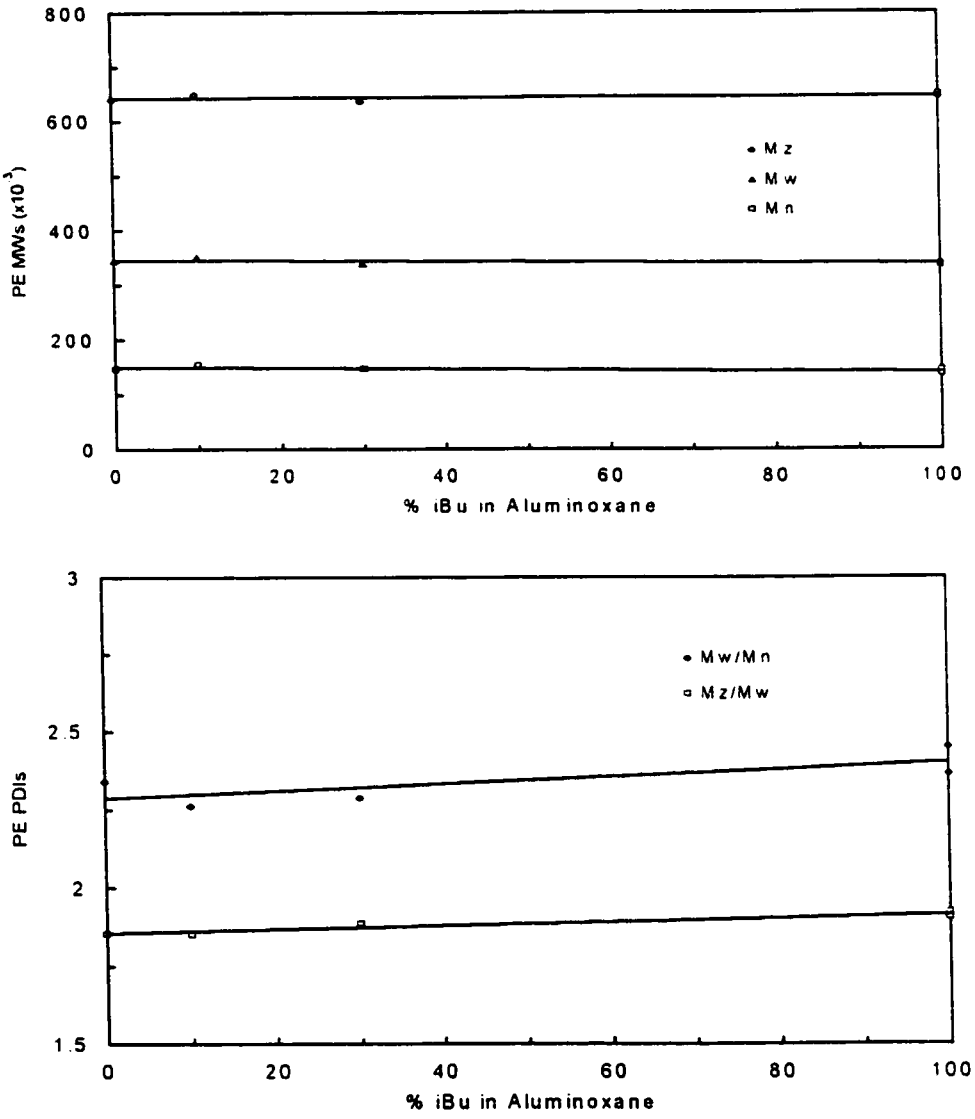

Figure 3.6 Effect of the % iBu in aluminoxane on A) the PE MWs and B) PE PDIs. The points are experimental data and the lines are linear least-square regression fit to the points. The polymerization conditions were: T = 70 °C, [ethylene] = 0.18 mol/L, [Zr] = 0.65 μM, Al/Zr = 1600, diluent = toluene.

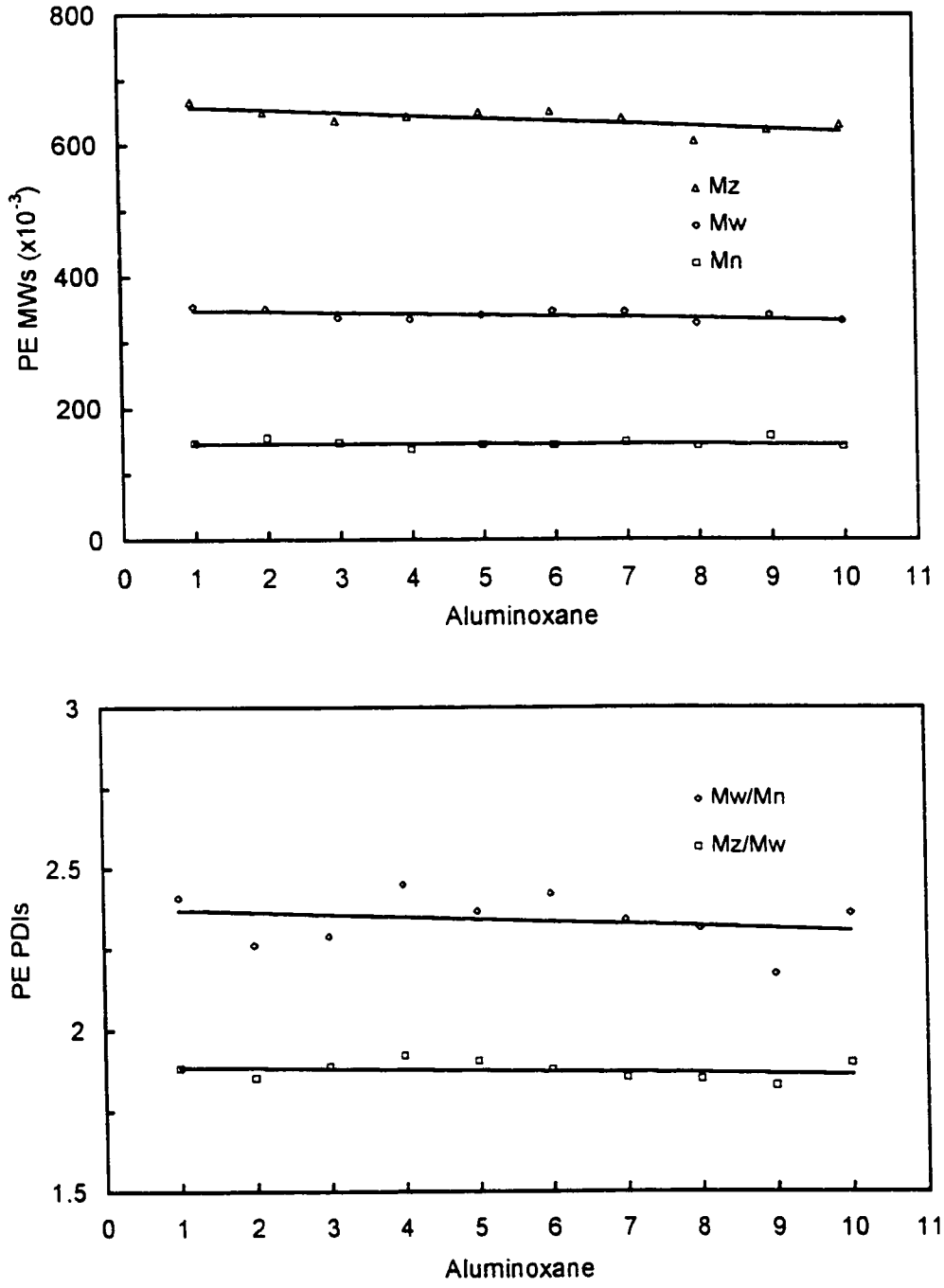

Figure 3.7 Effect of the aluminoxane type on A) PE MWs and B) PE PDIs. The points are experimental data and the lines are linear least-square regression fit to the points. The polymerization conditions were: T = 70 °C, [ethylene] = 0.18 mol/L, [Zr] = 0.65 μM, Al/Zr = 1600, diluent = toluene.

In order to determine the variation of PE MWs and PDIs produced a) from within a polymerization run and b) by the high temperature GPC, one of the polymerization runs was chosen at random and 6 samples of PE were run through the high temperature GPC. Figure 3.8 shows a boxplot (box-and-whisker plot) of the statistical comparison of the two means of a) the MWs produced from the 10 PE samples produced with different aluminoxane co-catalysts (M_n, M_w, and M_z) and b) the MWs from the 6 PE samples produced with the same aluminoxane within the same run (M_n(wr), M_w(wr) and M_z(wr)). In the boxplot diagram the circles give the mean of the data, the middle line of the box is the median, the bottom of the box is the first quartile (Q1) and the top is the third quartile (Q3) while the whiskers extend from the top and bottom of the box to the lowest and highest observations. It is clear from this plot that all the different aluminoxane co-catalysts produce PE with statistically identical MWs for this particular polymerization condition. Figure 3.9 compares the MWD determined from high temperature GPC with that predicted by Flory's most probable distribution.

This is a very important result as each of these aluminoxanes are produced by different processes with different starting materials and different formation conditions. The aluminoxanes have different compositions, some with different types of stabilizers present, and inevitably they have different degrees of oligomerization and different structures. Yet, each of these co-catalysts produce identical PE.

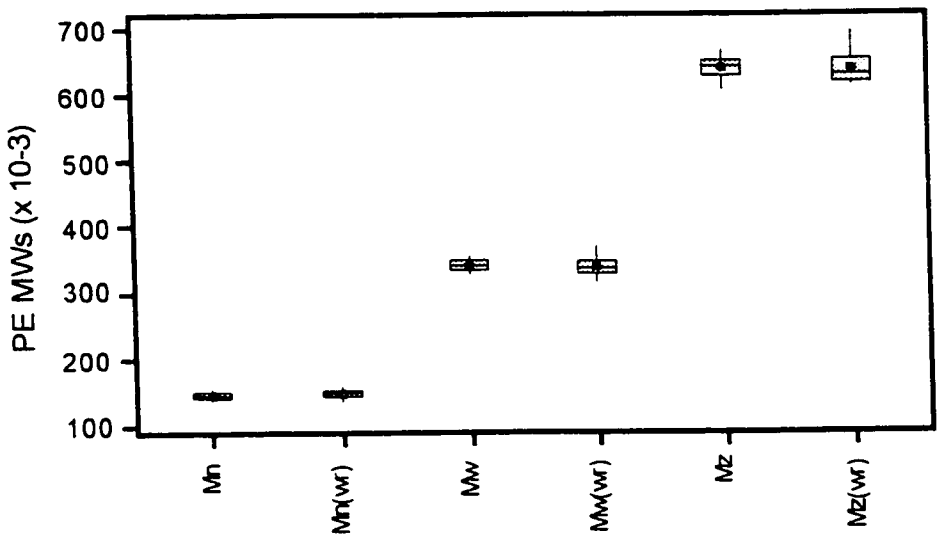

Figure 3.8 Boxplot of PE M_n, M_w, and M_z values for 10 different aluminoxanes used as co-catalyst versus variation of M_n, M_w, and M_z values for PE produced from a single run in the polymerization of ethylene with Cp_2ZrCl_2 as catalyst. The polymerization conditions were: T = 70 °C, [ethylene] = 0.18 mol/L, [Zr] = 0.65 μM, Al/Zr = 1600, diluent = toluene.

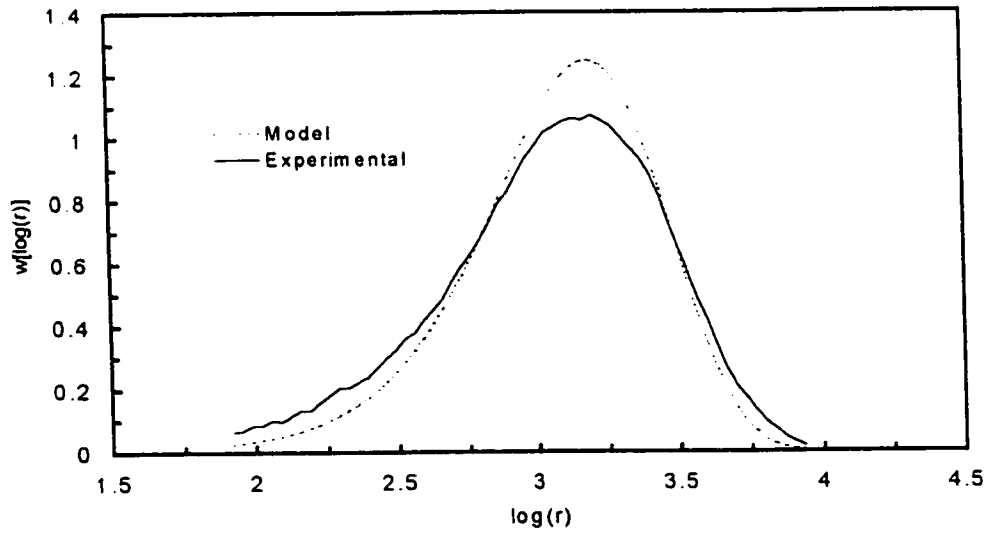

Figure 3.9 GPC trace comparing a typical PE sample to that predicted by Flory's most probable distribution.

3.4.3 *Effect of MAO Al/Zr Ratio and Added TMA on Catalyst Activity*

In order to investigate the effects of aluminoxane Al/Zr molar ratio on the catalyst activity and PE MWs and PDIs, polymerizations of ethylene were performed with Cp_2ZrCl_2 at 70 °C and varying Al/Zr ratios from 400-3200. Figure 3.10(A) gives the rate-time traces for polymerizations containing various concentrations of MAO. The rate-time traces are very similar for Al/Zr ratios from 1600-3200 with an almost immediate maximum in the rate of polymerization and then a rapid decay. With the Al/Zr ratio of 400 the induction period to reach the maximum is much longer and the rate-time curve is more constant with an apparent steady-state. Figure 3.10(B) provides plots of catalyst maximum and average activity versus Al/Zr molar ratio. We see that in the trace of maximum activity versus Al/Zr ratio a maximum in the curve is reached at an Al/Zr ratio of 2400 while further increasing the Al/Zr molar ratio decreases the activity. Notice that for the average activity the maximum is reached at an Al/Zr ratio of 1600 which remains constant up to the highest Al/Zr ratio studied of 3200.

In order to determine the effect on polymerization activity by adding TMA along with MAO to the polymerization mixture, two additional experiments were performed. Figure 3.11 gives the rate-time traces for runs with and without TMA based on the same total Al/Zr molar ratio. The runs with TMA give much lower initial rates of polymerization but also give more steady rate-time curves with less decay than those based on MAO at the same total Al/Zr molar ratio. With the same total Al/Zr molar ratio investigated here, MAO gives a higher initial rate of

polymerization than the combination of TMA and MAO, but similar average values.

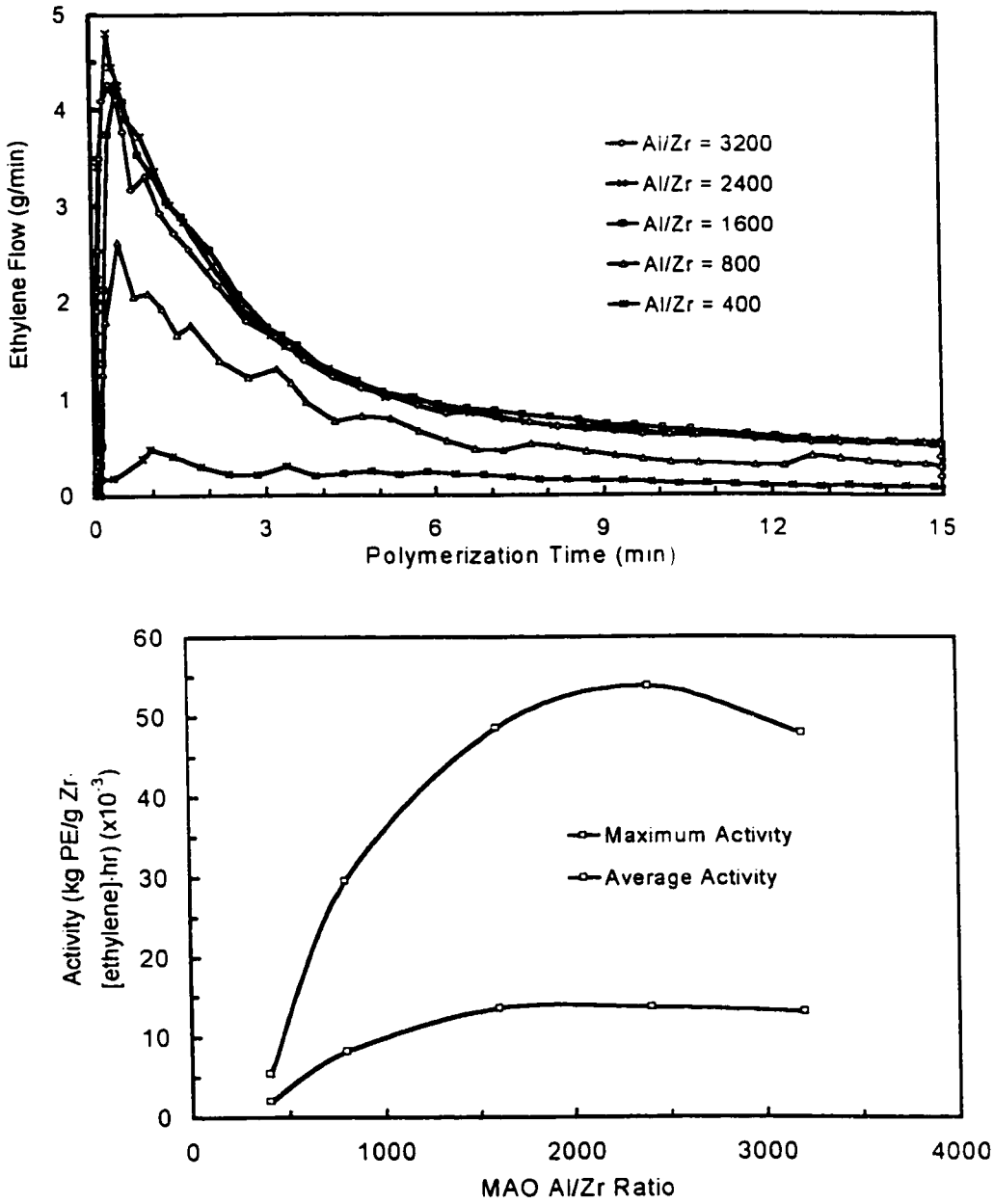

Figure 3.10 Effect of the MAO Al/Zr molar ratio on (A) polymerization rate-time curves (B) catalyst activity (kg PE/(g Zr·[ethylene]·hr)). The polymerization conditions were: T = 70 °C, [ethylene] = 0.18 mol/L, [Zr] = 0.65 μM, diluent = toluene.

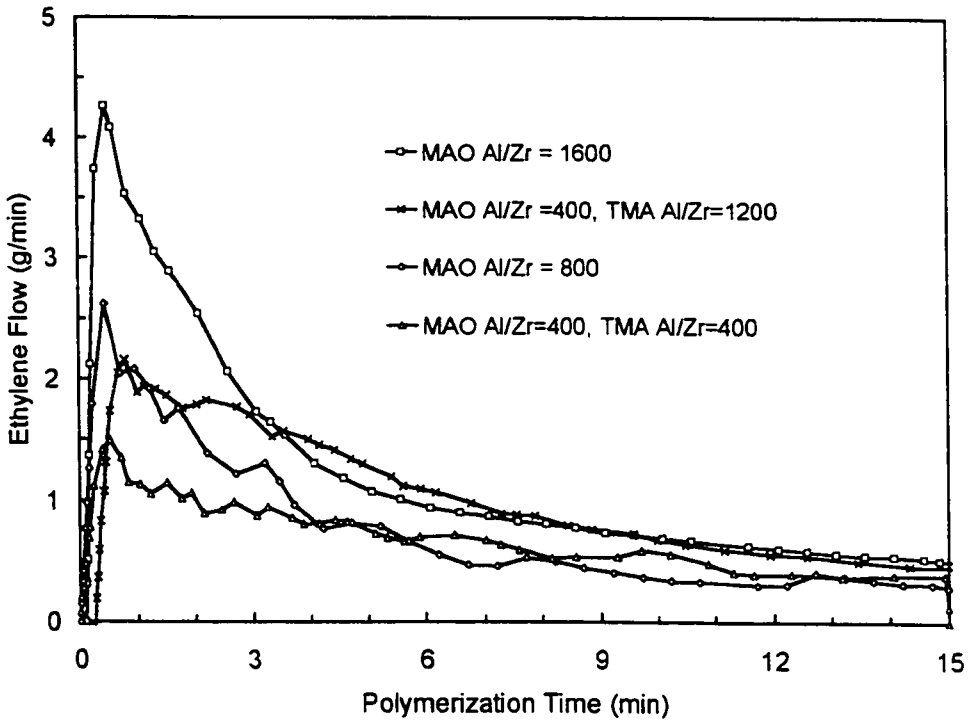

Figure 3.11 Rate-time curves for the polymerization of ethylene with Cp_2ZrCl_2 utilizing different Al/Zr ratios of MAO and TMA. The polymerization conditions were: T = 70 °C, [ethylene] = 0.18 mol/L, [Zr] = 0.65 μM, diluent = toluene.

3.4.4 Effect of MAO Al/Zr Ratio and Added TMA on PE MWD

Figure 3.12(A) plots the PE MWs versus Al/Zr molar ratio for runs with varying concentrations of MAO. The two runs with added TMA are also plotted. Figure 3.12(B) plots the PE PDIs versus Al/Zr molar ratio for varying concentration of MAO and the two runs with TMA added. It is clear from these plots that the Al/Zr molar ratio has no significant effect on the PE MWs or PDIs at 70 °C for the ranges of the ratio studied. It is also clear that the additional TMA

has no effect on the PE MWs or PDIs. Tables 3.3 and 3.4 give the experimental conditions and results for these polymerization runs.

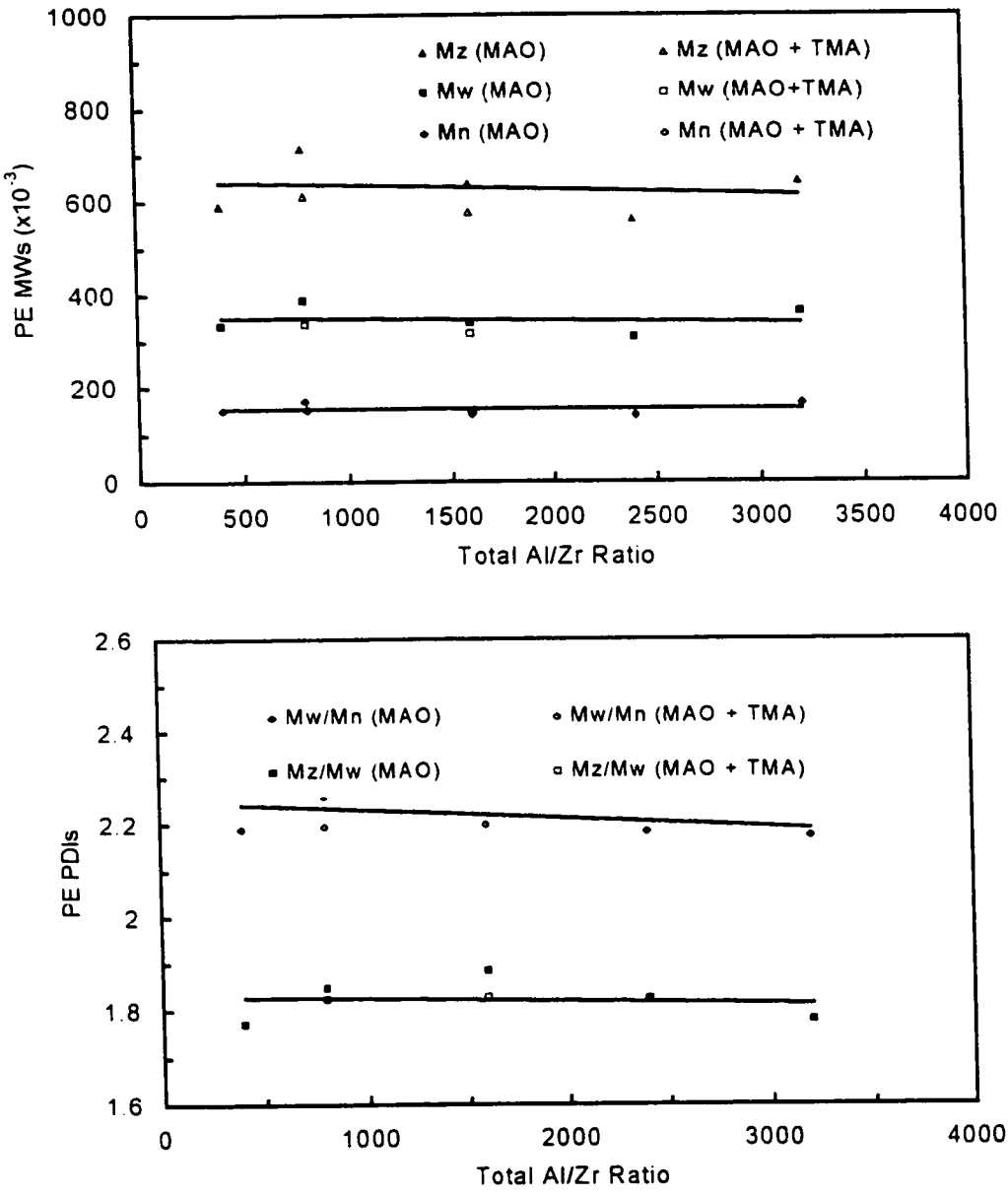

Figure 3.12 Effect of the molar Al/Zr ratio on (A) PE MWs and (B) PE PDIs. The points are experimental data and the lines are linear least-square regression fit to the points. The polymerization conditions were: T = 70 °C, [ethylene] = 0.18 mol/L, [Zr] = 0.65 μM, diluent = toluene.

Table 3.3. Effect of additional TMA on Catalyst Activities

MAO Al/Zr	TMA Al/Zr RAtio	Total Al/Zr	Maximum Activity ($x10^{-3}$) **	Average Activity ($x10^{-3}$) **
1600	0	1600	48.6	13.6
2400	0	2400	53.8	13.7
3200	0	3200	48	13.2
400	0	400	5.4	2
800	0	800	29.6	8.2
400	400	800	17	7.6
400	1200	1600	24.4	11.4

* Polymerization conditions: temperature = 70°C; $[Zr]_0$ = 0.65 μM; P_{Eth}= 35 psia; solvent = toluene

** Activity = kgPE/(gZr·[ethylene]·hr)

Table 3.4. Effect of additional TMA on PE MWs and PDIs

MAO Al/Zr	TMA Al/Zr RAtio	Total Al/Zr	M_n ($x\ 10^{-3}$)	M_w ($x\ 10^{-3}$)	M_z ($x\ 10^{-3}$)	M_w/M_n	M_z/M_w
1600	0	1600	147	337	637	2.29	1.88
2400	0	2400	141	307	561	2.18	1.83
3200	0	3200	166	361	643	2.17	1.78
400	0	400	152	333	590	2.19	1.77
800	0	800	171	387	714	2.26	1.85
400	400	800	153	335	612	2.19	1.82
400	1200	1600	143	315	576	2.20	1.83

* Polymerization conditions: temperature = 70°C; $[Zr]_0$ = 0.65 μM; P_{Eth}= 35 psia; solvent = toluene

** Activity = kgPE/(gZr·[ethylene]·hr)

3.4.5 *2^3 Designed Experiment for Comparison of MAO to Temperature and Al/Zr Ratio*

In order to compare the performance of MAO and MMAO at different Al/Zr and polymerization temperature levels and to see if the previous conclusions on the aluminoxane co-catalyst can be generalized in the semi-batch polymerization of ethylene using Cp_2ZrCl_2 in toluene, a 2^3 designed experiment (8 runs) was performed (Box, Hunter and Hunter, 1978). This experiment was designed to determine how polymerization activity and PE MWs and PDIs were effected by a) aluminoxane type (MAO = 0 % iBu and MMAO = 30 % iBu), b) Al/Zr ratio (800 and 2400), and c) polymerization temperature (50 and 90 °C). Table 3.5 summarizes the experimental conditions for the runs performed in this study while Table 3.6 summarizes the polymerization results. All analysis and plot generations were performed using Minitab for Windows v.11.

Figure 3.13 gives the effects plots generated from this analysis which illustrate how the maximum and average activities of polymerization are affected by the 3 variables of a) temperature, b) Al/Zr ratio and c) iBu content. For these effects plots, of the 8 total runs in the designed experiment, 4 are averaged at each of the levels i.e. for the maximum activity versus temperature, of the 4 different runs performed at 50 °C the average maximum activity value is plotted and of the 4 different runs performed at 90 °C the average maximum activity value is plotted, with a line drawn between the two average values to help visualize the trend. From this analysis we see that both the maximum and average activities increase

with increasing temperature, significantly with increasing Al/Zr molar ratio, and decreases slightly with increasing the iBu content in aluminoxane. Thus, for the designed experiments MAO and MMAO with iBu content up to 30% give very similar activities in the temperature range of 50-90 °C with the activities sharply increased with increasing aluminoxane concentration or Al/Zr ratio. Note: a further increase in the iBu content above 30% will significantly reduce the activity (refer to Figure 3.5).

Figure 3.14 gives the various effects plots for the PE MWs. The PE MWs (M_n, M_w, and M_z) were found to depend only on polymerization temperature and to be rather insensitive to the iBu content and Al/Zr molar ratio. Figure 3.15 gives the various effects plots for the PE PDIs which were found to be independent of temperature, Al/Zr ratio, and iBu content of the MAO (Note that the PDIs vary within small ranges of less than 0.2 which as we saw earlier in the GPC reproducibility study are not significant). We can safely conclude that the PE produced under these conditions with Cp_2ZrCl_2 in toluene approximates Flory's most probable distribution for the ranges studied.

Table 3.5. Experimental runs in comparison of MAO and MMAO in 2^3 designed experiment

Run Number	Polymerization Temperature (°C)	Al/Zr Ratio	iBu Content
1	50	800	0
2	50	2400	29
3	50	800	29
4	90	2400	0
5	90	800	29
6	90	800	0
7	90	2400	29
8	50	2400	0

* Polymerization conditions: $[Zr]_0$ = 0.65 μM, P_{Eth}= 35 psia; solvent = toluene

Table 3.6. Polymerization results for designed experiment

Run #	Max. Activity ($x10^{-3}$) **	Average Activity ($x10^{-3}$) **	M_n ($x\ 10^{-3}$)	M_w ($x\ 10^{-3}$)	M_z ($x\ 10^{-3}$)	M_w/M_n	M_z/M_w
1	11.6	4.3	124	262	470	2.1	1.79
2	13.3	6.7	162	376	696	2.32	1.85
3	8.5	4	176	431	871	2.45	2.02
4	60	19.4	73	158	269	2.17	1.70
5	2.6	0.1	53	116	191	2.17	1.65
6	5.1	0.8	65	138	232	2.12	1.68
7	58.5	20.4	77	167	285	2.17	1.70
8	19.6	6.1	152	334	620	2.2	1.86

** Activity = kgPE/(gZr·[ethylene]·hr)

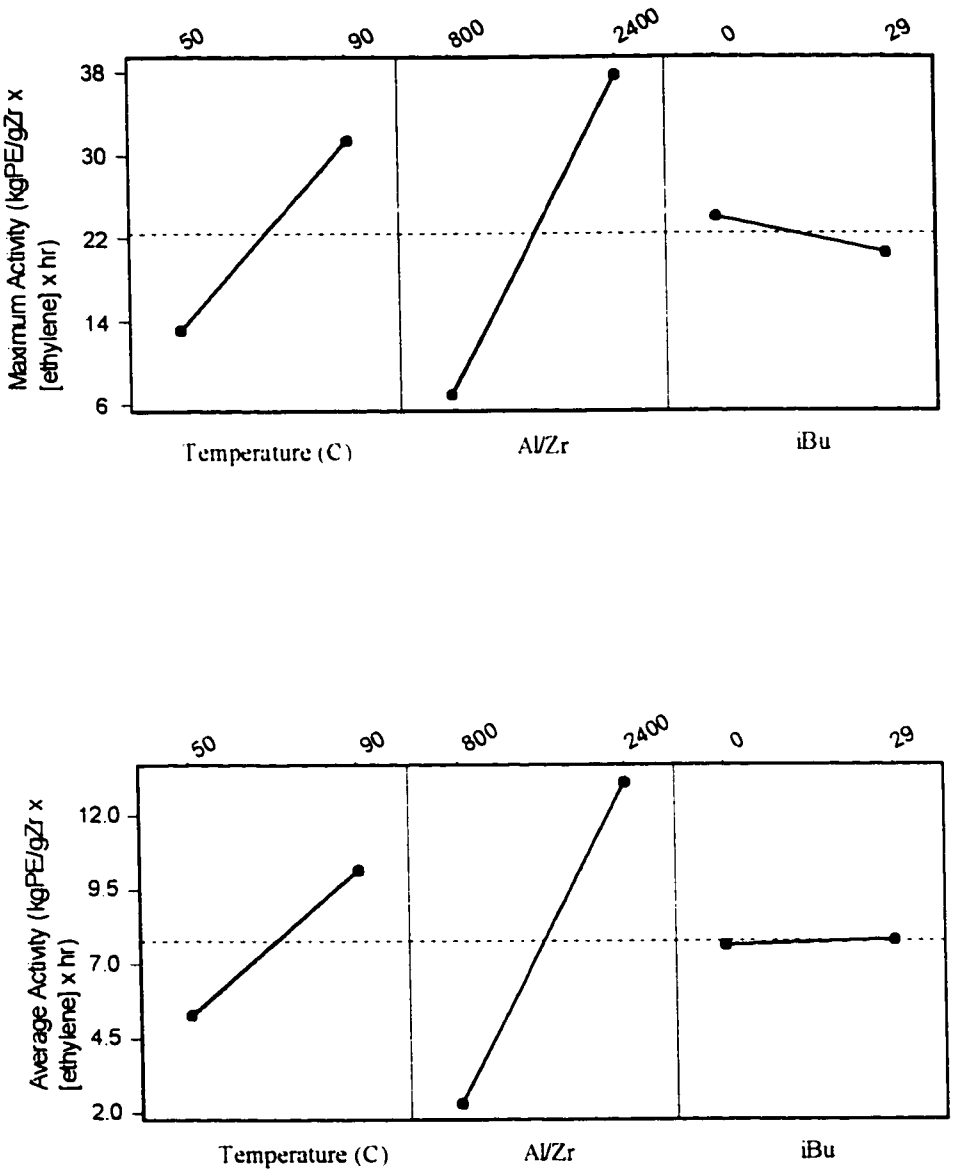

Figure 3.13 Effects plots for (A) maximum catalyst activity and (B) average catalyst activity in the polymerization of ethylene utilizing Cp_2ZrCl_2. The polymerization conditions were P_{ETH} = 35 psia, [Zr] = 0.65 μM, diluent = toluene.

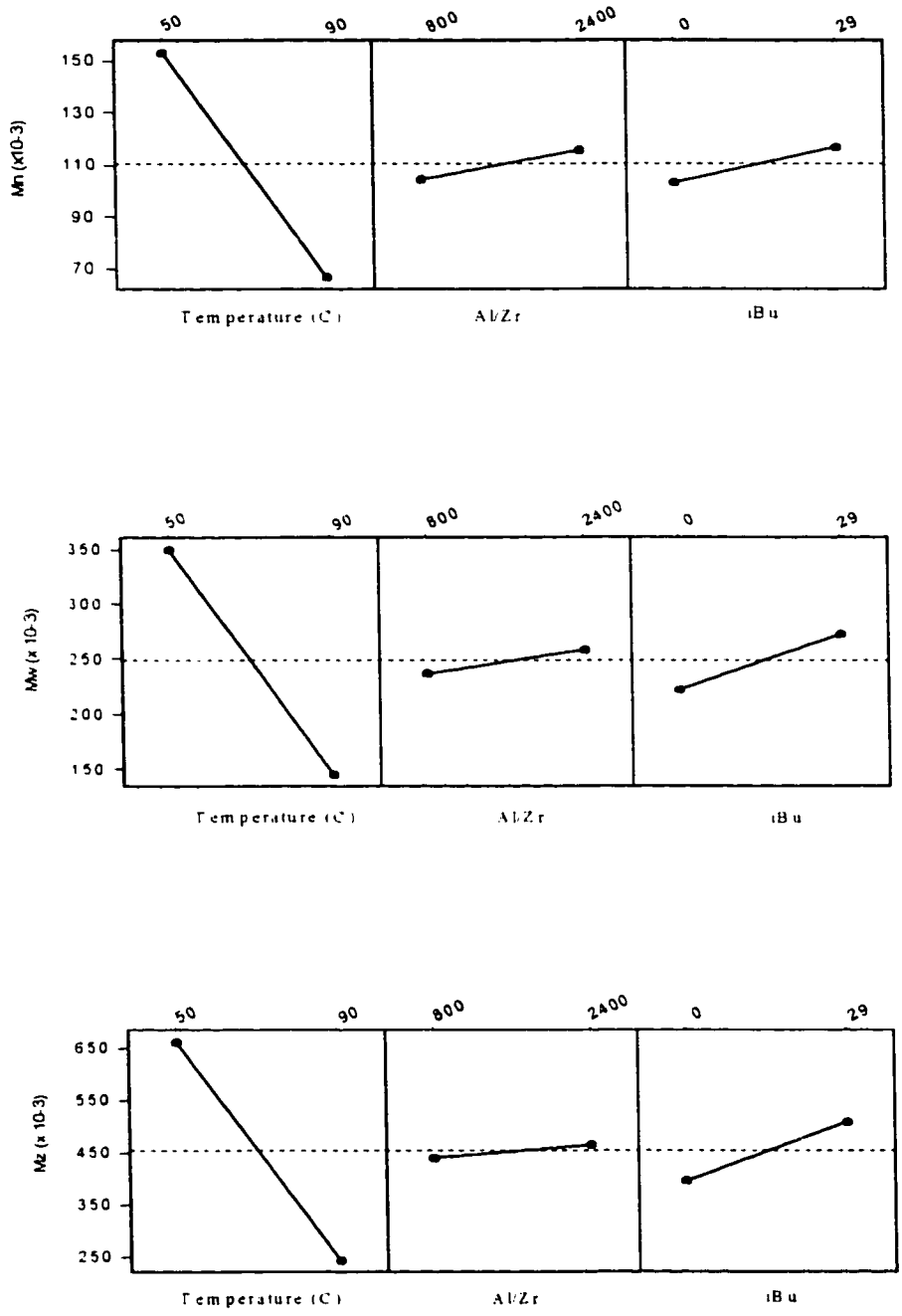

Figure 3.14 Effects plots of PE (A) M_n (B) M_W and (C) M_Z in the polymerization of ethylene utilizing Cp_2ZrCl_2. The polymerization conditions were P_{ETH} = 35 psia, [Zr] = 0.65 μM, diluent = toluene.

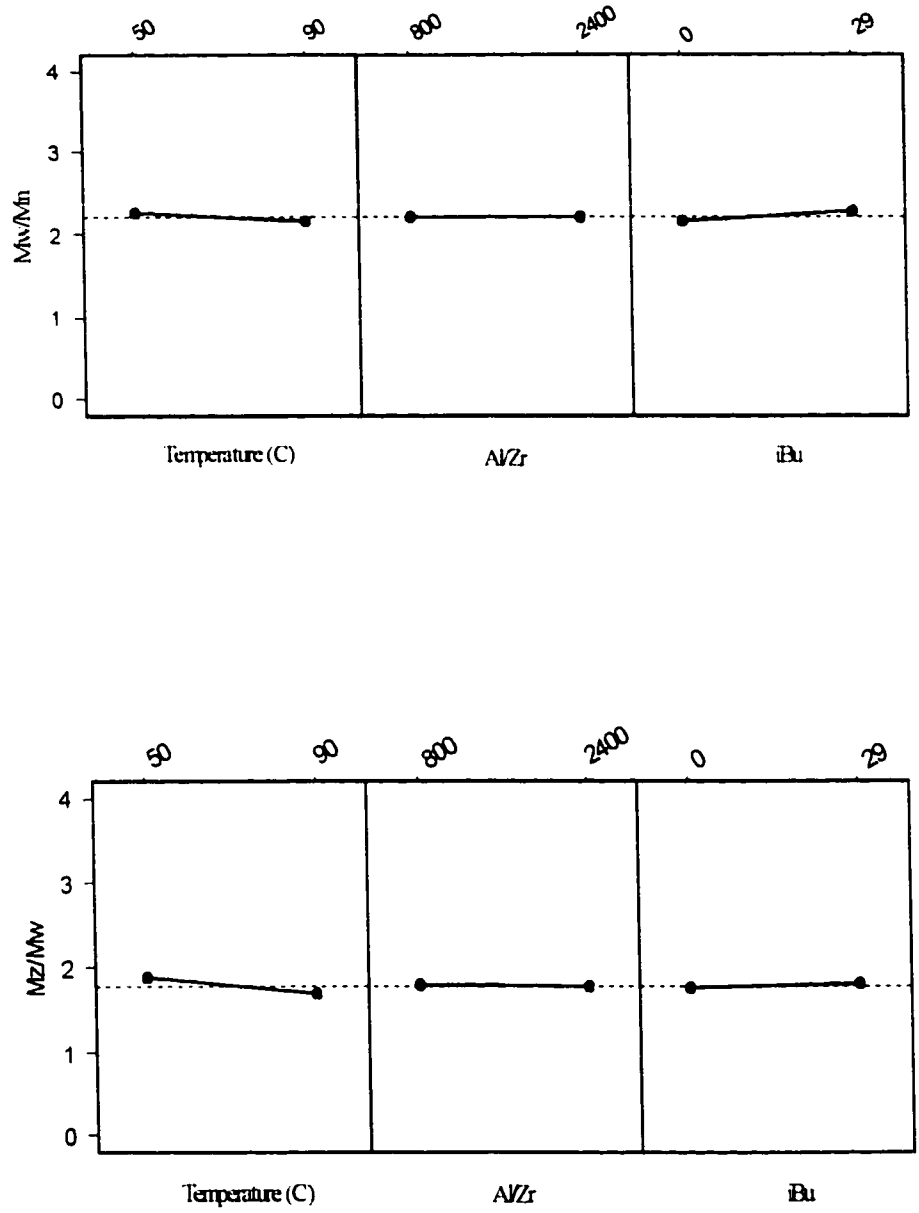

Figure 3.15 Effects plots of PE (A) M_W/M_n and (B) M_Z/M_W in the polymerization of ethylene utilizing Cp_2ZrCl_2. The polymerization conditions were P_{ETH} = 35 psia, [Zr] = 0.65 μM, diluent = toluene.

3.5 Discussion

Although there has been data published in the literature about the effect of aluminoxane structure on polymerization activity, very little information is available as to the effect of aluminoxane type, concentration and structure on the PE MWD. As each site-type produces PE with a M_w/M_n PDI = 2.0 and M_z/M_w PDI = 1.5, as defined by Flory's most probable distribution (Flory, 1953), careful examination of the GPC traces of PE produced with different types and concentrations of aluminoxane provides definitive information on the active catalytic site-type(s) and if those active site-type(s) are being effected by the structure and concentration of the aluminoxane co-catalyst.

Increasing the iBu content in aluminoxane was found to only minimally decrease the Cp_2ZrCl_2 catalyst activity in the polymerization of ethylene over the range of 0-30 % whereas 100 % iBu content (or IBAO) was found to give very low activities. The iBu groups of MMAO or IBAO which alkylate zirconocene catalyst to initiate polymerization, may give a less active cationic center than the cationic center formed when the CH_3 group of plain MAO alkylates it. The iBu alkylated form of zirconocene catalyst presumably has a significantly higher activation energy for the first few steps of ethylene insertion. This higher barrier to ethylene insertion may be due to both steric and electronic considerations. Although the iBu content in aluminoxane affected the activity of polymerization, no significant effect was observed on the PE MWD. For all of the various aluminoxane co-catalysts studied, with both known and unknown compositions,

the PE MWD was unaffected in the semi-batch polymerization of ethylene with Cp_2ZrCl_2 from 50-90 °C.

Due to the high levels of aluminoxane necessary for polymerization (Al/Zr ratios upwards of 1000:1 were most reproducible) MAO is believed to act as a scavenger mopping up active-site impurities in the diluent like O_2 and H_20. Aluminoxanes are known for their ability to react with the impurities O_2 and H_2O (Pasynkiewicz, 1990; Belov, 1995). As metallocene polymerization is essentially cationic in nature, this form of polymerization is extremely sensitive to impurities which would react with the active site and kill polymerization. In order to have a significant active-site/impurity ratio, a sufficient amount of aluminoxane must be present in order to mop up impurities in the diluent for a reproducible polymerization.

In the evolution of metallocene polymerization of olefins from academic interest to commercial success, it has been necessary to reduce the amount of MAO co-catalyst in order to reduce material costs and minimize separation problems. Chien has reported that approximately 90 % of MAO can be replaced with traditional alkylaluminum co-catalysts with little effect on the catalyst performance towards the polymerization of ethylene (Chien & Wang, 1988). We found that addition of extra TMA to MAO gave significantly lower activity than pure MAO at the same total Al/Zr molar ratio. We also found that addition of extra TMA to MAO had no effect on the PE MWD when ethylene was polymerized with Cp_2ZrCl_2/MAO/TMA.

For all the different aluminoxanes studied here, and for all the different MAO and TMA concentrations, it is clear that the role of MAO or TMA/MAO mixture is that of a co-catalyst in the activation of the catalyst. Our results are consistent with the idea that depending on co-catalyst structure, concentration, presence of additives, etc., the aluminoxane forms different concentrations of active cationic catalytic site-types. The greater the number of active cationic catalyst site-types the higher the polymerization activity. However, under conditions where the site types are not starved for monomer, and termination of polymer chains is mainly due to β-hydride elimination and transfer to monomer, the PE MWD is independent of the number of active catalyst site-types. There is no evidence that the aluminoxane is actively involved in the active cationic catalyst site-type once formed as the catalyst termination to propagation ratio, τ, is unaffected by both type and concentration of MAO, and the addition of any extra TMA. In all cases Flory's most probable distribution was approximated for polymerization with a single site type catalyst with resultant PE M_w/M_n values approaching 2.0 and M_z/M_w approaching 1.5 as predicted. There was also no evidence from this study that chain transfer to Al is occurring to any significant extent for the termination of polymer chains and hence may be ignored in any kinetic analysis. MAO may also act as a scavenger in the removal of impurities from the polymerization mixture and may, as an oligomer or polymeric form, have a role in the prevention of the precipitation of polymer chains.

The fact that the structure and type of aluminoxane show no effect on the PE MWD lead us to believe that the active cationic form of the metallocene catalyst Cp_2ZrCl_2 is not coordinated with the active anionic form of the co-catalyst MAO. The active MAO is most likely in the form of a non-coordinating anion, similar to that of the non coordinating anion, $CH_3B(C_6F_5)_3^-$, which is formed upon reaction of tri(pentafluorophenyl)boron and a metallocene dimethyl compound. This anion is often used as the co-catalyst of choice in the polymerization of olefins with a purely cationic metallocene such as the Dow Chemical Company's constrained geometry catalyst (Lai et al., 1993). To be a non-coordinating anion, the coordination of the anionic co-catalyst to the metal center must not be competitive with the coordination of the olefin to the metal center. It has been found by electrochemical and optical spectroscopy means that MAO forms an exceptionally non-coordinating anion in toluene, even more non-coordinating than $CH_3B(C_6F_5)_3^-$ anion (Siedle, 1995). Clearly, if the coordination of aluminoxane co-catalyst was competitive with coordination of ethylene to the active form of zirconocene complex, changes in the aluminoxane structure and concentration would affect the catalyst termination to propagation ratio, τ, and one would observe changes in the PE MWD, which were not observed.

3.6 Conclusions

Aluminoxane structure and any added stabilizers were found to have no effect on the catalytically active zirconocene site type. The type of aluminoxane influenced the activity of the catalyst with generally, MAO > MMAO >> IBAO for polymerization activity. By increasing the MAO concentration (increasing Al/Zr molar ratio), the polymerization activity was found to increase up to a maximum at an Al/Zr ratio of 2400. The studied polyethylene MWs and PDIs were found not to vary with MAO type or concentration. Use of TMA, along with MAO, gives lower activity than MAO by itself for a given Al/Zr molar ratio but has no effect on MWs or PDIs of the formed PE.

Our results, by carefully studying the PE MWD and catalytic activity, agree with the hypothesis of a single active cationic metallocene site-type for the simple metallocene system Cp_2ZrCl_2/MAO/TMA. For the polymerization of ethylene with zirconocene dichloride, the aluminoxane was found to function solely as a co-catalyst in activating the catalyst and was not found to be involved in the catalyst site-type having no effect on the termination to propagation ratio τ.

3.7 Acknowledgments

We greatly appreciate the financial support from the Natural Sciences and Engineering Research Council of Canada (NSERC) for this work. We also thank and Dr. Kris Kostanski for analysis of PE samples by GPC.

3.8 Notation

CCD	Chemical Composition Distribution
DIBAL-O	Tetraisobutyldialuminoxane
IBAO	Isobutylaluminoxane
MAO	Methylaluminoxane
MMAO	Modified methylaluminoxane
MWD	Molecular weight distribution
PDI	Polydispersity index
PE	Polyethylene
PS	Polystyrene
GPC	Gel permeation chromatography
TCB	Tri-chlorobenzene
TIBA	Triisobutylaluminum
TMA	Trimethylaluminum
τ	termination/propagation ratio

3.9 Literature Cited

Andresen, A.; Cordes, H.G.; Herwig, J.; Kaminsky, W.; Sinn, H.; Vollmer, H.J. *Angew. Chem. Int. Ed. Engl.*, **1976**, 15, 630.

Barron, A.R. *Macromol. Symp.* **1995**, 97, 15.

Belov, G.P.; Korneev, N. *Macromol. Symp.*, **1995**, 97, 63.

Boleslawsky, M.; Pasynkiewicz, S.; Kunicki, A.; Serwatowski, J. *J. Organometal. Chem.*, **1976**, 116, 285.

Box G.; Hunter,W.; Hunter, J. *Statistics for Experimenters-An Introduction to Design, Data Analysis, and Model Building*, John Wiley & Sons, 1978.

Box, G.; Draper, N. *Empirical Model-Building and Response Surfaces*, John Wiley & Sons, 1987.

Charpentier, P.; Hamielec A.E.; Brook, M.; Zhu, S. *Submitted*, **1997**.

Chien, J.C.W.; Wang, B.P. *J. Polym. Sci. Polym. Chem. Ed.* **1988**, 26, 3089.

Crapo, C.C.; Malpass, D.B. *U.S. Patent* 4,960,878, **1990**

Crapo, C.C.; Malpass, D.B. *U.S. Patent* 5,041,584, Aug. 20, **1991**.

Deavenport, D.L.; Hodges; J.T.; Malpass, D.B.; Tran, N.H. *U.S. Patent* 5,041,585, **1991**

Eisch, J.J.; Pombrik, S.I.; Zheng, G.-X. *Organometallics*, **1993**, 12, 3856.

Flory, P.J. *Principles of Polymer Chemistry*; Cornell University Press, Ithaca, New York, 1953.

Giannetti, E.; Nicoletti, G.M.; Mazzocchi, R. *J. Polym. Sci. Polym. Chem. Ed.* **1985**, 23, 2117.

Hagendorf, W.; Harder, A.; Sinn, H. *Macromol. Symp.*, **1995**, 97, 127.

Hamielec, A. E.; Soares, J.P.; *Prog. Polym. Sci.* **1996**, 21, 651.

Harlan, C.J.; Mason, M.R., Barron, A.R. *Organometallics*, **1994**, 13, 2957.

Howie, M.S. Proceedings of MetCon'93, May 26-29, 1993 Houston TX, USA, p. 253.

Jordan, R.F.; Bajgur, C.S.; Willett, R.; Scott, B. *J. Am. Chem. Soc.* **1986**, 108, 7410

Kaminsky, W. *Angew. Chem., Int. Ed. Engl.*, **1980**, 19, 390

Kaminsky, W. in *Transition Metal Catalyzed Polymerization*, Quirk, R.P., ed., Vol. 4, MMI Press, London, 1983, pp. 225-244.

Kaminsky, W.; Miri, M.; Sinn, H.; Woldt, R. *Makromol. Chem. Rapid Commun.* **1983**, 4, 417.

Kaminsky, W.; Hahnsen, H. *U.S. Pat.* 4,544,762, **1985**

Kaminsky, W. in *Catalytic Polymerization of Olefins*, Keii, T.; Soga, K. eds., Kodausha-Elservier: Tokyo, 1986; pp 293-304.

Kaminsky, W.; Kulper, K.; Niedoba, S. *Makromol. Chem., Makromol. Symp.* **1986**, 3, 377.

Kaminsky W. ed, *Transition Metals and Organometallics as Catalysts for Olefin Polymerization*, Springer-Verlag, New York Proceedings of an

International Symposium, Hamburg, FRG, September 21-24, 1987, pages 257-268.

Kaminsky, W.; Bark, A.; Spiehl, R.; Moller-Lindenhof, N.; Niedoba, S. in *Transition Metals and Organometallics as Catalysts for Olefin Polymerization*, Kaminsky,W.; Sinn, H., eds., Springer-Verlag, Berlin, 1988, pp. 291-301.

Kaminsky,W.; Steiger, R. *Polyhedron* **1988**, 7, 2375.

Kaminsky, W.; Kulper, K.; Brintzinger, H.H.; Wild, F.R.W.P. *Angew. Chem. Int. Ed. Engl.* **1992**, 31, 1347.

Lai, S.Y.; Wilson, J.R.; Knight, G.W.; Stevens, J.C.; Chum, P.W.S. (to Dow Chemical Co.). *U.S. Patent* 5,272,236, **1993**.

Long, W.P.; Breslow, D.S. *Liebigs Ann. Chem.* **1975**, 463.

Manyik et.al. *U.S. Patent* 3,300,458, **1967**.

Mason, M.R.; Smith, J.M.; Bott, S.G.; Barron, A.R. *J. Am. Chem. Soc.* **1993**, 115, 4971.

Michiels W.; Munoz-Escalona, A. *Macromol. Symp.* **1995**, 97, 171.

Pasynkiewicz, S. *Polyhedron*, **1990**, 9,429.

Razuvaev, G.A. Sangalov, J.A. *Izv. Akad. Nauk USSR, Ser. Chim*, **1975**, 19, 2547.

Reichert, K.H.; Meyer, K.R.; *Makromol Chem*, **1973**, 169, 163.

Reichert, K.H., in *Transition Metal Catalyzed Polymerization*, Quirk, R.P., ed., Vol. 4, MMI Press, London, 1983, pp. 465-493.

Resconi, L.; Bossi, S. *Macromolecules*, **1990**, 23, 4489.

Schoenthal; G. W.; Slaugh; L. H., *U.S. Patent* 4,730,071, **1988**.

Schoenthal; G. W.; Slaugh; L. H., *U.S. Patent* 4,730,072, **1988**.

Siedle, A.R.; Hanggi, B.; Newmark, R.A. *Macromol. Symp.* **1995**, 89, 299.

Sinn, H.; Kaminsky, W. *Adv. Organomet. Chem.* **1980**, 18, 99.

Sinn, H.; Kaminsky, W.; Volmer, H.J.; Woldt, R. *Angew. Chem. Int. Ed. Engl.*, **1980**, 19, 390.

Sinn, H.; Bliemeister, J.; Clausnitzer, D. Tikwe, L.; Winter, H.; Zamke, O. in *Transition Metals and Organometallics as Catalysts for Olefin Polymerization*, Kaminsky,W.; Sinn, H., ed., Springer-Verlag, Berlin, 1988, pp. 257.

Sinn, H., *Macromol. Symp.* **1995**, 97, 27.

Soares, J.P.; Hamielec, A. E. *Macromol. Theory Simul.* **1996**, 5, 547.

Stockmayer, W.H. *J.Chem.Phys.*, **1945**, 13, 199.

Tritto, I.; Li, S.; Sacchi, M.C.; Zannoni, G. *Macromolecules* **1993**, 26, 26.

Tritto, I.; Sacchi, M.C.; Locatelli, P. *Macromol. Symp.* **1995**, 89, 289.

Tritto, I.; Sacchi, M.C.; Locatelli, P.; Li, S.X. *Macromol. Symp.* **1995**, 97, 101.

Tritto, I.; Li, S.X.; Sacchi, M.C.; Locatelli, P.; Zannoni, G. *Macromolecules*, **1995**, 28, 5358.

Tritto, I.; Sacchi. M.C. Locatelli, P.; Li, S.X. *Macromol. Chem. Phys.* **1996**, 197 1537.

Welborn, Jr.; H.C.; Tornqvist; E.M. *U.S. Pat* 4,665,208, **1987.**

Wild, F.R.W.P.; Zsolnai, L.; Huttner, G.; Brintzinger, H.H. *J. Organomet. Chem.*, **1982**, 232, 233.

CHAPTER 4 CONTINUOUS SOLUTION POLYMERIZATION OF ETHYLENE USING METALLOCENE CATALYST SYSTEM Cp_2ZrCl_2/MMAO/TMA

P.A. Charpentier, S. Zhu*, A.E. Hamielec,

Department of Chemical Engineering

McMaster University, Hamilton, Ontario, Canada L8S 4L7

M. A. Brook

Department of Chemistry

McMaster University, Hamilton, Ontario, Canada L8S 4M1

Paper accepted by *IECR* August, 1997.

Keywords: CSTR, solution polymerization, metallocene catalyst, zirconocene dichloride, methylaluminoxane, polyethylene

* Author to whom correspondence should be addressed.

Email: zhuship@mcmaster.ca.

Phone: (905) 525-9140 ext 24962.

Fax: (905) 528-5114

4.1 Abstract

A high pressure, high temperature continuous stirred-tank reactor (CSTR) system having approximately an ideal residence time distribution (RTD) has been set up for the polymerization of olefins utilizing metallocene catalysts. Preliminary experiments of ethylene polymerized with the metallocene catalyst system Cp_2ZrCl_2/MMAO/TMA in toluene at 1,500 psig have been carried out. The reactor system showed good control over temperature, pressure and ethylene feed rate. The steady state was obtained after 4 mean residence times (4 τ's). With increasing Cp_2ZrCl_2 concentration, the molecular weight (MW) of polyethylene (PE) decreased and the catalyst activity (kg PE/([ethylene] g catalyst)) increased. With increasing temperature between 140-200 °C, the MW of PE decreased and molecular weight distribution (MWD) polydispersity increased. PE with weight-average molecular weight (M_w) 18,000-52,000 g/mol were obtained. The catalyst activity decreased with increasing temperature with an apparent activation energy of -93 kJ/mol. The deactivation of the catalyst is first-order with the rate constant $k_d=2.1\times10^{-3}$ s^{-1} at 140 °C. The rate constants of propagation and β-scission at 140 °C are $k_p=5\times10^{3}$ $(M\cdot s)^{-1}$ and $k_{tr,\beta}=3$ s^{-1}.

4.2 Introduction

In industry, the manufacture of polyolefins is performed exclusively with continuous reactors while most academic researchers can only produce resins with batch or semi-batch autoclaves. We have therefore setup a continuous stirred tank reactor (CSTR) for the polymerization of olefins utilizing metallocene catalysts. The work reported here utilized a simple metallocene catalyst system, Cp_2ZrCl_2/MMAO/TMA for the polymerization of ethylene in solution in our CSTR at 1,500 psig.

In the past few years, metallocene catalysts have revolutionized the polymer industry for producing both specialty and commodity polyolefins (Thayer, 1995). Besides the large resin manufacturers individually producing metallocene resins, many joint ventures have developed to produce, market and sell gas phase HDPE and LLDPE, as well as isotactic and syndiotactic PP, syndiotactic PS, and EPR and EPDM elastomers using metallocene catalysts (Karol, 1995, Thayer, 1995).

The advantages of metallocene catalysts include extremely high activities and narrow molecular weight distributions (MWDs) with polydispersity indexes (PDIs) approaching 2 (Kaminsky et al., 1983; Chien and Wang, 1988) as defined by Flory's most probable MWD (Flory, 1953). They also give extremely narrow chemical composition distributions (CCDs) for copolymers as defined by Stockmayer's bivariate distribution (Stockmayer, 1945). This unique behavior is a

result of the metallocene catalyst having a single site-type. This may be compared to a traditional Ziegler-Natta catalyst (e.g. $TiCl_4$/TMA) which has multiple site-types. Each site-type of the metallocene catalyst gives a unique activity, chain transfer to propagation rate, reactivity ratios and stereoselectivity so that by variation of catalyst site structure, each of these can be tailored to give a polymer with a desired blend of properties.

Monocyclopentadienyl type metallocenes allow high incorporation of higher α-olefin comonomers to readily control the density of a polymer not achievable with a traditional heterogeneous Ziegler-Natta (Z-N) catalyst. These catalysts can also polymerize and copolymerize many unusual monomers and combinations of monomers that are not possible with traditional Z-N catalysts. As a result, the use of metallocene catalysts allows polymer products with uniform composition and specific desired properties These novel polymers are only beginning to be studied in industry and academia and are providing physical, chemical and electrical properties that are very promising.

The utilization of certain metallocenes also provides the ability to control the melt rheology of the formed polyolefin by incorporating long chain branches (LCBs) (Lai et al., 1993). A CSTR is most desirable for producing polyolefins with LCBs and in a later paper we will report on the polymerization of ethylene utilizing Dow Chemical's constrained geometry catalyst with our research CSTR system.

4.3 Experimental

4.3.1 *Reactor Setup*

A high pressure, high temperature reactor system has been set up as shown in Figure 4.1. The reactor is an Autoclave Engineers 3" inner diameter 600 mL autoclave utilizing both a 6-blade 1.25" Dispersimax impeller and a 1" 45° pitched-blade turbine impeller. The reactor system can be used at a pressure up to 3,000 psi and 300 °C. Three Neptune 500-S-N3-FA chemical metering pumps are used for the high-pressure pumping of catalyst, co-catalyst and co-monomer. A Neptune 500-D-N3-FA metering pump is used for high-pressure pumping of diluent. The pumps are rated for up to 3,000 psi, run at 1,800 rpm and have 1 HP explosion-proof motors. The compressor for the ethylene feed is an Aminco Model 46-14025-1 vertical unit consisting of an 8-inch single-end air operator directly connected to a 9/16 inch diameter hydraulic plunger rated for a maximum operating pressure of 10,000 psi.

The inlet feed enters the reactor from two separate stainless steel (SS 314) dip tubes, one containing the monomer and the other the catalyst and co-catalyst solution. An outlet SS dip tube was used for removal of reactor contents. The inlet dip tubes were sent to the bottom of the reactor near the agitator and the outlet dip tube was placed near the top of the reactor to ensure good mixing of reactants and products. A ratio of the distance from inlet to outlet over the reactor

diameter (L/D) of approximately 1.6 was obtained. All wetted parts in the continuous reactor system are either 316 stainless steel or teflon. All experiments were performed at 1,000 rpm using toluene as solvent and with temperatures high enough to ensure that polymerization was conducted in solution. Tracer studies to measure the residence time distribution (RTD) for our CSTR system are discussed later.

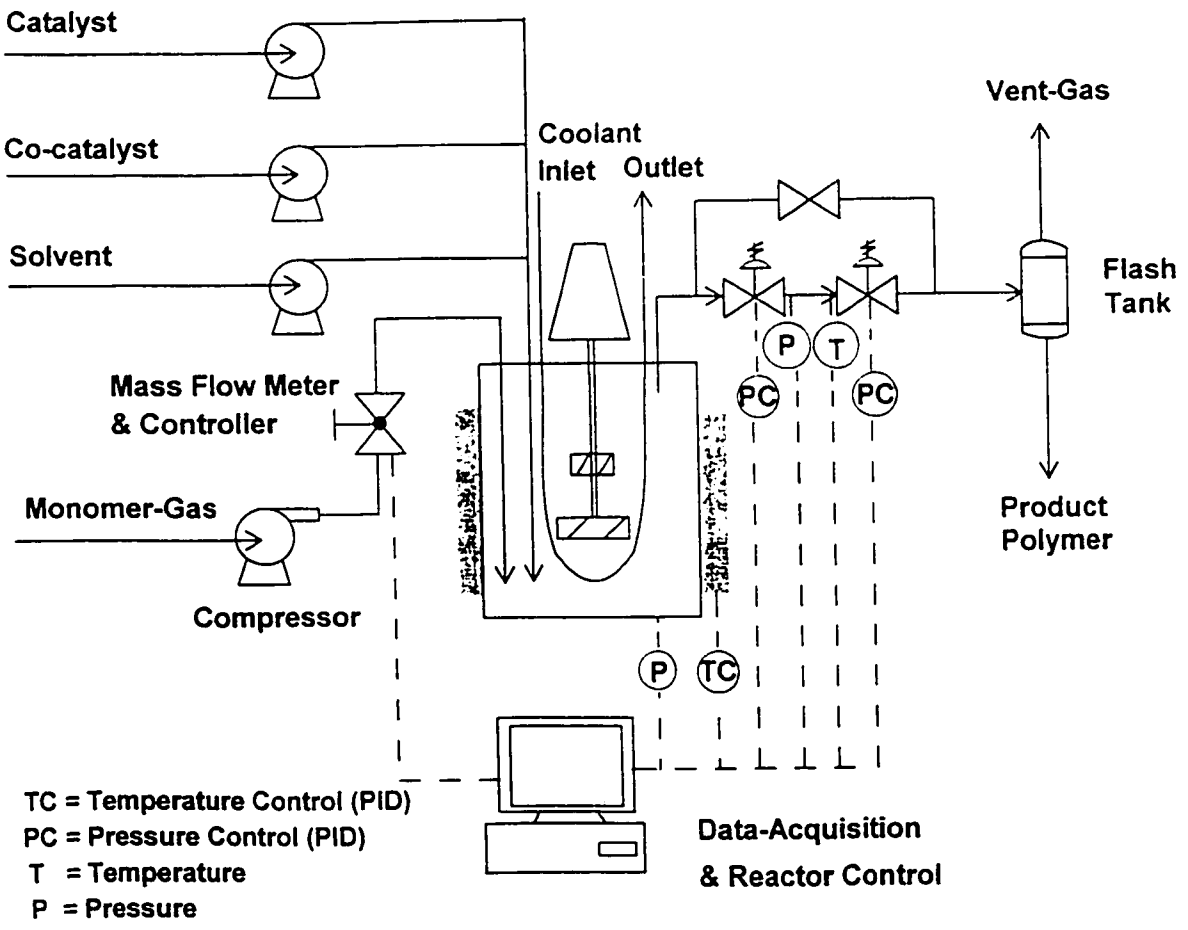

Figure 4.1 Schematic of the research high pressure high temperature CSTR system.

4.3.2 *Polymerization Procedure*

A toluene/Cp_2ZrCl_2/TMA solution was injected into a 1 L catalyst feed tank and a toluene/MAO solution was injected into the co-catalyst feed tank to provide the desired concentrations. Solvent, catalyst and co-catalyst feed tanks were maintained under an inert N_2 blanket throughout the reaction. The Neptune metering pumps were used for pumping the three inlet streams at a rate to give the proper residence time and the desired catalyst and co-catalyst concentrations. The three streams were joined into a single inlet stream at the reactor entrance. All pumps were calibrated at the reaction pressure of 1,500 psig.

The startup procedure consisted of initially heating up the product lines and reactor to the desired reaction temperature. The toluene pump was then started at a low flow rate and the flow rate gradually increased to normally provide 80% of the final toluene flow. Pressure and temperature were monitored closely with alarm settings for pre-defined deviations from the set-point. All reactions were performed at a pressure of 1,500 psig. After pressure and temperature were stabilized, the air-driven ethylene compressor was turned on and ethylene flow was then introduced to the reactor. Next, the catalyst and co-catalyst pumps were started. Once all pumps and ethylene flow were at desired settings, the time of reaction was considered to be 0.

The exiting polymer stream was fed to sampling containers filled with anhydrous ethanol in order to quench the reaction and cool the polymer product. The polymer samples were then filtered and dried under vacuum.

4.3.3 *Reactor Control*

An automated industrial subsystem (OPTO 22) consisting of a 16 I/O points control-enclosure and a brain board and mounting rack purchased from Transduction Ltd. were used for containing data-acquisition and control modules. I/O Modules were also from Transduction Ltd. There are three separate parts for control of the continuous reactor: i) temperature control, ii) pressure control, and iii) control of monomer feed rate.

i) The control of temperature was performed with a modular controller (Autoclave Engineers) with an integrated circuit control board utilizing a PID algorithm in a time proportional heating of an Autoclave Engineers furnace and the time proportional actuation of a solenoid valve for allowing cooling fluid through the cooling loop of the reactor. This type of control was found sufficient to maintain the reaction temperature at set point.

ii) Pressure control of the reactor was performed utilizing the SCADA (Control and Design) mode of Intellution FIX MMI V 6.0 for Windows 95 software purchased from Transduction Ltd. Fisher Type 646 explosion proof transducers receive a 4-20 mA dc input signal from the OPTO subsystem and transmit a proportional 3-15 psig pneumatic output pressure to the 1/4" Badger Type 807 control valves for control of reactor pressure. A PID algorithm was used in the control of the Badger control valves.

iii) Control of the ethylene flow rate was performed with a mass flowmeter and controller (Brooks 5850 TRP) purchased from and calibrated by Trillium

Controls Ltd. with N_2 at an inlet pressure of 1,500 psig and 7.5 standard liters per minute (slpm). A 1-5 Vdc control signal was used to control the ethylene flow by the Brooks MFC.

4.3.4 *Data Acquisition*

Data acquisition was performed by the OPTO 22 subsystem and the reactor and product temperatures were monitored continuously with thermocouples. Signal conditioning was performed on the thermocouple input voltage by the FIX software to give readings in centigrade. Ametek Model 88C explosion-proof mini pressure transmitters were utilized for continuous pressure measurement and to transmit a 4-20 mA proportional signal to the OPTO subsystem for data-acquisition of: 1) reactor pressure (0-5,000 psi), 2) pressure after the first control valve (0-5,000 psig), and 3) ethylene pressure after the compressor (0-3,000 psig) as illustrated in Figure 4.1. The signal conditioning was performed on the proportional signal by the FIX software in a linear fashion. Data-acquisition of the ethylene flow rate was performed by a 1-5 Vdc output from the Brooks mass flow controller which was linearized by the FIX software.

4.3.5 *Materials for Polymerization*

Zirconocene dichloride and 2.0M trimethylaluminum (TMA) in toluene were purchased from Aldrich Chemical and used as received. MMAO-4 was purchased from Akzo-Nobel Corporation and used as received. All manipulations

of catalyst and co-catalyst were performed in a Vacuum Atmospheres glovebox which controls O_2 and H_2O levels down to a few ppm.

Toluene was used as diluent for all reactions and purchased from Caledon Laboratories Ltd. The diluent was dried over a mixture of 5Å and 13X molecular sieves from Fisher Scientific and silica gel from Caledon Labs. The diluent was de-oxygenated by sparging with ultra high purity (UHP) nitrogen. UHP nitrogen (99.999%) and polymerization grade ethylene (> 99.5%) were purchased from Matheson Gas and further purified by passing through columns containing supported CuO from Aldrich to remove O_2, Ascarite from Fisher Scientific to remove CO_2, and finally, Grace-Davidson molecular sieves to remove H_2O.

4.3.6 *RTD Studies*

All studies of the RTD of the reactor system were performed by a pulse injection of dye into the post pump. Oil Blue dye was purchased from Aldrich Chemical and diluted with toluene to the desired concentration to be injected to the reactor. Samples were collected from the reactor effluent over the period of 25 minutes. A Hewlett-Packard 8452A diode array spectrophotometer was used for measuring the absorbance of all samples.

4.3.7 *High Temperature GPC*

All gel permeation chromatography (GPC) measurements were performed on a Waters-Millipore SEC instrument model 150-C high temperature GPC at 140

°C using trichlorobenzene (TCB) as solvent. The following operation conditions were adopted: 1) column and sample compartment temperature, 140 °C, 2) flow rate of mobile phase, 1.0 mL min^{-1}, 3) sample injection volume, 200 μL, 4) no sample spinning, 5) no sample filtering, 6) sample concentration of 0.1 wt% in trichlorobenzene.

Calibration of the high temperature GPC was performed at 140 °C directly with a calibration curve obtained using narrow MWD PE standards purchased from the National Bureau of Standards. Narrow polystyrene (PS) standards were purchased from Tosoh Corporation and broad PE standards were purchased from American Polymer Standards and Polymer Laboratories Ltd., both were used to check the calibration curve. The Mark-Houwink constants for the universal calibration curve were $K=1.21\times10^{-4}$ and a = 0.707 for PS and $K=3.92\times10^{-4}$ and a = 0.725 for PE.

4.4 Results

4.4.1 *RTD Studies*

The residence time distribution function E(t) is characteristic of the mixing that occurs in the chemical reactor (Levenspiel, 1962). The E(t) of a particular reactor can significantly affect the reactor performance so its measurement is crucial. A dye tracer pulse was used to measure the RTD for the research reactor

and the normalized RTD, i.e. $E(\theta)$ is reported. The initial RTD for the first experimental setup was found to give a higher value for $E(\theta)$ at approximately 0.2 τ and 0.75 τ. This indicates both channeling and dead space in the original internal configuration of the reactor and that mixing was not ideal as indicated in Figure 4.2. The research reactor configuration was then altered by removing the original cooling coil and replacing it with a cooling loop which allowed the addition of an additional 1" pitched-blade (45°) turbine agitator to be placed above the original 1.25" dispersimax impeller. This re-configuration of the reactor was found to provide better mixing and very little dead space in the reactor and give a RTD that approximates an ideal CSTR as evidenced in Figure 4.2. The presence of the dispersimax impeller, which is designed for good gas dispersion and axial flow, along with the pitched-blade turbine, gives both axial and radial flow and promotes turbulence. We conclude that the mixing in the experimental reactor sufficiently approaches ideality for a CSTR for our purposes. All experimental polymerization runs reported here were carried out using the second improved reactor configuration.

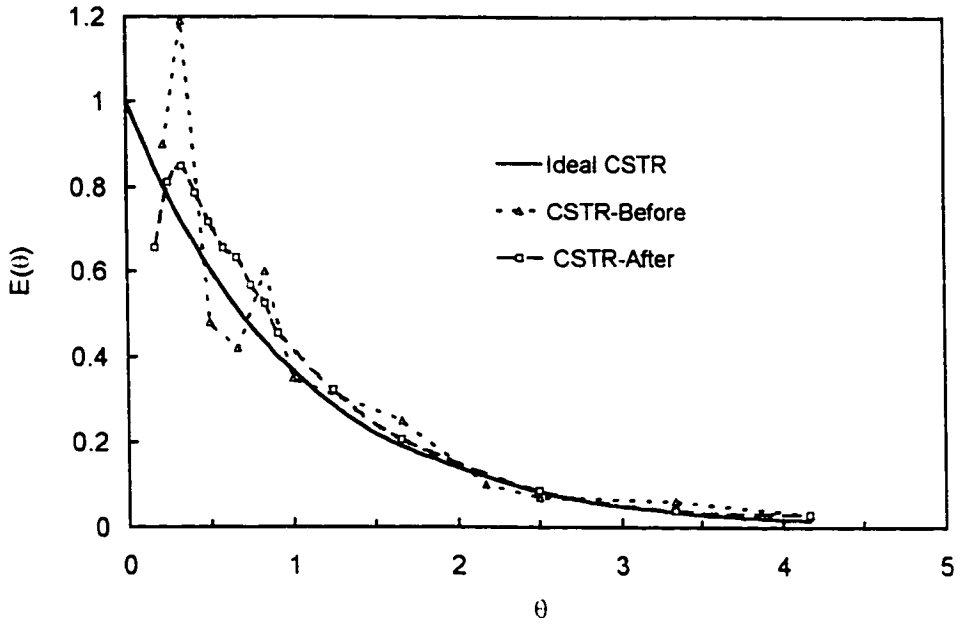

Figure 4.2 Residence Time Distribution (RTD) curves of the research CSTR illustrating a) an ideal CSTR b) the research reactor in its original configuration and c) the research reactor in its final configuration. The points are experimental data.

4.4.2 *Polymerization Runs*

All ethylene polymerization runs were performed at 1,500 psig in toluene utilizing Cp_2ZrCl_2 as catalyst, with MAO and TMA as co-catalysts. The total Al/Zr molar ratio was always maintained at 1,000 with 600 from TMA and 400 from MAO. TMA was mixed with the catalyst solution in the catalyst feed tank and MAO was added to the co-catalyst feed tank (refer to Figure 4.1). Polymerization was initiated within 10 minutes of adding catalyst and co-catalyst to the feed tanks. Table 4.1 summarizes the reactor conditions for all polymerization runs.

Table 4.1. Experimental conditions for the CSTR solution polymerization runs

Run #	P (psig)	T (°C)	Q (mL/min)	$\nu_{Ethylene}$ (g/min)	$[Et]_0$ (mol/L)	τ (min)	$[Zr]_0$ (μM)	[Al]/[Zr]
1	1,500	140	120	7.7	2.3	5	4	1,000
2	1,500	140	120	7.7	2.3	5	2	1,000
3	1,500	140	120	7.7	2.3	5	1	1,000
4	1,500	200	120	7.7	2.3	5	1.5	1,000
5	1,500	180	120	7.7	2.3	5	1.5	1,000
6	1,500	160	120	7.7	2.3	5	1.5	1,000
7	1,500	140	120	7.7	2.3	5	1.5	1,000
8	1,500	140	120	5.6	1.7	5	1.5	1,000
9	1,500	140	120	3.8	1.1	5	1.5	1,000
10	1,500	140	120	1.9	0.6	5	1.5	1,000
11	1,500	140	60	4.2	2.5	10	1.5	1,000
12	1,500	140	80	5.4	2.4	7.5	1.5	1,000

Note: [TMA]/[Zr] = 600, [MAO]/[Zr] = 400, Q = total flowrate of toluene in mL/min, $[Et]_0$ = ethylene concentration in feed, $[Zr]_0$ is the catalyst concentration in feed.

4.4.3 *Polymerization Control and Steady-State Attainment*

For a CSTR operated at steady-state, the polymer product, unreacted monomers and catalytic species leave the reactor continuously, and the temperature and concentrations of all species in the reactor are spatially and time-independent. Figure 4.3 gives the output from the data-acquisition of the experimental CSTR for Run #12. Here we see the three controlled variables of reactor pressure, temperature and ethylene flow rate plotted versus time. It is clear that control of the reactor is excellent with all 3 controlled variables varying within very close tolerances at steady-state. This run is consistent with the control

of all other reported runs. Figure 4.4 illustrates the GPC traces of these samples for the various τ's during the continuous polymerization run. Note that the GPC traces of the four PE samples taken during the course of the reaction at various times are very similar, and in fact, overlap one-another. This indicates that the catalyst site-type is not changing significantly during the polymerization and can be considered constant after 4 τ's. Figures 4.5-4.6 illustrate that the catalyst activity, PE MWs and PDIs are very similar during the polymerization and reach a steady-state value after 4 τ's of running time. All GPC results reported in this paper were taken from PE samples collected between 9-10 τ's after the start of polymerization, when the reactor is clearly under steady-state conditions.

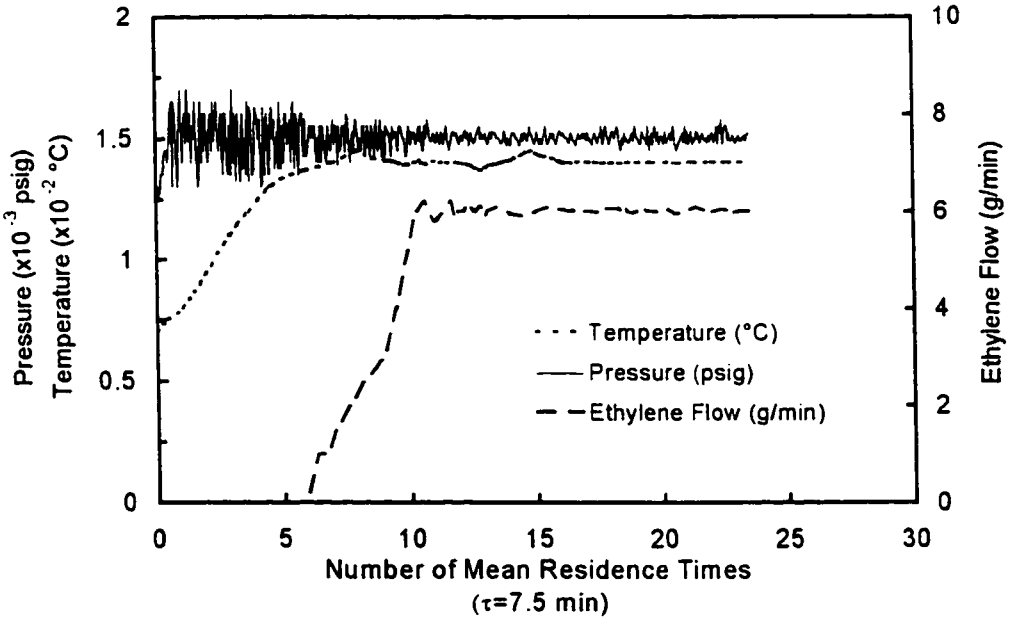

Figure 4.3 Data-acquisition from Run 12 showing traces of the reactor temperature, reactor pressure, and ethylene flow rate from the initial start up of the reactor to the start of polymerization at τ = 10. The polymerization conditions were P = 1500 psig, T = 140 °C, ν_E = 6 g/min, [Zr] = 1.5 μM, Al/Zr = 1000, and τ = 7.5 minutes.

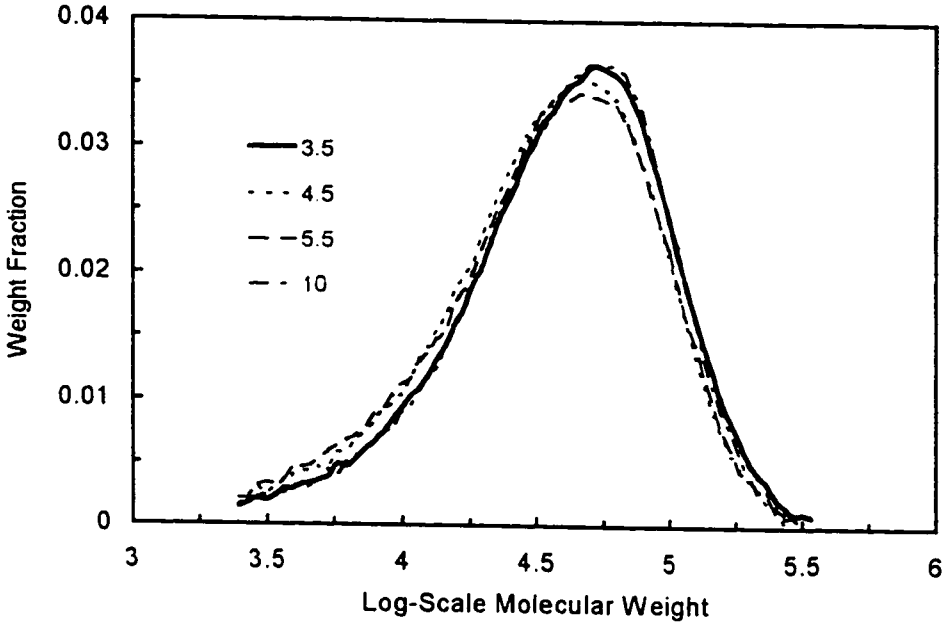

Figure 4.4 High temperature GPC traces of PE samples taken from Run 12. Four PE samples were taken at various times during the polymerization run corresponding to t = 3.5, 4.5, 5.5, and 10 mean residence times (τ's) after the start of polymerization. The polymerization conditions were the same as Figure 3.

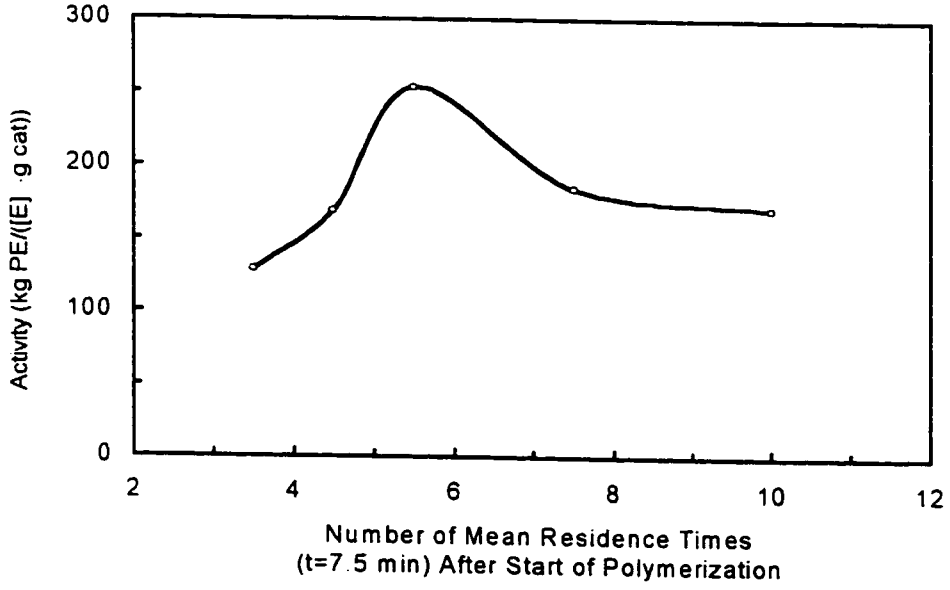

Figure 4.5 Effect of polymerization time on the catalyst activity corresponding to t = 3.5, 4.5, 5.5, 7.5 and 10 mean residence times (τ's) after the start of polymerization taken from Run 12. The points are experimental data. The polymerization conditions were the same as Figure 3.

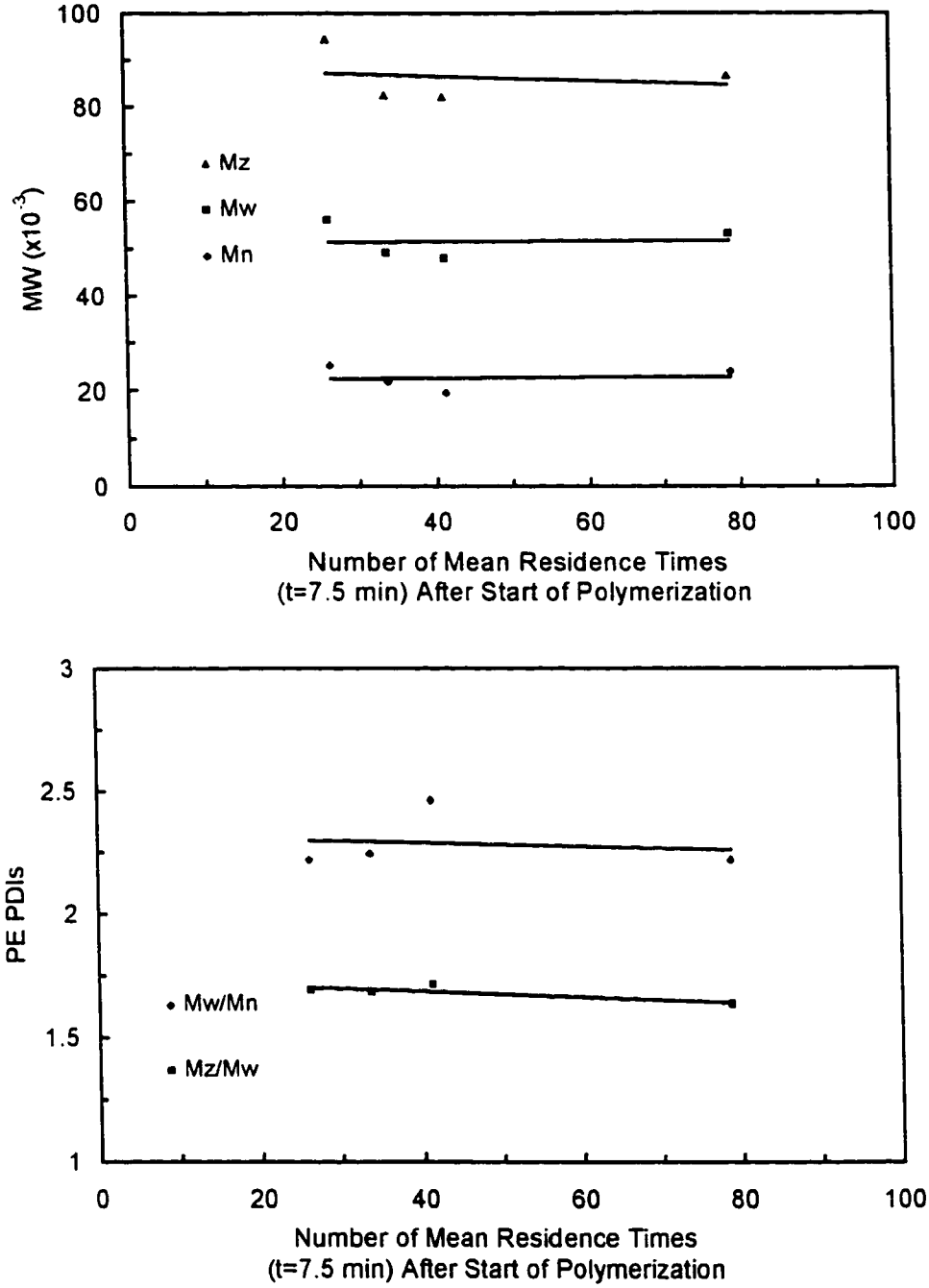

Figure 4.6 Effect of polymerization time on the formed PE (A) MWs and (B) PDIs corresponding to τ = 3.5, 4.5, 5.5, 7.5 and 10 mean residence times (τ's) after the start of polymerization taken from Run 12. The points are experimental data and the line is a linear least-squares regression fit to the points. The polymerization conditions were the same as Figure 3.

4.4.4 *Effect of Zr Concentration*

The first set of polymerization runs were performed in order to determine the effect of Zr concentration on reactant conversion and to choose a catalyst concentration for the remaining runs. The total Al/Zr molar ratio was held constant at 1,000 for all catalyst concentrations studied. Figure 4.7 gives the monomer conversion (X) and catalyst activity (activity = kg polymer/[ethylene] g of catalyst) versus Zr concentrations. It should be pointed out that the ethylene concentration in this definition of activity was determined by mass balance. We know the amount of ethylene going into the reactor. We also know the amount of polyethylene coming out from the reactor. Based on the mass balance, we calculated the ethylene concentration in the reactor, [ethylene]. This definition of activity has an advantage of including the actual concentration of ethylene in the reactor thus reflecting the reaction kinetics more directly. It also has a drawback that when the ethylene concentration approaches zero it becomes infinity. The activity by this definition is also termed as productivity. However, the terms of catalyst activity and productivity are often used interchangeably in the literature. In Figure 4.7, both conversion and activity increase with increasing Zr concentration. The reactant conversion increases with increasing Zr concentration. The activity increases slowly but linearly with increasing Zr concentration until the concentration of catalyst is approached where X is almost 100%. At this concentration of catalyst, the concentration of ethylene in the reactor approaches 0, thereby sharply increasing the activity as we have defined it.

Figure 4.8(A) shows how M_n, M_w, and M_z decrease with increasing catalyst concentration. As the number of active sites increase due to the increased catalyst concentration in the feed, while the ethylene concentration in the feed is held constant at 2 M, the active sites become starved for monomer and the propagation/termination ratio $(k_p \cdot M)/k_{tr}$ decreases, lowering the PE MWs. Figure 4.8(B) indicates that both of the PDIs, i.e., M_w/M_n and M_z/M_w, remain constant with increasing catalyst concentration. When β-hydride elimination controls the molecular weight development, $M_n = k_p M/k_{tr,\beta}$ and $M_w = 2k_p M/k_{tr,\beta}$. Thus, $M_w/M_n = 2$ and the PDI is independent of the catalyst concentration as the results illustrate.

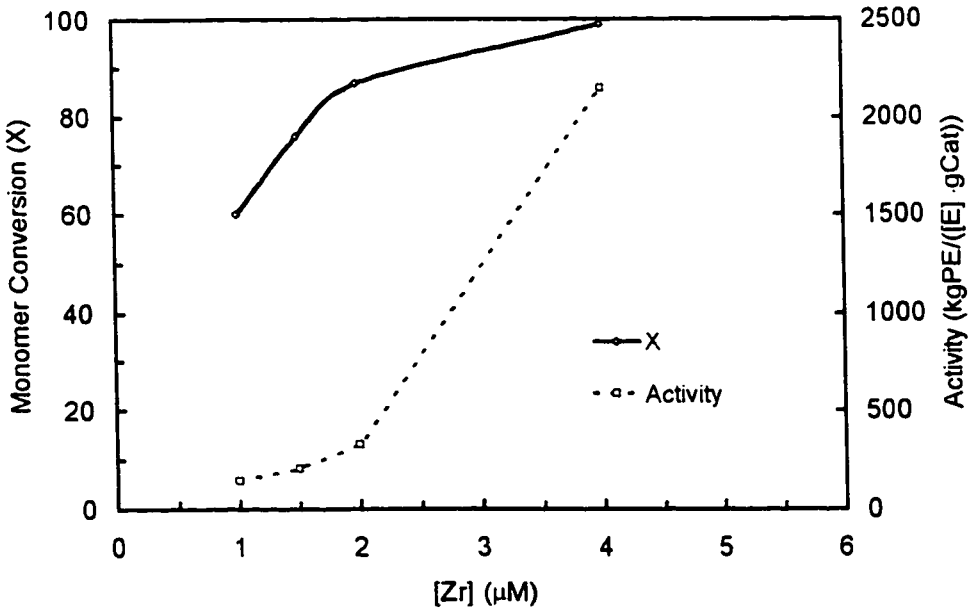

Figure 4.7 Effect of Cp_2ZrCl_2 catalyst concentration on the monomer conversion (X) and catalyst activity (kg PE/([ethylene]·g of catalyst)). The points are experimental data. The polymerization conditions were P = 1500 psig, T = 140 °C, ν_E = 8 g/min, Al/Zr = 1000, and τ = 5 minutes.

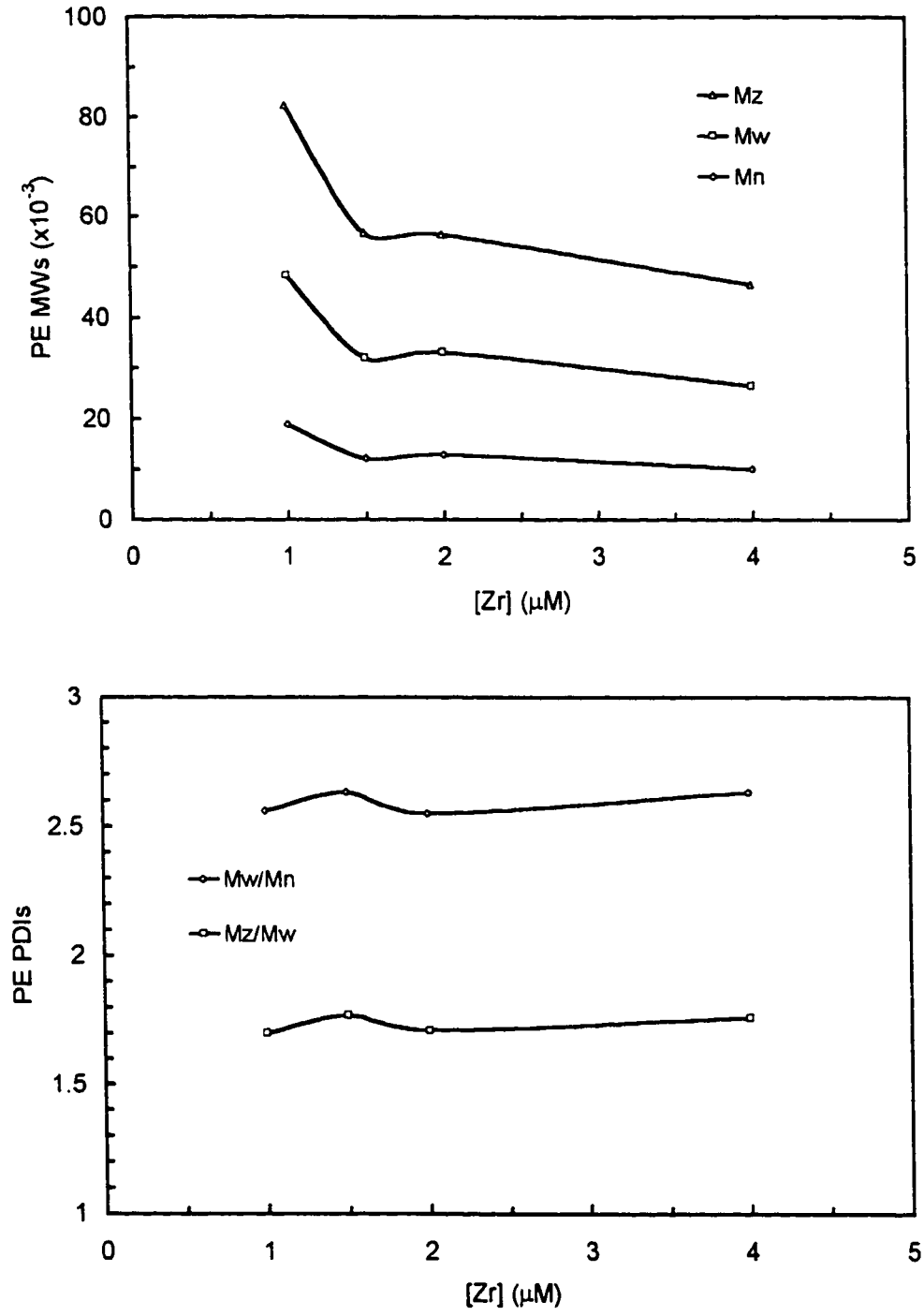

Figure 4.8 Effect of Cp_2ZrCl_2 catalyst concentration on the PE (A) MWs and (B) PDIs. The points are experimental data. The polymerization conditions were the same as Figure 4.7.

4.4.5 *Effect of Temperature*

Figure 4.9 illustrates the effect of temperature on ethylene conversion and catalyst activity for the polymerization of ethylene using the Cp_2ZrCl_2/MAO/TMA system. The conversion is seen to decrease with increasing temperature in a linear fashion. The activity decreases with increasing temperature in a non-linear fashion. It is clear that the deactivation of this catalyst system with increasing temperature is very pronounced.

Figure 4.10(A) illustrates how M_n, M_w, and M_z decrease linearly with increasing temperature. Figure 4.10(B) shows that the PDIs of the formed PE increase linearly with increasing temperature. One possible explanation for the increasing polydispersity index with increasing temperature is the existence of multiple site types in this catalyst system at elevated temperatures. However, we would like to leave this point open for discussion.

Some degradation of product PE was encountered at 200 °C and, to a lesser degree, at 180 °C. Small chunks of hardened PE were observed in the product polymer and some light yellow discoloration was also observed. It was concluded, at these elevated temperatures, that a residence time of 5 minutes is probably too long for ethylene polymerization under these conditions. As the maximum practical flow rate of the pumps was being reached at 1,500 psig for these experiments (lowest τ possible), the subsequent experimental runs were performed exclusively at 140°C.

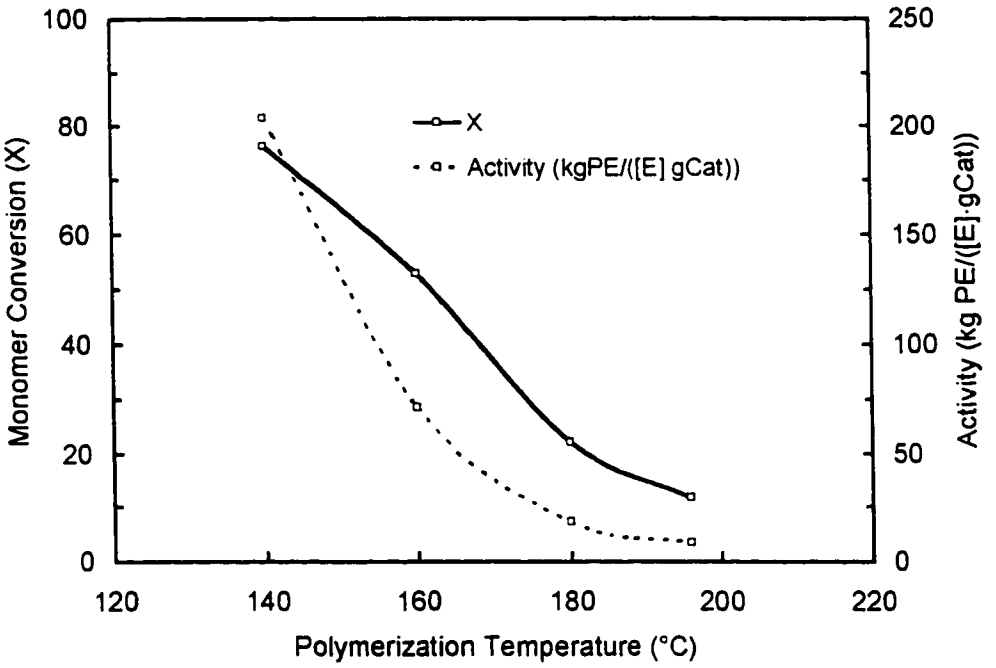

Figure 4.9 Effect of polymerization temperature on the monomer conversion (X) and catalyst activity (kg PE/([ethylene]·g of catalyst)). The points are experimental data. The polymerization conditions were P = 1500 psig, ν_E = 8 g/min, [Zr] = 1.5 μM, Al/Zr = 1000, and τ = 5 minutes.

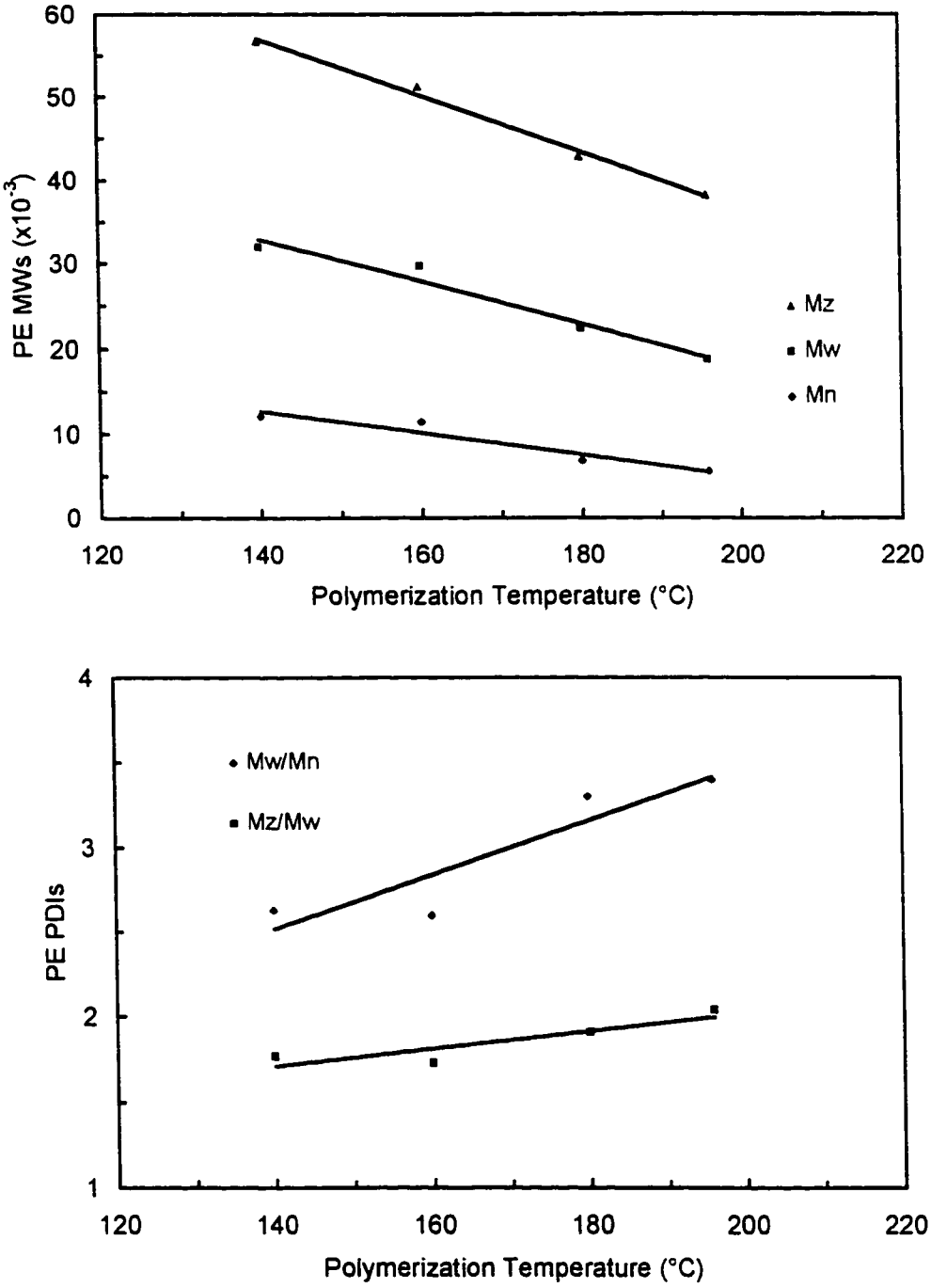

Figure 4.10 Effect of polymerization temperature on the formed PE (A) MWs and (B) PDIs. The points are experimental data and the line is a linear least-squares regression fit to the points. The polymerization conditions were the same as Figure 4.9.

4.4.6 *Effect of Inlet Ethylene Concentration (v_E)*

Four different reactor inlet ethylene concentrations were studied for their effect on ethylene polymerization. Figure 4.11 illustrates how the M_n, M_w, and M_z of the formed polyethylene increase with increasing inlet ethylene concentration and then plateau. Figure 4.12 indicates that the PDIs are constant with increasing inlet ethylene concentration up to a point and then increase slightly with increasing concentration.

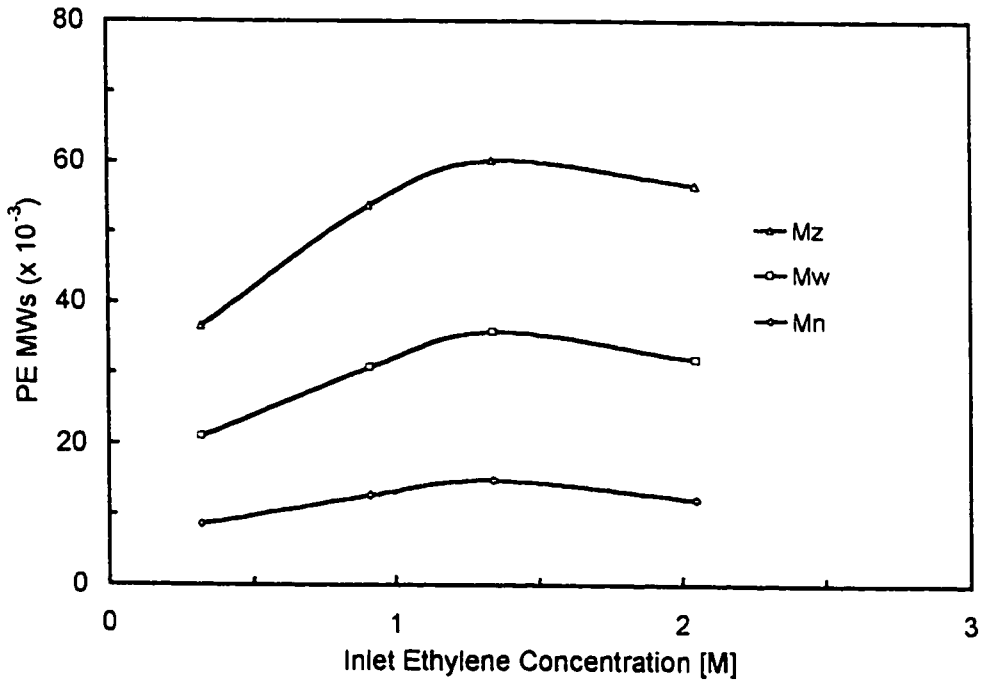

Figure 4.11 Effect of inlet ethylene concentration on the MWs of PE. The points are experimental data. The polymerization conditions were P = 1500 psig, T= 140 °C, [Zr] = 1.5 μM, Al/Zr = 1000, and τ = 5 minutes.

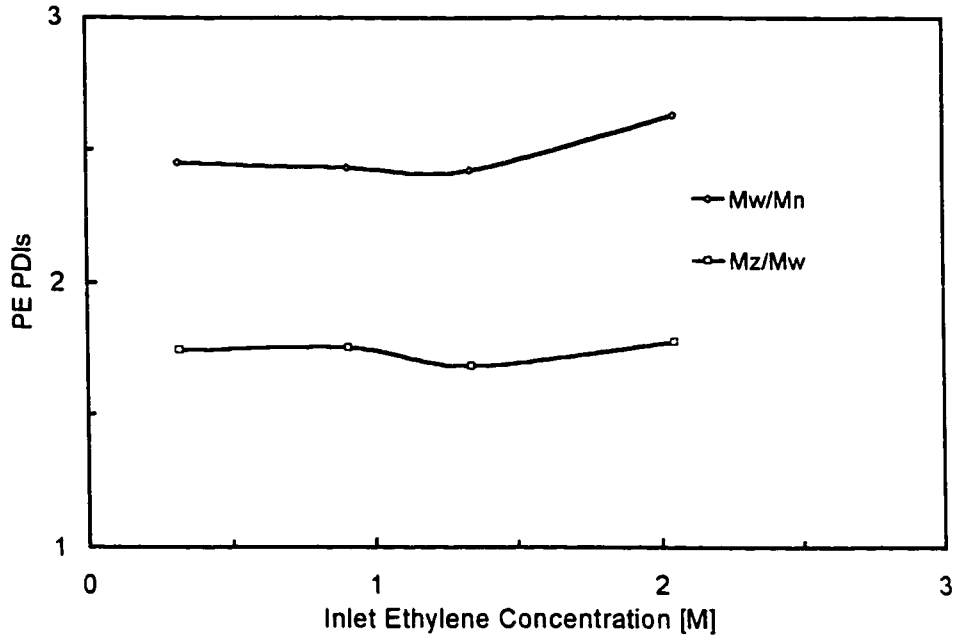

Figure 4.12 Effect of inlet ethylene concentration on the PDIs of PE. The points are experimental data. The polymerization conditions were the same as Figure 4.11.

4.4.7 *Effect of Residence Time (τ)*

The effect of residence time on the polymerization of ethylene, as controlled by the flow of reactants and polymer, was investigated at 5, 7.5 and 10 minutes. The inlet concentrations of catalyst, co-catalyst, and ethylene in toluene were maintained equal for the three τ values studied. Figure 4.13 illustrates the change in the monomer conversion and activity for the three different τ values. Both conversion and activity decrease slightly with increasing residence time. Figure 4.14(A) gives the M_n, M_w, and M_z values while Figure 4.14(B) gives the PDIs of the PE for each of the three residence times.

From Figure 4.14(A), a maximum in MW is found at a τ of 7.5 minutes and Figure 4.14(B) shows that this τ gives the lowest PDI of the three residence times studied. As the lifetime of an individual polyethylene chain is only a few seconds (Chien, 1990), the reactor residence time should not affect the instantaneous MWD or PDI of the formed PE. In a well mixed flow reactor (CSTR) with an ideal residence time distribution, the chain length distribution produced is the instantaneous distribution and in this case should be Flory's most-probable distribution (Hamielec, 1992). The increased residence time lowers the number of effective catalyst sites and monomer concentration in the reactor. The lower catalyst concentration leads to a significant increase in the MWs of the formed PE at higher residence times. Table 4.2 gives the summary of the results for the kinetic data for the polymerization runs while Table 4.3 summarizes the GPC data.

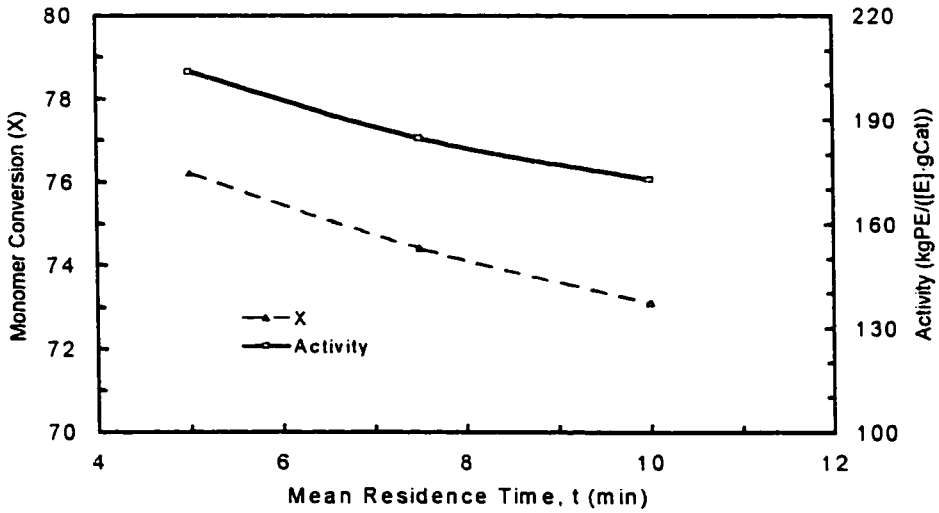

Figure 4.13 Effect of mean residence time, τ, on the monomer conversion (X) and catalyst activity (kg PE/([ethylene]·g of catalyst)). The points are experimental data. The polymerization conditions were P = 1500 psig, T= 140 °C, [Zr] = 1.5 μM, Al/Zr = 1000.

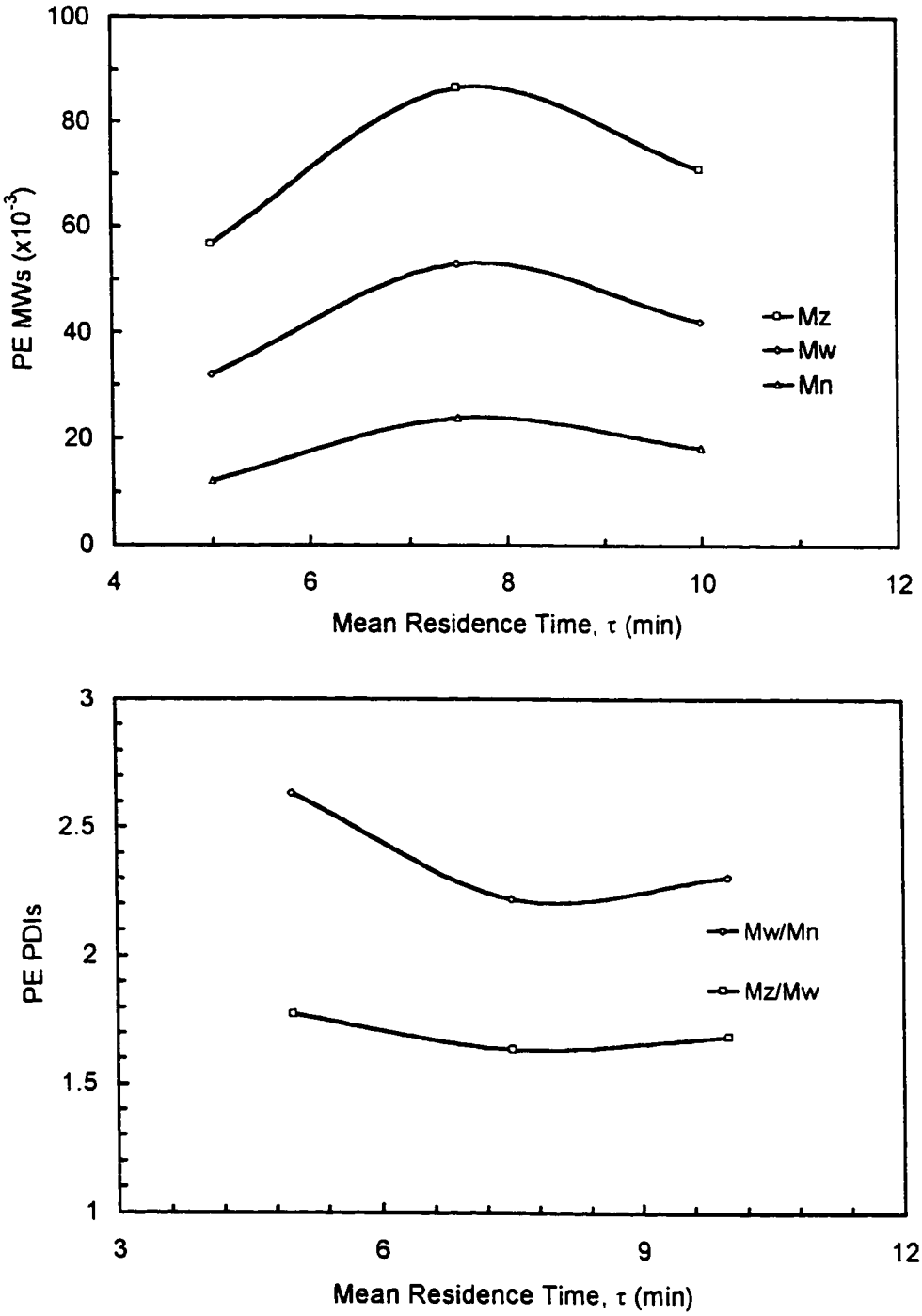

Figure 4.14 Effect of mean residence time, τ, on the formed PE (A) MWs and (B) PDIs. The points are experimental data. The polymerization conditions were the same as Figure 4.13.

Table 4.2. Summary of the reaction kinetic data.

Run #	Activity(kg PE /[E] g catalyst)	Activity(kg PE /[E] g Zr)	X (%)	[E]* (mol/L)	R_p (M/s) $\times 10^3$	k_p $(M \cdot s)^{-1} \times 10^{-3}$
1	2,100	6,900	99	0.02	7.5	82
2	330	1,050	87	0.3	6.6	11
3	140	460	60	0.9	4.6	5.0
4	8	27	12	2.0	0.9	0.3
5	18	58	22	1.8	1.7	0.6
6	71	230	53	1.1	4.0	2.5
7	204	650	76	0.5	5.8	7.1
8	138	440	68	0.5	3.8	4.8
9	145	470	70	0.3	2.6	5.1
10	59	190	48	0.3	0.9	2.0
11	173	550	73	0.7	3.1	3.0
12	185	590	74	0.6	4.0	4.3

* [E] calculated by mass balance.

Table 4.3. Summary of the GPC data for PE

Run #	$M_n \times 10^{-3}$ g/mol	$M_w \times 10^{-3}$ g/mol	$M_z \times 10^{-3}$ g/mol	M_w/M_n	M_z/M_w
1	10.0	26.4	46.5	2.63	1.76
2	13.0	33.0	56.4	2.55	1.71
3	18.9	48.4	82.3	2.56	1.70
4	5.5	18.7	38.2	3.40	2.04
5	6.8	22.4	42.8	3.30	1.91
6	11.4	29.6	51.2	2.60	1.73
7	12.1	31.9	56.6	2.63	1.77
8	14.8	35.8	60.2	2.42	1.68
9	12.7	30.8	53.8	2.43	1.75
10	8.6	21.0	36.6	2.45	1.74
11	18.2	42.0	70.8	2.30	1.69
12	23.9	53.0	86.6	2.22	1.64

4.5 Discussion

The productivity or activity of a Ziegler-Natta catalyst in a continuous system is normally given in either kg of polymer per gram of catalyst or kg of polymer per gram of transition metal. As the concentration of monomer in the solvent is also very important, we have defined the activity of catalyst in our work as A = kg PE produced/([ethylene] g of catalyst). Notice that the units of time are removed from activity in a continuous system operated at steady-state.

One may compare the activity of this simple metallocene catalyst to a traditional Ziegler-Natta catalyst. A silica supported chromium oxide catalyst, such as those produced by Phillips Petroleum Co., exhibit activities of 3-10 kg HDPE/g catalyst, corresponding to 300-1,000 kg HDPE/g Cr. The Dow Chemical Company has reported activities of 275 kg PE/g Ti (Gessell et al., 1978) for their solution process and Amoco has reported activities of 10 kg PE/g catalyst (Hoff, 1978) for their gas-phase process. We see from Table 4.2 that our activity for this simplest of metallocene catalyst systems reaches a maximum of 130 kg HDPE/g catalyst (based on Cp_2ZrCl_2) or 420 kg HDPE/g Zr. The metallocene catalyst, Cp_2ZrCl_2, is more than 10× more active than the extremely high activity Phillips catalyst on a g of catalyst basis while giving roughly similar activity on a g transition metal basis to the Phillips and Dow's heterogeneous catalysts. The activity of this simple metallocene catalyst decreases linearly with temperature due

to catalyst deactivation: a more advanced metallocene catalyst would require a greater stability at elevated temperatures in order to provide high activity.

The weight average molecular weights (M_w) obtained with the zirconocene dichloride/MMAO/TMA catalyst system in this study range from 55,000 g/mol to 18,000 g/mol without the addition of any hydrogen. Chien (1990) reports for a $MgCl_2$ supported titanium catalyst a M_w of 460,000 at a polymerization temperature of 70 °C, without the addition of hydrogen, and M_w/M_n's greater than 14. In general, a supported Z-N catalyst gives significantly higher MWs than a simple metallocene catalyst. One of the main reasons for this is the very high rate of termination of chains by β-hydride elimination in metallocene polymerization whereas Z-N polymerizations experience little if any of this type of termination reaction. We suspect that a more geometrically constrained soluble metallocene catalyst would provide higher MWs than this simple metallocene catalyst at similar elevated temperatures in solution due to decreased β-hydride elimination from a more stable cationic active site.

We know from Flory's most probable distribution that for an instantaneously produced polymer chain, the lowest M_w/M_n PDI is 2.0 for a single site-type catalyst. As the lowest PDI that we measured was 2.2 for the formed PE, a single site-type catalyst is assumed to exist at the lowest polymerization temperature studied of 140 °C.

Assuming that the polymer chain is sufficiently long (long chain assumption), the polymerization rate R_p is given by:

$$R_p = k_p[C^*][M] \qquad (1)$$

where k_p is the propagation rate constant, $(M \cdot s)^{-1}$, [C*] and [M] are molar active site and reactor ethylene concentrations in mol/L. In order to determine the propagation rate constant, k_p, for a CSTR reactor we must first take the mass balance for monomer around the reactor:

$$R_p = ([M]_{in}-[M])/\tau \qquad (2)$$

where M_{in} and M are the molar inflow and outflow of monomer. From Equations (1) and (2), we have

$$[M] = [M]_{in}/\left(1 + k_p[C^*]\tau\right) \qquad (3)$$

Combined with the definition of monomer conversion, $X = 1-[M]/[M]_{in}$. Equation (3) becomes

$$k_p = X/\left((1 - X)[C^*]\tau\right) \qquad (4)$$

Equation (4) is used to give estimate for the propagation rate constants reported in Table 4.2. Since the real active site concentration in the reactor is unknown due to decay, we use the influent catalyst concentration for the rate constant estimation. The temperature dependence of the propagation rate constant is given by the Arrhenius equation, $k_p = A_p\exp(-E_p/RT)$. Thus, from Equation (1), the rate of polymerization can be expressed as

$$R_p = A_p\exp(-E_p/RT)[C^*][M], \qquad (5)$$

and substituting into Equation (2) and rearranging yield

$$\ln(X/(1-X)) = -(E_p/R)\cdot(1/T) + \ln(A_p[C^*]\tau) \qquad (6)$$

From Equation (6), The activation energy of propagation, E_p, can be estimated from the slope of the curve of ln (X/(1-X)) versus 1/T, as shown in Figure 4.15, giving a value of E_p = -93 kJ/mol or -22 kcal/mol. This negative value of the apparent activation energy indicates significant catalyst deactivation occurring with increasing temperature such as that found occasionally with cationic polymerization (Hamielec and Tobita, 1992).

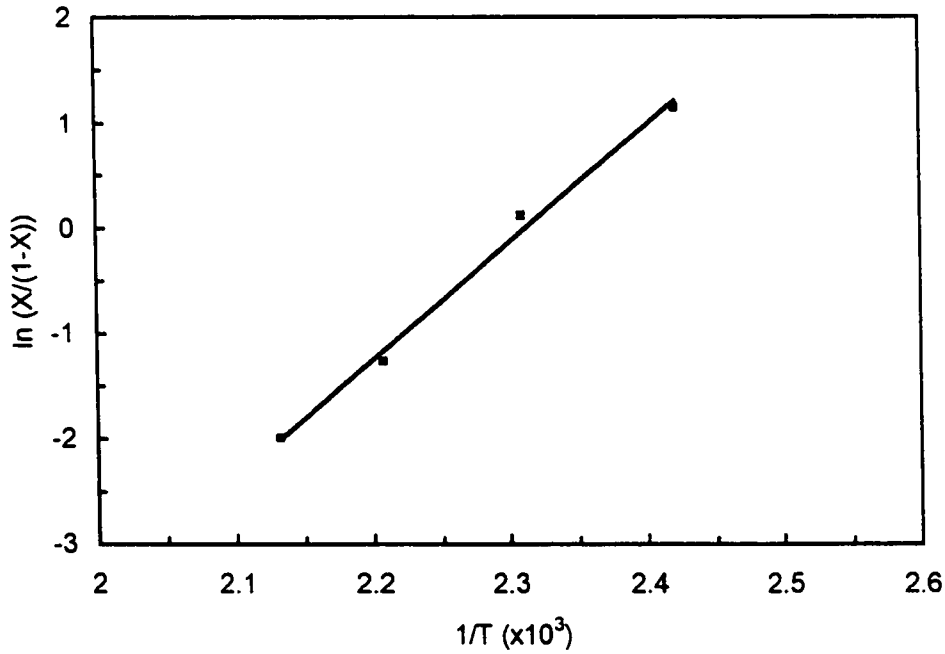

Figure 4.15 Estimation of polymerization activation energy by plotting ln (X/(1-X)) versus 1/T. The points are experimental data and the line is a linear least-squares regression fit to the points. The experimental conditions were: P = 1500 psig, ν_E = 8 g/min, [Zr] = 1.5 μM, Al/Zr = 1000, and τ = 5 minutes.

The spontaneous process of the β-hydride elimination, $k_{tr,\beta}$ is widely recognized as the primary mechanism for termination of polymer chains when using metallocene/MAO catalysts (Chien, 1985). The value of $k_{tr,\beta}$ can be obtained from the variation of number average molecular weight with monomer concentration,

$$m/M_n = k_{tr,M}/k_p + k_{tr,\beta}/(k_p[M]) + k_{tr,Al}/(k_p[M]) \qquad (7)$$

where m is the molecular weight of the monomeric unit (28 for PE). Since $k_{tr,\beta} \approx 25k_{tr,Al}$ (Chien and Wang, 1990), we can ignore $k_{tr,Al}$ and thus,

$$m/M_n = k_{tr,M}/k_p + k_{tr,\beta}/(k_p[M]) \qquad (8)$$

From the slope of m/M_n versus $[\text{ethylene}]^{-1}$ in Figure 4.16, we obtain $k_{tr,\beta}/k_p = 5.8\times10^{-4}$ and since $k_p \cong 5\times10^3$ $(M\cdot s)^{-1}$ (Table 2) thus giving $k_{tr,\beta} = 2.9$ s^{-1} for the conditions $[Cp_2ZrCl_2] = 1.5$ μM, Al/Zr = 1,000, T = 140°C, P = 1,500 psig. The intercept of the line gives $k_{tr,M}/k_p$ which is 9.4×10^{-4}, i.e., $k_{tr,M} \approx 5$ $(M\cdot s)^{-1}$. From our experimental data, we estimated the kinetic chain lifetimes in the order of 10^{-1} second. Note that these chain length lifetimes at 140°C are much shorter than that reported by Chien and Wang of 4 seconds at the much lower temperature of 70°C (Chien & Wang, 1990).

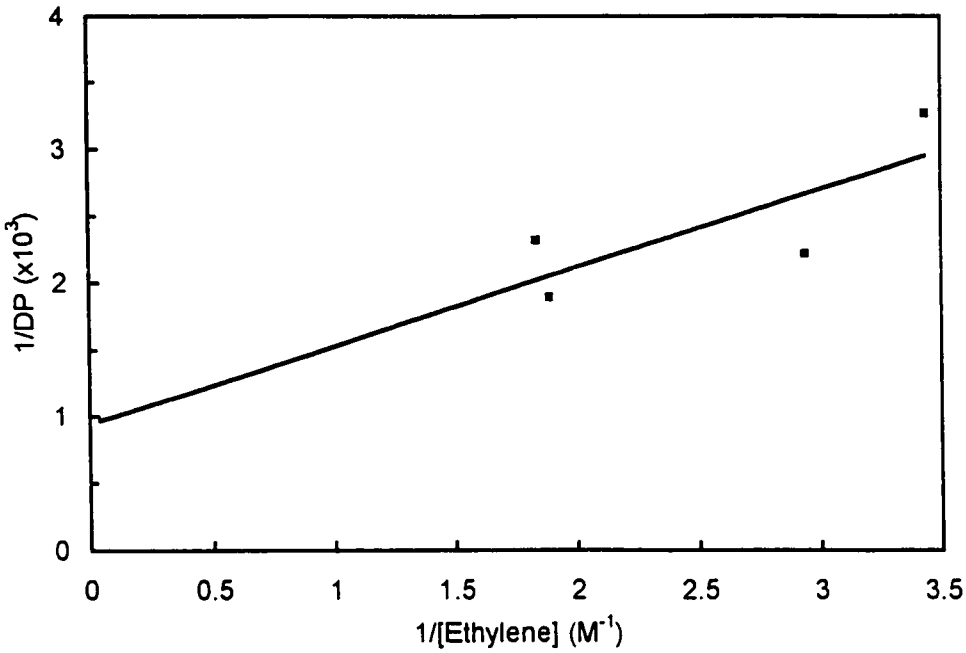

Figure 4.16 Plot of 1/DP versus 1/[ethylene]. The points are experimental data and the line is a linear least-square regression fit to the points. The experimental conditions were: P = 1500 psig, T= 140 °C, [Zr] = 1.5 μM, Al/Zr = 1000, and τ = 5 minutes.

The active site generated when a metallocene catalyst is activated by the appropriate co-catalyst is widely believed to have a large degree of cationic behavior (Jordan, 1986). Like a carbocation in cationic polymerization, the propagating metallocene active site is very reactive and hence vulnerable to impurities in the reaction medium. These impurities can never be totally removed and metallocene active sites are consumed to a significant extent by deactivation. For first order decay of catalyst (Levenspiel, 1962):

$$R_p = k_p[M][C^*]_0 e^{-k_d t} \qquad (9)$$

The plot of $\ln R_p$ versus residence time is given in Figure 4.17. The linear shape of this plot indicates first order decay of catalyst and a deactivation rate constant, $k_d = 2.1 \times 10^{-3}\ s^{-1}$ is obtained from the slope.

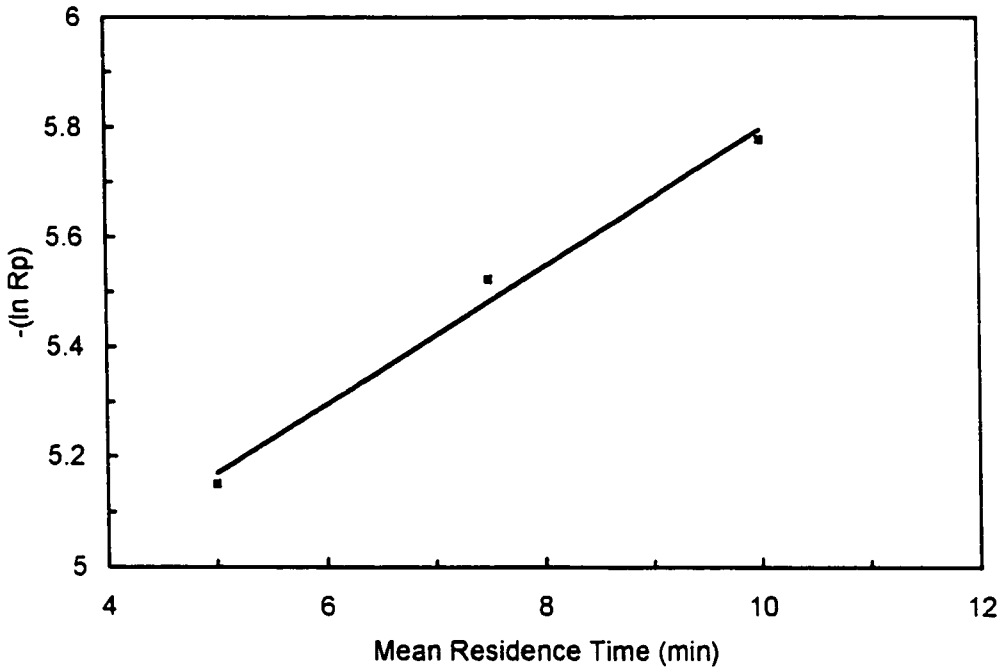

Figure 4.17 Plot of ln R_p versus the reactor mean residence time, τ, to estimate catalyst deactivation. The points are experimental data and the line is a linear least-squares regression fit to the points. The polymerization conditions were P = 1500 psig, T= 140 °C, [Zr] = 1.5 μM, Al/Zr = 1000.

4.6 Conclusions

A high pressure high temperature CSTR system having approximately an ideal RTD has been demonstrated. Preliminary experiments of ethylene polymerized with the metallocene catalyst system of Cp_2ZrCl_2/MMAO/TMA in toluene at 1,500 psig show good control over temperature, pressure and ethylene feed rate. The reactor steady state was obtained after 4 τ's.

Increasing Cp_2ZrCl_2 concentration gave increased activity and decreased PE MWs while PDI's were unaffected. Increasing reactor temperature from 140 to 200 °C gave a linear decrease in activity, a linear decrease in PE MWs and a linear increase in PE PDIs. Catalyst deactivation was found to be first order kinetics. Increasing influent ethylene flow was found to increase PE MWs up to a maximum which then leveled off. Increasing reactor residence time from 5 to 10 minutes gave a maximum PE MW at 7.5 minutes.

4.7 Acknowledgments

The authors are grateful to the National Science and Engineering Research Council of Canada (NSERC) for support for this research. The CSTR supporting systems were purchased using the Grant EQP173683. The autoclave was donated by McMaster Institute for Polymer Production Technology (Prof. A.E. Hamielec). The compressor was donated by Department of Chemical Engineering. Thanks to Peter Hajak for much of the reactor setup and RTD measurements and to Daryoosh Beigzadeh for help in the reactor setup and reactor control. Thanks to Dr. Kris Kostanski for analysis of PE samples by GPC.

4.8 Literature Cited

Chien, J.C.W; Kuo, C.I.; Ang, T.J. Magnesium Chloride Supported High Mileage Catalyst for Olefin Polymerization. VIII. Decay and Transformation of Active Sites. *J. Polym. Sci. Polym. Chem. Ed.* **1985**, *23*, 761.

Chien, J.C.W.; Wang, B.P. Metallocene-Methylaluminoxane Catalysts for Olefin Polymerization. I. Trimethylaluminum as Coactivator. *J. Polym. Sci. Polym. Chem. Ed.* **1988**, *26*, 3089.

Chien, J.C.W.; Wang, B.P. Metallocene-Methylaluminoxane Catalysts for Olefin Polymerization. V. Comparison of Cp_2ZrCl_2 and $CpZrCl_3$. *J. Polym. Sci. Polym. Chem. Ed.* **1990**, *28*, 15.

Flory, P.J. *Principles of Polymer Chemistry*; Cornell University Press, Ithaca, New York, 1953.

Gessell, G.L.; Dighton, D.E.; Valenzuela-Bernal, L.D.; (to Dow Chemical Co.). U.S. Patent 4,067,822, 1978.

Giannetti, E.; Nicoletti, G.M.; Mazzocchi, R. Homogeneous Ziegler-Natta Catalysis. II. Ethylene Polymerization by IVB Transition Metal Complexes/Methyl Aluminoxane Catalyst Systems; *J. Polym. Sci. Polym. Chem. Ed.* **1985**, *23*, 2117.

Hamielec, A.E.; Tobita, H. *Ullmann's Encyclopedia of Industrial Chemistry*; **1992**, p.331.

Hoff, G.R. (to Standard Oil Co. Indiana). U.S. Patent 4,104,199, 1978.

Jordan, R.F.; Bajgur, C.S.; Willett, R.; Scott, B. Ethylene Polymerization by a Cationic Dicyclopentadienylzirconium (IV) Alkyl Complex, *J. Am. Chem. Soc.* 1986, *108*, 7410.

Kaminsky, W. Polymerization and Copolymerization with a Highly Active, Soluble Ziegler-Natta Catalyst. In *Transition Metal Catalyzed Polymerization*, Quirk, R.P., Ed.; vol.4, MMI Press, London, 1983, pp.225.

Kaminsky, W.; Miri, M.; Sinn, H.; Woldt, R. Bis(cyclopentadienyl)zirkon-Verbindungen und Aluminoxan als Ziegler-Katalysatoren fur die Polymerisation und Copolymerisation von Olefinen. *Makromol. Chem. Rapid Commun.* **1983**, *4*, 417.

Kaminsky, W. Preparation of Special Polyolefins from Soluble Zirconium Compunds with Aluminoxane as Cocatalyst. In *Catalytic Polymerization of Olefins*; Keii, T., Soga, K., Eds.; Kodausha-Elservier: Tokyo, 1986; p.293.

Kaminsky, W.; Kulper, K.; Niedoba, S. Olefin Polymerization with Highly Active Soluble Zirconium Compounds using Aluminoxane as Co-catalyst. *Makromol. Chem., Makromol. Symp.* **1986**, *3*, 377.

Kaminsky, W.; Bark, A.; Spiehl, R.; Moller-Lindenhof, N.; Niedoba, S. Isotactic Polymerization of Olefins with Homogeneous Zirconium Catalysts. In *Transition Metals and Organometallics as Catalysts for Olefin Polymerization*; Kaminsky,W., Sinn, H., Eds.; Springer-Verlag, Berlin, 1988, p.291.

Kaminsky,W.; Steiger, R. Polymerization of Olefins with Homogeneous Zirconocene/Alumoxane Catalysts, *Polyhedron* **1988**, *7*, 2375.

Karol, F.J. Catalysis and the Unipol® Process in the 1990s, *Macromol. Symp.* **1995,** *89*, 563.

Lai, S.Y.; Wilson, J.R.; Knight, G.W.; Stevens, J.C.; Chum, P.W.S. (to Dow Chemical Co.). Elastic substantially linear olefin polymers, U.S. Patent 5,272,236, **1993**.

Lai, S.Y.; Wilson, J.R.; Knight, G.W.; Stevens, J.C. (to Dow Chemical Co.). Elastic substantially linear olefin polymers, U.S. Patent Application WO 93/08221, **1993**.

Levenspiel, O. *Chemical Reaction Engineering*, John Wiley & Sons, New York, 1962.

Short, J.N. *Transition Metal Catalyzed Polymerizations: Alkenes and Dienes*, R.P. Quirk, Ed., Harwood Academic Publishers, New York, **1983**, p.651.

Soares, J.P.; Hamielec, A. E. Bivariate chain length and long chain branching distribution for copolymerization of olefins and polyolefin chains containing terminal double-bonds. *Macromol. Theory Simul.* **1996**, *5*, 547.

Stockmayer, W.H. Distribution of chain lengths and compositions in copolymers. *J. Chem. Phys.* **1945**, *13*, 199.

Swogger, K.W.; Kao, C.I. in "*Polyolefins VIII*", *Tech. Pap., Reg. Tech. Conf.-Soc. Past. Eng.*, **1993**, 14.

Thayer, A.M. Metallocene Catalysts Initiate New Era in Polymer Synthesis. *Chem. Eng. News* **1995,** *73*, 15.

CHAPTER 5 LONG-CHAIN BRANCHING IN POLYETHLENE PRODUCED BY ZIRCONOCENE DICHLORIDE IN SEMI-BATCH AND CONTINUOUS REACTORS

P.A. Charpentier, A.E. Hamielec*, S. Zhu

Department of Chemical Engineering

McMaster University, Hamilton, Ontario, Canada L8S 4L7

M.A. Brook

Department of Chemistry

McMaster University, Hamilton, Ontario, Canada L8S 4M1

Submitted to *Macromolecules* September, 1997.

Keywords: metallocene catalyst , long-chain branching, polyethylene, CSTR, semi-batch process, solution polymerization

* Author to whom correspondence should be addressed.

Email: hamielec@mcmaster.ca

Phone: (905) 525-9140 ext. 24950

Fax: (905) 528-5114.

5.1 Abstract

Significant long chain branch formation (LCBing) was found in polyethylene (PE) produced using the metallocene catalyst bis(cyclopentadienyl) zirconium dichloride (Cp_2ZrCl_2) in the semi-batch polymerization of ethylene at 70 °C in the diluent toluene. Branching densities per 1000 carbons (λ_N) up to 1.2 were found and the ratio of melt flow indexes indicating shear thinning, I_{10}/I_2, were found up to 15. In comparison, ethylene polymerized using the same catalyst in a continuous stirred tank reactor (CSTR) at 1500 psig and 140 °C was found to have $\lambda_N \cong 0.6$ and I_{10}/I_2's $\cong 6$. Polymerization of ethylene in the CSTR at 500 psig and 140 °C using the Dow Chemical Company's constrained geometry catalyst Titanium [N-(1,1-dimethylethyl)-1,1-dimethyl-1-[(1,2,3,4,5-η)-2,3,4,5 tetramethyl- 2,4-cyclopentadien-1-yl] silanaminato (2-)-N] dimethyl- (CGC-Ti) was found to provide $\lambda_N = 0.9$.

5.2 Introduction

Metallocene polymerization is revolutionizing the polymer industry for producing both specialty and commodity polyolefins. The main advantages of metallocene catalysts are that they are extremely active (Kaminsky, 1983; Chien, 1988) and their structure can be modified to an almost limitless number of possibilities by variation of: a) ligand type, b) bridge joining ligands, c) substituents on ligand and bridge to modify the steric and electronic surroundings of the transition metal and, d) transition metal type (Hamielec & Soares, 1996). This well defined and controllable catalyst structure allows formation of unique and specific active site-types (normally one per catalyst) compared to a traditional Ziegler-Natta (Z-N) catalyst (e.g. $TiCl_4$/TMA) which is a multiple site-type catalyst with very little control of the individual site-types. Each site type gives narrow molecular weight distributions (MWDs) (Chien, 1988; Kaminsky, 1987) with polydispersity indexes (PDIs) approaching 2 as defined by Flory's most probable distribution (Flory, 1953) and extremely narrow chemical composition distributions (CCDs) in the formation of copolymers, as defined by Stockmayer's bivariate distribution (Stockmayer, 1945). Each site-type gives a unique activity, chain transfer to propagation rate, reactivity ratio and stereoselectivity so that by variation of catalyst site structure, each of these can be tailored to give a polymer with a desired blend of properties.

Due to their narrow MWD's, polymer resins produced by metallocenes normally provide higher zero-shear viscosities (η_o) than conventional Z-N resins at the same weight-average molecular weights. This higher η_o leads to many favorable mechanical and physical properties such as improved toughness. However, one major problem with these resins, as with other narrow MWD resins, is that they are difficult to process (i.e., extrusion, calendering, injection molding, etc.) due to a lack of shear thinning. The Dow Chemical Company was the first to report that their constrained geometry metallocene catalysts, in the solution polymerization of ethylene with/without comonomers, gave resins with significant shear thinning, attributed to the presence of long chain branches (Lai et. al, 1993). The branching densities λ_N's (LCBs per 1000 C atoms) were reported from 0.01-3 and B_N's (LCBs per polymer chain) were reported from 0.2-0.66. By variation of reactor conditions it was reported that this system could independently control both LCBing and short chain branching (SCBing). Shear thinning, as measured by the ratio of melt flow indexes, I_{10}/I_2, were reported varying from 5.6 to 16.1. Increasing LCBing is reported to lead to improved rheological behavior of the resins over traditional LLDPE that includes: 1) greater shear thinning in which the polymer has a lower viscosity at a higher shear rate; 2) decrease in sharkskin or melt fracture effects at higher shear rates (higher production output); 3) higher melt strength of the polymer which allows for superior film properties to be produced (Lai et. al., 1993). Figure 5.1 illustrates how LCBs are believed to be

formed: first a growing PE chain is terminated by β-hydride elimination (also possible by chain transfer to monomer or other mechanism) giving a terminal unsaturated macromonomer; and secondly, the macromonomer is added to a growing polymer chain to form a branched chain.

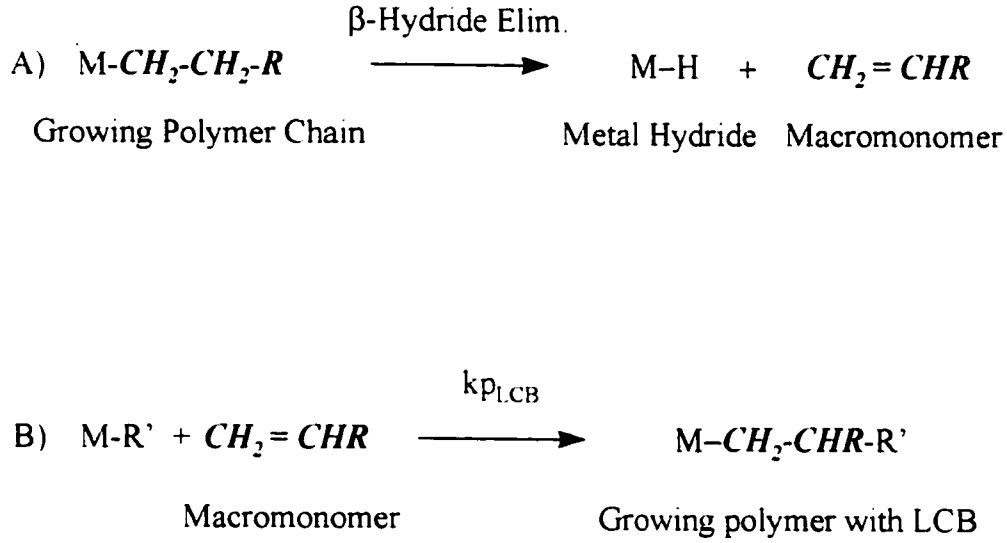

Figure 5.1 Schematic illustrating how LCBs are formed by: (A) formation of a macromonomer and (B) incorporation of the macromonomer into a growing polymer chain.

The viscosity (η) versus shear rate (γ) curve characterizes the shear-thinning behavior of a polyolefin resin. Shear-thinning is caused by molecular disentanglements and alignments of the polymer chains in the direction of flow of the polymer melt with increasing shear rate, thus reducing the viscosity of the polymer melt. Increasing the amount of LCBing was first demonstrated to decrease the melt viscosity at a given molecular weight by Mendelson et. al, 1970; and Wild et. al, 1971. It is believed that the effective LCB length for shear thinning is the molecular weight between entanglements, M_e (Graessley, 1984). M_e has been reported for metallocene polymerized HDPE to be comparable to that found in conventional HDPE of 1830 g/mol (Vega, et.al, 1996) or 131 CH_2 units long.

We have prepared several PE resins in our laboratory using metallocene catalysts in both semi-batch and CSTR processes. These resins have been characterized by GPC, ^{13}C NMR, I_{10}/I_2, T_m and we are reporting on finding significant LCBing using the simple metallocene catalyst Cp_2ZrCl_2 with both semi-batch and CSTR polymerization using toluene as diluent. We compare the branching frequency obtained using this simple metallocene catalyst to that obtained using the Dow Chemical Company's constrained geometry catalyst in our CSTR. Figure 5.2 gives the structure of these two metallocene catalysts. Presently, our research group is focusing on how to control the frequency of LCBs in PE using metallocene catalysts and to understand the enhanced physical and mechanical properties and shear thinning behavior of these resins.

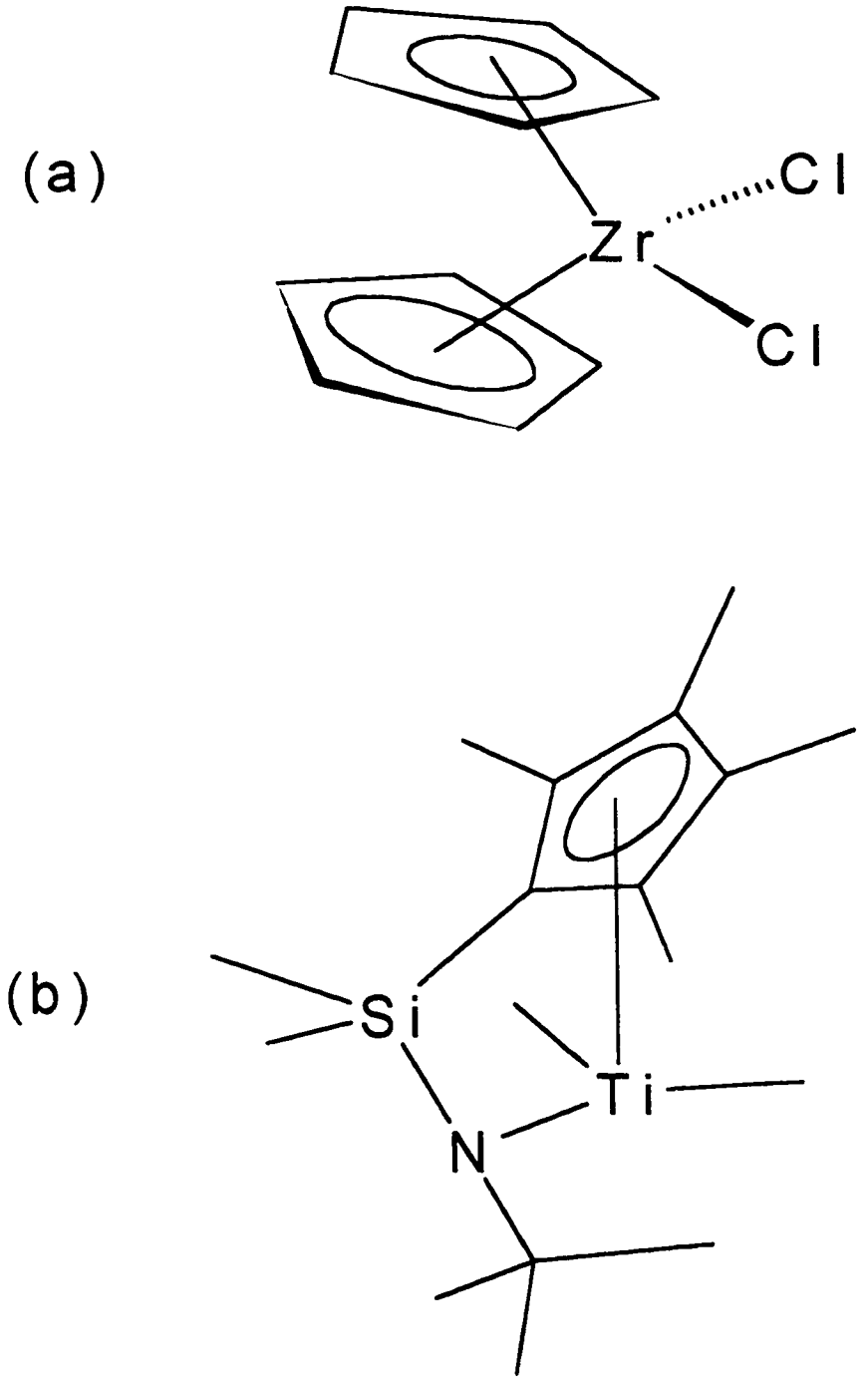

Figure 5.2 (A) Cp_2ZrCl_2 bent sandwich metallocene (B) the Dow Chemical Company's constrained geometry metallocene catalyst.

5.3 Experimental

5.3.1 *Polymerization Procedure*

The procedure for polymerization of ethylene in semi-batch has been reported earlier (Charpentier et al., 1997(a)) as has the procedure for polymerization of ethylene in the research CSTR (Charpentier et al., 1997(c)).

5.3.2 *High Temperature GPC*

All GPC measurements were performed with a Waters-Millipore SEC instrument model 150-C high temperature GPC with a differential refractive index detector at 140 °C using TCB as solvent. The following operation conditions were adopted: 1) column and sample compartment temperature, 140 °C; 2) flow rate of mobile phase, 1.0 ml min^{-1}; 3) sample injection volume, 200 µl; 4) no sample spinning: 5) no sample filtering; 6) sample concentration, 0.1 wt % in 1,2,4-trichlorobenzene.

Calibration of the high temperature GPC was performed at 140 °C directly with a calibration curve obtained using narrow MWD PE standards purchased from the National Bureau of Standards. In addition, both narrow MWD polystyrene (PS) standards from Tosoh Corporation and broad MWD PE standards from American Polymer Standards and Polymer Laboratories Ltd. were

used to check the calibration curve. The Mark-Houwink constants for the calibration curve were for PS K = 1.21 x 10^{-4} and a = 0.707 and for PE were K = 3.92 x 10^{-4} and a = 0.725.

5.3.3 *Differential Scanning Calorimetry (DSC)*

All polymer melting points and heats of fusion were measured with a DuPont model 910 DSC which was calibrated with an Indium standard. Weighed polymer samples (2-3 mg) were transferred to DSC pans, heated up to 180 °C at a heating rate of 10 °C/min.

5.3.4 *^{27}Al NMR*

All reported ^{27}Al NMR spectra were measured using a Bruker AC 300 spectrometer under the following experimental conditions.

Spectral frequency	78.2 MHz	Memory size	32 Kbytes
Spectral Width	29,412 Hz	Pulse width	6 μsec
Pulse angle	90°	Relaxation delay	1 ms
Acquisition time	0.28 sec		

5.3.5 *^{13}C NMR*

All reported ^{13}C NMR spectra of polyolefins were measured using a Bruker AC 300 spectrometer under the following experimental conditions. PE samples were prepared after polymerization by washing the polymer with methanol and drying under vacuum. No additives or melt processing of any form was performed. PE samples were homogenized for 4-5 hours at 150 °C in a ODCB-d_4/TCB mixture.

Pulse angle	90°	Relaxation delay	10 ms
Sample Temperature	130 °C	Sample Concentration	30 %
Spectral frequency	75.5 MHz	Memory size	32 Kbytes
Spectral Width	17,900 Hz	Pulse width	8.5 μsec
Acquisition time	0.92 sec		

5.3.6 *Melt Flow Indexes*

Melt Flow Indexes were determined with a Kayeness Melt Flow Indexer at 190 °C according to the method of ASTM D-1238. I_2 used a 2.3 kg weight whereas I_{10} used a 10 kg weight. PE samples were prepared by mixing Irganox 1010 (an antioxidant) in acetone, adding to PE, mixing by hand, then drying under vacuum to give a 0.3 wt. % Irganox 1010 in PE mixture. Polymer extrudates were normally white with little discoloration. All samples were repeated at least twice

with the average value reported. Reproducibility of individual samples was within 3 %.

5.4 Results and Discussion

5.4.1 *Al Content in PE*

An initial examination was performed in order to determine if all of the Al was removed from the polymer chain ends (if $k_{tr,Al}$ is important) and/or to make sure no aluminoxane was left in the PE samples to complicate ^{13}C NMR, GPC, and DSC spectra and rheological testing. As shown in Figure 5.3 for the various mechanisms believed possible for termination of PE chains with metallocene catalysts, chain transfer to Al should provide a chain terminated by an aluminoxane residue, which will give a saturated chain end when hydrolyzed by methanol. All polymerization reactions were quenched by the addition of methanol in this study. Figure 5.4 gives the ^{27}Al NMR traces of a) before methanol washing from a PE sample, b) after the washing, and c) the background aluminum probe. From this figure we can clearly observe that any aluminum that was initially present has been removed from the PE samples. All PE samples reported in this work were washed in a similar manner and we believe any effects due to Al or aluminoxane in the samples have been eliminated.

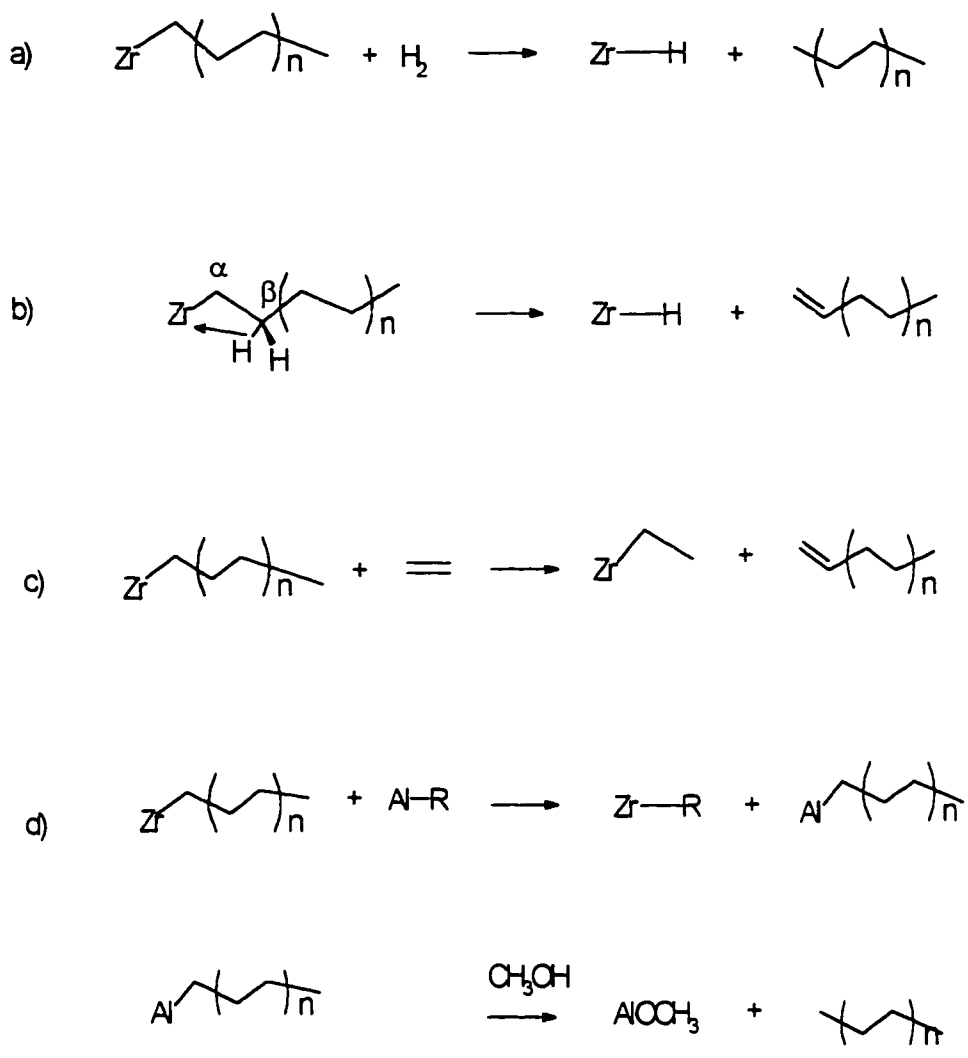

Figure 5.3 Chain Transfer Mechanisms for termination of PE chains using metallocene catalysts; (A) transfer to hydrogen; (B) β-Hydride elimination; (C) transfer to monomer; (D) transfer to aluminum.

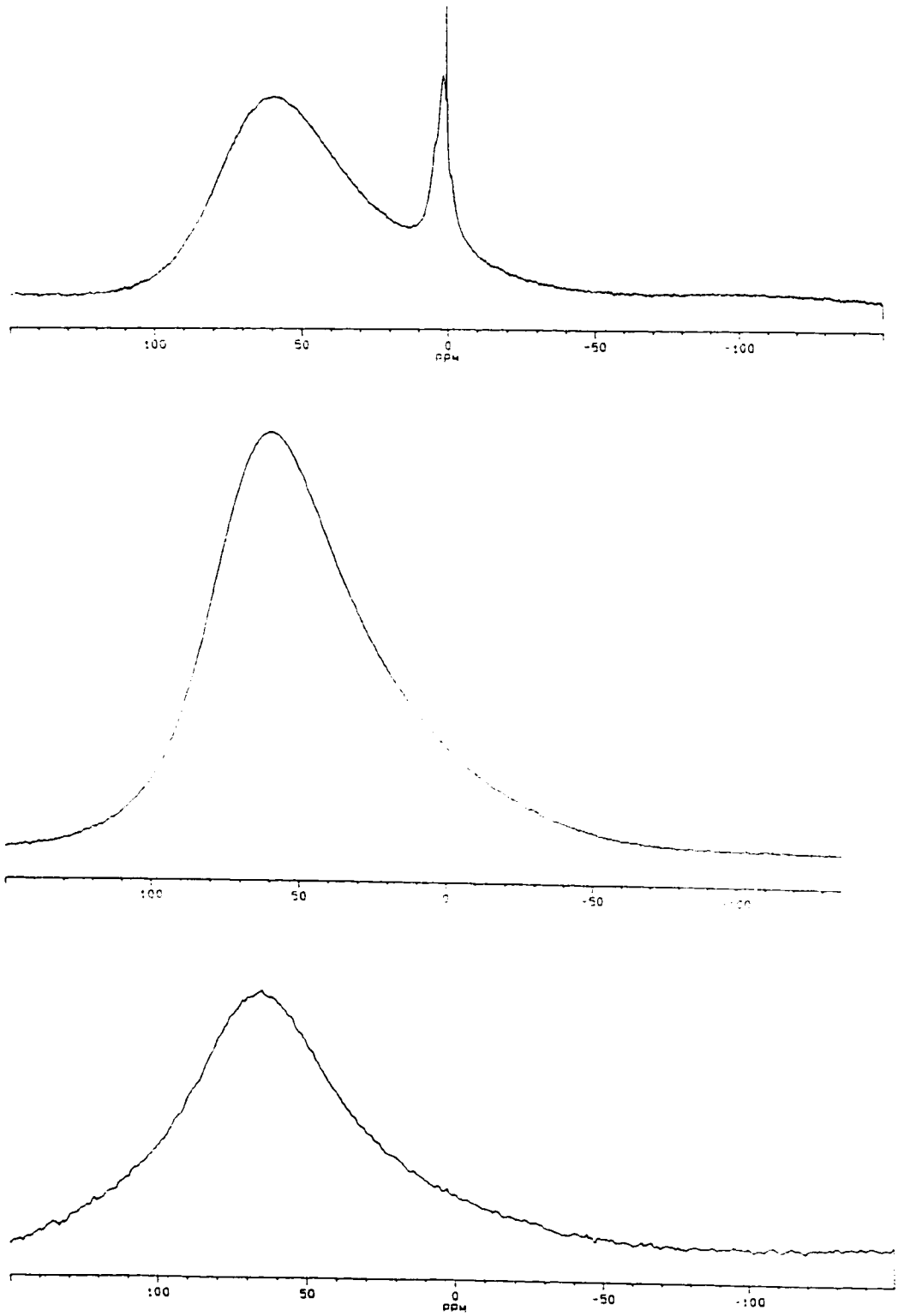

Figure 5.4 ^{27}Al NMR spectra of a PE sample: (A) before methanol washing; (B) PE sample after the washing; (C) aluminum probe background.

5.4.2 *Determination of Long Chain Branching and Shear-Thinning in PE Samples*

In order to determine λ_N or the number of LCBs/1000C atoms for the PE samples produced with no comonomer, ^{13}C NMR was used according to the method of Randall (Randall, 1989). Figure 5.5 gives a schematic of: a) a PE chain with a branch point and the peak assignments of the various C atoms, and b) a schematic of a PE chain with both saturated and unsaturated end groups and the peak assignments of the various C atoms. The equations proposed by Randall for LCBing in PE are:

$$\lambda_N = [(1/3)\alpha/T_{TOT}] \times 10^3 \qquad (1)$$

where λ_N is the branches per 1,000 carbon atoms; α is the average intensity of a carbon from the branch carbon $\alpha\delta^+$; and

$$T_{TOT} = 1s + 2s + 3s + \delta^+\delta^+ + 3a \qquad (2)$$

is the total carbon intensity.

I_{10}/I_2 is a quick and simple shear-thinning test which is defined as the ratio of the melt flow index (MFI) using a 10 kg weight divided by the MFI using a 2.3 kg weight. This property is simply the ratio of two points from the viscosity versus shear-rate curve of the polymer with I_2 being the higher viscosity on the curve at a lower shear-rate and I_{10} the lower viscosity on the curve at a higher shear-rate.

A)

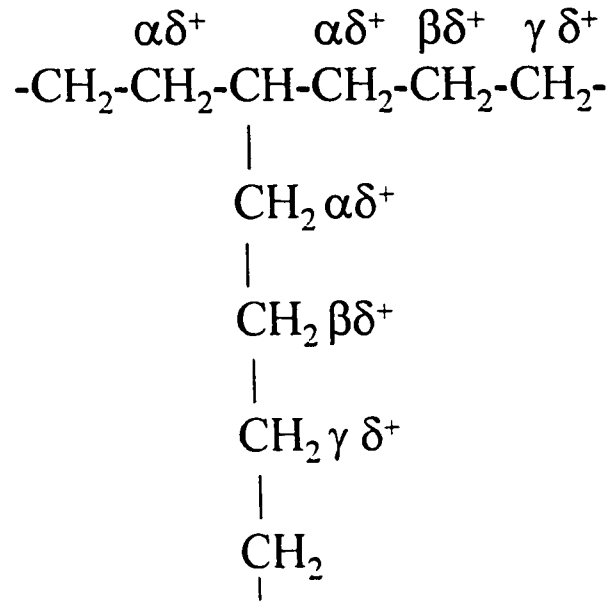

1s 2s 3s $\delta^+\delta^+$ a

B) $CH_3\text{-}CH_2\text{-}CH_2\text{-}(CH_2)_n\text{-}CH_2\text{-}[CH_2\text{-}CH{=}CH_2]$

Figure 5.5 (A) Schematic of a branch point and the peak assignments of the various C atoms according to Randall; (B) schematic of a PE chain with both saturated and unsaturated end groups and the peak assignments according to Randall.

5.4.3 *Long-Chain Branching and Shear Thinning in Semi-Batch Polymerization*

Table 5.1 summarizes the polymerization conditions, while Table 5.2 provides the integral areas of the key peak assignments from ^{13}C NMR for all PE samples reported. The integral areas of the key peak assignments were utilized in Eqs. (1) and (2) from above to calculate λ_N for the PE samples investigated. High temperature GPC characterization results are given in Table 5.3 while λ_N's as well as the shear-thinning melt flow index I_{10}/I_2 characterization results are reported in Table 5.4.

Table 5.1. Polymerization Conditions for formation of PE Samples.

PE Sample #	Experimental Conditions						
	Reactor Type	Temp. (°C)	Solvent	Catalyst Type	[Catalyst] (μM)	[Ethylene] (mol/L)	τ (min)
1	SB	70	Toluene	Cp_2ZrCl_2	6.5	0.05	-
2	SB	70	Toluene	Cp_2ZrCl_2	6.5	0.05	-
3	SB	70	Toluene	Cp_2ZrCl_2	6.5	0.10	-
4	SB	80	Toluene	Cp_2ZrCl_2	0.67	0.09	-
5	SB	70	Toluene	Cp_2ZrCl_2	0.67	0.18	-
6	SB	90	Toluene	Cp_2ZrCl_2	0.67	0.14	-
7	CSTR	140	Toluene	Cp_2ZrCl_2	1.5	0.3*	5
8	CSTR	140	Toluene	Cp_2ZrCl_2	1.5	0.7*	10
9	CSTR	140	Toluene	Cp_2ZrCl_2	1.5	0.6*	7.5
10	CSTR	140	Isopar-E	CGC*	40	0.2*	4

SB = Semi-Batch Reactor; τ = Residence Time for continuous reactor; CSTR = Continuous Stirred Tank Reactor; * [ethylene] for CSTR determined by mass balance; CGC* = the Dow Chemical Company's constrained geometry catalyst, Titanium:(N-1,1-dimethylethyl)dimethyl(1-(1,2,3,4,5-eta)-2,3,4,5-tetramethyl-2,4-cyclopentadien-1-yl)silanaminato))(2-)N)-dimethyl.

Table 5.2. Intregal Areas of ^{13}C NMR Chemical Shifts for PE Samples

PE Sample #	Peak Assignment (Integral Area)				
	1s[a)]	2s[b)]	a[c)]	Delta(+)[d)] Delta(+)	alpha-delta(+)[e)]
1	0.03	0.05	0	33.8	0.12
2	0.03	0.04	0	34	0.12
3	0.05	0.07	0	60	0.16
4	0.04	0.07	0	160	0.3
5	0.03	0.06	0	200	0.23
6	0.05	0.08	0	140	0.2
7	0.15	0.2	0	70	0.12
8	0.05	0.07	0.03	65	0.12
9	0.04	0.08	0.07	70	0.16
10	0.06	0.08	0	100	0.18

a) δ = 14.1 ppm b) δ = 22.9 ppm; c) δ = 34 ppm; d) δ = 30 ppm;
e) δ = 34.6 ppm

Table 5.3. GPC Characterization Results for the PE Samples.

PE Sample #	M_n ($x10^{-3}$)	M_w ($x10^{-3}$)	M_z ($x10^{-3}$)	M_w/M_n	M_z/M_w
1	31	74	138	2.3	1.86
2	30	73.5	139	2.45	1.89
3	28.8	65.3	120	2.27	1.84
4	92	202	366	2.19	1.81
5	141	307	561	2.18	1.83
6	73	158	269	2.17	1.7
7	12.7	30.8	53.8	2.43	1.75
8	18.2	42	70.8	2.3	1.69
9	23.9	53	86.6	2.22	1.64
10	175	365	621	2.1	1.7

Table 5.4. Long-Chain Branching Results for PE Samples.

PE Sample #	T_m (°C)	λ_N*	I_2	I_{10}/I_2
1	134	1.2	0.65	15
2	134	1.2	0.73	15.5
3	133	0.9	1.5	12.9
4	136	0.6	0.11	8.7
5	137	0.4	0.01	9.4
6	136	0.5	0.5	8
7	134	0.6	29	5.6
8	134	0.6	11	5.7
9	135	0.7	12	5.7
10	136	0.89	0	N/M

*λ_N = LCB's per 1000 C determined by ^{13}C NMR (Randall, 1989); N/M = Not Measurable

Figure 5.6 and 5.7 gives two of the ^{13}C NMR spectra and peak assignments of PE samples prepared from the semi-batch polymerization of ethylene using Cp_2ZrCl_2/MAO in the diluent toluene. From these ^{13}C NMR results (summarized in Table 5.4 by λ_N), it is clear that significant amounts of LCBing in PE can occur with the simple metallocene catalyst Cp_2ZrCl_2 in semi-batch polymerization in the diluent toluene. Here we found λ_N's up to 1.2 and I_{10}/I_2's up to 15 in PE resins produced using a semi-batch reactor at 70 °C.

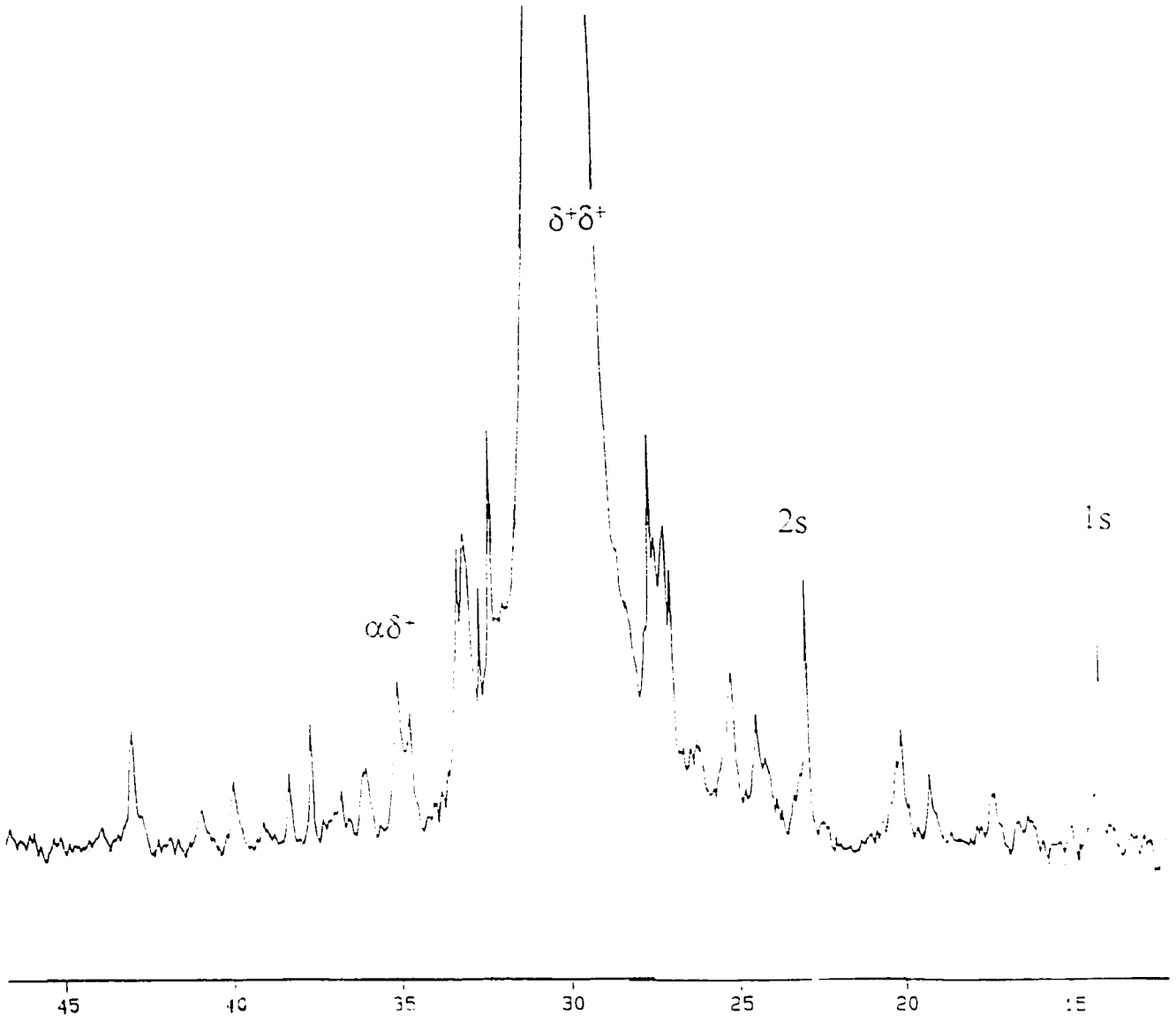

Figure 5.6 ^{13}C NMR spectra with chemical shifts for semi-batch produced PE sample. The polymerization conditions were: Catalyst Type = Cp_2ZrCl_2, [Catalyst] = 6.5 μM, Al/Zr = 1600, T = 70 °C, [Ethylene] = 0.05 mol/L.

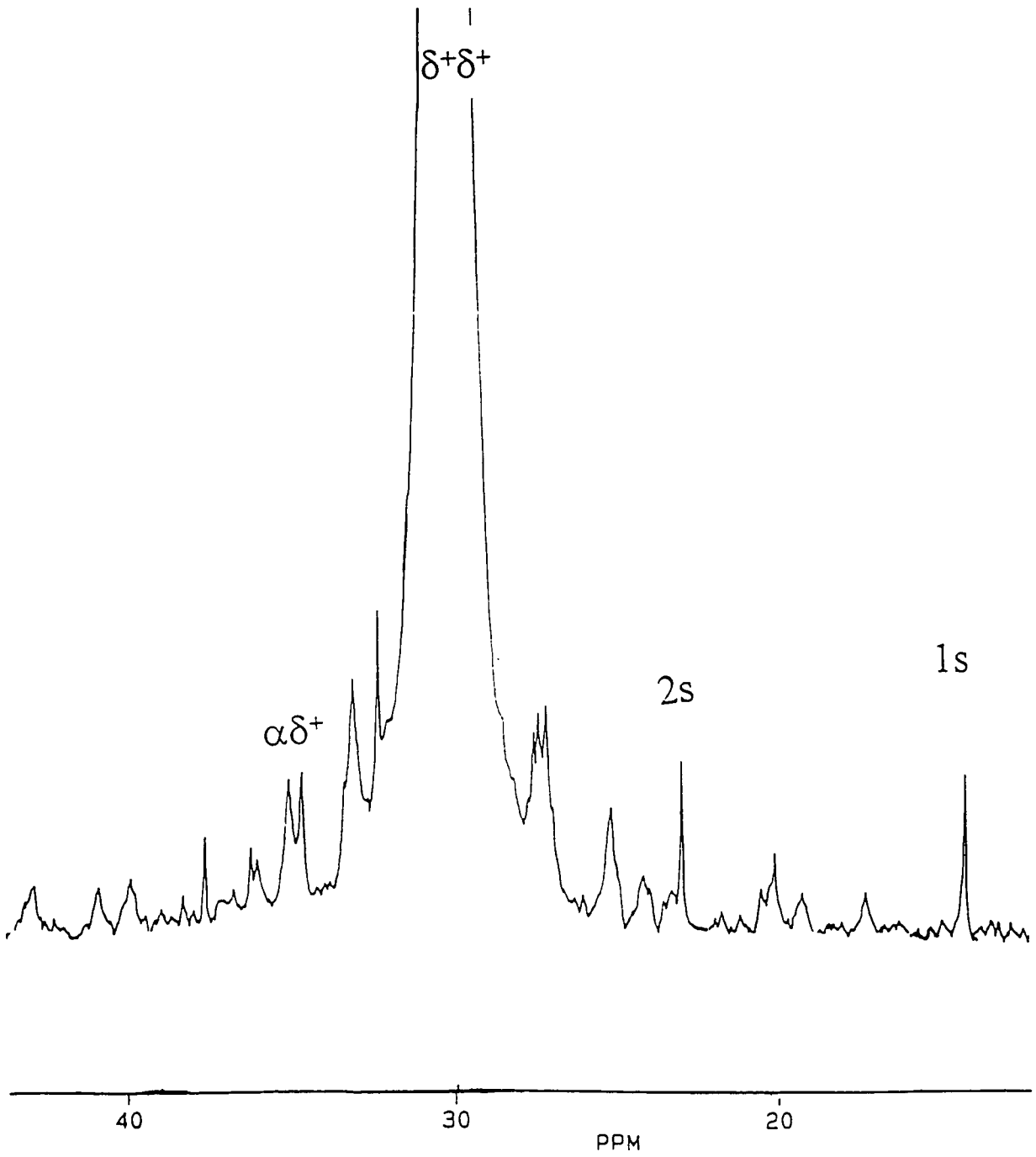

Figure 5.7 ^{13}C NMR spectra with chemical shifts for semi-batch produced PE sample. The polymerization conditions were: Catalyst Type = Cp_2ZrCl_2, [Catalyst] = 6.5 μM, Al/Zr = 1600, T = 70 °C, [Ethylene] = 0.10 mol/L.

We believe that in the semi-batch polymerization of ethylene utilizing the metallocene catalyst Cp_2ZrCl_2 that a two-phase type polymerization is occurring. In the solvent phase the catalyst and co-catalyst interact to form cationic active sites which polymerize ethylene monomer to form polymer chains. The polymer chains are believed to precipitate out of solution upon formation (Charpentier et. al. 1997a). The precipitated polymer chains, when swelled by solvent, form a polymer rich phase. Catalyst, co-catalyst and ethylene diffuse into this polymer rich phase and additional polymerization occurs. In the polymer rich phase the concentration of macromonomer is much higher than in the solvent phase and thus the formation of LCBs is facilitated.

We have no knowledge of any other researchers reporting on the formation of LCBs with this simple metallocene catalyst in the literature. This may be related to: a) the extremely long run times with the ^{13}C NMR instrument in order to provide sufficient resolution to resolve the LCBing peaks for PE, and b) the use of toluene as a diluent instead of hexane or heptane. We have used toluene as a diluent in this study for the polymerization of ethylene with Cp_2ZrCl_2 because it is much better than hexane or heptane at swelling PE chains, as evidenced in any chemical compatibility chart. For the two-phase type of polymerization proposed, swelling of the chains is believed necessary for the formation of LCBs under semi-batch conditions.

5.4.4 *Long-Chain Branching and Shear Thinning in Continuous Polymerization*

In solution polymerization using our research CSTR with Cp_2ZrCl_2 at 140 °C, amounts of LCBing were found in PE resins with λ_N's up to 0.7 and I_{10}/I_2's up to 6 (see Table 5.3). These values are lower than the semi-batch results at 70 °C using the same catalyst where λ_N's up to 1.2 and I_{10}/I_2's up to 15 were found. Figure 5.8 gives one of the ^{13}C NMR spectra and peak assignments from a PE sample prepared using our research CSTR with Cp_2ZrCl_2 at 140 °C. For comparison purposes, the Dow Chemical Company's constrained geometry catalyst was investigated in the solution polymerization of ethylene using our research CSTR with Isopar E (an industrial solvent composed primarily of C8-C10 saturated hydrocarbons with a boiling temperature of 137 °C) as diluent in the absence of any hydrogen. LCBing in metallocene polymerization is believed to be maximized by monocyclopentadienyl type catalysts with open faces such as Dow's CG catalyst, which provide a low steric barrier to addition of a sterically demanding macromonomer. Figure 5.9 gives the ^{13}C NMR spectra and peak assignments from the PE sample prepared with the Dow catalyst which gave a λ_N = 0.9 at a reactor temperature of 140 °C. This was higher than that produced under similar conditions with Cp_2ZrCl_2 at 140 °C in solution polymerization (λ_N = 0.7).

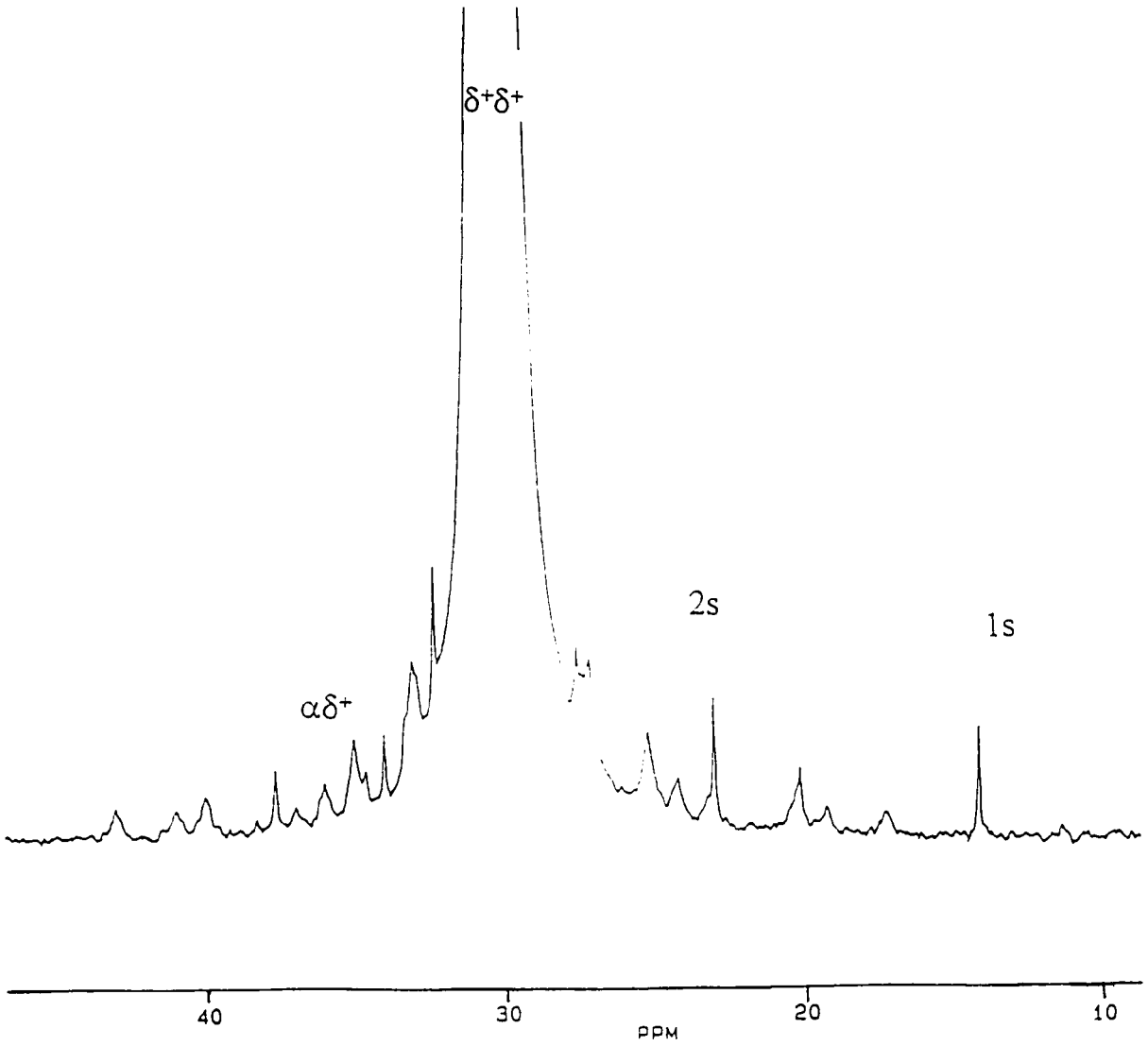

Figure 5.8 ^{13}C NMR spectrum with chemical shifts for CSTR produced PE sample using Cp_2ZrCl_2. The polymerization conditions were: [Catalyst] = 1.5 μM, Al/Zr = 1000, T = 140 °C, [Ethylene] = 0.6 mol/L, τ = 7.5 minutes.

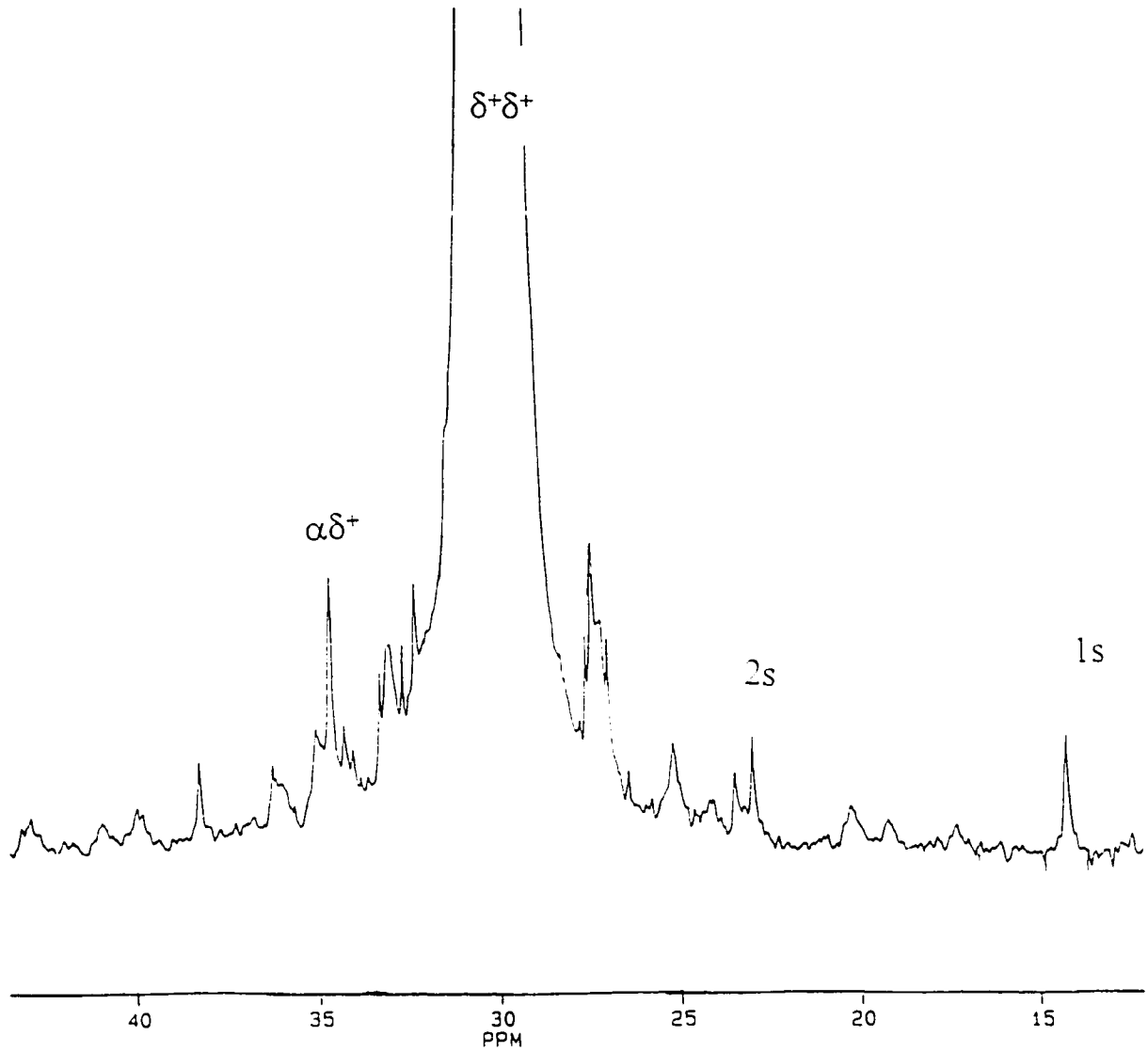

Figure 5.9 ^{13}C NMR spectrum with chemical shifts for CSTR produced PE sample using Dow's CG catalyst. The polymerization conditions were: [Catalyst] = 40 μM, Co-catalyst/Catalyst = 2, T = 140 °C, [Ethylene] = 0.2 mol/L, τ = 4 minutes.

Of additional difference between the continuous and semi-batch polymerization of ethylene is that the concentration of ethylene was higher in the CSTR (0.3-0.7 mol/L) than in the semi-batch reactor (< 0.2 mol/L). Higher [macromonomer]/[ethylene] molar ratios should increase the amount of LCBing, as there is a higher probability that a macromonomer, rather than monomer, will add to a growing polymer chain. Lower ethylene concentrations should help to increase the [macromonomer]/[monomer] ratio, thus increasing LCBing. Similarly, increasing the reactor residence time (τ) may help to maximize the monomer conversion (X) and thus increase the [macromonomer]/[monomer] ratio. However, from Table 5.3, we see that for the different residence times (5-10 minutes), studied with Cp_2ZrCl_2 in the CSTR at 140 °C, no strong dependence of LCBing or shear-thinning was noticed.

In the CSTR experiments, the polymerization of ethylene was conducted in solution, at a temperature higher than the melting point of the polymer. Polymerization at this temperature in solution should be homogeneous, occurring in a uniform phase with little polymer precipitation compared to that in semi-batch at lower temperatures. Solution polymerization is believed to increase the segmental diffusion of the polymer chains hence making them more mobile and available for formation of LCBs. Increasing the polymerization temperature will increase the segmental diffusion of polymer chains, and thus make it easier for a macromonomer to be added to a growing polymer chain at a metallocene active site. However, in our experiments, higher levels of LCBing and shear thinning

were found in semi-batch PE produced at much lower temperatures than those produced in the homogeneous solution CSTR. This finding could be attributed to the presence of a two-phase type polymerization occurring in semi-batch conditions.

The resolution with our ^{13}C-NMR instrument for the identification of LCBs with these PE samples, was limited. Further, we were limited to runs of 24 hours with our NMR setup. Unfortunately, even doubling the run time to 48 hours would only improve the resolution by $\sqrt{2}$ = 41% and further problems may arise such as losing the NMR lock signal, increasing the oxidation of PE, etc. Due to the limited resolution available, we view the calculation of LCBs/1000 C atoms from this data as being semi-quantitative. Further refinements in technique or the use of solid state NMR may make future studies in this area more accurate. This will be very important as, when the branching distribution gets more complicated, more elaborate methods will be necessary to elucidate branching frequency and distribution.

It is generally believed that LCBs are formed by the incorporation of a macromonomer into a growing polymer chain. We have no evidence that the mechanism for formation of LCBs in either semi-batch or in solution CSTR polymerization using the metallocene catalysts Cp_2ZrCl_2 or the Dow Chemical Company's CG catalyst is anything other than the incorporation of a macromonomer into a growing PE chain. However, other mechanisms for

formation of LCBs cannot be ruled out and we hope that later research by our group or others will clarify this point.

5.4.5 *Ethylene-Octene Copolymers*

We will report on two ethylene-octene copolymers produced under the same conditions as the homopolymerization of ethylene in semi-batch at 70 °C (Charpentier et. al, 1997a). This is important for two reasons: First, the SCB from the incorporated octene-1 comonomer is indistinguishable from a LCB peak (Randall, 1989). The presence of this peak for the ethylene-octene copolymers at the ^{13}C NMR chemical shift δ = 34.6 ppm (relative to TMS), compared to the $\alpha\delta^-$ peak at the identical chemical shift of δ = 34.6 ppm for ethylene homopolymers provides strong evidence that the PE homopolymer has LCBs, as no comonomer was present during polymerization. Second, the reactivity ratio calculated for Cp_2ZrCl_2 with octene-1 in toluene at 70 °C in semi-batch gives an indication of the ability of this metallocene to incorporate a relatively sterically hindered monomer. This should be indicative of the metallocene catalysts ability to incorporate a macromonomer, which is believed necessary to form a LCB.

Figures 5.10 and 5.11 give the DSC traces of the two ethylene-octene copolymers illustrating sharp uniform peaks indicating that incorporation of comonomer is uniform corresponding to that predicted by Stockmayer's chemical composition distribution. Table 5.5 gives the polymerization conditions for the

formation of the ethylene-octene copolymers. Figure 5.12 and 5.13 give the ^{13}C NMR spectras of the copolymers, while Table 5.6 gives the integral areas from the NMR spectra of the copolymers. The incorporation of octene-1 comonomer was calculated from the ^{13}C NMR spectra according to ASTM Method D 5017.

Table 5.5. Polymerization Conditions in Semi-Batch for Ethylene-Octene Copolymer Formation

Condition	Copolymerization 1	Copolymerization 2
$[Octene\text{-}1]_0$(mol/L)	0.265	0.13
$[Octene\text{-}1]_F$ (mol/L)	0.242	0.108
Mole % Octene-1 (^{13}C NMR)	1.72	1.13
br/1000C (^{13}C NMR)	8.2	5.5
T_m (°C)	118.5	123

Copolymerizations performed in toluene at 70 °C with [ethylene] = 0.18 mol/L, $[Cp_2ZrCl_2]$ = 0.65 μM. [Al]/[Zr] = 1600.

Table 5.6. Calculation of Octene-1 Incorporation by ^{13}C NMR According to ASTM D 5017 Method

Area	Region for Integration (ppm)	Integral of Copolymer 1	Integral of Copolymer 2
A	41.5 to 40.5	0.04	0.04
B	40.5 to 39.5	0.05	0.04
C	39.5 to 37.0	0.55	0.33
D	35.8	0	0
D+E	36.8 to 33.2	1.86	1.11
F+G+H	33.2 to 25.5	72.15	68.2
H	28.5 to 26.5	1.82	1.27
I	25.0 to 24.0	0.11	0.09
P	24.0 to 22.0	0.44	0.3

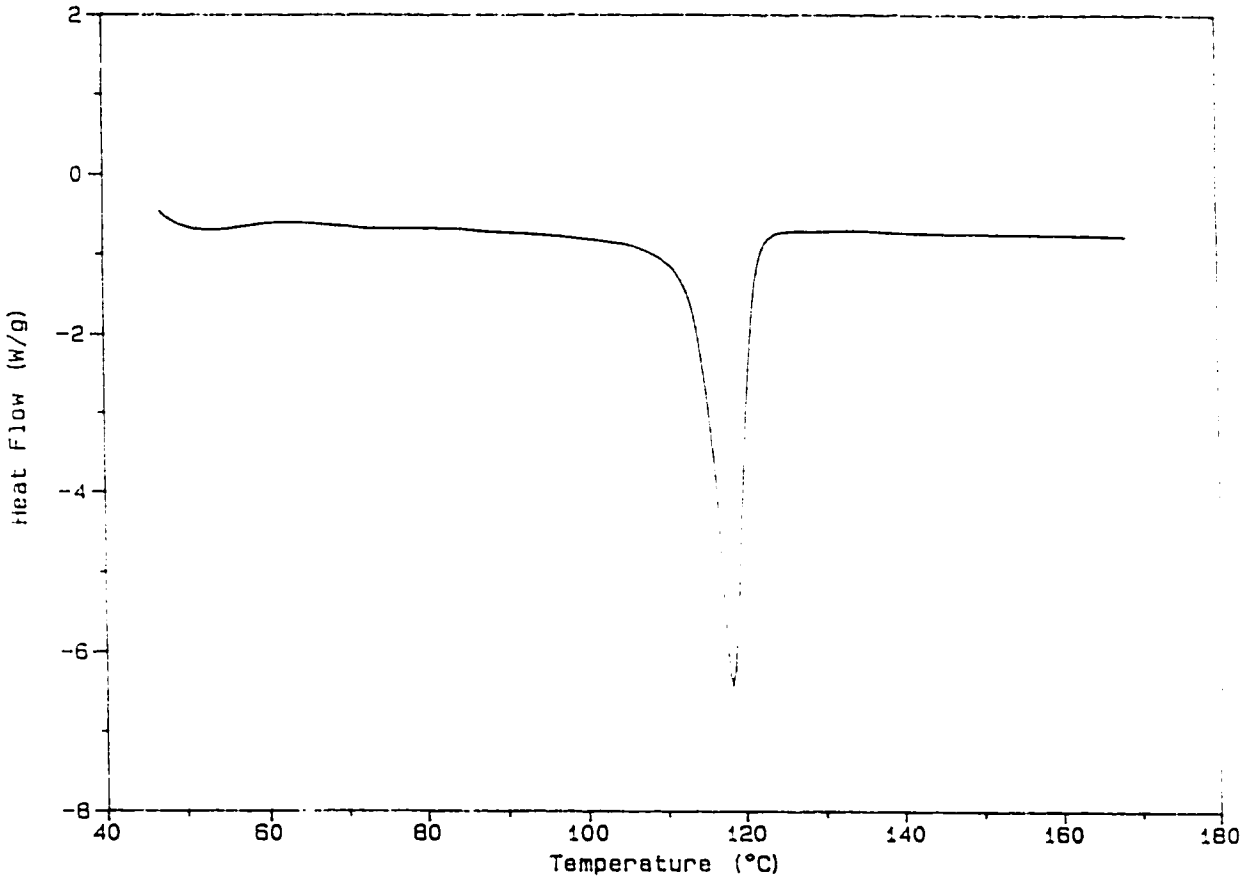

Figure 5.10 DSC curve of ethylene-octene copolymer. The polymerization conditions in semi-batch were: T = 70 °C, $[Cp_2ZrCl_2]$ = 0.7 μM, Al/Zr = 1600, [ethylene] = 0.18 mol/L, $[\text{octene-1}]_0$ = 0.27 mol/L.

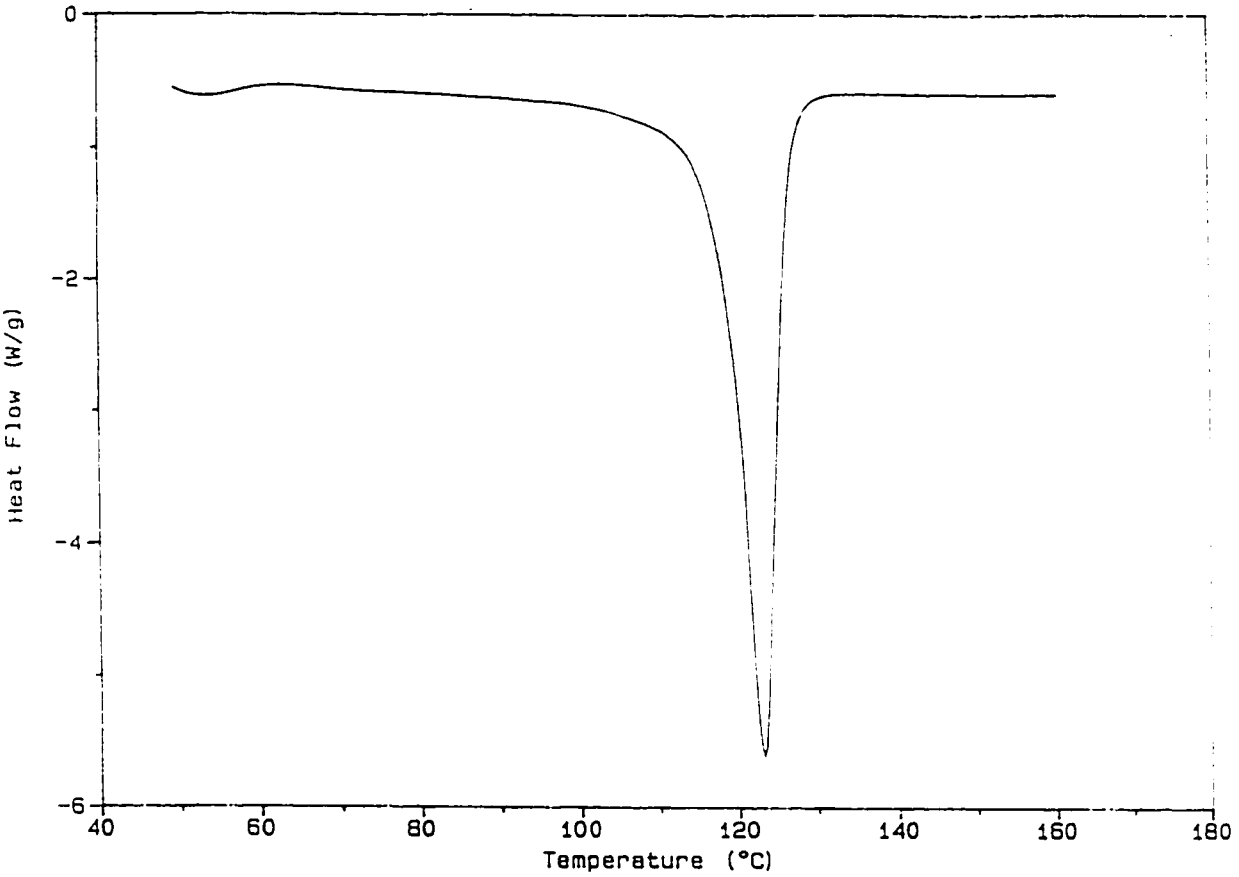

Figure 5.11 DSC curve of ethylene-octene copolymer. The polymerization conditions in semi-batch were: T = 70 °C, $[Cp_2ZrCl_2]$ = 0.7 μM, Al/Zr = 1600, [ethylene] =0.18 mol/L, $[\text{octene-1}]_0$ = 0.13 mol/L.

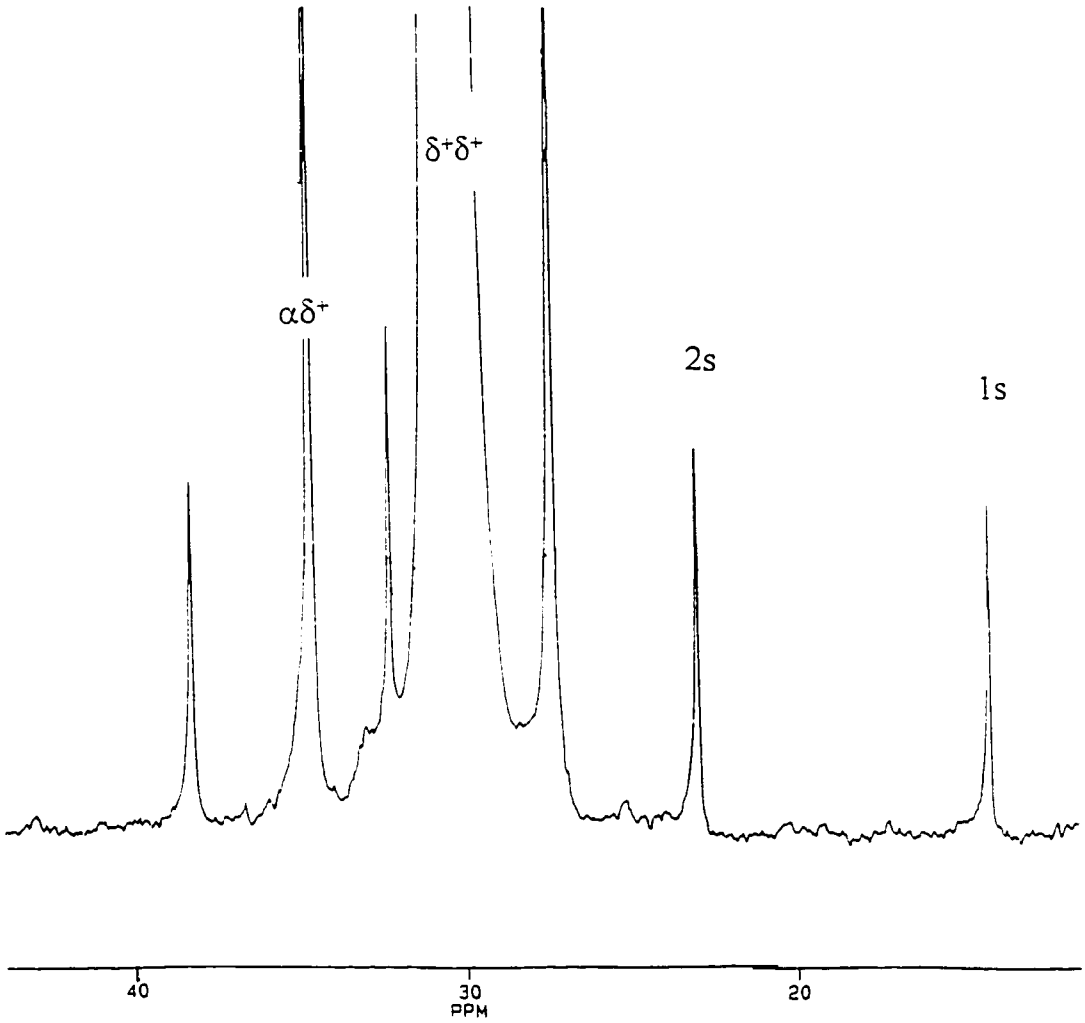

Figure 5.12 ^{13}C NMR Spectrum for ethylene-octene copolymers. Polymerization conditions were the same as in Figure 5.10.

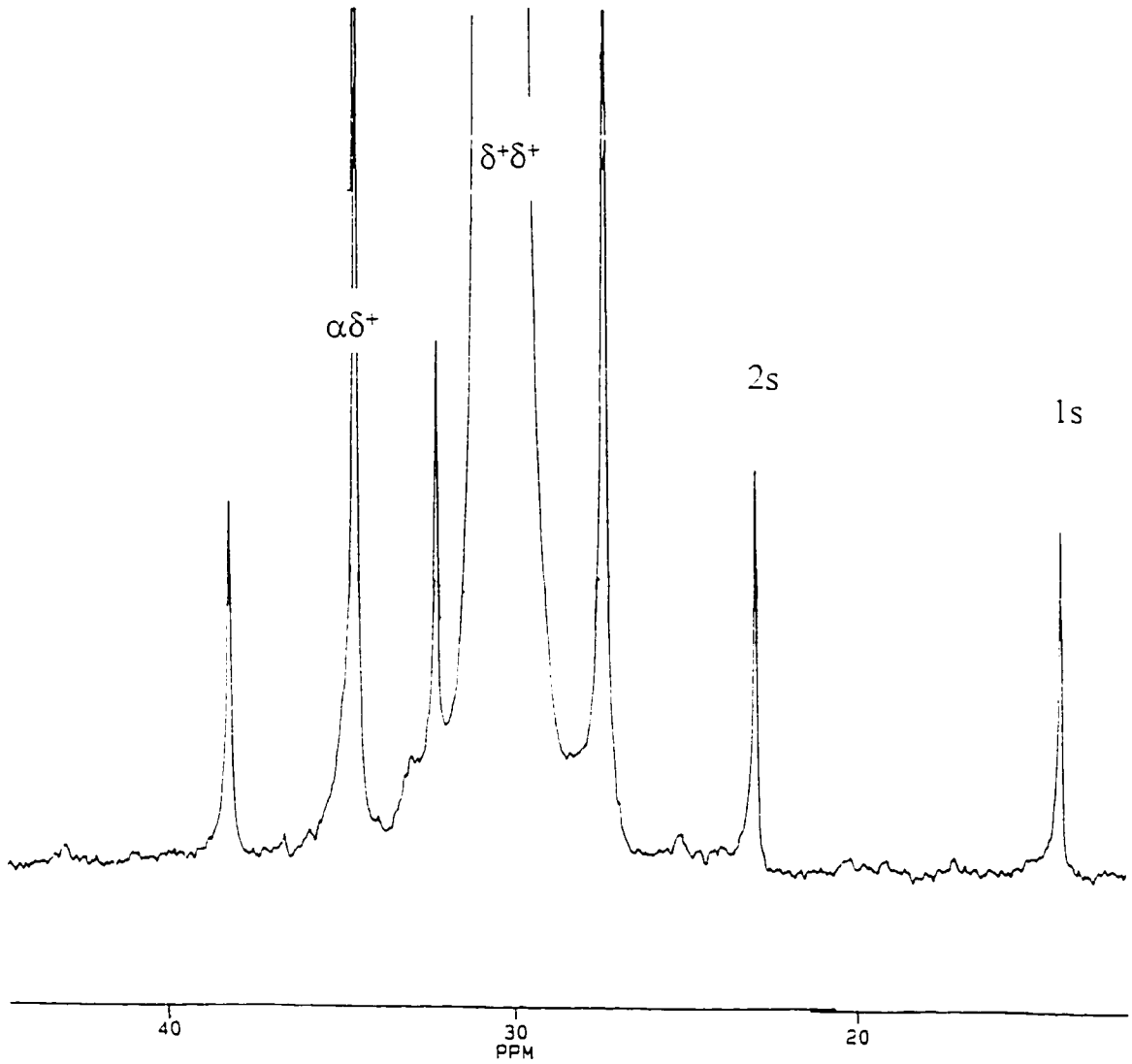

Figure 5.13 ^{13}C NMR Spectrum for ethylene-octene copolymers. Polymerization conditions were the same as in Figure 5.11.

In order to calculate the reactivity ratios for ethylene (M_1) and octene-1 (M_2) from the above copolymerizations, the following equation (3) is utilized (Odian, 1970):

$$F_1 = \frac{r_1 f_1^2 + f_1 f_2}{r_1 f_1^2 + 2 f_1 f_2 + r_2 f_2^2} \qquad (3)$$

where F_1 is the mole fraction of M_1 in the copolymer; f_1 is the mole fraction of monomer M_1 in the feed. Fitting the above equation to the data from Table V extracts the reactivity ratios for ethylene and octene-1, respectively: $r_1 = 46$ and $r_2 \sim 0$. Note that only two data points were used for this calculation so the reactivity ratios should be viewed as only approximate values. However, it is quite clear that ethylene is far more reactive than octene-1 which gives a rather significant steric barrier to its incorporation into a growing polymer chain under these co-polymerization conditions.

5.5 Conclusions

Significant long chain branch formation was found by ^{13}C NMR in PE produced using the simple homogeneous catalyst Cp_2ZrCl_2 in semi-batch polymerization with λ_N's (LCBs/1000C atoms) up to 1.2 and I_{10}/I_2's up to 15. The $\alpha\delta^+$ peak in the ethylene-octene copolymers and the $\alpha\delta^+$ peak from the LCBs in PE were both found to have identical chemical shifts at $\delta = 34.6$ ppm, providing confirmation of the presence of LCBs in the ethylene homopolymers. A two-phase type polymerization is believed responsible for the formation of LCBs in semi-

batch where localized high macromonomer/ethylene ratios are present. In comparison, the polymerization of ethylene using the catalyst Cp_2ZrCl_2 in solution with a research CSTR at 1500 psig and 140 °C was found to provide $\lambda_N \cong 0.6$ and I_{10}/I_2's $\cong 6$. The polymerization of ethylene in solution with a CSTR at 500 psig and 140 °C using the Dow Chemical Company's CG catalyst was found to provide $\lambda_N \cong 0.9$, higher than that from Cp_2ZrCl_2 under similar polymerization conditions.

5.6 Acknowledgments

We greatly appreciate the financial support from the Natural Sciences and Engineering Research Council of Canada (NSERC) for this work. We also thank Dr. Kris Kostanski for GPC analysis, Dr. Brian Sayer for ^{13}C and ^{27}Al NMR, and Dajing Yan for performing a few of the MFI values reported.

5.7 Nomenclature

CCD	chemical composition distribution
CSTR	continuous stirred tank reactor
GPC	gel permeation chromatography
LCB	long chain branching
M	concentration of monomer (mol/l)
M_o	concentration of monomer in feed
MMAO	modified methylaluminoxane

MWD	molecular weight distribution
PDI	polydispersity index (M_w/M_n)
PE	polyethylene
PS	polystyrene
RTD	residence time distribution (τ)
TCB	trichlorobenzene
TMA	trimethylaluminum
X	conversion (moles of reactant polymerized/moles of reactant fed to reactor)
Z-N	Ziegler-Natta catalyst

5.8 References

Charpentier, P.; Hamielec, A.E.; Brook, M.; Zhu, S. "Semi-Batch Polymerization of Ethylene Utilizing Metallocene Dichloride/Methylaluminoxane — Diffusion Limitations"; Submitted for Publication to *AIChE J.*

Charpentier, P.; Hamielec, A.E.; Brook, M.; Zhu, S. "Effect of Aluminoxane on Semi-Batch Polymerization of Ethylene Using Zirconocene Dichloride"; Submitted for Publication to *Polymer*.

Charpentier, P.; Zhu, S.; Hamielec A.E., Brook M.; "Continuous Solution Polymerization of Ethylene using the Metallocene Catalyst System, Zirconocene Dichloride/MMAO/TMA; Accepted for publication in *Ind.Eng. Chem. Res.*

Chien, J.C.W., Wang, B.P. *J. Polym. Sci., Polym. Chem. Ed.* **1988**, 26, 3089.

Flory, P.J. in "Principles of Polymer Chemistry", Cornell University Press, Ithaca, New York, 1953, p.161.

Graessley,W.W. In *Physical Properties of Polymers*, Mark, J.E.; ACS, Washington D.C., 1984, p 126.

Hamielec, A.E.; Soares J.P.; *Prog. Polym. Sci.*, **1996**, 21, 651.

Kaminsky, W. in "Transition Metal Catalyzed Polymerization" (Ed. R.P. Quirk), vol.4, MMI Press, London, 1983, p.225

Kaminsky, W., Miri, M., Sinn, H., Woldt, R. *Makromol. Chem., Rapid Commun.* **1983**, 4, 417

Lai, S. Y.; Wilson, J.R.; Knight, G.W.; Stevens, J.C.; Chum, P.W.S. (to Dow Chemical Co.). Elastic substantially linear olefin polymers, U.S. Patent 5,272,236, **1993**.

Lai, S. Y.; Wilson, J.R.; Knight, G.W.; Stevens, J.C. (to Dow Chemical Co.). Elastic substantially linear olefin polymers, U.S. Patent Application WO 93/08221, **1993**.

Mendelson, R.A.; Bowles, W.A.; Finger, F.L.; *J. Polym. Sci.* **1970**, A-2, 8, 105.

Odian, G. *Principles of Polymerization*, McGraw-Hill Book Company, New York, 1970.

Randall, J.C. *Rev. Macromol. Chem. Phys*, **1989**, C29 (2&3), 201.

Soares, J.P.; Hamielec, A. E. *Macromol. Theory Simul.* **1996**, 5, 547.

Stockmayer, W.H. *J.Chem.Phys.*, **1945**, 13, 199.

Vega, J.F.; Munoz-Escalona, A.; Santamaria, A.; Munoz, M.E.; Lafuente, P. *Macromolecules*, **1996**, 29, 960-965.

Wild, L. Ranganath, R.; Ryle, T. *J. Polym. Sci.*, **1971**, A-2, 9, 2137.

CHAPTER SIX SIGNIFICANT RESEARCH CONTRIBUTIONS TO POLYMER SCIENCE AND ENGINEERING

I believe that significant contributions to polymer science and engineering have been made in this research. These follow in the order outlined within the thesis.

(1) Determination from the semi-batch polymerization of ethylene in the temperature region 20-90 °C that the metallocene catalyst Cp_2ZrCl_2 is a single-site type catalyst. Earlier kinetic models developed based on PE MWDs > 3 and bimodal distributions were most likely caused by the high activity of the metallocene catalyst giving significant diffusion limitation problems leading to significant temperature and monomer concentration gradients within the reactor. Diffusion limitations and polymer precipitation were found to create significant problems with homogeneous polymerization utilizing these high activity metallocenes in semi-batch which can account for reactor fouling and the decay-type polymerization rate-time curves observed. The use of a comonomer such as octene-1 with ethylene was found to prevent the decay-type polymerization rate-time curves as the SCBs incorporated into the polymer chains presumably prevent precipitation of the chains and removal of active sites from

solution. It was also determined that hydrogen: i) only slightly decreases the rate of polymerization of ethylene utilizing Cp_2ZrCl_2, ii) significantly lowers the PE MWs but does not increase the PE PDIs or number of catalytic site types.

(2) Determination that the aluminoxane co-catalyst functions as a true co-catalyst in the polymerization of ethylene in that: 1) its structure and concentration have a strong influence on the Cp_2ZrCl_2 catalyst activity by the formation of active sites; and, 2) its structure and concentration were not found to have any effect on the produced PE MWD. Hence, the aluminoxane co-catalyst was found not to be actively involved in the catalytic site-type for the polymerization of ethylene. It was determined that the only significant chain transfer mechanisms for polymerization of ethylene with Cp_2ZrCl_2 were i) β-hydride elimination, ii) chain transfer to hydrogen and iii) chain transfer to ethylene. Chain transfer to polymer and chain transfer to Al (from MAO and TMA) were not found to be of significant importance.

(3) The first description of the high temperature continuous solution polymerization of ethylene using metallocene polymerization in a CSTR with approximately ideal RTD. With the metallocene catalyst Cp_2ZrCl_2 in the temperature range of 140-200 °C in solution, significant deactivation of

the catalyst was observed which could be approximately described as a 1st order deactivation. With Cp_2ZrCl_2 in the temperature range of 140-200 °C in solution, PE MWs significantly decrease and PE PDIs increase. I have shown that the constrained geometry of the Dow catalyst provides significantly higher MWs than Cp_2ZrCl_2 at 140-200 °C in solution and hydrogen must be utilized as a chain transfer agent to obtain PE MWs in the range of interest.

(4) For semi-batch polymerization of ethylene utilizing Cp_2ZrCl_2 in toluene, significant LCBing was observed, this was highest using low concentrations of monomer and high concentrations of catalyst. For the polymerization of ethylene in the CSTR at high temperatures (140-200 °C) utilizing Cp_2ZrCl_2 in toluene, LCBing was observed but less than that found from semi-batch under optimum conditions. For polymerization of ethylene in the CSTR utilizing the Dow Chemical Company's constrained geometry catalyst in Isopar-E, higher LCBing was observed than with Cp_2ZrCl_2 in toluene under similar conditions.

CHAPTER SEVEN FUTURE RESEARCH

This Ph.D. thesis has exposed several different areas for future research:

7.1 *Long-Chain Branching in Semi-Batch and Solution Polymerization*

This research has shown that significant numbers of long-chain branches are present in PE produced in semi-batch polymerization in toluene even with the most simple of metallocene catalysts, i.e., Cp_2ZrCl_2. Metallocene catalysts permit one to prepare resins with a desired microstructure. However, the effects of catalyst structure on formation of LCBs is not well understood. It is believed that: 1) a more open structure will lead to increased LCBing and increased comonomer incorporation; and, 2) bridged metallocenes normally give increased comonomer incorporation and thus should give increased long chain branching.

The effects of LCBing on rheological properties are not well understood as extremely small changes in long-chain branching frequency can cause profound changes in rheological responses. Careful characterization will be required to examine the microstructure of the polymer. More advanced ^{13}C NMR techniques will be required to determine more accurately long-chain branching frequency at such low levels. Longer NMR run times will give higher resolution. Use of solid-state NMR will allow samples to be run for longer times at lower temperatures and

thus without significant polymer degradation. This will allow a more quantitative determination of the number of long-chain branches. Also the use of a well calibrated GPC with an online viscometer and LALLS detectors should help to accurately determine the frequency and distribution of LCBs as a function of MW. Careful examination of the molecular weight distribution is encouraged, especially the higher moments of the distribution such as M_z and M_{z+1}. These are difficult to determine accurately and accurate calibration curves for GPC will be required. These higher moments are believed to be most closely related to the rheological properties. Once the exact number of long-chain branches can be determined, their effect on rheological properties can be elucidated.

7.2 *Impurities in Polymerization*

One of the roles of aluminoxanes is widely believed to be the 'scavenging of ' impurities such as O_2, H_2O, and CO from the solvent and monomer feed which reduces the deactivation of catalyst sites and allows the polymerization of monomer by metallocene catalysts. However, very little information or data in the academic literature is available on this subject of metallocene catalyst poisons and their effect on polymerization. The role of the aluminoxane, alkyl aluminum and metallocene catalyst in this area could be greatly expanded upon. The exact role of aluminoxanes (e.g., MAO, MMAO, IBAO) and alkyl aluminum's (e.g., TMA, TEAL, TIBA) and the metallocene catalyst in scavenging impurities can be elucidated by studying the levels of impurities present in a functioning metallocene

polymerization at reaction temperature with an on-line gas chromatograph (GC) and how various purification methods can lower them. Industrially, there is always the potential of catalyst poisons accumulating in the recycle diluent, particularly if the catalyst poison has a boiling point similar to that of the diluent.

7.3 *Supported Catalyst*

In the unsupported metallocene polymerization of ethylene in slurry or solution, there are no heterogeneous particles for the polymer to form from, such as that found with traditional Z-N polymerization. This lack of powder properties of the PE chains in slurry greatly increases the viscosity of the reacting medium. Supporting the metallocene catalyst on a spherical macrosupport particle consisting of spherical primary crystallite particles may greatly improve the apparent viscosity of the polymerization. The spherical primary crystallite particles will act as a template for polymerization of PE which will grow radially outwards in a fashion similar to that encountered in a traditional Z-N polymerization (often called *replication*). Another way to reduce apparent viscosity would be to use a prepolymerization with either a spherical Z-N catalyst or a spherical supported metallocene catalyst to: a) slow down the initial R_p; b) provide good "replication"; and c) provide good bulk density. Then, in a second step, use homogenous metallocene polymerization to take advantage of the extremely high activities and narrow MWD and other favorable physical properties.

It is also important to examine supported catalysts for polypropylene polymerization in the gas phase and even in the supercritical region where polypropylene concentration is much higher and novel properties can be produced.

7.4 *Bench Scale Gas Phase Polymerization*

Most industrial commodity polymerization of HDPE/LLDPE/PP is presently performed using a fluidized bed gas-phase reactor (e.g. Unipol) which will most likely continue into the future as this type of reactor: a) requires no solvent; b) can operate at lower temperatures than solution polymerization; c) can produce much higher MWs than solution polymerization where high viscosity's prevent high MWs; d) can grow polymer particles to a size large enough for sale without subsequent extrusion and pelletizing; and, e) can incorporate several comonomers for LLDPE production which is not possible with slurry technology.

Several areas of research could be addressed with a bench scale semi-batch reactor equipped for gas phase polymerization: 1) kinetic modeling of the gas phase process for metallocene catalysts; and, 2) analysis of novel supported catalysts and their kinetic behavior.

7.5 *Long Chain Branching in Gas Phase*

Due to the present and future importance of gas-phase polymerization, it is important to determine for metallocene catalysts: a) if LCBs can be made in the gas phase; and, b) how they can be controlled. It is also important to determine

how sufficient shear thinning can be produced with a gas phase polymer and if the presently popular bimodal resins can be produced in the bench scale gas phase reactor and if they increase shear thinning and other physical and mechanical properties.

APPENDIX A ANALYSIS OF Cp_2ZrCl_2 SITE-TYPE INCREASE WITH TEMPERATURE IN CSTR

A.1 Introduction

We observed in Chapter 4 for the experimental runs performed with the research CSTR in the polymerization of ethylene utilizing the metallocene catalyst system Cp_2ZrCl_2/MMAO/TMA, that increasing polymerization temperature led to an approximately linear increase in PE polydispersity indexes. In order to analyze the increase in polydispersity indexes with temperature, the size exclusion chromatography (SEC) traces of the PE samples were analyzed using mathematical models based on the most probable weight chain length distribution (Soares & Hamielec, 1996). This analysis was performed in order to provide information on the actives sites and if the number of active sites were increasing with increasing polymerization temperature.

During polymerization, each site type instantaneously produces dead polymer chains that have the most probable weight chain length distribution (WCLD). The instantaneous WCLD of the total polymer produced instantaneously can be considered to be an average of that produced by the individual site types, weighted by the weight fraction of polymer produced by each site type. Assuming that the polymerization conditions are such that the WCLD of the accumulated polymer is equal to the instantaneous WCLD, it is possible to

obtain information about the number of active site types by decomposing the WCLD of the whole polymer into individual most probable WCLD for each site type (Vickroy et al., 1993).

A.2 Numerical Methodology to Deconvolute the SEC Chromatograms

The most probable WCLD of linear homopolymer may be expressed by the equation:

$$w(r,j) = \tau^2(j) r e^{-\tau(j) r} \qquad (A.1)$$

where

$w(r,j)$ most probable WCLD (weight fraction of polymer of chain length r produced on site type j instantaneously)

$\tau(j)$ ratio of rate of production of dead polymer chain to rate of propagation

r polymer chain length

j active site type

It is assumed that $\tau(j)$ is independent of conversion and also spatially independent utilizing the research CSTR.

The instantaneous WCLD of the whole polymer is obtained by averaging the distributions of each individual site type:

$$W(r) = \sum_{j=1}^{n} m(j)w(r,j) \qquad (A.2)$$

where,

W(r) instantaneous WCLD of the whole polymer produced by n site types

m(j) weight or mass fraction of polymer made by site type j

n number of active site types

Equation (A.2) is modified to include the constraint:

$$\sum_{j=1}^{n} m(j) = 1 \qquad (A.3)$$

and is finally expressed as:

$$W(r) = w(r,n) + \sum_{j=1}^{n-1} m(j)[w(r,j) - w(r,n)] \qquad (A.4)$$

In order to determine the adjustable parameters: i) τ(1), τ(2),... τ(n); and, ii) m(1), m(2),...,m(n); we need to minimize the difference between W'(r) computed by equation (A.4), and the measured distribution W(r).

Equation (A.4) is valid for describing an instantaneous WCLD formed by the superposition of several individual most probable WCLDs. Thus, to apply this model to the experimental WCLDs (from GPC traces) we must assume that the WCLD for the accumulated polymer is the same as the instantaneous WCLD. This assumption is valid: 1) for a CSTR reactor operated at steady-state where the WCLD is spatially independent; and, 2) the ratio of chain transfer to propagation

rates of all active sites does not change during the polymerization; and, 3) the relative amounts of polymer made be each site type does not change during the polymerization; and 4) mass and heat transfer effects which would cause the instantaneous WCLD to be spatially dependent, are negligible. In chapter 4 we determined that our CSTR was operated at steady-state and that mass and heat transfer effects should be negligible for the nonsupported metallocene catalyst system Cp_2ZrCl_2/MMAO/TMA in solution polymerization.

A.3 Numerical Solution

A.3.1 *Obtaining first estimates*

In order to estimate τ(1), τ(2), and m(1) we can firstly assume a two site type model and use the number, mass and z average chain lengths (n_n,n_w,n_z) from the experimental WCLD. This initial approximation was valuable for starting the decomposition algorithm.

For a two site type model, the chain length averages are defined by the equations:

$$n_n = \frac{1}{m(1)\tau(1) + m(2)\tau(2)} \tag{A.5}$$

$$n_w = 2\left[\frac{m(1)}{\tau(1)} + \frac{m(2)}{\tau(2)}\right] \tag{A.6}$$

$$n_2 = 3\left[\frac{m(1)}{\tau^2(1)} + \frac{m(2)}{\tau^2(2)}\right]\left[\frac{m(1)}{\tau(1)} + \frac{m(2)}{\tau(2)}\right]^{-1} \qquad \text{(A.7)}$$

Equations (A.5) to (A.7) may be solved with any algorithm for finding the roots of non-linear algebraic equations, such as Newton's method (Press et al., 1992). This will provide initial estimates for τ(1), τ(2), and m(1) for a 2 site-type model.

A.3.2 *Higher Site Type Models (n > 2)*

Two nonlinear least-squares numerical methods can be utilized to fit equation (A.4) to the experimental WCLDs provided by the SEC traces: i) the Levenberg-Marquardt method (Bates and Watts, 1988) and the Golub and Pereyra method (1973). For this analysis of the SEC traces, the Golub and Pereyra method was utilized due to its faster convergence (Soares & Hamielec, 1996).

The Golub and Pereyra proposed a method to minimize:

$$r_2(\tau) = \left|W - A(\tau)m(\tau)\right|^2 \qquad \text{(A.8)}$$

which depends only on the nonlinear parameters. The objective function is first optimized in relation to the nonlinear parameters $\tau(j)$ and then the linear parameters m(j) are calculated. For this method, for each of the site types n, only $\tau(j)$ needs to be estimated. This method was utilized as implemented in the FORTRAN subroutine VARPRO (Dongarra and Grosse, 1987).

A.4 Simulation Results

Table 1 gives the GPC results for the four polyethylene samples prepared in the research CSTR at different polymerization temperatures which were analyzed by deconvolution analysis (see Chapter 4).

Table A.1 Polydispersity Indexes of Polyethylene Samples

Run #	Polymerization Temperature (° C)	M_w/M_n	M_z/M_w
7	140	2.6	1.77
6	160	2.6	1.73
5	180	3.3	1.91
4	200	3.4	2.04

Polymerizations were performed at 1500 psig in toluene. τ = 5minutes; $[Zr]_0$ =1.5 μM and [Al]/[Zr] =1000.

For the highest polymerization temperature investigated with the research CSTR, i.e. 200 °C, the polydispersity index M_w/M_n was found to 3.4 as given in Table A.1. Figure A.1(A) gives both the experimental chain length distribution, as determined by high temperature GPC, and the chain length distribution as predicted by Flory's most probable distribution (Flory, 1953). It is clear that Flory's most probable distribution is not an adequate description of the SEC trace under these conditions and it is questionable whether or not a one site model is appropriate for these elevated polymerization temperatures.

Figure A.1(B) deconvolutes the experimental chain length distribution into two most probable chain length distributions. We observe that even with two site-types, the model chain length distribution is still not close to the experimental

distribution. Figure A.2(A) further deconvolutes the experimental chain length distribution into three most probable distributions. In order to determine whether the model is adequate, an analysis of the residuals is required. Correlated residuals are a good indication of model inadequacy (Bates and Watts, 1988). For the three site type model for this polyethylene sample prepared in the CSTR at 200 °C, the residuals are not randomly distributed and are significantly correlated as shown in Figure A.2(B). For this polyethylene sample, the three site type model does not give a good description. Increasing the site-types from three to four as shown in Figure A.3(A) gives residuals that are almost randomly distributed with no significant correlation as evidenced in Figure A.3(B). Thus for this polyethylene sample a four site-type model is required to give an adequate numerical description.

For polymerization at 180 °C, the experimental chain length distribution was deconvoluted into three most probable distributions as shown in Figure A.4(A) with the residuals given in A.4(B). It is clear that at 180 °C, a three site type model is not adequate and a four site type model must be invoked. Figure A.5(A) deconvolutes the chain length distribution into four most probable distributions while Figure A.5(B) provides the residuals which are uncorrelated. For polymerization at 160 °C, the experimental chain length distribution was deconvoluted into three most probable distributions as shown in Figure A.6(A).

Figure A.6 (B) indicates that the residuals are not highly correlated. Thus at 160 °C, a three site type model is adequate to describe the experimental SEC trace.

For the lowest polymerization temperature studied, 140 °C, the experimental chain length distribution was deconvoluted into two most probable distributions as shown in Figure A.7(A). For this two site type model, the residuals are highly correlated as shown in Figure A.7(B). Increasing the site-types from two to three as shown in Figure A.8(A) gives residuals that are almost randomly distributed with no significant correlation as evidenced in Figure A.8(B). Thus at 140 °C, a three site type model is adequate to describe the experimental SEC trace.

It is clear that a three site-type model is adequate to model the experimental SEC traces at the lowest polymerization temperatures studied of 140 °C and 160 °C, but clearly inadequate at 180 and 200 °C. A four site-type model is required to describe the SEC traces for these higher temperature polymerized polyethylene samples. It is possible that the increasing polydispersity index, M_w/M_n, found with increasing polymerization temperature from 140-200 °C in the research CSTR using the metallocene catalyst system Cp_2ZrCl_2/MMAO/TMA, is due to the formation of a new site type with a low τ value which forms low molecular weight polyethylene. Significant catalyst deactivation was observed at elevated temperatures with this simple metallocene catalyst system, and it may be possible that a different site type was created.

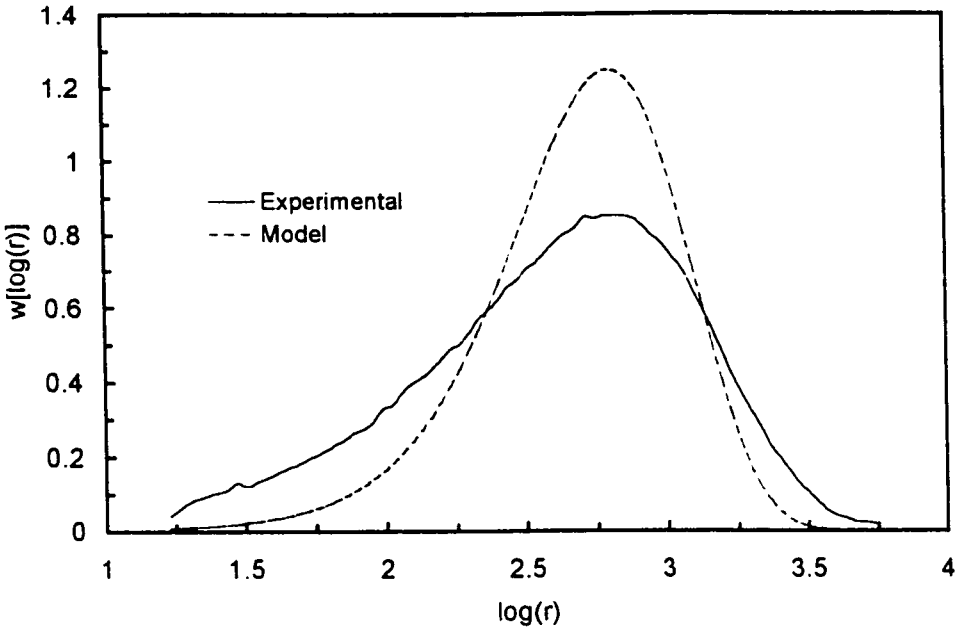

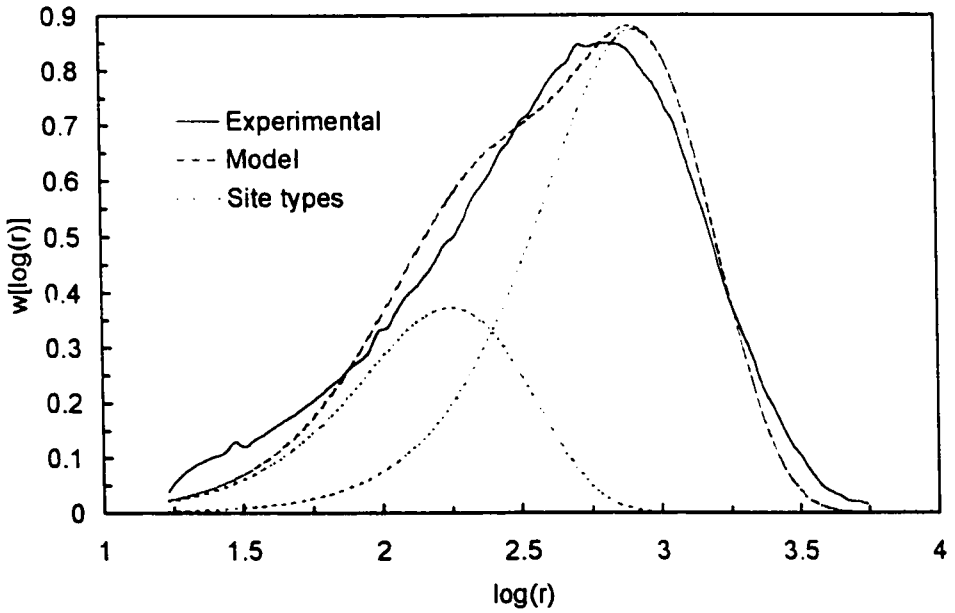

Figure A.1 (A) Comparison of an experimental polyethylene chain length distribution to that predicted by Flory's most probable distribution (B) deconvolution of the experimental polyethylene chain length distribution into two most probable chain length distributions. The PE sample was prepared in the research CSTR at 200 °C with the catalyst system Cp_2ZrCl_2/MMAO/TMA.

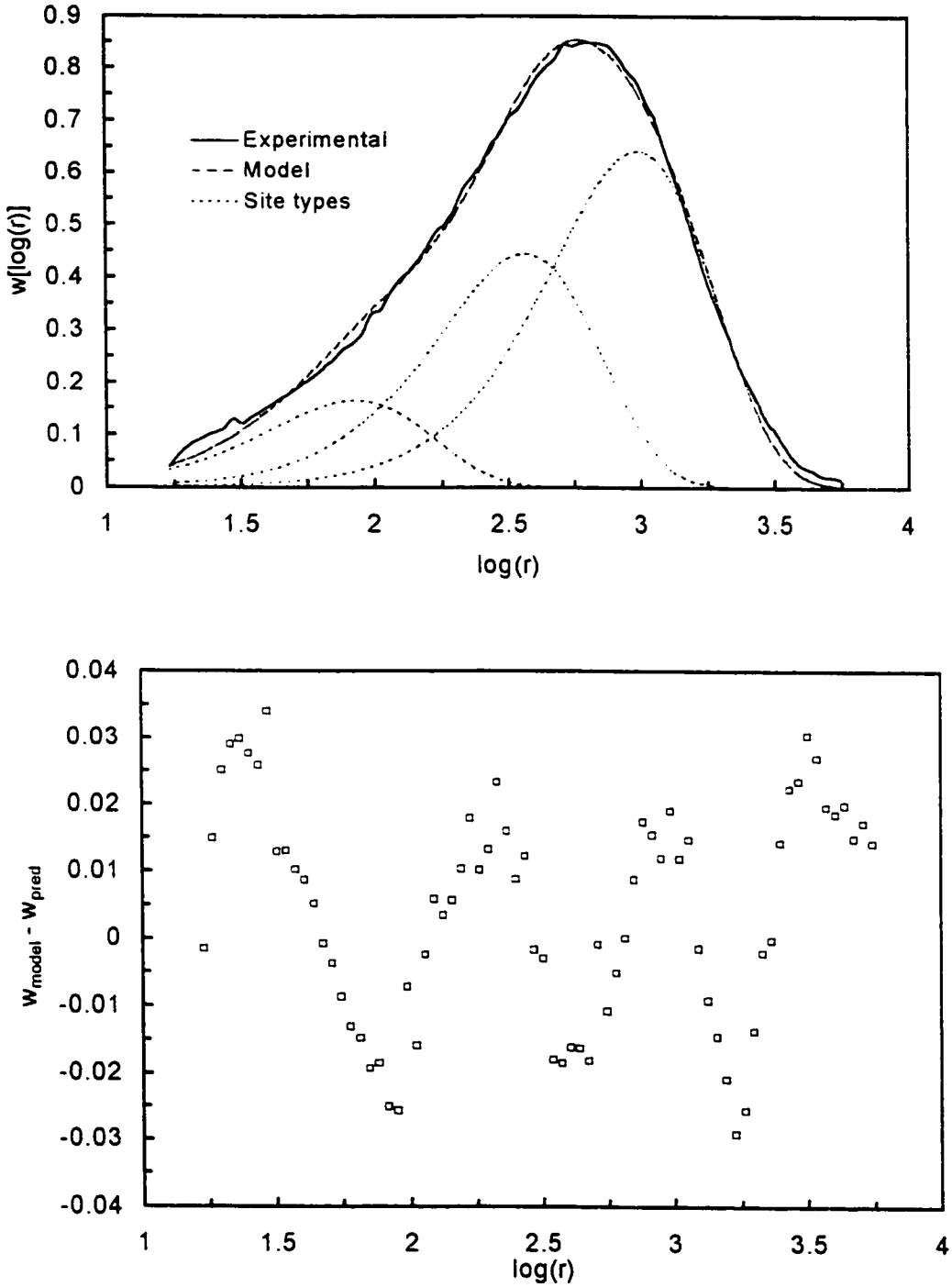

Figure A.2 Deconvolution of an experimental polyethylene chain length distribution into: (A) three most probable chain length distributions; and, (B) residuals of the predicted three site type chain length distribution. The PE sample is the same as from Figure A.1.

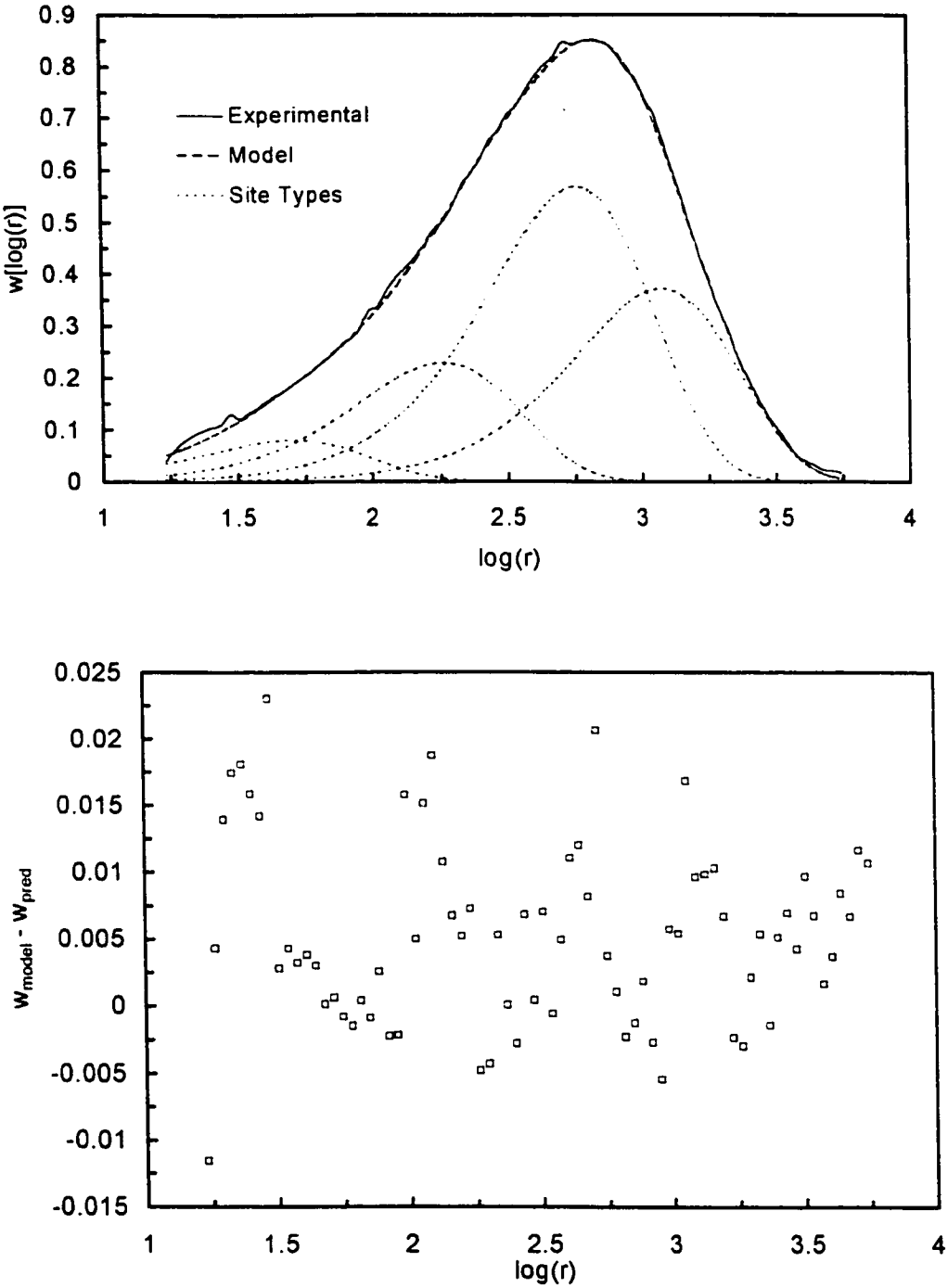

Figure A.3 Deconvolution of an experimental polyethylene chain length distribution into: (A) four most probable chain length distributions; and, (B) residuals of the predicted four site type chain length distribution. The PE sample is the same as from Figure A.1.

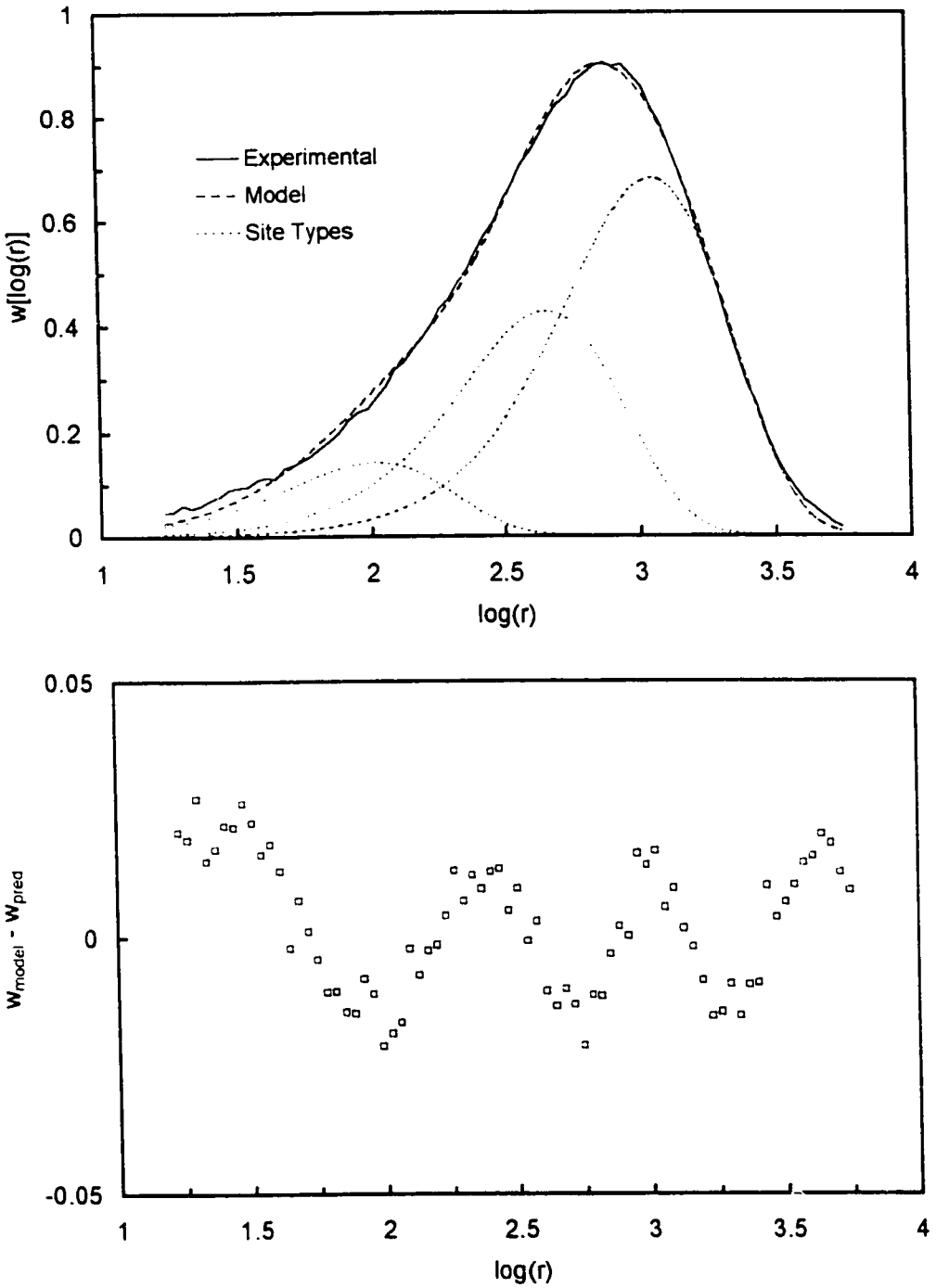

Figure A.4 Deconvolution of an experimental polyethylene chain length distribution into: (A) three most probable chain length distributions; and, (B) residuals of the predicted three site type chain length distribution. The PE sample was prepared in the research CSTR at 180 °C with the catalyst system Cp_2ZrCl_2/MMAO/TMA.

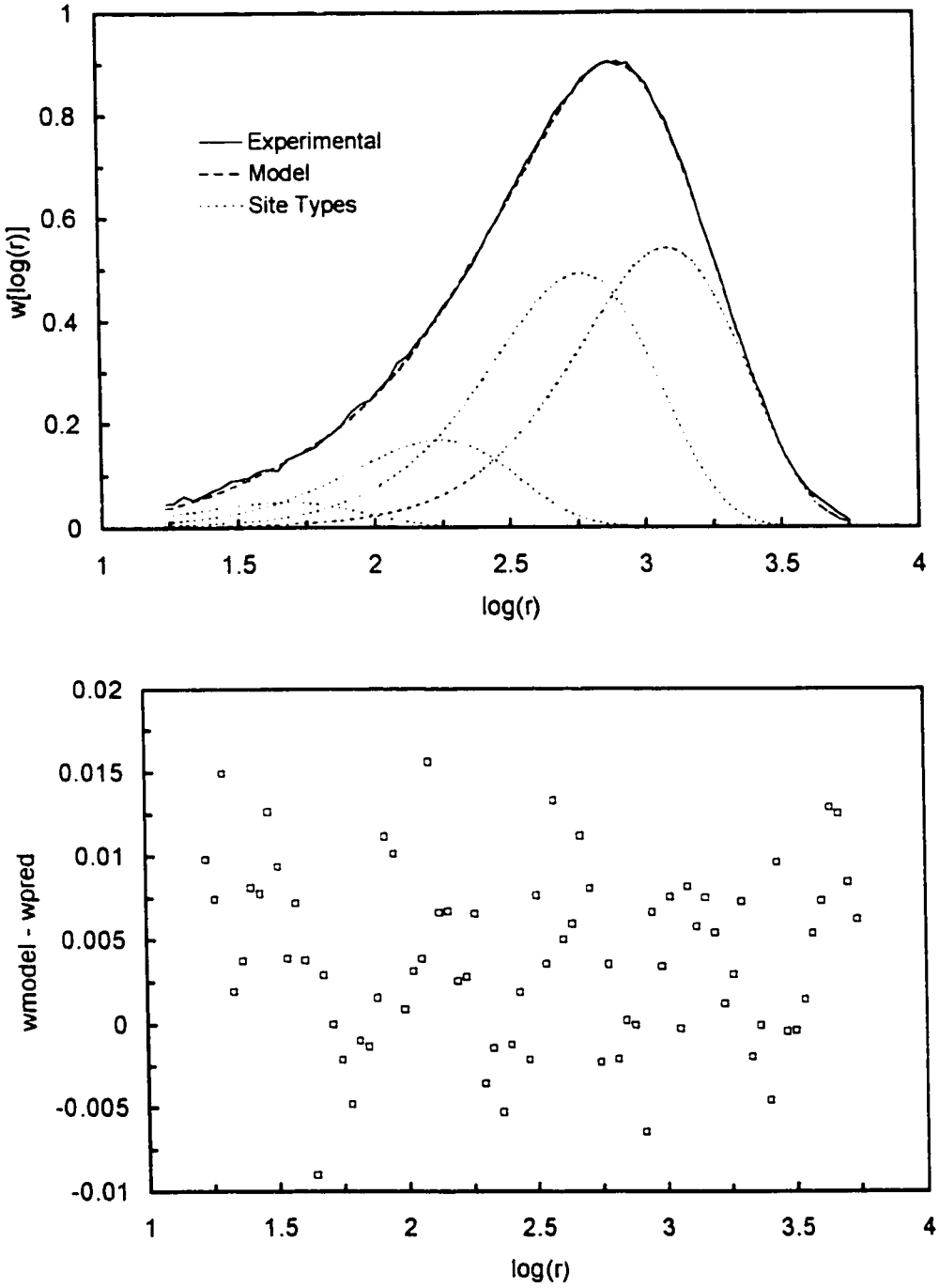

Figure A.5 Deconvolution of an experimental polyethylene chain length distribution into: (A) four most probable chain length distributions; and, (B) residuals of the predicted four site type chain length distribution. The PE sample was prepared in the research CSTR at 180 °C with the catalyst system Cp_2ZrCl_2/MMAO/TMA.

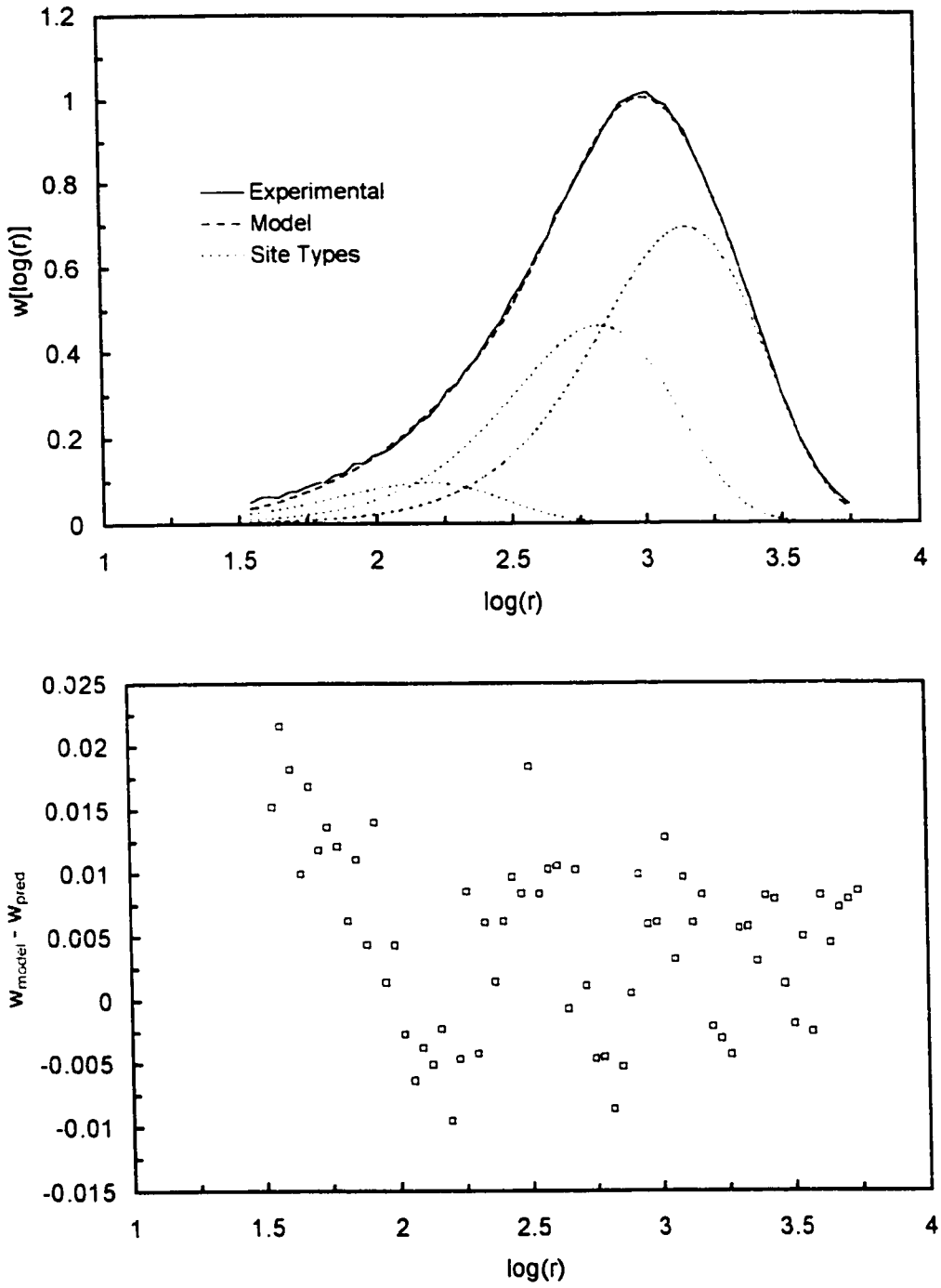

Figure A.6 Deconvolution of an experimental polyethylene chain length distribution into: (A) three most probable chain length distributions; and, (B) residuals of the predicted three site type chain length distribution. The PE sample was prepared in the research CSTR at 160 °C with the catalyst system Cp_2ZrCl_2/MMAO/TMA.

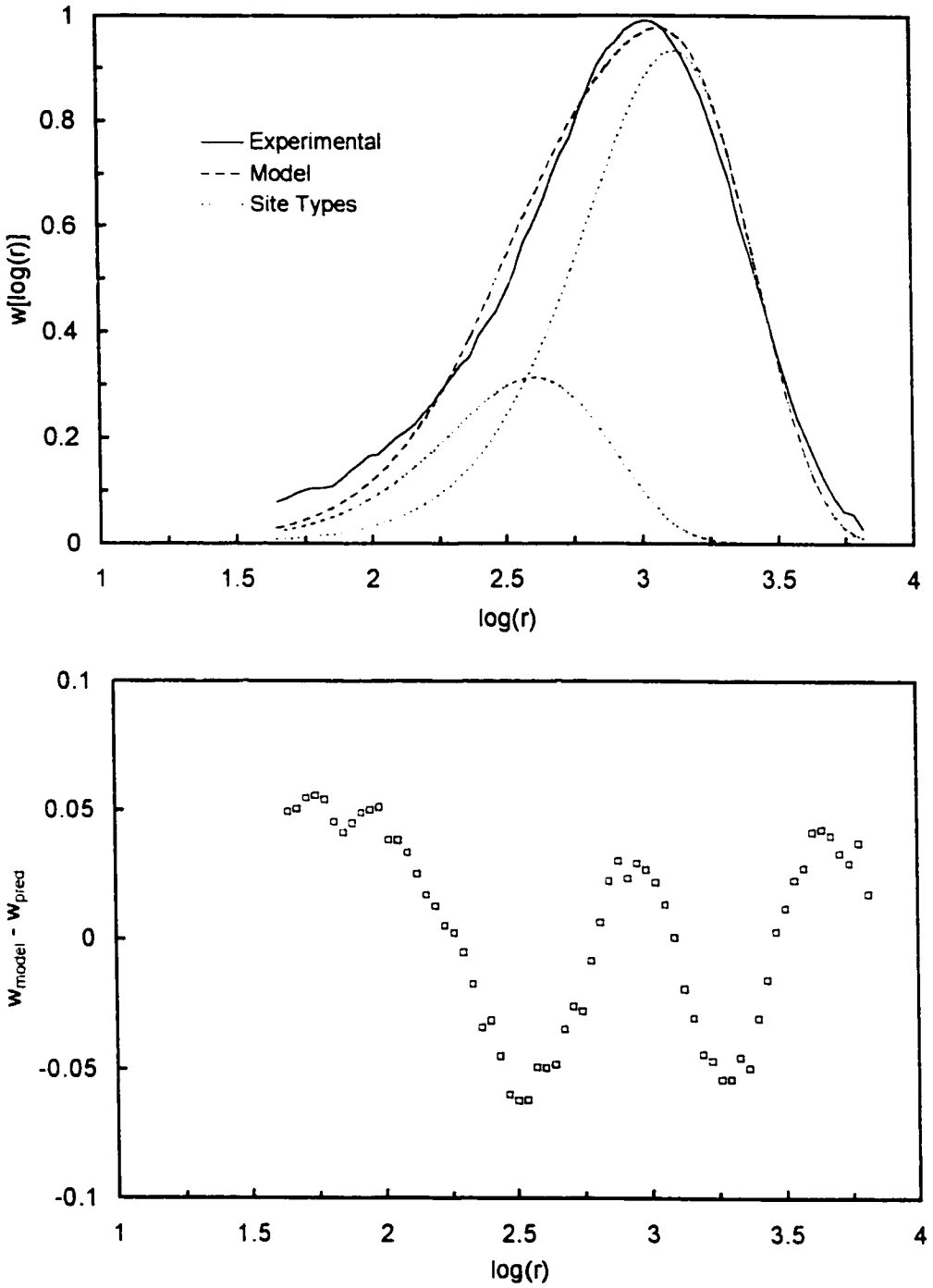

Figure A.7 Deconvolution of an experimental polyethylene chain length distribution into: (A) two most probable chain length distributions; and, (B) residuals of the predicted two site type chain length distribution. The PE sample was prepared in the research CSTR at 140 °C with the catalyst system Cp_2ZrCl_2/MMAO/TMA.

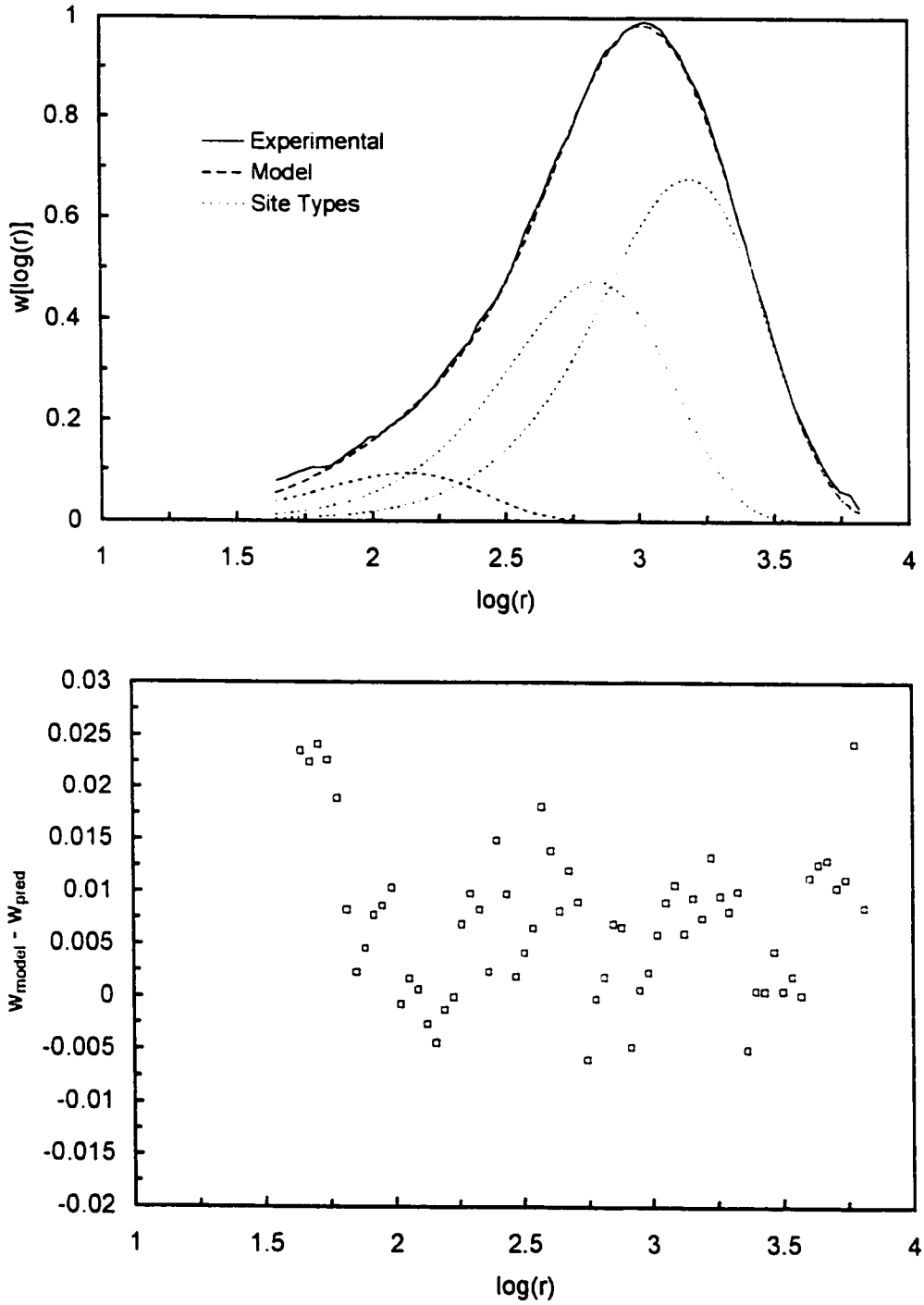

Figure A.8 Deconvolution of an experimental polyethylene chain length distribution into: (A) three most probable chain length distributions; and, (B) residuals of the predicted three site type chain length distribution. The PE sample is the same as from Figure A.7.

Literature Cited

Bates, D.M.; Watts, D.G. *Nonlinear Regression Analysis and its Applications*, John Wiley & Sons, New York, **1988**.

Boor, J., Jr. *Ziegler-Natta Catalysts and Polymerization*, Academic Press, New York, **1979**.

Chien, J.C.W.; Wang, B.P. *J. Polym. Sci. Polym. Chem. Ed.* **1988**, *26*, 3089.

Chien, J.C.W.; Wang, B.P. *J. Polym. Sci. Polym. Chem. Ed.* **1990**, *28*, 15.

Dongarra, J.J.; Grosse, E. *Commun. ACM*, **1987**, 30, 403.

Flory, P.J. *Principles of Polymer Chemistry*; Cornell University Press, Ithaca, New York, **1953**.

Golub, G.H.; Pereyra, V. *SIAM J.Numer. Anal.*, **1973**, 10, 413.

Hamielec, A.E.; Tobita, H. *Ullmann's Encyclopedia of Industrial Chemistry*; **1992**, p.331.

Hamielec, A.E., Soares, J.P. *Progr. Polym. Sci.*. **1996**, 21, 651.

James, D.E. In *Encyclopedia of Polymer Science and Engineering*, 2nd ed.; Mark, H.F., Bikales, N.M., Overberger, C.C., Menges, G., Eds.; Wiley-Interscience: New York, **1987**, Vol. 6.

Kaminsky, W. In *Transition Metal Catalyzed Polymerization*, Quirk, R.P., Ed.; vol.4, MMI Press, London, **1983**, pp.225.

Kaminsky, W.; Miri, M.; Sinn, H.; Woldt, R. *Makromol. Chem. Rapid Commun.* **1983**, *4*, 417.

Karol, F.J. *Macromol. Symp.* **1995,** *89*, 563.

Kuhlke, W.C.; World Polyolefin Market Forecast, ANTEC, **1994**, 2689.

Lai, S.Y.; Wilson, J.R.; Knight, G.W.; Stevens, J.C.; Chum, P.W.S. (to Dow Chemical Co.)., U.S. Patent 5,272,236, **1993**.

Lai, S.Y.; Wilson, J.R.; Knight, G.W.; Stevens, J.C. (to Dow Chemical Co.), U.S. Patent Application WO 93/08221, **1993**.

Press, W.H.; Teukolsky, S.A.; Vetterling, W.T.; Flannery B.P. *Numerical Recipes in Fortran*, Cambridge University Press, Cambridge, 2nd ed., **1992**.

Sinclair, K.B.; *ANTEC*, **1994**, 2697.

Soares, J.P.; Hamielec, A. E., *Macromol. Theory Simul.* **1996**, *5*, 547.

Soares, J.P.; Hamielec, A.E. *Polymer*, **1995,** 36,11,2257.

Speed, C.S.; Trudell, B.C.; Mehta, A.K.; Stehling, F.C.; *Polyolefins VII Conference Proceedings*, **1991**, 45.

Stockmayer, W.H. *J. Chem. Phys.* **1945**, *13*, 199.

Swogger, K.W.; Kao, C.I. in "*Polyolefins VIII*", *Tech. Pap., Reg. Tech. Conf.-Soc. Past. Eng.*, **1993**, 14.

VanderSanden, D.; Halle, R.W.. *ANTEC*, **1993**, 46.

Vela Estrada, J.M.; Hamielec, A.E. *Polymer*, **1994**, 35, 808.

Vickroy, V.V.; Schneider, H.; Abbott, R.F., *J. Appl. Polym Sci.*, **1993**, 50, 551.

Walton, K.L.; Patel, R.M.; (Dow Chemical Co.) *ANTEC*, **1994**, 1430.

Whiteley, K.S.; Heggs, T.G.; Koch, H.; Mawer, R.L.; Immel, W. In *Ulmann's Encyclopedia of Industrial Chemistry*, A21, B.Elvers, S.Hawkins, G. Schultz (eds), Weinheim, VHC Publishers Inc., **1992**, 487.